Dissertation zur Erlangung des Doktorgrades der
Fakultät für Chemie und Pharmazie der
Ludwig-Maximilians-Universität München

Processing of viral nucleic acids

Beatrice Theres Laudenbach

Aus
Rottweil, Deutschland

2018

Erklärung

Diese Dissertation wurde im Sinne von §7 der Promotionsordnung vom 28. November 2011 von Herrn Professor Dr. Matthias Mann betreut.

Eidesstattliche Versicherung

Diese Dissertation wurde eigenständig und ohne unerlaubte Hilfe erarbeitet.

München, den 26.06.2018

Beatrice Theres Laudenbach

Dissertation eingereicht am 26.06.2018
1. Gutachter: Prof. Dr. Matthias Mann
2. Gutachter: Prof. Dr. Andreas Pichlmair
Mündliche Prüfung am 29.10.2018

Für meine Eltern

Über die Geduld

Man muss den Dingen
die eigene, stille
ungestörte Entwicklung lassen,
die tief von innen kommt
und durch nichts gedrängt
oder beschleunigt werden kann,
alles ist austragen – und
dann gebären...

Reifen wie der Baum,
der seine Säfte nicht drängt
und getrost in den Stürmen des Frühlings steht,
ohne Angst,
dass dahinter kein Sommer
kommen könnte.

Er kommt doch!

Aber er kommt nur zu den Geduldigen,
die da sind, als ob die Ewigkeit
vor ihnen läge,
so sorglos, still und weit...

Man muss Geduld haben

Mit dem Ungelösten im Herzen,
und versuchen, die Fragen selber lieb zu haben,
wie verschlossene Stuben,
und wie Bücher, die in einer sehr fremden Sprache
geschrieben sind.

Es handelt sich darum, alles zu leben.
Wenn man die Fragen lebt, lebt man vielleicht allmählich,
ohne es zu merken,
eines fremden Tages
in die Antworten hinein.

Rainer Maria Rilke

CONTENTS

ABBREVIATIONS

5'-PPP - 5'-triphosphorylated
ADAR - Double-stranded RNA-specific adenosine deaminase
AGS - Aicardi-Goutières syndrome
AIM2 - Absent in melanoma 2
APOBEC - Apolipoprotein B mRNA editing enzyme
ALR - AIM2-like receptor
AMP - Adenosine monophosphate
AP - Affinity purification
ASC - Apoptosis-associated speck-like protein containing CARD
CARD - Caspase-recruitment domain
cGAMP - Cyclic GMP-AMP
cGAS - Cyclic GMP-AMP synthase
DCP1 - mRNA decapping enzyme 1
DCP2 - mRNA decapping enzyme 2
DcpS - Scavenger decapping enzyme
DIS3 - Exosome complex exonuclease
DNase - Deoxyribonuclease
ETS - External transcribed spacer
GMP - Guanosine monophosphate
HA - Hemagluttinin
HBV - Hepatitis B virus
HCV - Hepatitis C virus
HCl - Hydrochloric acid
IAV - Influenza A virus
IFIT1,2,3 - Interferon-induced tetratricopeptide repeat protein 1/2/3
IFN - Interferon
Interleukin - Interleukin
IRF - Interferon regulatory factor
ISRE - IFN-stimulated response element
ITS - Internal transcribed spacer
LPS - Lipopolysaccharide
LTR - Lymphotoxin beta receptor
MAVS - Mitochondrial antiviral signaling
MDA5 - Melanoma differentiation factor 5
mRNA - Messenger RNA
mRNP - Messenger ribonucleoprotein
MYD88 - Myeloid differentiation primary response 88
ms - Mouse
NA - Neuraminidase
NaCl - Sodium chloride
ncRNA - Non-coding RNA
NFκB - Nuclear factor 'kappa-light-chain-enhancer' of activated B-cells
NLR - NOD-like receptor
NMD - Nonsense mediated decay

Abbreviations

NRD - Non-functional rRNA decay
NSD - No-stop decay
NOD - Nucleotide-binding oligomerization domain
OAS - 2'-5'-oligoadenylate synthetase
OH - Hydroxyl group
PARN - Poly(A)-specific ribonuclease
PAMP - Pathogen associated molecular pattern
PNPase - Polynucleotide phosphorylase
PKR - Protein kinase R
PPP - Triphosphate
PRR - Pattern-recognition-receptor
rb - Rabbit
RIG-I - Reinoic acid-inducible gene I
RNA - Ribonucleic acid
RNP - Ribonucleoprotein
rRNA - Ribosomal RNA
RVFV - Rift Valley Fever Virus
SAMHD1 - SAM domain and HD domain-containing protein 1
SINV - Sindbis Virus
SKIV2L - Superkiller viralicidic activity 2-like
SLE - Systemic Lupus Erythematosus
snoRNA - Small nucleolar RNA
snRNA - Small nuclear RNA
STAT - Signal transducer and activator of transcription 1
STING - Stimulator of IFN genes
TBK1 - TANK-binding kinase 1
TREX1 - Three prime repair exonuclease 1
TRIF - TIR-domain-containing adapter-inducing interferon-
tRNA - Transfer RNA
TLR - Toll-like receptor
UPR - Unfolded protein response
VSV - Vesicular stomatitis virus
wt - Wild type
XRN1 - Exoribonuclease 1
XRN2 - Exoribonuclease 2

ABSTRACT

The innate immune system evolved a plethora of germline encoded pattern recognition receptors that are able to sense viral nucleic acids in order to restrict infection. Exceptional progress has been made in the understanding of viral nucleic acid sensing. However, surprisingly little is known about the ability of cells to degrade viral nucleic acids. RNA turnover is a highly conserved process and tightly controlled to only target erroneous RNAs for degradation. Intact cellular messenger RNAs are protected from 5'-degradation by a 5'-cap structure. Before being a substrate for 5'-exonucleases, the 5'-cap structure has to be removed by the decapping protein 2 (DCP2 or NUDT20). This decapping leaves a monophosphorylated RNA that can serve as a substrate for the exonuclease 1 (XRN1). Nucleic acids of some RNA viruses bear a triphosphorylated 5'-end. This chemical structure is a feature exclusively foreign nucleic acids introduce into cells and does not serve as a substrate for XRN1.

In this dissertation, I discovered a novel mechanism that prepares viral 5'-triphosphorylated RNAs for degradation. Employing a siRNA screen, recombinant proteins as well as *in vitro* and *in vivo* experiments, I identified the protein Nudix hydrolase 2 (NUDT2) as central protein to prepare 5'-PPP-RNA for degradation by XRN1. I could show that the activity of NUDT2 is unspecific in terms of the 5'-triphosphorylated RNA substrate and can dephosphorylate substrates of a broad range without showing any sequence or structural requirements. NUDT2 releases two phosphate groups in a sequential manner, leaving a monophosphorylated RNA that can serve as a substrate for XRN1. Thereby, NUDT2 initiates a RNA decay mechanism that is specific for viral 5'-PPP RNA. Its importance is highlighted by the increased replication of PPP-RNA generating Vesicular stomatitis virus infected cells lacking the *Nudt2* gene.

Besides identifying this novel pathway to process and remove 5'-PPP-RNA, I also contributed to gain a better understanding on how the viral restriction factor interferon-induced protein with tetratricopeptide repeats 1 (IFIT1) discriminates host from viral nucleic acids. Infection of IFIT1 mutant cells emphasized the importance of IFIT1 mediated virus restriction and expanded our knowledge on important RNA binding sites.

Abstract

Taken together, this work describes the functional characterization of a viral RNA specific degradation route involving the phosphatase NUDT2 and gives further insights into the discrimination of self and non-self nucleic acids by the viral restriction factor IFIT1. Both projects deepen and enhance our understanding of the execution mechanisms of innate nucleic acid immunity.

PREFACE

This thesis is written in a cumulative style. The first part of chapter one introduces general knowledge of RNA biology, particular focusing on RNA degradation pathways. The second part of chapter one describes nucleic acid immunity including pattern recognition receptors, the discrimination of self and non-self RNA, antiviral restriction factors, and an introduction to the role of nucleases and immunopathologies triggered by the deregulation of nucleic acid immunity. Section I.2.4 of the introduction was published in the *Journal of Interferon & Cytokine Research*:

Anna Gebhardt, **Beatrice T. Laudenbach**, Andreas Pichlmair, Discrimination of Self and Non-Self Ribonucleic Acids. *J Interferon Cytokine Res* 37, 184-197 (2017).

The third and fourth part of the introduction describes viral RNA degradation pathways and a general introduction to the background of mammalian phosphatases.

The second chapter includes my results in form of manuscripts already published or prepared for submission:

Beatrice T. Laudenbach, Alexander Reim, Markus Moser, Arno Meiler, Janos Ludwig and Andreas Pichlmair. NUDT2 initiates viral RNA degradation by removal of 5'-phosphates. Submitted to *Science* (2018)

Yazan M. Abbas, **Beatrice T. Laudenbach**, Saúl Martínez-Montero, Regina Cencic, Matthias Habjan, Andreas Pichlmair, Masad J. Damha, Jerry Pelletier, and Bhushan Nagar. Structure of human IFIT1 with capped RNA reveals adaptable mRNA binding and mechanisms for sensing N1 and N2 ribose 2'-O methylations. *Proc Natl Acad Sci U S A* 114, E2106-E2115 (2017).

The last chapter features the discussion and outlook.
All publications are reprinted with permission and copyright of the publications belongs to the publishers.

Part I

Introduction

CHAPTER

1

RNA BIOLOGY

Contents

1.1 Ribonucleic Acids

The amount of ribonucleic acid (RNA) that is produced by a eukaryotic cell is striking. Over 2000 ribosomal RNA molecules are synthesized per minute along with messenger RNAs (mRNAs) coding for thousands of genes, transfer RNAs (tRNAs), small nuclear RNAs (snRNAs) and small nucleolar RNAs (snoRNAs). The metabolic expenses are huge. The synthesis of all RNA species involves several processing reactions, transitions between subcellular compartments and cycling between different protein complexes.
The different types of RNA are generated in the nucleus by three cellular RNA polymerases (RNA Pol-I, RNA Pol-II, and RNA Pol-III). All three polymerases give rise to a precursor transcript bearing a 5'-triphosphate (5'-PPP) group. Before being exported to the cytoplasm the RNA precursors get variably processed.
Ribosomal RNAs (rRNAs) constitute the largest portion accounting for about 80% of total RNA. Transcription by RNA Pol-I gives rise to a 45S primary transcript (pre-rRNA) carrying a 5'-PPP-RNA structure. A considerable amount of chemical modifications are made to the precursor rRNA including hundreds of isomerizations of uridines to pseudouridines and methylations of the 2'OH position of the nucleotide sugars[1]. Endonucleolytic cleavage and removal of the external and internal transcribed spacer regions (ETS and ITS) leads to the maturation of the precursor into the 28S, 18S, and 5.8S rRNAs[2]. The processed ribosomal RNAs then carry a 5'-monophosphate structure (Figure 1).
RNA Pol-III transcribes an additional set of three different classes comprising the 5S rRNA (Class I), tRNAs (Class II) - the second largest proportion of RNAs accounting for 15% of total RNA in a cell - as well as many small noncoding genes (Class III)[3;4]. The latter include 7SK RNA, 7SL RNA, U6 snRNA, vault genes (HVG), hY RNA, H1 RNA, MRP RNA and others[5]. tRNAs undergo by far the most extensive processing in order to provide correct function and structure. First, Ribonuclease P and Ribonuclease Z cut the 5'-leader and 3'-trailer sequence, respectively, leaving a 5'-monophosphorylated tRNA precursor. Second, tRNA nucleotidyltransferase - a specialized RNA polymerase - adds the essential three 3'-terminal nucleotides CCA to the tRNA (Figure 1)[6]. Moreover, some tRNA precursors contain introns that have to be spliced out. In addition, over 17% of all nucleotides in precursor tRNAs are chemically modified. More than 50 different types of tRNA modifications are known including methylations, isomerization from uridines to pseudouridines and the widespread deaminations of adenines to inosines and cytidines to uridines[7].
Transcription of RNA Pol-II gives rise to mRNAs and many nonprotein-coding noncoding(nc)RNAs, such as micro RNAs (miRNAs), snRNAs and snoRNAs. In case of

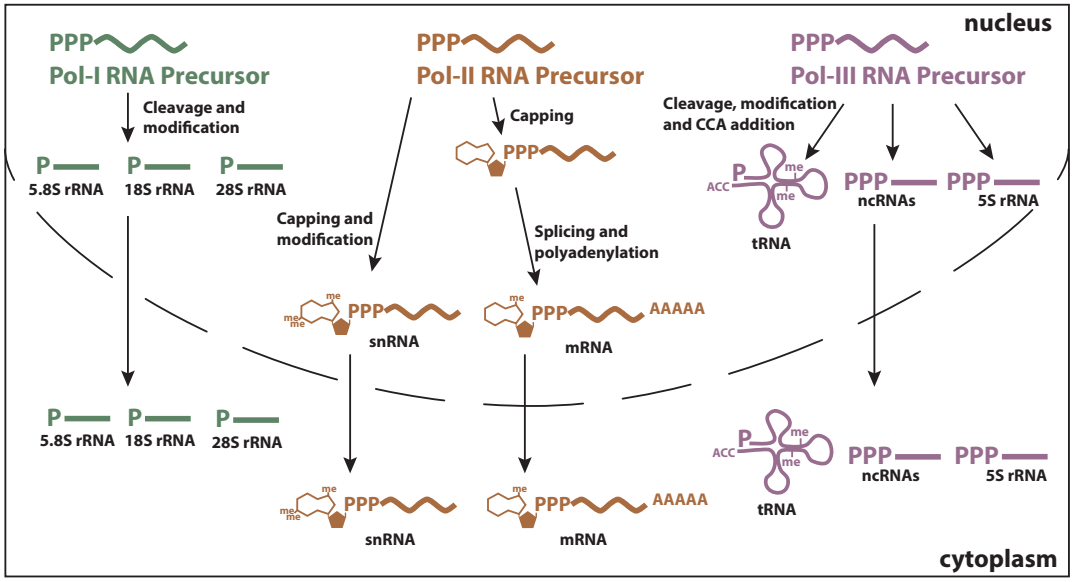

Figure 1: Processing and maturation of cellular RNA transcripts originating from the three RNA polymerases RNA polymerase I, RNA polymerase II and RNA polymerase III.

mRNAs, the nascent RNA molecule is processed by coupling a guanine monophosphate nucleoside to the RNA precursor forming the 5'-cap structure (Cap)[8]. The 5'-cap is further processed by methylating the N7-position of the guanosine directly after capping, thereby generating the N7-methylguanylate cap (Cap-0). In addition, the 2'-O-position of the first (Cap-1) and second ribose (Cap-2) can be methylated[9].

After capping, a poly(A) tail is added to the 3'-end of the mRNA chain to protect the molecule from rapid decay in the cytoplasm, to facilitate export from the nucleus and to aid transcription termination[10;11]. The poly(A) tail interacts with poly(A) binding proteins (PABP) in order to protect the structure from exonucleases.

In the final step of mRNA processing, introns are removed and exons are again conjugated (Figure 1). This splicing reaction is carried out by a large protein complex called the spliceosome. The 5'-end of snRNAs is processed as well by unique 5'-cap structures including 5'-trimethylguanosine caps (Sm-class snRNAs) or 5'-monomethylphosphate caps (LSM-class snRNAs transcribed by RNA Pol III)[12]. Spliceosomal snRNAs are as well extensively 2'-O- methylated and pseudouridylated at conserved residues important for proper function similar to rRNAs[13].

Only recently, through development of high-throughput sequencing techniques, it was found that internal nucleotides of mRNAs can be chemically modified to pseudouridines as well[14;15]. Observations indicate that pseudouridylation of mRNAs may play an

important biological role since cellular stress, such as starvation, immune stimulation or heat shock can lead to pseudouridylation of completely novel sites[14;16].
The pervasiveness of all RNA modifications is important for proper structure and function of RNAs and, importantly also allows quality-control mechanisms to distinguish mature RNA from their precursors.

1.2 RNA Degradation

The synthesis of proteins is one of the most costly biochemical processes. It requires a remarkable amount of energy and has to dynamically adapt to environmental changes the cell encounters in order to exclusively produce proteins that are needed at a given time. This regulation is partially achieved by degradation of mRNA, eventually leading to changing patterns of protein synthesis. By decay of RNA molecules, ribonucleotides can be recycled and incorporated into newly synthesized RNAs.
Besides controlling protein synthesis, RNA degradation machineries need to prevent the accumulation of nonfunctional RNAs with defects in folding, defective RNA modifications or incorrectly assembled proteins. RNA degradation is a fundamental cellular process that has to be tightly controlled to accurately spot RNAs to target them for destruction.
RNA decay processes can be subdivided into RNA quality control, mRNA turnover and the processing of RNAs. In RNA quality control all classes of RNA are monitored. Surveillance pathways constantly detect aberrant RNAs that can originate from various events, including mutations in the gene leading to premature termination of translation, error-prone transcription or pre-RNA processing. Quality control pathways are also able to detect non-functional RNAs which are generated by the transcription of intergenic regions[17] or parasitic RNAs originating from transposons. Turnover of mRNAs is another cause for RNA degradation and regulates protein synthesis and abundance. Related to mRNA turnover, ncRNAs are constitutively degraded and thereby form a contrast to the very stable group of rRNAs. Processing of RNAs in the nucleus represents the third cause for RNA degradation since all types of RNA are synthetized in the nucleus as larger precursors by the three RNA polymerases before they undergo trimming of the 5'- or 3'-ends. This trimming events, but also the generation of excised fragments or introns, necessitates their removal and governs large parts of the nuclear RNA degradation machinery.
RNA polymerase I, II, and III are able to generate very different types of RNA molecules however cellular RNA decay pathways seem to not distinguish between their products but rather constitute a universal arsenal surveilling all cellular RNAs.

1.2.1 Degradation of RNA Polymerase II transcripts

RNA Polymerase II transcription leads to the generation of different classes of RNA including mRNA, snRNAs, snoRNAs and miRNAs. In eukaryotic cells, two main mRNA degradation pathways are responsible for the turnover of bulk mRNAs: 5' to 3' decay employing the exonuclease 1 (XRN1) and 3' to 5' degradation through the exosome complex. Both pathways are commenced by the removal of the poly(A) tail in a process called deadenylation. As a second step, either the 5'-cap is removed by decapping enzymes and cellular nucleases proceed with 5'-3' degradation of the RNA body or alternatively, the second major mRNA decay route proceeds in 3'-5' direction through engaging the exosome complex[18].

In addition to the two main mRNA degradation pathways there are more specialized mechanisms in place to detect and degrade non-functional RNAs. RNAs containing premature stop codons are recognized and degraded in a process called nonsense-mediated decay (NMD), whereas turnover of RNAs lacking translation termination codons occurs via nonstop decay (NSD)

1.2.1.1 RNA Deadenylation

The initial and rate-limiting step for bulk mRNA decay is deadenylation. The main cytoplasmic deadenylase complexes are the C-C-chemokinrezeptor type 4 - negative regulator of transcription (CCR4-NOT), poly(A)-nuclease 2 and 3 (PAN2-PAN3) and poly(A) ribonuclease (PARN) complexes. Each of these complexes has unique properties. In eukaryotes, the predominant deadenylase activity comes from the CCR4-NOT complex including five conserved subunits: CCR4, NOT1, NOT2, NOT3/5, and CAF1/ POP2[19]. Two of the subunits, namely CCR4 and CAF1/POP2, are responsible for the catalytic 3'-5' poly(A) exoribonuclease activity of the complex (Figure 2). CCR4 - originally identified in yeast - has several homologs in mammals that form a similar complex containing CNOT6 (Ccr4a), CNOT6L (Ccr4b). Similarly, CAF1/POP2 constituting the second catalytic subunit of the CCR4-NOT complex, is widely conserved and has three mammalian homologues: CNOT7 (hCaf1), CNOT8 (hPop2) and CAF1Z[20]. The activity of CCR4-NOT is inhibited PABP[21].

The second enzyme complex exerting cytoplasmic mRNA deadenylation activity is the PAN2-PAN3 complex. Interestingly, in comparison to the CCR4-NOT complex the PAN2-PAN3 complex is dependent on PABP. PAN2 executes the catalytic function of the complex (Figure 2). Although the PAN2-PAN3 complex does not degrade the entire poly(A) tail, it is responsible for an initial shortening of the poly(A) tail to a length of

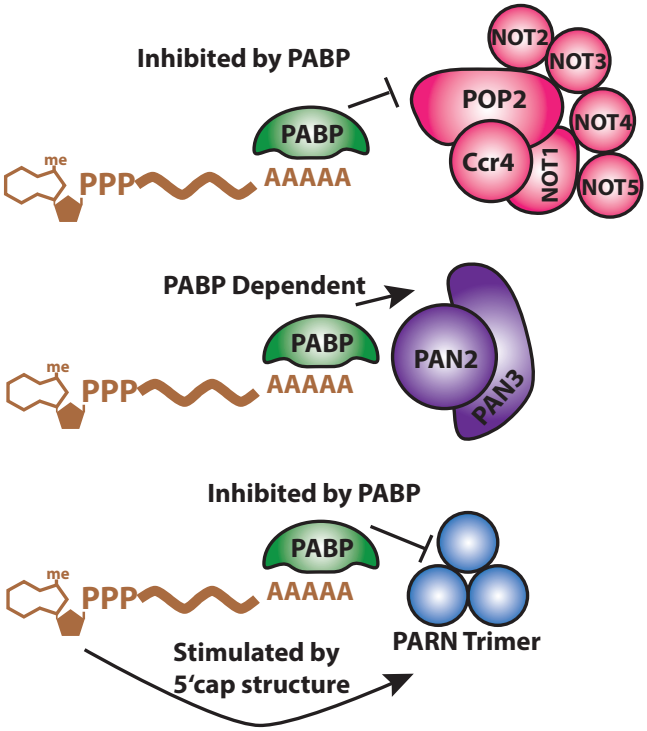

Figure 2: Eukaryotic polyadenation complexes including the CCR4-NOT, PAN2-PAN3 and PARN complex. CCR4-NOT and the PARN complex select RNAs for polyadenylation that are not bound by PABP, whereas the PAN2-PAN3 complex is only active on RNAs bound by PABP.

80 nucleotides[22]. Deadenylation is then continued by the CCR4-NOT complex.
PARN is the final enzyme known to deadenylate mRNAs and is unique in that its activity is increased by the existence of a 5'-cap structure[23] but inhibited by cap-binding proteins (Figure 2)[24]. The catalytic subunits CCR4, CAF1, PAN2 and PARN belong to the RNAse D-type family having Mg^{2+}-dependent 3'-5' exoribonuclease domains. Interestingly, biochemical studies indicate that the different deadenylase complexes prefer specific mRNA substrates. The CCR4-NOT complex and PARN select mRNAs without PABP bound to the poly(A) tail for deadenylation, whereas the activity of the PAN2-PAN3 complex depends on PABP binding. This selection of messenger ribonucleoprotein (mRNP) substrates shows that deadenylation and therefore mRNA turnover can be controlled by the architecture of mRNPs and the associated proteins.

1.2.1.2 The exosome complex

Following deadenylation of mRNAs, one possible degradation route is 3'-5' decay by the exosome complex. The RNA exosome is a large multiprotein complex forming a barrel-like structure. In eukaryotes, the core part with its nine subunits (barrel: RRP41, RRP42, RRP43, RRP45, RRP46, MTR3 and cap: CSL4, RRP4, RRP40) is highly conserved (Figure 3A). It is very similar to the structure and domain organization of

the bacterial proteins polynucleotide phosphorylase (PNPase) and RNase PH. RNase PH is a bacterial tRNA processing enzyme forming a hexameric ring of six RNase PH proteins[25], whereas PNPase is a RNA degrading protein using phosphate as attacking group. PNPase forms a trimeric complex of one KH and S1 RNA binding domain and two RNase PH domains[26], a structure very similar to the one of the exosome. The trimeric ring of the exosome is composed of proteins containing S1 and KH domains and the hexameric ring of RNAse PH-like proteins. However in contrast to these bacterial RNA degrading complexes, the internal chamber of the exosome is catalytically inactive. Only an additional subunit (RRP44 or DIS3) confers catalytic activity to the complex[27]. Therefore, single-stranded RNA molecules that enter the exosome through a pore in the S1 and KH-domain containing cap are then channeled through the barrel to the catalytic DIS3 subunit (Figure 3A). Although catalytically inactive, the barrel itself is important as it serves as a scaffold for the binding of regulatory proteins and to guide and restrain the substrate to the catalytic active site[28]. The chemical reaction performed by DIS3 constitutes a hydrolysis reaction. This is in contrast to the bacterial phosphorylytic reactions of PNPase and RNase PH. However, the hydrolase activity has the advantage that the RNA substrate is irreversibly cleaved, while phosphorylytic reactions can be reversed[29]. During the hydrolysis reaction, single nucleotides are cleaved off from the polynucleotide chain and no intermediates are released until the mRNA chain is trimmed to a four-nucleotide remnant, which is eventually released. The scavenger decapping enzyme (DcpS) is then able to decap this short oligonucleotides and release an m^7GMP cap structure[30].

In addition to its exoribonuclease activity (RNase II-like domain) DIS3 also provides endonuclease activity. In the nucleus the exosome also associates with an additional subunit (RRP6) constituting the eleventh subunit and contributing for another exoribonuclease activity[31]. RRP6 plays an important role in trimming rRNAs, snRNAs and snoRNAs during RNA processing in the nucleus[32].

In order to degrade RNA, the exosome has to associate with regulatory protein complexes: the nuclear TRAMP complex[33] and the cytoplasmic SKI complex (Figure 3B)[34], both of which have ATP-dependent helicase activity. The nuclear TRAMP complex adds short poly(A) tails to the 3'-end of its substrates. This adenosine-tag is supposed to provide a single-stranded interaction site for the exosome complex in the nucleus (Figure 3B)[17]. In the cytoplasm, the Ski complex is suggested to directly link RNA unwinding by its helicase activity to RNA degradation by the exoribonuclease activity of DIS3 through one uninterrupted channel[35].

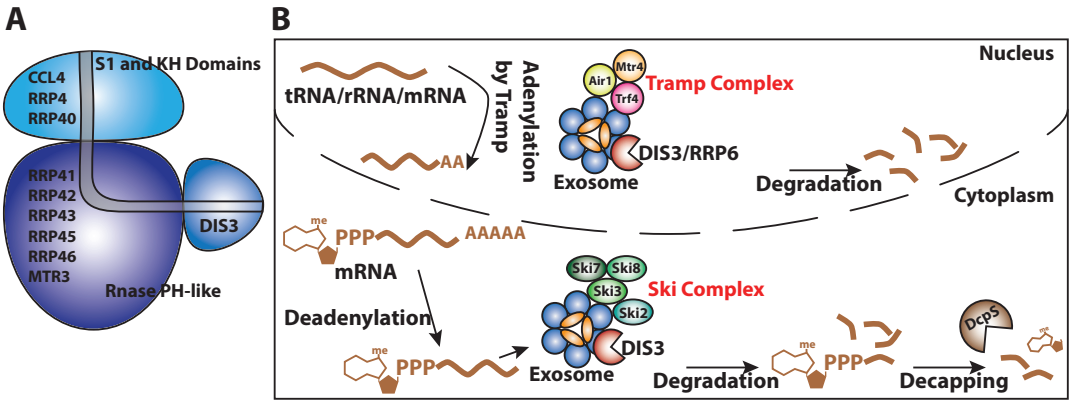

Figure 3: The eukaryotic exosome complex. A: Domain structure and organization of the exosome complex. **B:** Degradation of nuclear and cytoplasmic RNA species by the exosome complex

1.2.1.3 Canonical 5' to 3' mRNA decay

As an alternative to being directly degraded by the exosome, deadenylated RNA can be subject to the second main route of RNA degradation, where deadenylation is followed by decapping.

The protein with main decapping activity in humans is mRNA-decapping enzyme 2 (DCP2)[36]. However in vivo, the decapping activity of DCP2 alone is not sufficient and additional activators, the so called enhancers of decapping (EDCs), are required for full activity. In humans, DCP1 interacting with DCP2 strongly stimulates decapping activity. Additionally, the heptameric Sm-like protein 1-7 (LSM1-7) complex binds the 3'-end of deadenylated RNAs, thereby promoting decapping (Figure 4). Other LSM proteins like enhancer of decapping-3 (EDC3 or LSM16), RNA-associated protein of 55kDa (RAP55 or LSM14) are also involved in decapping[37]. The proteins DExD/H-box RNA helicase DHH1 and PAT1 are able to directly mediate translational repression through which decapping is stimulated since decapping and translation are two distinct processes directly competing with each other.

EDCs interact with each other, with DCP2 directly as well as with the ribonuclease XRN1, providing a direct connection between 5'-3' RNA degradation and decapping[38]. In general DCP1 and DCP2 bind their mRNA substrate as part of a ribonucleoprotein complex containing EDCs and favor longer RNA as substrates. This contrasts the activity of DcpS, which uses short capped oligonucleotides as substrate originating from degradation by the exosome. In *C.elegans* it was shown that DCP2 does not associate with the 5'-cap directly and is not inhibited by cap analogs but rather binds the RNA

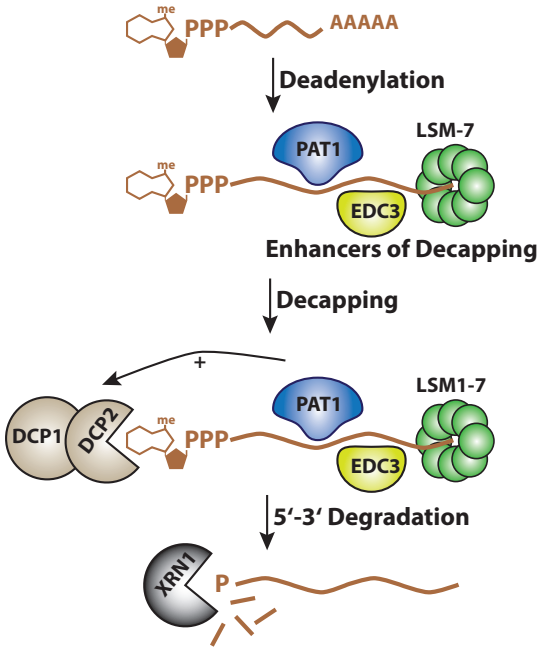

Figure 4: Eukaryotic 5'-3' RNA Degradation pathway. After deadenylation, proteins of the family of enhancers of decapping strengthen the activity of the decapping complex including DCP1 and DCP2. Decapping leaves a monophosphorylated RNA species that is a substrate for the cellular exonuclease XRN1.

body with a length requirement of 50 nucleotides[39]. In addition to the canonical decapping protein DCP2, other proteins were shown to have decapping activity as well. Amongst those is NUDT16, which was shown to work on other subsets of RNAs compared to DCP2[40;41]. Only recently, NUDT3 was identified to possess mRNA decapping activity on substrates modulating cell migration[42]. Interestingly, NUDT16, NUDT3 and DCP2 (NUDT20) all belong to the same family of Nudix hydrolases.
After decapping, the RNA body is subject to exonucleolytic cleavage by the nuclease XRN1 that is localized in the cytoplasm of cells (Figure 4). Another member of the XRN family, namely XRN2 (Rat1) is mainly nuclear. Both proteins are Mg^{2+}-dependent 5'-3' exoribonucleases acting on single-stranded, unstructured, 5'- monophosphorylated RNAs[43]. Capped RNAs or RNAs bearing 5'-hydroxyl or 5'-triphosphate groups renders them as unsusceptible to degradation by XRN1[44]. By deleting over 40 components of the mRNA processing pathways, Sun et al. identified that XRN1 alone leads to an imbalance between RNA synthesis and degradation. Thereby, XRN1 was suggested to be a key factor contributing to the buffering of mRNA levels[45].

1.2.1.4 mRNA quality control

In the cytoplasm, multiple adaptor proteins are able to distinguish aberrant from normal mRNAs targeting them for degradation. mRNAs with premature translation termination codons are recognized by the Upf proteins in a process called nonsense-

mediated decay (NMD). After recognition, these proteins are targeted for deadenylation followed by 3'-5' degradation by the exosome complex, or decapping and degradation by XRN1[46]. In yeast, stalled ribosomes causing a pause during elongation are recognized by the proteins Hbs1 and Dom34. These mRNAs are then targeted for endonucleolytic cleavage in a process called No-Go decay (NGD)[47]. Hbs1 and Dom34 are paralogs of the eukaryotic release factors 1 and 3 (eRF1 and eRF3), respectively where Hbs1 was suggested to recognize the stop codon in the A site of the ribosome and Dom34 to display endonuclease activity[48]. This finding however could not be supported in recent reports[49]. After an initial cleavage, the mRNA body is degraded by XRN1 and the exosome complex. When stop codons are missing, the Ski complex identifies those stalled ribosomes and engages the cytoplasmic exosome for RNA turnover by the Non-stop decay (NSD) pathway[50].
Intergenic regions that are erroneously transcribed by RNA polymerase II are as well rapidly degraded in the nucleus by the actions of the TRAMP complex through adding of short poly(A) tails and subsequent degradation by the exosome complex[17]. Additionally, in a process called unfolded protein response (UPR), mRNA levels are reduced when the amount of newly synthesized proteins exceeds the folding capacity of the ER. Inositol-requiring enzyme 1 (IRE1) promotes this in a process called regulated IRE-1-dependent RNA decay (RIDD), where ER-associated mRNAs are degraded to reduce the load of freshly generated proteins[51]. However, the products of IRE-1-mediated cleavages contain 2'3'-cyclic phosphates that could potentially be recognized as harmful aberrant RNA species by the innate immune system[52].

1.2.1.5 Similarities in eukaryotic and bacterial mRNA degradation

New discoveries suggest unappreciated similarities between pro- and eukaryotic RNA degradation. For long time it was thought that RNA molecules and proteins involved in the RNA degradation pathways differ a lot between both kingdoms. One reason for this notion is the quite diverse chemical structure and organization of RNA molecules in bacterial and eukaryotic cells. Eukaryotic mRNAs are protected by the 5'-cap structure connected by an unusual 5'-5' triphosphate linkage. In contrast, bacterial mRNA is protected by a 5'-triphosphate group and miss additional post-transcriptional chemical modifications on the RNA 5'-end. Additionally, the 3'-end of eukaryotic mRNAs is elongated by the post-transcriptionally added poly(A) tail. Bacterial mRNA commonly ends with a stem loop. Moreover, the 5'-cap structure and poly(A) tail of eukaryotic mRNA are bound by proteins like the eukaryotic translation initiation factor 4F (eIF4F) and PABP, respectively. Both proteins can interact with each other forming a closed

loop. Bacterial mRNA is not complexed by proteins of that kind.

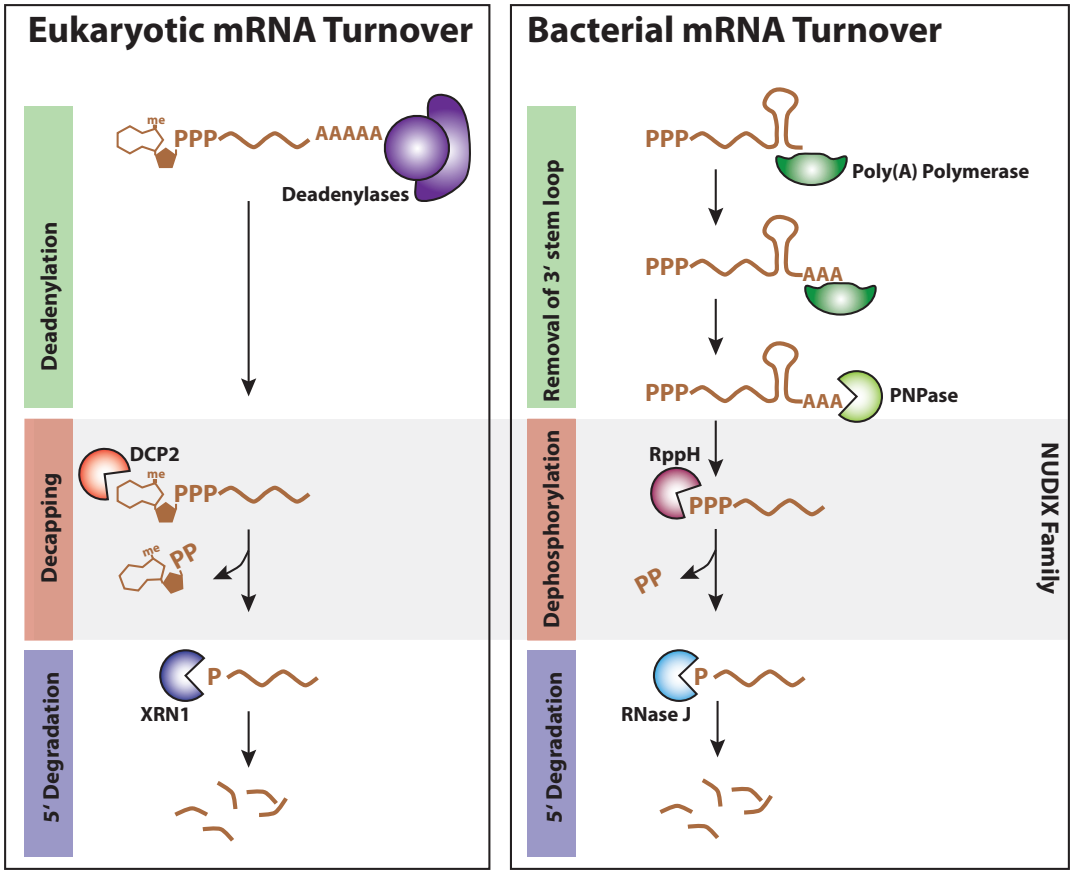

Figure 5: Comparison of eukaryotic and bacterial mRNA Degradation pathways. Despite differences in the preparation of 3'-ends, the eukaryotic and prokaryotic RNA degradation shows striking commonalities in regard of 5'-processing involving proteins of the same protein family namely the Nudix hydrolase family.

The long-standing model for RNA degradation in bacteria comes mostly from studies in E.coli, which contains several 3'-exonucleases and endonucleases. The stem-loop structure at the 3'-end of bacterial mRNA protects it from 3'-exonucleolytic cleavage and therefore it was thought that degradation needs to be initiated with endonucleolytic cleavage. This model was supported by the finding that the endonuclease RNase E seems to play a general role in bacterial mRNA turnover[53]. However, this model was challenged by the discovery of polyadenylation of bacterial mRNA and its major importance for RNA degradation[54]. Similar to the TRAMP complex - the nuclear exosome regulator in eukaryotes - a bacterial poly(A) polymerase transiently adds adenosines to the 3'-end of RNAs. This short poly(A) tail renders it susceptible to 3'-exonucleolytic cleavage

by PNPase (Figure 5) which requires single-stranded RNA to initiate cleavage[55]. The PNPase complex is structurally related to the eukaryotic exosome complex. Besides commonalities in 3'-5' degradation between pro- and eukaryotes, discovery of an additional mRNA decay pathway in bacteria shows similarities to eukaryotic degradation pathways. The RNA pyrophosphorylase RppH is able to dephosphorylate the bacterial 5'-PPP RNA[56;57]. This reaction is very similar to the eukaryotic process of decapping (Figure 5). Notably, the eukaryotic decapping enzyme DCP2 and the bacterial pendant RppH belong to the family of Nudix hydrolases, suggesting an evolutionary conserved mechanism. Both, the eukaryotic and bacterial reactions yield a monophosphorylated RNA as product, which can be further processed by 5'-3 exonucleases: XRN1 in eukaryotes or RNase J or E in bacteria, both of which can only use monophosphorylated substrates for degradation[58].

Despite these striking similarities in bacterial and eukaryotic mRNA degradation, notable differences remain. The 3'- and 5'-terminal degradation processes, including deadenylation, decapping and exonuclease cleavage, dominate in eukaryotic cells whereas endonucleolytic cleavage still plays the major role in bacteria. The limited activity of endonucleases in eukaryotic cells is much more restrained and shows high specificity in comparison to endonucleases in bacteria. Moreover, the poly(A) tails play distinct roles in pro- and eukaryotes. Contrary to eukaryotic poly(A) tails, which mainly serve as stabilizing features of the RNA molecules regulating their half-lives, the bacterial polyadenylation has solely destabilizing function and initiates 3'-degradation.

1.2.2 Degradation of RNA Polymerase I transcripts

The maturation of ribosomes requires more than 170 proteins and 70 snoRNAS. A mature ribosome is then assembled from 82 ribosomal proteins and the four rRNAs[59]. Three out of the four rRNAs are produced from one single transcript by endo- and exonucleolytic cleavage reactions. Therefore, the removal of the ETS and ITS from the longer rRNA precursor produces a huge amount of nuclear junk RNA due to the high production rate of ribosomes. Degradation of these RNAs therefore requires most of the RNA degradation machinery. The resulting ETS and ITS rRNA fragments as well as defective pre-ribosomes are modified by the nuclear TRAMP complex, thereby stimulating exosome mediated RNA degradation (Figure 6).

Involvement of the TRAMP complex was discovered in yeast mutants by David Tollervey where nuclear export of rRNAs was blocked. In these strains, pre-rRNAs were rapidly degraded and polyadenylated species of the rRNAs were detected. Moreover, deletion of a member of the TRAMP complex suppressed polyadenylation and prohibited

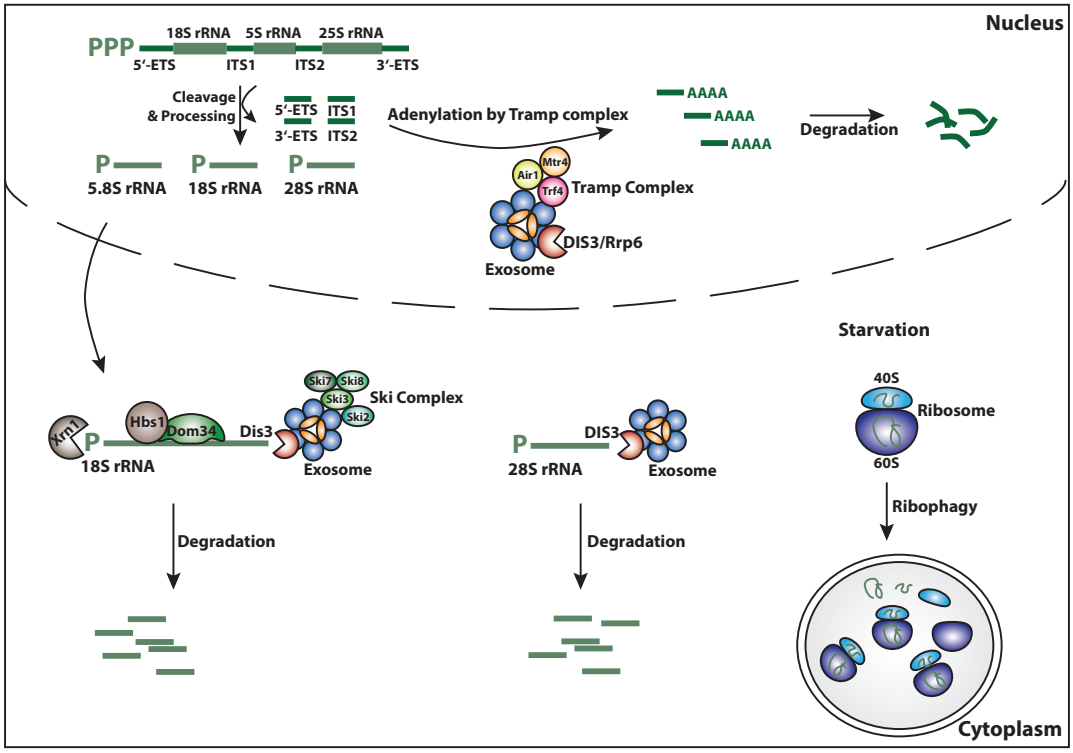

Figure 6: Degradation of RNA Polymerase I transcripts. Nuclear surveillance pathways including the TRAMP complex remove cleavage and processing products of the rRNA maturation pathway. In the cytosol, defective 18S and 28S rRNA transcripts are recognized and finally degraded by the exosome complex. Ribophagy removes whole ribosomes under starvation conditions.

degradation[60]. After being exported to the cytoplasm and assembled into ribosomal subunits, the rRNAs are very stable and degradation is essentially undetectable.

Interestingly, there seems to be a cytoplasmic rRNA quality control pathway that controls if rRNAs are still functional. In an elegant study in yeast, LaRivière et al. mutated sites important for ribosome function namely in the 25S peptidyl transferase center and the 18S decoding sequence. This resulted in a decrease in levels of those rRNAs whereas levels of rRNAs containing mutations in non-conserved positions stayed constant[61]. The cellular discrimination of functional and non-functional rRNAs led to the discovery of the non-functional rRNA decay (NRD) pathway. Turnover of the 18S rRNA employs Hbs1 and Dom34, the same protein complexes used in the mRNA No-Go decay pathway (Figure 6)[62]. Degradation of 25S rRNA remains more enigmatic since the RNA itself seems to be degraded by the exosome complex whereas the Ski complex is indispensable. Thus, how the 25S rRNA is recruited to the exosome is still unclear.

In addition, monitoring green fluorescent protein-fused ribosomal proteins revealed that under starvation conditions ribosomes were targeted and degraded in the vacuole in an autophagy-dependent manner. Because of the analogy to the autophagy pathway, this process has been named “ribophagy” (Figure 6). In a genetic screen the ubiquitin protease Ubp3 and its activator Bre5 were found to be required for the packaging of ribosomes in the autophagosome or their fusion to the vacuole[63].

1.2.3 Degradation of RNA Polymerase III transcripts

Knowledge of surveillance of RNA Pol-III transcripts (5S rRNA, U6 snRNA and tRNAs) is more limited. However, comparable to RNA Pol-I transcripts, RNA Pol-III transcripts are also under surveillance by the TRAMP complex in the nucleus. First evidence came from a study identifying that the hypomethylated $tRNA_i^{Met}$ is polyadenylated and degraded by the exosome[64].

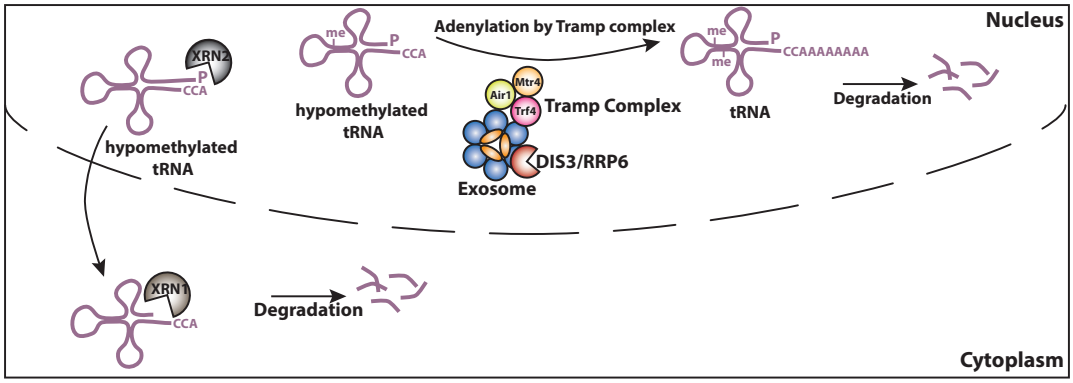

Figure 7: Degradation of RNA Polymerase III transcripts. tRNAs with processing defects are recognized by the nuclear TRAMP complex leading to degradation by the nuclear exosome complex.

Besides this nuclear pre-tRNA surveillance, mature hypomodified tRNAs like $tRNA^{Val(AAC)}$ lacking two specific methylations are rapidly degraded by a process called rapid tRNA decay (RTD) pathway which is independent of the TRAMP complex[65] but employs a 5'-degradation pathway by the proteins XRN2 and XRN1 (Figure 7)[66].

CHAPTER

2

NUCLEIC ACID IMMUNITY

Contents

2.1 Introduction to Nucleic Acid Immunity

The innate immune system is considered to be simple and non-specific and in recent years major discoveries led to tremendous advances in the field of innate immunity. All forms of life installed complex mechanisms in order to detect pathogens, in particular foreign genetic material. Recent advances include the identification of pathways that are restricting the spread of pathogen-derived nucleic acids including the identification of pattern recognition receptors, nucleic acid restriction factors and the turnover of nucleic acids. These processes are integral parts of a nucleic acid-targeting defense system, which can be termed nucleic acid immunity (Figure 8)[67].

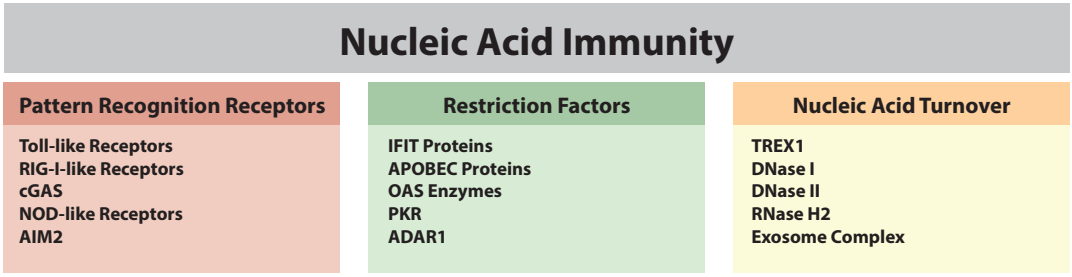

Figure 8: Nucleic Acid Immunity is shaped by pattern recognition receptors, restriction factors and nucleic acid turnover

Pattern recognition receptors (PRRs) are germline-encoded sensors that detect molecules bearing features that mark them as non-self as for instance foreign nucleic acids. They can be divided in nucleotide-binding-oligomerization domain (NOD) -like receptors (NLRs), which sense viral PAMPs and cellular stress, retinoic acid inducible gene I (RIG-I)-like receptors (RLRs) sensing RNA, Toll-like receptors (TLRs), (absent in melanoma 2) AIM2-like receptors (ALRs) that sense DNA, and cyclic GMP-AMP synthase (cGAS). Whereas PRRs elicit a broad range of effector functions by activating signaling cascades, nucleic acid restriction factors have a direct inhibitory effector function. Restriction factors include interferon induced proteins with tetratricopeptide repeats (IFIT) proteins, protein kinase R (PKR), apolipoprotein B mRNA editing enzyme (APOBEC), double-stranded RNA-specific adenosine deaminase (ADAR) or 2'-5'-oligoadenylate synthetase (OAS) enzymes. The third part includes proteins of nucleic acid turnover pathways, which regulate the abundance of nucleic acids. This group includes nucleases like DNase II, three prime repair exonuclease 1 (TREX1), the exosome complex, SAM domain and HD domain-containing protein 1 (SAMHD1), and RNase H2.

The importance of all three parts becomes apparent in rare monogenetic inflammatory

disorders like type I interferonopathies where monogenic defects in PRRs, restriction factors or nucleases result in autoimmune and autoinflammatory diseases. Therefore, nucleic acid immunity has fundamental implications for human health and disease.

2.2 Immune sensing receptors

The paradigm of pattern recognition introduced by Charles Janeway in the late 1980ies revolutionized our understanding of the immune system. In the introductory words for the Cold Spring Harbor Symposium on quantitative biology, Janeway hypothesized in a conceptual paper that infections are detected by germline-encoded pattern recognition receptors (PRRs) of the innate immune system. These receptors should be able to sense molecules of microbial origin so called pathogen-associated molecular patterns (PAMPs)[68]. At first, Charles Janeway's ingenious insights did not catch a lot of attention, however remarkably major parts of his conceptual work turned out to be correct.

By now we know that mammalian cells are equipped with a defined set of receptors that are able to detect very different pathogenic nucleic acids derived from different classes of viruses. Following the sensing of nucleic acids, an immune response is initiated by the induction of cytokines, chemokines and the expression of antiviral genes.

As a first milestone, Isaacs and Lindenmann could demonstrate that foreign nucleic acids are able to induce the antiviral cytokine type I interferon[69;70]. But only three decades later, after Jules Hoffmann found that the Drosophila protein Toll plays a role in antifungal defense[71], the mammalian Toll homolog was discovered as the first bona-fide mammalian PRR. Indeed this protein showed an immune function and led to the expression of antiviral cytokines[72]. Several additional members of the family of Toll-like receptors (TLRs) were identified. The identity of the first TLR ligand was discovered one year later by Paul Godowsky and colleagues, who showed that crude extracts of the bacterial constituent lipopolysaccharide (LPS) led to a direct response of TLR2[73]. The first pattern recognition receptor shown to detect foreign nucleic-acids was the cell-type specific TLR9 (Figure 9), which senses unmethylated CpG motifs in DNA[74]. Besides TLR9, other Toll-like receptors were identified to sense nucleic acids. Amongst those are TLR3 a sensor of double-stranded RNA[75] and TLR7 and TLR8 sensing RNA degradation products like nucleosides or short polynucleotides[76]. Those endosomal TLRs induce the expression of pro-inflammatory cytokines and type I interferons via the signaling adapter molecules TIR-domain-containing adapter-inducing interferon-β (TRIF)/TANK-binding kinase 1 (TBK1) (in case of TLR3) or myeloid

differentiation primary response 88 (MYD88) (in case of TLR7, TLR8, and TLR9) thereby activating the transcription factors interferon regulatory factor 3/7 (IRF3/7) or nuclear factor 'kappa-light-chain-enhancer' of activated B-cells (NFκB) (Figure 9).

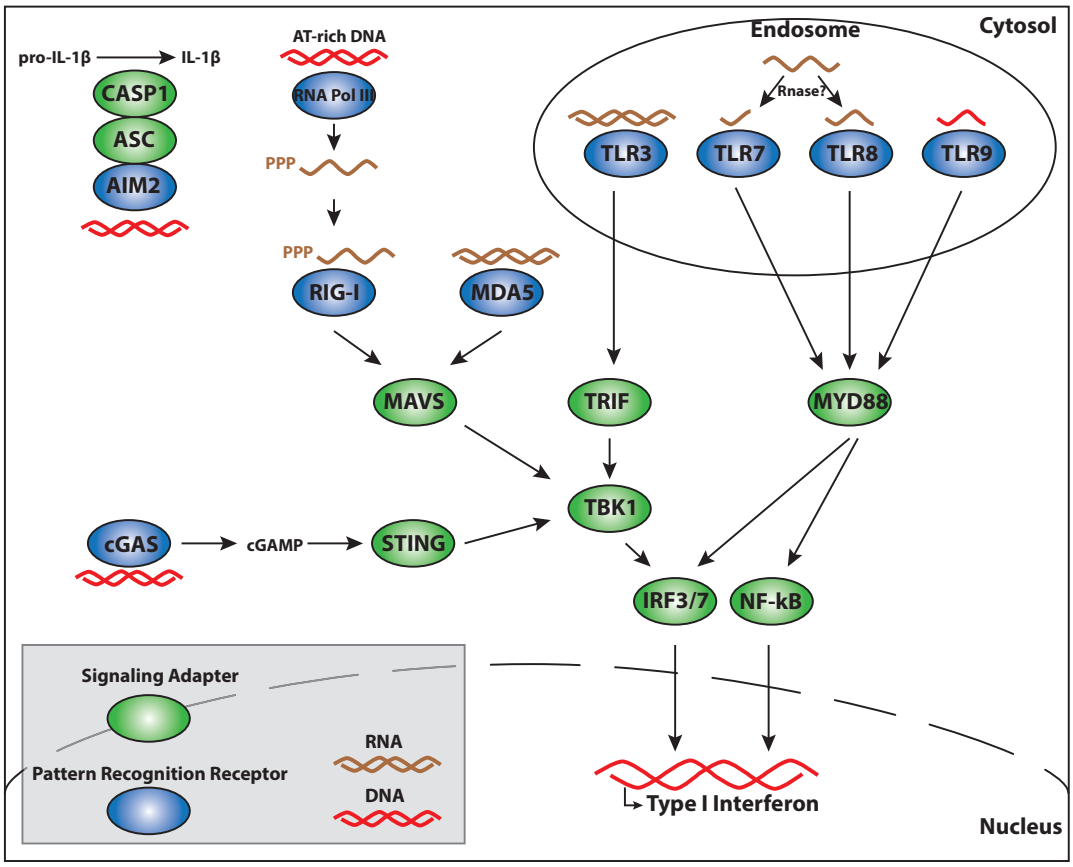

Figure 9: Pattern recognition receptors important for nucleic acid immunity. Diverse ligands are sensed by a very distinct repertoire of receptors in the endosome or cytoplasm of cells. Sensing of foreign nucleic acids results in the activation of signaling cascades and the induction of type I interferons.

In 2004, the pattern recognition receptors RIG-I and melanoma differentiation antigen 5 (MDA5) were identified[77]. RIG-I was identified to sense blunt-ended RNA with 5'-triphosphate ends[78;79]. In addition, RIG-I ligands can originate from AT-rich templates used by RNA polymerase III yielding 5'-triphosphorylated double-stranded RNA[80]. MDA5 recognizes long double-stranded RNA generally not present in healthy cells. Both, RIG-I and MDA5 engage with the signaling adapter protein mitochondrial antiviral-signaling protein (MAVS) leading to the expression of type I interferons, pro-inflammatory cytokines and ultimately in the expression of interferon stimulated genes

(ISGs) (Figure 9).
Moreover, Jürg Tschopp discovered that the inflammasome, a multiprotein complex, is able to induce the caspase 1-dependent secretion of pro-inflammatory cytokines like interleukin-1 (IL-1)[81]. One activator of the inflammasome is the sensor AIM2 that detects cytosolic DNA thereby activating the inflammasome and leading to a release of bioactive IL-1β (Figure 9)[82].
Since the inflammasome did not result in the induction of type I interferons, but yet this response was observed when DNA was delivered into cells, it was clear that an additional sensing pathway needs to be involved in the detection of cytoplasmic DNA. In 2012, James Chen discovered the DNA binding enzyme cGAS[83]. Upon ligand engagement, cGAS synthesizes the cyclic second messenger cyclic guanosine monophosphate–adenosine monophosphate (cGAMP) that in turn activates stimulator of interferon genes (STING) to induce expression of type I interferons (Figure 9)[84].
The repertoire of these diverse receptors that are positioned in different subcellular compartments allow the cell to swiftly and appropriately respond to virus infections. While the receptors are distinct in affinity to the diverse ligands, they overlap in their ability to engage signaling pathways that culminate in the expression of pro-inflammatory cytokines and type I interferons.

2.3 Discrimination of self and non-self RNA

The identification of pattern recognition receptors was an essential requirement to understand how the cell discriminates pathogenic nucleic acids from cellular nucleic acids. In a special issue of the *Journal of Interferon & Cytokine Research*, we review the principles underlying the discrimination of self and non-self nucleic acids. First, we provide an overview of the discriminative chemical properties of cellular and viral nucleic acids. Then, the current literature on RNA sensing is summarized with a spotlight on the discrimination of these differential RNA features and modifications leading to a terminal restriction of specifically viral nucleic acids.

JOURNAL OF INTERFERON & CYTOKINE RESEARCH
Volume 37, Number 5, 2017

DOI: 10.1089/jir.2016.0092

REVIEWS

Discrimination of Self and Non-Self Ribonucleic Acids

Anna Gebhardt,* Beatrice T. Laudenbach,* and Andreas Pichlmair

Most virus infections are controlled through the innate and adaptive immune system. A surprisingly limited number of so-called pattern recognition receptors (PRRs) have the ability to sense a large variety of virus infections. The reason for the broad activity of PRRs lies in the ability to recognize viral nucleic acids. These nucleic acids lack signatures that are present in cytoplasmic cellular nucleic acids and thereby marking them as pathogen-derived. Accumulating evidence suggests that these signatures, which are predominantly sensed by a class of PRRs called retinoic acid-inducible gene I (RIG-I)-like receptors and other proteins, are not unique to viruses but rather resemble immature forms of cellular ribonucleic acids generated by cellular polymerases. RIG-I-like receptors, and other cellular antiviral proteins, may therefore have mainly evolved to sense non-processed nucleic acids typically generated by primitive organisms and pathogens. This capability has not only implications on induction of antiviral immunity but also on the function of cellular proteins to handle self-derived RNA with stimulatory potential.

Keywords: ribonucleic acid sensing, antiviral mechanisms, interferon, MDA5, RIG-I, PRR

Introduction

The host immune system is constantly encountering pathogen invasion. Viruses, the most abundant pathogens on earth, can infect eukaryotes and prokaryotes and require the supportive environment of the cell to proliferate and spread. For this reason, organisms evolved barriers including the innate and adaptive immune system to suppress growth of pathogens. Protection against viral infections is to a large extent mastered by the innate immune system, which is able to sense incoming virus particles, viral proteins, viral replication products, and changes in the general integrity of the cell (Isaacs and Lindenmann 1957; Rassa and Ross 2003; Sancho and Reis e Sousa 2013). As a result, the organism mounts an appropriate antiviral response that impairs virus growth and allows virus clearance.

Activation of the antiviral innate immune system is characterized by secretion of antiviral cytokines, particularly type I interferons (IFN-α/β). These cytokines were identified by Isaacs and Lindenmann (1957) who demonstrated that cells secrete antiviral factors upon exposure to heat inactivated viruses. The main stimulatory agent was identified to be nucleic acids that are delivered through the viral infection process (Goubau and others 2013). Viral replication greatly enhances the abundance of stimulatory nucleic acids and thereby regulates the magnitude of the response (Rehwinkel and others 2010; Weber and others 2013). Both, viral RNA and DNA (vRNA/DNA) can stimulate pattern recognition receptors (PRRs) and recently molecular principles underlying the basis for detecting viruses and immune-stimulatory nucleic acids were discovered (Schlee 2013; Ahmad and Hur 2015). Besides activation of the innate immune system, viral nucleic acids modulate the activity of general cellular machineries such as protein translation, RNA degradation, or cell death (Fig. 1). At the same time viral nucleic acids are directly targeted by cellular proteins with antiviral functions. Thus, it becomes more and more evident that the innate immune system is not only a blunt alarm system that reacts to a single stimulus. It rather consists of a highly sophisticated network of proteins that target pathogen-derived nucleic acids. Importantly, the innate immune system has dramatic impact on the cellular and organismal level and its activation has to be modulated in a very tight manner. In this regards, the discrimination between ''pathogen derived'' and ''host'' nucleic acids is of central importance.

In this review we will focus on the features of RNAs that are in place to discriminate between self and non-self nucleic acids. Viral nucleic acids can be sensed by their localization in nucleic acid free organelles (such as endosomes), and by their chemical modifications and secondary structures. Considering current knowledge, it appears that large parts of the cellular sensing mechanisms are targeting ''missing-self'' modifications rather than nucleic acids specific to a certain pathogen. This concept is reminiscent of the adaptive immune system that is also predominantly

Innate Immunity Laboratory, Max-Planck Institute of Biochemistry, Munich, Germany.
*Both these authors contributed equally to this work.

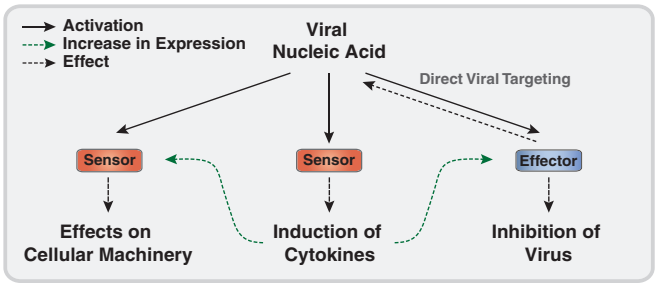

FIG. 1. Viral nucleic acids trigger a variety of events that are governed by a variety of specific cellular sensor proteins. Despite that these sensor proteins can identify the same type of viral nucleic acid, the antiviral and cellular effects are diverse. A key function of viral nucleic acids is the induction of cytokines, which regulate expression of many antiviral proteins, including sensor or effector proteins with affinity for the same viral nucleic acids. Engagement of these proteins with viral nucleic acid leads to changes in biological activity of cellular functions or in direct viral inhibition.

targeting missing-self structures and has proven to work well to protect against a wide range of invading pathogens.

Generation and Properties of Cellular RNA

To explain how intruding vRNAs are sensed by the innate immune system it is important to consider basic processes that are in place to generate cellular nucleic acids in higher eukaryotes. Generation of cellular RNAs is limited to the nucleus and mitochondria. The cytoplasm, however, is the compartment in which most RNAs are active and it is the site that is best surveyed by PRRs. Three cellular RNA polymerases (Pol-I, Pol-II, and Pol-III) are responsible for the generation of different types of RNAs. In a first step these polymerases generate precursor transcripts that carry a 5′ triphosphate (5′ PPP) group on their RNA (Fig. 2). However, before translocation to the cytoplasm, the 5′ end of these transcripts gets variably modified. In case of Pol-II transcripts, such as messenger RNA (mRNA) and most small nuclear RNAs (snRNAs), a guanosine nucleotide is coupled to the 5′ PPP group of the nascent RNA and forms the 5′ cap structure (McCracken and others 1997; Furuichi and Shatkin 2000). Moreover, the 5′ cap structure is further modified by a methylation mark at the N7-position of the guanosine (N7 methylation), the 2′O-position of the first (to generate Cap1 mRNA) and possibly also on the second ribose (Cap2 mRNA) (Byszewska and others 2014). All these modifications are co-transcriptionally added to the newly generated transcript (Topisirovic and others 2011) and are important for further processing and transport to the cytoplasm (Kohler and Hurt 2007; Muller-McNicoll and Neugebauer 2013). Lower eukaryotes, such as yeast, which appear not to use an IFN-based antiviral defense system, lack 2′O methylation on capped RNA (Byszewska and others 2014).

Ribosomal RNAs (rRNAs) are transcribed by Pol-I as a 45S-pre-rRNA with a 5′ PPP-RNA structure. After cleavage of the precursor into 28S, 18S, and 8S, rRNA, a 5′ monophosphate (5′ P) is obtained on the individual RNAs (Fig. 2) (Drygin and others 2010). Similarly, Pol-III generates a subset of additional RNAs comprising transfer RNA (tRNA), some small nucleolar RNA (snoRNAs), 5S rRNA, 7SK RNA, and U6 snRNA (Hopper 2013; Kirchner and Ignatova 2015). Like Pol-I transcribed rRNAs, tRNAs bear a 5′ P after cleavage of a 5′ oligonucleotide. U6 snRNA and 7SK RNA are not cleaved but bear a 5′ gamma-monomethyltriphosphate (5′ P_mPP-RNA) after processing (Singh and Reddy 1989).

In addition to the 5′ end modifications, host RNAs are highly modified on internal nucleotides (Sarin and Leidel 2014; Rosenthal 2015). However, the function of only a few modifications has been elucidated to date. Deamination of adenosines to inosines (A-to-I) by the RNA editing enzyme adenosine deaminase acting on RNA 1 (ADAR1), for instance, was recently shown to destabilize stem loop structures of Alu elements located in the 3′ untranslated region (UTR) of some mRNAs (George and others 2014). Repetitive Alu elements form double-stranded (ds) RNA structures that can stimulate IFN responses (Athanasiadis and others 2004; Levanon and others 2004). Deamination of such Alu elements in the 3′ UTR of mRNA leads to destabilization of dsRNA and reduced activation of the innate immune system (Hartner and others 2009). It still has to be determined how specificity to certain adenines is mediated and to what extent such deamination events also affect coding regions of proteins by accumulating mutations, potentially leading to protein misfolding. However, genetic evidence clearly shows that lack of ADAR1 is embryonically lethal in mice presumably due to elevated levels of dsRNA (Rice and others 2012). Deleting critical innate immune signaling molecules [eg, mitochondrial antiviral-signaling (MAVS) protein (also called IPS-1, VISA, or Cardif)] in these mice reduces this phenotype clearly suggesting that inability to deaminate RNAs on internal residues results in an IFN-dependent pathology (Liddicoat and others 2015; Pestal and others 2015; George and others 2016).

Another type of RNA that is prominently modified on internal residues are tRNAs. Internal modifications, such as ribose 2′O methylation on guanosine at position 18 and 34, have been shown to be important to dampen potential immune-stimulatory activity of tRNAs (Gehrig and others 2012; Jockel and others 2012; Kaiser and others 2014). It is quite likely that other not yet defined chemical modifications exist to prevent activation of the innate immune system.

Besides chemical modifications of RNA it is important to note that most RNAs are bound by RNA-binding proteins under steady-state conditions. Proteins associating to RNA can either contribute to activation or inhibition of the innate immune system. Viral proteins such as the E3L protein of Vaccinia virus, the nonstructural protein 1 (NS1) protein of Influenza A virus (IAV) or B2 of Flock house virus are binding dsRNA and can reduce the potential of stimulatory RNA likely by restricting accessibility to PRRs (Lingel and others 2005; Ayllon and Garcia-Sastre 2015). Similarly, the

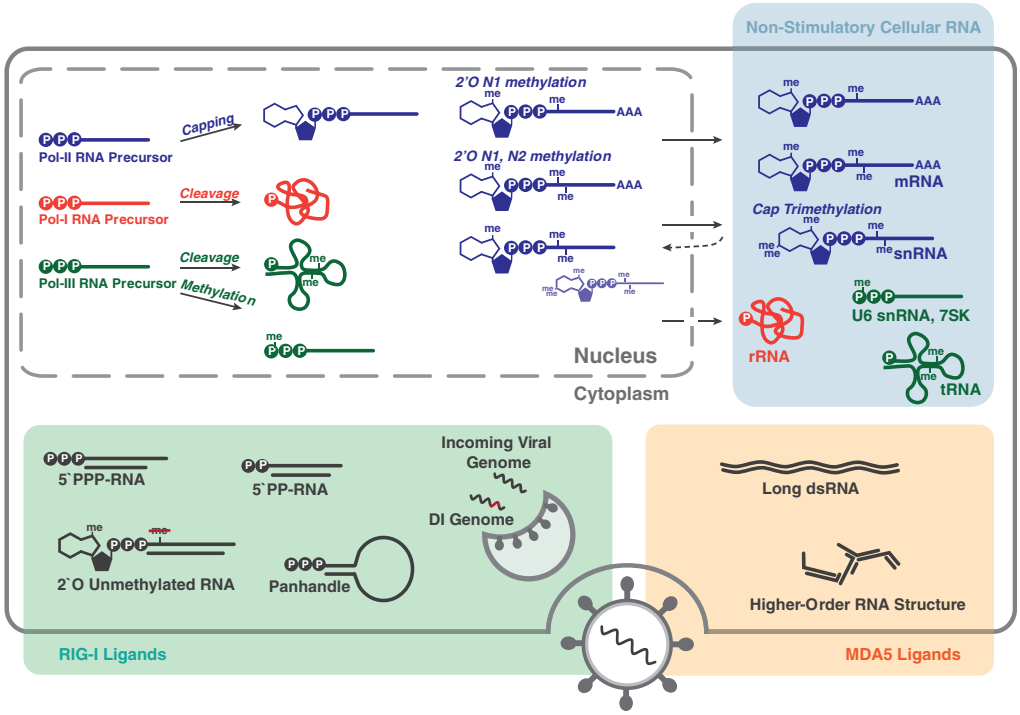

FIG. 2. Stimulatory and nonstimulatory RNAs in cells. This schematic provides an overview of the main proportion of cellular RNAs and cytoplasmic RIG-I and MDA5 stimulatory RNAs. Host RNAs are synthesized by RNA polymerase I–III (Pol-I, Pol-II, and Pol-III) in the nucleus. The RNAs are generated as a precursor RNA bearing a 5′ triphosphate group, which is extensively modified in the nucleus before getting transported to the cytoplasm where they perform their biological function. snRNAs are further modified in the cytoplasm and reimported to the nucleus. Nonstimulatory cytoplasmic cellular RNA (*blue box*) are not activating cytoplasmic PRRs. Specific viruses can introduce different types of stimulatory RNA during the infection process. These RNAs often resemble premature forms of cellular RNA and can be classified into RIG-I (*green box*) and MDA5 ligands (*orange box*). AAA, poly(A) tail; DI genomes, defective interfering genomes; dsRNA, double-stranded ribonucleic acid; MDA5, melanoma differentiation-associated protein 5; me, methyl group; mRNA, messenger RNA; P, phosphate group; PRR, pattern recognition receptor; RIG-I, retinoic acid-inducible gene I; rRNA, ribosomal RNA; snRNA, small nuclear RNA; tRNA, transfer RNA.

cellular RNA binding protein laboratory of genetics and physiology 2 (LGP2) reduces the stimulatory potential of certain RNAs (Venkataraman and others 2007), presumably by steric interference with activation of cellular PRRs (Yoneyama and others 2005; Saito and others 2007). However, LGP2 has also been shown to promote induction of IFN by a subset of viruses (Venkataraman and others 2007). Cellular RNA helicases can prepare viral ligands to be better sensed by effector proteins of the innate immune system (Ahmad and Hur 2015; Yao and others 2015). This is likely happening through displacement of other RNA binding proteins from the stimulatory RNA or due to changes in the secondary structure of the RNA. In recent years, a surprisingly high number of cellular helicases including DEAD-box protein (DDX) DDX1 (Zhang and others 2011a), DDX3 (Oshiumi and others 2010; Thulasi Raman and others 2016), DEAH-box helicase DHX9 (Zhang and others 2011b), DDX17 (Moy and others 2014), DDX60 (Miyashita and others 2011), and others, have been shown to be involved in induction of type I IFN. These proteins mostly do not directly bind to signaling molecules of the canonical IFN pathway but appear to have important accessory functions to properly activate the innate immune system. However, the contribution of RNA binding proteins to modulate innate immune responses can be diverse and needs to be characterized on an individual level.

Features of vRNA

Viruses often use relatively simple replication machineries resulting in RNAs that are only partially processed and therefore resemble a premature state of cellular RNAs. A number of PRRs evolved to sense such unprocessed RNA. The simplest evidence for this is the ability of cells to sense 5′ PPP-RNA, which constitutes the most basic product of RNA polymerases, through the cellular PRR retinoic acid-inducible gene I (RIG-I) (Hornung and others 2006; Pichlmair and others 2006). Delivery of 5′ PPP-RNA into the

cytoplasm activates type I IFN expression in an RIG-I-dependent manner. Many negative strand RNA viruses such as orthomyxo-, paramyxo-, and most bunyaviruses generate 5′ PPP-RNA constituting either the genomic RNA, replication by-products [eg, complementary RNA (cRNA)], or short subgenomic RNAs (Pichlmair and others 2009; Goubau and others 2013; Habjan and Pichlmair 2015). Interestingly, most viruses that generate 5′ PPP-RNA express auxiliary factors (eg, NS1 of IAV, V protein of Measles virus, etc.) that actively impair activation of the innate immune system (Versteeg and Garcia-Sastre 2010). Viruses that do not express such dedicated viral proteins, commonly process the 5′ RNA terminus to escape immune surveillance. Bornaviruses and a subset of Bunyaviruses including Crimean–Congo hemorrhagic fever virus, for instance, employ a 5′ trimming event as part of their replication strategy (Schneider and others 2007; Habjan and others 2008). Thereby the terminal nucleotides are cleaved by a viral nuclease leaving a 5′ P on the genomic RNA. Picorna- and caliciviruses shield their genomic 5′ PPP-end with the covalently linked VPg protein (Flanegan and others 1977; Lee and others 1977; Habjan and others 2008), which impairs binding of cellular PRRs to the 5′-end of vRNAs.

Viruses, such as flavi-, corona-, pox-, and reoviruses encode their own capping enzymes to generate 5′ capped mRNA (Decroly and others 2012). In addition to capping, these viruses independently evolved proteins that methylate the first ribose at the 2′O-position to generate RNA that resembles cellular mRNA modifications, indicating a strong selective pressure to favor this modification. Interestingly, viruses that lack the ability to methylate the 2′O position on the first ribose are sensed by the innate immune system (Daffis and others 2010; Habjan and others 2013; Schuberth-Wagner and others 2015). Orthomyxo- and bunyaviruses employ an alternative approach to gain a fully processed cap structure called ''cap-snatching.'' The first 10–13 nucleotides of a cellular mRNA are fused to the 5′ end of a vRNA, which thereby acquire cellular marks that allow evasion from host sensing mechanisms (Dias and others 2009; Decroly and others 2012; Reich and others 2014; Koppstein and others 2015).

In addition to 5′-end modifications vRNA has structural properties that allow discrimination from cellular RNAs. In particular, RNA double-strandedness of certain length is a feature that is often sensed by PRRs. Such long dsRNAs are generated by genome replication of dsRNA viruses or as replication by-products of many single-stranded (ss) RNA viruses. Even DNA viruses such as pox- and herpes viruses generate dsRNA through convergent transcription (Weber and others 2006; Feng and others 2012).

In the last years, genomic viral secondary structure elements generating portions of double-strandedness on ssRNA genomes like panhandle structures or stem loops have been shown to be recognized by antiviral mechanisms (Schlee and others 2009; Resa-Infante and others 2011; Moy and others 2014; Xu and others 2015). Although the underlying data are very compelling, it is still challenging to explain how the cell distinguishes viral from cellular dsRNA, particularly given the well-documented existence of natural dsRNA (Portal and others 2015) and high frequency of stem loops commonly found in RNAs of human origin. Different explanations for the increased immunogenicity of viral nucleic acids are possible: A certain threshold of dsRNA may have to be reached to activate the innate immune system. The abundance of vRNAs present in infected cells by far exceeds the abundance of cellular dsRNA. A threshold model is also supported by experiments using the poxvirus Modified Vaccinia Virus Ankara (MVA): Although poxviruses naturally generate dsRNA, a genetically engineered MVA strain that expresses increased levels of dsRNA shows superior immunogenicity (Wolferstatter and others 2014). Another explanation could be the subcellular localization of dsRNA since the majority of cellular dsRNA should remain in the nucleus or membrane covered cytoplasmic virus factories (Mackenzie 2005; Paul and Bartenschlager 2015), which cannot be surveyed by PRRs. Additionally, specific sequences associated to viral dsRNAs may contribute to signaling strength. Interestingly, the presence of double-strand portions within RNA is not always beneficial for virus sensing. Alphaviruses exhibit a secondary structural motif within the 5′ UTR, which prevents binding and activation of innate immune restriction proteins (Hyde and others 2014). Mechanistically, this high affinity dsRNA portion may not be accessible to cellular proteins and therefore most likely evolved as virus countermeasure against immune surveillance by the immune system (Hyde and others 2014).

Sensors of Viral or Nonprocessed RNA

A number of germline-encoded receptors have the ability to sense the presence of viral nucleic acids and initiate a variety of downstream events aiming at clearance of the invading pathogen. These receptors can be grouped in respect to their subcellular localization (endosomal or cytoplasmic), their ligand specificity (DNA, dsRNA, and ssRNA) and their effect after vRNA engagement (regulators of transcription, translation, or direct effect on vRNA). Here, we focus on cytoplasmic sensors of viral-derived RNAs and refer to other excellent reviews dealing with sensing in endosomes or of other viral ligands (O'Neill and others 2013; Cai and others 2014; Hornung and others 2014; Pelka and others 2016; Roers and others 2016).

RIG-I-Like Receptor-Mediated Recognition

The discovery of the PRR RIG-I by Takashi Fujita's laboratory opened a new era in the understanding of RNA virus sensing (Yoneyama and others 2004) and led to the identification of a class of receptors named RIG-I-like receptors (RLRs) (Onoguchi and others 2011). The highly conserved family of RLRs is comprised of three structurally related proteins named RIG-I, melanoma differentiation-associated protein-5 (MDA5), and LGP2 (Yoneyama and others 2005; Onoguchi and others 2011). All members belong to the Asp-Glu-Ala-Asp (DEAD) box family and consist of a RNA helicase domain with ATPase activity and a C-terminal domain (CTD), which is important to mediate specificity to virus-derived nucleic acid sensing (Takahasi and others 2008). RIG-I and MDA5 accommodate two N-terminal caspase activation and recruitment domains (CARDs), which initiate downstream signaling through CARD-dimerization with the MAVS protein.

Genetic deletion of RIG-I and MDA5 showed that RIG-I and MDA5 exhibit specificity for certain viruses indicating that distinct nucleic acids are sensed by these receptors. RIG-I is able to detect viruses of the rhabdoviridae family

such as Vesicular stomatitis virus and viruses of the paramyxoviridae family including Newcastle disease virus, Sendai virus (SeV), and Measles virus. MDA5 detects viruses of the Picornaviridae family such as Encephalomyocarditis virus and Polio virus (Gitlin and others 2006; Kato and others 2006). Some flaviviruses (eg, Dengue virus, West Nile virus, and Semliki forest virus) activate both, RIG-I and MDA5 (Fredericksen and others 2008; Akhrymuk and others 2016).

In contrast to RIG-I and MDA5, the role of LGP2 is less well understood particularly since this protein is missing a CARD. Depending on the experimental system, it was shown that LGP2 could serve as a negative regulator of RLR signaling (Saito and others 2007; Venkataraman and others 2007) or activate induction of IFN (Venkataraman and others 2007). However, more recent studies strengthen the finding that LGP2 operates as a positive regulator of MDA5 (Satoh and others 2010; Bruns and others 2014; Uchikawa and others 2016).

An important property of all RLRs is their ability to interact with dsRNA. However, although it became evident that binding to dsRNA is important to activate RLRs, RNA double-strandedness is not always sufficient to induce signaling. Additional requirements on stimulatory RNA, particularly chemical modifications, may serve as safeguard to reduce accidental activation of type I IFN signaling, particularly if the double-stranded stretch on RNA is only short.

Activation and Downstream Signaling of RLRs

Activation of RIG-I requires ligand binding, a cascade of regulatory post-translational modifications and binding of proteins resulting in the exposure of the CARDs. In uninfected cells, RIG-I CARDs and the CTD are constitutively phosphorylated at Ser8 and Thr170 by Protein Kinase C alpha/beta and Casein Kinase II (CKII) (Sun and others 2011; Maharaj and others 2012). In the phosphorylated state RIG-I adopts a ''closed'' conformation sequestering the CARDs from signaling due to interactions with the C-terminal repressor domain. The ATPase activity of the helicase domain allows RIG-I to constantly scan RNAs for the presence of viral motifs and was shown to be a key element to prevent recognition of self-RNA (Lassig and others 2015). ATP hydrolysis facilitates the release of RIG-I from self-RNA, while presence of viral motifs detected through the CTD leads to stalling and activation of RIG-I. Subsequently, the constitutive Ser/Thr phosphorylation sites in the CARDs are removed by serine/threonine-protein phosphatase α and γ (PP1α and PP1γ) resulting in Riplet-mediated ubiquitination of the CTD. This is followed by dimerization and a conformational rearrangement of RIG-I leading to the exposure of CARDs (Oshiumi and others 2013; Peisley and others 2013), binding of ubiquitin/ISG15-conjugating enzyme (TRIM25) to CARD1, and subsequent K63-linked ubiquitination in CARD2 (Gack and others 2007). After activation, the CARDs of RIG-I form a helical tetramer in a lock washer conformation. Multiple lock washer tetramers form a helical trajectory that allows MAVS filament assembly along this structure (Wu and others 2014). This results in clustering of multiple MAVS molecules and activation of downstream signaling.

In contrast to RIG-I, MDA5 oligomerizes as filaments in a head-to-tail fashion along dsRNA to reach high-affinity interactions with long dsRNA ligands (Peisley and others 2011; Berke and others 2012). After oligomerization, the CARDs of MDA5 point outward of the filament and oligomerize in structures that can bind to MAVS and activate downstream signaling (Wu and others 2013). Interestingly, MDA5 activation is significantly increased by LGP2, which does not contain a CARD itself. Structural analysis showed that LGP2 binds the end of dsRNAs (very much like RIG-I) and thereby initiates MDA5 filament oligomerization on dsRNA (Uchikawa and others 2016). LGP2 and MDA5 have been shown to bind similar stimulatory RNAs, which is in line with cooperative activity of LGP2 in MDA5 activation. LGP2-precipitated RNAs induce IFN-α/β in a MDA5-dependent manner providing a functional link between LGP2 and MDA5 (Deddouche and others 2014).

A key uniting feature of all RLRs is signaling through MAVS. Under physiological conditions, MAVS is kept inactive by an autoinhibitory mechanism. Upon binding to oligomerized CARDs of RLRs, the regions responsible for downstream signaling including TANK-binding kinase 1 (TBK1)/Interferon regulatory factor 3 (IRF3) and IκB kinase (IKK)/nuclear factor kappa-light-chain-enhancer of activated B cells (NF-κB) activation sites are exposed and induce signaling events that result in expression of type I IFNs and proinflammatory cytokines (Shi and others 2015).

Sensing of 5′ Modifications by RIG-I

RIG-I activation requires two features that co-occur on one RNA molecule. The first essential feature for RIG-I activation is a chemical modification on the 5′ terminus of the RNA. The best described 5′ modifications that activate RIG-I are 5′ tri- and 5′ di-phosphates (Hornung and others 2006; Pichlmair and others 2006; Goubau and others 2014). However, more recently it has been shown that RIG-I is also activated by capped RNA that lack a methylation mark at the 2′O ribose position of the first nucleotide (Schuberth-Wagner and others 2015; Devarkar and others 2016). A conserved residue (Histidine 830) within the CTD of RIG-I sterically prevents binding of cellular 2′O-methylated RNA, and therefore serves as molecular gatekeeper to pertain activation by cellular mRNAs. Silencing of the endogenous cap-specific mRNA (nucleoside-2′-O-)-methyltransferase 1 (MTr1) converts nonstimulatory into stimulatory mRNA and triggers a spontaneous RIG-I-dependent type I IFN response (Schuberth-Wagner and others 2015). The second essential feature for RIG-I activation is a short stretch of blunt-ended dsRNA. While chemically synthesized 5′ PPP-ssRNA is not sufficient to prominently activate RIG-I, 5′ PPP-dsRNA molecules with the same sequence show very strong activity (Schlee and others 2009; Schmidt and others 2009). Reports regarding the minimum length of this dsRNA stretch range from at least 10 base pairs (bp) (Schmidt and others 2009; Kohlway and others 2013) to 19 bp (Schlee and others 2009). Experiments transfecting differently modified RNA clearly show that 3′ overhangs at the 5′-end are sufficient to impair activation of RIG-I (Schlee and others 2009) and may even serve as dominant negative decoy substrate (Marq and others 2011).

Besides dsRNA with 5′ PPP modifications, short 5′ hydroxyl (5′ OH) and 3′ monophosphoryl (3′ P) dsRNA cleavage products of 2-5A-dependent ribonuclease (RNAseL) have been proposed to serve as RIG-I ligands (Malathi

and others 2007, 2010). Although this notion is supported by many functional data, the exact mechanism of RIG-I activation is not clear to date, particularly since this appears to happen in a cell type-dependent manner (Banerjee and others 2014).

Sensing of RNA in Virus-Infected Cells

Despite formidable progress that allowed defining optimal activation of RIG-I by synthetic ligands much less is known about the nature of the physiological ligand generated during virus infections. Many elegant studies aimed to define the physiological RIG-I stimulus. Compelling evidence suggests that viral genomic RNA delivered by virus infection activates RIG-I. Here, we discuss data that support this notion and also consider questions that still remain to be answered. Evidence for vRNA being the physiological ligand for RIG-I was already provided by Isaacs and Lindenmann (1957), who found that cells treated with high amounts of heat-inactivated viruses activate type I IFN. More recently this was supported by data that show that delivery of replication incompetent viral particles activate RIG-I (Weber and others 2013). Furthermore, shortly after infection, vRNA of infectious viral particles closely associates with mitochondria, which are serving as signaling hubs for the induction of type I IFN (Liedmann and others 2014). However, the magnitude of an antiviral response triggered by incoming vRNA appears to be relatively low and viral replication appears to be required to elicit high amounts of IFN (Crotta and others 2013; Killip and others 2014). One reason could be insufficient abundance of stimulatory RNAs, which questions whether incoming viral nucleic acids are significantly contributing to type I IFN production under physiological conditions.

Genomic vRNA isolated from virus particles and transfected into cells potently stimulates RIG-I (Hornung and others 2006; Pichlmair and others 2006). This is in agreement with the notion that vRNA isolated from IAV particles spontaneously forms the so-called panhandle structure. This structure is formed due to base-pairing of terminal ssRNA sequences of many negative ssRNA viruses and serves as promoter for the viral polymerase complex (Hsu and others 1987; Fodor and others 1994; Tiley and others 1994). The panhandle structure resembles *in vitro* synthesized blunt ended 5′ PPP RNA. In line with RIG-I activation by synthetic ligands, the panhandle thus constitutes a perfect stimulus for RIG-I activation and explains the very strong stimulatory activity of isolated vRNA. Interestingly, mismatches in the panhandle structure of some IAV strains disrupt RNA complementarity and results in reduced activation of RIG-I (Anchisi and others 2016). Such an adaptation may therefore represent a viral strategy to evade RIG-I activation (Anchisi and others 2016). Supporting evidence that viral genomic RNA stimulates RIG-I comes from experiments using minireplicon systems. vRNA of defined length generated by the IAV polymerase complex activates RIG-I (Rehwinkel and others 2010). Interestingly, PPP-RNA is not only generated by viruses but also by bacteria. mRNA in bacteria is not capped and intracellular bacteria such as Listeria and Legionella have been shown to activate RIG-I (Monroe and others 2009; Abdullah and others 2012).

Although the notion that genomic vRNA is the major ligand activating RIG-I in virally infected cells is elegant, a number of additional aspects linked to the replication process of viruses complicate this simple model: During viral replication, vRNA is constantly bound by viral proteins, which theoretically prevent activation of RIG-I. In case of many negative strand RNA viruses the viral polymerase complex is located at the 5′-end of vRNAs potentially shielding the terminal PPP group from being sensed by RIG-I. Indeed, for IAV it has been shown that association of the polymerase complex to the vRNA polymerase protects from innate sensing by RIG-I (Weber and others 2013; Liedmann and others 2014). Variants of the viral polymerase complex featuring weaker affinity for viral genomic RNAs have reduced ability to impair activation of the innate immune system (Weber and others 2013) suggesting that under certain conditions vRNAs can be a physiological activator of RIG-I and that the presence of proteins actively impair RIG-I activation. Besides a potentially inaccessible 5′-end, the relative contribution of the panhandle structure to provide a dsRNA platform for RIG-I binding is not so clear: Although isolated genomic RNA of IAV clearly generates blunt double-stranded ends, the structure of the panhandle bound to the viral polymerase complex, as it exists in virally infected cells, adopts a partially single-stranded conformation (Tiley and others 1994). This notion is supported by low affinity binding of the negative strand RNA virus polymerases to the double-stranded panhandle structure compared to binding to ssRNA (Pflug and others 2014; Gerlach and others 2015). Thus, the panhandle structure most likely either exists as a ''corkscrew'' (Neumann and Hobom 1995; Flick and others 1996) or as a ''fork'' (Fodor and others 1994, 1995; Kim and others 1997) structure in virally infected cells. Both structures presumably only allow suboptimal activation of RIG-I and it is therefore still not finally solved what type of RNA prominently activates RIG-I in virus infected cells.

A possibility is the activation of RIG-I by viral replication intermediates or by defective interfering (DI) particles, which are commonly generated during infections with viruses including SeV, IAV, and Measles virus (Strahle and others 2006; Baum and others 2010; Runge and others 2014). Although DI particles are not replicating, they prominently activate the innate immune system (Killip and others 2012).

Besides generating stimulatory nucleic acids from viral templates, RNA-dependent RNA polymerases (RdRP) also have the ability to use cellular RNA as templates resulting in the generation of host-derived stimulatory RNAs. Expression of Simian foamy virus RdRP, for instance, leads to induction of IFN-β in the absence of viral templates (Nikonov and others 2013). In addition, expression of RdRP in transgenic animals induces a constant IFN response that leads to increase virus resistance in these animals (Painter and others 2015). The ability of viral polymerases to generate cellular RNA copies with IFN inducing capability indicates that RdRP transcripts feature stimulatory modifications rather than the actual sequence being sensed by innate immune sensors. Interestingly, the ability to generate stimulatory RNA from cellular templates has so far only been shown for RdRPs that are active in the cytoplasm. A possible explanation for this could be the absence of RNA-modifying enzymes in the cytoplasm, which does not allow RNA processing to minimize the stimulatory potential of RdRP generated RNA.

Sensing of dsRNAs by MDA5

In contrast to ligands for RIG-I, requirements for MDA5 activation are less well understood. MDA5 recognizes long dsRNA (greater than ~0.5 kB) that is normally not present in the cytoplasm of uninfected cells (Kato and others 2008). A commonly used synthetic activator for MDA5 is poly-I:C, which is generated through annealing of enzymatically synthesized poly-I and poly-C homopolymers of undefined length. Although poly-I:C is regarded as dsRNA analog, the structure of poly-I:C is most likely not a uniform double-strand but may rather adopt a web-like structure (Pichlmair and others 2009). Interestingly, similarly synthesized poly-A:U or poly-G:C have very little stimulatory potential suggesting features associated with poly-I:C that are not yet well understood.

The best characterized viruses leading to MDA5 activation are picornaviruses [eg, Encephalomyocardidits virus (EMCV), Theiler's murine encephalitis virus, Poliovirus, or Norovirus] featuring a positive ssRNA genome (Gitlin and others 2006; Kato and others 2006; Loo and others 2008; McCartney and others 2008). While RIG-I activating viruses have the ability to induce PRR signaling through viral genome recognition, activation of MDA5 by EMCV strictly requires transcription of the viral genome and generation of a dsRNA intermediate resulting in a 7.5 kb replicative form of EMCV (Feng and others 2012; Triantafilou and others 2012). Furthermore, it is likely that additional replication intermediates representing higher order structural RNAs are generated and sensed by MDA5 (Pichlmair and others 2009).

Unbiased Approaches to Identify PRR-Associated vRNA

More recently, next generation sequencing was used to characterize the RNA ligand bound to MDA5 or RIG-I. An issue with such approaches is that the helicase domain of RLRs can generally associate with dsRNA and that this affinity does not directly lead to activation of RIG-I or MDA5. However, next generation sequencing helped to identify commonalities and differences in RNA binding between MDA5 and RIG-I. In Measles virus-infected cells, for instance, both, MDA5 and RIG-I preferentially bind to viral AU-rich sequences, particularly in the Measles virus L-region (Runge and others 2014). However, MDA5 shows superior enrichment for the Measles virus (+) sense RNA, while RIG-I preferentially bind to RNA of negative polarity. In a similar approach, Sanchez David and colleagues used next-generation sequencing analysis to investigate RNA precipitated with RIG-I, MDA5, and LGP2 in Measles and Chikungunya virus-infected cells. The authors showed that each of the RLRs binds distinct regions of the viral genome. RIG-I bound specifically the 3′ UTR of the Chikungunya virus genome and DI genomes of Measles virus, whereas, MDA5 and LGP2 sensed nucleoprotein coding regions of Measles virus (Sanchez David and others 2016). The shared RNAs targeted by MDA5 and LGP2 strongly support a functional relationship between these two PRRs, which is also confirmed by alternative functional and structural approaches (Goubau and others 2014) (Uchikawa and others 2016).

In sum, it is evident that distinct RNA species trigger RIG-I and MDA5 activation. These RNA species may even be expressed at different time points during the infection process. Indeed, it was shown that vRNA products generated at different time points after West Nile virus infection sequentially stimulate RIG-I and MDA5, whereby, RIG-I triggers an early and MDA5 a later response (Errett and others 2013).

Direct Effectors of Viral Nucleic Acids

Besides RLRs, which have the ability to sense nucleic acids and regulate transcriptional programs, a set of additional proteins exist that are binding to specific viral nucleic acids (Habjan and Pichlmair 2015). These proteins either have the ability to regulate cellular processes that are unrelated to transcription or directly bind and thereby impair the activity of viral nucleic acids. Often these additional vRNA binding proteins are inducible by type I IFNs underlining their involvement in antiviral processes. This concept of multiple cellular proteins associating to a given type of stimulatory RNA is best illustrated by dsRNA binding proteins (Fig. 3). dsRNA activates the PRR MDA5, which is activating a transcriptional program culminating in expression of type I IFN. Besides MDA5, dsRNA-dependent Protein Kinase R (PKR) and 2′-5′-oligoadenylate synthetase (OAS1) directly bind dsRNAs. PKR regulates a plethora of antiviral processes after binding to dsRNA including inhibition of translation through continuous phosphorylation of eukaryotic initiation factor 2 alpha (eIF2-a), induction of apoptosis and autophagy (Kang and Tang 2012), and activation of NF-kB through interacting with the IKK complex (Zamanian-Daryoush and others 2000). PKR has additionally been linked to regulation of type I IFN expression (Diebold and others 2003; Gilfoy and Mason 2007). While this accessory function of PKR is dispensable for RIG-I-dependent responses, IFN induction by viruses that activate MDA5 appears to be critically relying on additional activity by PKR (Schulz and others 2010; Wolferstatter and others 2014; Pham and others 2016). After binding to dsRNA OAS1 generates 2′-5′-linked oligoadenylates (2′-5′-OA) that serve as second messengers and have the ability to activate the latent RNAseL. Only after activation, RNAseL cleaves RNA eventually resulting in cell death (Chakrabarti and others 2011). Furthermore, vRNAs bind to a number of DEAD- and DEAH-box helicases, which often appear to have auxiliary functions to regulate IFN-α/β expression and also bear direct virus inhibitory function. DDX3, for instance, has been shown to be important for activation of the IFN signaling pathway (Oshiumi and others 2010; Gu and others 2013). DDX3 was also shown to restrict HBV replication and, thereby, acting as an antiviral effector protein (Ko and others 2014).

As for dsRNA, 5′ PPP-RNA, which activates RIG-I, can associate with additional cellular proteins. Unbiased AP-MS experiments and follow-up studies using mutational approaches identified the interferon-induced protein with tetratricopeptide repeats (IFIT) 1 and -5, which directly associate with 5′ PPP-RNA (Pichlmair and others 2011; Fensterl and Sen 2015). Depending on the exact experimental setup, IFIT1-deficient mice appear to be more susceptible to 5′ PPP-RNA generating viruses such as Vesicular stomatitis virus (Pichlmair and others 2011). However, while RIG-I activation requires dsRNA, IFIT proteins specifically bind only ssRNAs in a helical positively charged binding cleft (Abbas and others 2013). Besides associating with 5′ PPP-RNA, IFIT1 has the ability to directly associate with capped RNA that lacks a methylation mark at the first ribose (2′O N1 unmethylated RNA) (Habjan and others 2013; Kumar and

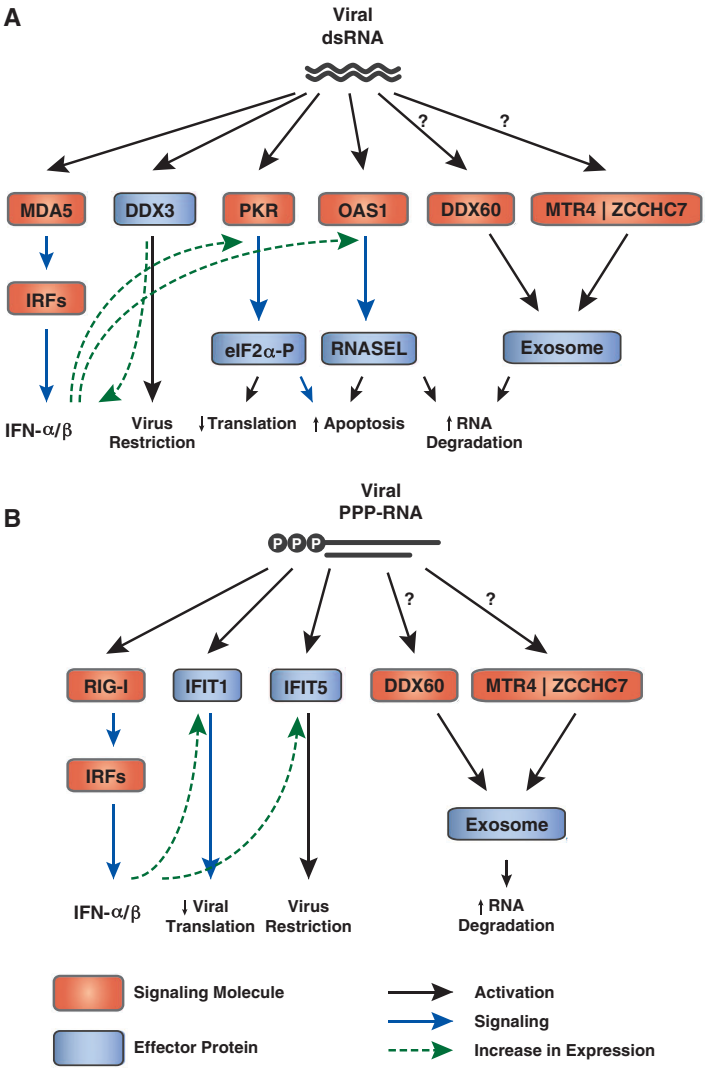

FIG. 3. Cellular sensor and effector proteins binding viral nucleic acids. **(A)** Sensing of dsRNAs by MDA5 results in expression of IFN-α/β. These in turn upregulate additional sensors including dsRNA-dependent PKR and OAS1. Binding of PKR to dsRNA phosphorylates the translation initiation factor eIF2-leading to an inhibition of translation and an induction of apoptosis. OAS1 synthesizes 2′-5′-oligoadenylates activating RNASEL. Activation of RNASEL results in RNA degradation and apoptosis. DDX60, ATP-dependent RNA helicase SKIV2L2 (MTR4) and ZCCHC7 promote vRNA degradation via the exosome complex upon virus infection. DDX3 activates IFN signaling and restricts virus replication. **(B)** Engagement of 5′-triphosphorylated-RNA by RIG-I leads to the expression of type I IFNs, thereby inducing the expression of the effector proteins IFIT1 and IFIT5. Sensing of PPP-RNA by IFIT1 and IFIT5 leads to decreased viral translation and restriction of virus, respectively. vRNA can be recognized and degraded by the exosome cofactors DDX60, MTR4, and ZCCHC7. DDX3, DEAD box protein 3; DDX60, DEAD box protein 60; eIF2, eukaryotic initiation factor 2; IFIT, interferon-induced protein with tetratricopeptide repeats; IFN, interferon; IRFs, interferon regulatory factors; MTR4, ATP-dependent RNA helicase SKIV2L2; OAS1, 2′-5′-oligoadenylate synthetase 1; PKR, double-stranded RNA-dependent protein Protein Kinase R; PPP-RNA, triphosphorylated RNA; vRNA, viral RNA; ZCCHC7, Zinc finger CCHC domain-containing protein 7.

others 2014). Viruses that fail to methylate the 2′O position of the first ribose are attenuated in wild-type mice but are highly pathogenic in IFIT-deficient animals (Daffis and others 2010; Leung and Amarasinghe 2016). It is yet not entirely clear how IFIT1 and -5 impair virus growth but the high amounts of IFIT proteins expressed after IFN treatment suggests stoichiometric interference with viral nucleic acids rather than enzymatic activity of IFIT proteins (Habjan and others 2013; Kumar and others 2014). Pathogenic alphaviruses that generate high affinity dsRNA secondary structures on the 5′-end of their genome evade surveillance by IFIT proteins (Hyde and others 2014). IFIT1 appears to show surprisingly little efficiency against negative strand RNA viruses *in vivo* despite that these viruses are known to generate 5′ PPP-RNA (Pinto and others 2015). Potential explanations may be evasion strategies of these viruses, including replication in the nucleus that is not surveyed by IFIT proteins (eg, for IAV) or generation of secondary structures of the RNA 5′-end as has been shown for alphaviruses (Pinto and others 2015). IFITs have also been proposed to be (Berchtold and others 2008; Zhang and others 2013; Imaizumi and others 2016) or not to be (Pichlmair and others 2011; Habjan and others 2013) involved in regulation of antiviral gene expression. Thus, the activity of IFIT proteins is not yet fully understood and highlights the importance of functional studies that will give further mechanistic insights.

While the induction of type I IFNs and cellular restriction mechanisms are partially well understood, relatively little is known about the cellular machinery that specifically degrades vRNA. A prominent machinery responsible

for RNA degradation is the exosome, a large molecular complex with 3′-5′ exonuclease activity. However, this complex requires accessory factors that mark RNA for degradation. Recently, the Ski2-like protein DDX60 was identified as cellular protein that promotes degradation of vRNA of diverse viruses through the exosome (Oshiumi and others 2015). Furthermore, DDX60 has been proposed to support RIG-I and MDA5-dependent induction of type I IFNs (Oshiumi and others 2015). However, the role of DDX60 appears complex since other laboratories found little effect of DDX60 in antiviral immunity (Goubau and others 2015; Grunvogel and others 2015). More recently, superkiller viralicidic activity 2-like 2 (SKIV2L2; also called Mtr4) and Zinc finger CCHC domain-containing protein 7 (ZCCHC7), components of the Trf4/Air2/Mtr4p polyadenylation (TRAMP) complex, were identified to colocalize with vRNA and the exosome in the cytoplasm of infected cells (Molleston and others 2016) and the helicase SKI2W (SKIV2L) RNA exosome has been shown to prevent autoimmunity by regulating the abundance of RIG-I ligands (Eckard and others 2014) suggesting that vRNAs are specifically targeted for decay.

Concluding Remarks

The knowledge on virus sensing and restriction has dramatically increased in recent years. It became evident that the innate immune system particularly senses RNA that is insufficiently processed and therefore lacks motifs commonly found on cellular RNA. The ability of cytoplasmic PRRs to sense such missing-self motifs allows them to be broadly active and to detect nucleic acids generated by viruses and other pathogens such as bacteria. In case of failure to properly process cellular RNA this ability also bears the risk of inducing unwanted immune responses that can lead to autoimmune disorders. Besides nucleic acid sensors, a set of cellular proteins exists that directly restricts viruses or leads to changes in cellular machineries ranging from translational control to cell death. More mechanistic insights into the regulation and function of nucleic acid binding proteins are important to understand antiviral immunity and to exploit this knowledge for therapeutic interventions.

Acknowledgments

We want to thank the members of the innate immunity laboratory, particularly Philipp Hubel and Pietro Scaturro, for input and critical discussions. The work in the authors' laboratory is funded by a Max-Planck free floater program, ERC starting grant (StG 311339, iVIP), the German Research Foundation (PI1084/2-1, PI1084/3-1, and TRR179), and the Federal Ministry for Education and Research (ERA-Net grant ERASe).

Author Disclosure Statement

No competing financial interests exist.

References

Abbas YM, Pichlmair A, Gorna MW, Superti-Furga G, Nagar B. 2013. Structural basis for viral 5′-PPP-RNA recognition by human IFIT proteins. Nature 494(7435):60–64.

Abdullah Z, Schlee M, Roth S, Mraheil MA, Barchet W, Bottcher J, Hain T, Geiger S, Hayakawa Y, Fritz JH, Civril F, Hopfner KP, Kurts C, Ruland J, Hartmann G, Chakraborty T, Knolle PA. 2012. RIG-I detects infection with live Listeria by sensing secreted bacterial nucleic acids. EMBO J 31(21): 4153–4164.

Ahmad S, Hur S. 2015. Helicases in antiviral immunity: dual properties as sensors and effectors. Trends Biochem Sci 40(10):576–585.

Akhrymuk I, Frolov I, Frolova EI. 2016. Both RIG-I and MDA5 detect alphavirus replication in concentration-dependent mode. Virology 487:230–241.

Anchisi S, Guerra J, Mottet-Osman G, Garcin D. 2016. Mismatches in the influenza A virus RNA panhandle prevent retinoic acid-inducible gene I (RIG-I) sensing by impairing RNA/RIG-I complex formation. J Virol 90(1):586–590.

Athanasiadis A, Rich A, Maas S. 2004. Widespread A-to-I RNA editing of Alu-containing mRNAs in the human transcriptome. PLoS Biol 2(12):e391.

Ayllon J, Garcia-Sastre A. 2015. The NS1 protein: a multitasking virulence factor. Curr Top Microbiol Immunol 386: 73–107.

Banerjee S, Chakrabarti A, Jha BK, Weiss SR, Silverman RH. 2014. Cell-type-specific effects of RNase L on viral induction of beta interferon. MBio 5(2):e00856-14.

Baum A, Sachidanandam R, Garcia-Sastre A. 2010. Preference of RIG-I for short viral RNA molecules in infected cells revealed by next-generation sequencing. Proc Natl Acad Sci U S A 107(37):16303–16308.

Berchtold S, Manncke B, Klenk J, Geisel J, Autenrieth IB, Bohn E. 2008. Forced IFIT-2 expression represses LPS induced TNF-alpha expression at posttranscriptional levels. BMC Immunol 9:75.

Berke IC, Yu X, Modis Y, Egelman EH. 2012. MDA5 assembles into a polar helical filament on dsRNA. Proc Natl Acad Sci U S A 109(45):18437–18441.

Bruns AM, Leser GP, Lamb RA, Horvath CM. 2014. The innate immune sensor LGP2 activates antiviral signaling by regulating MDA5-RNA interaction and filament assembly. Mol Cell 55(5):771–781.

Byszewska M, Smietanski M, Purta E, Bujnicki JM. 2014. RNA methyltransferases involved in 5′ cap biosynthesis. RNA Biol 11(12):1597–1607.

Cai X, Chiu YH, Chen ZJ. 2014. The cGAS-cGAMP-STING pathway of cytosolic DNA sensing and signaling. Mol Cell 54(2):289–296.

Chakrabarti A, Jha BK, Silverman RH. 2011. New insights into the role of RNase L in innate immunity. J Interferon Cytokine Res 31(1):49–57.

Crotta S, Davidson S, Mahlakoiv T, Desmet CJ, Buckwalter MR, Albert ML, Staeheli P, Wack A. 2013. Type I and type III interferons drive redundant amplification loops to induce a transcriptional signature in influenza-infected airway epithelia. PLoS Pathog 9(11):e1003773.

Daffis S, Szretter KJ, Schriewer J, Li J, Youn S, Errett J, Lin TY, Schneller S, Zust R, Dong H, Thiel V, Sen GC, Fensterl V, Klimstra WB, Pierson TC, Buller RM, Gale M, Jr, Shi PY, Diamond MS. 2010. 2′-O methylation of the viral mRNA cap evades host restriction by IFIT family members. Nature 468(7322):452–456.

Decroly E, Ferron F, Lescar J, Canard B. 2012. Conventional and unconventional mechanisms for capping viral mRNA. Nat Rev Microbiol 10(1):51–65.

Deddouche S, Goubau D, Rehwinkel J, Chakravarty P, Begum S, Maillard PV, Borg A, Matthews N, Feng Q, van Kuppe-

veld FJ, Reis e Sousa C. 2014. Identification of an LGP2-associated MDA5 agonist in picornavirus-infected cells. Elife 3:e01535.

Devarkar SC, Wang C, Miller MT, Ramanathan A, Jiang F, Khan AG, Patel SS, Marcotrigiano J. 2016. Structural basis for m7G recognition and 2′-O-methyl discrimination in capped RNAs by the innate immune receptor RIG-I. Proc Natl Acad Sci U S A 113(3):596–601.

Dias A, Bouvier D, Crepin T, McCarthy AA, Hart DJ, Baudin F, Cusack S, Ruigrok RW. 2009. The cap-snatching endonuclease of influenza virus polymerase resides in the PA subunit. Nature 458(7240):914–918.

Diebold SS, Montoya M, Unger H, Alexopoulou L, Roy P, Haswell LE, Al-Shamkhani A, Flavell R, Borrow P, Reis e Sousa C. 2003. Viral infection switches non-plasmacytoid dendritic cells into high interferon producers. Nature 424(6946):324–328.

Drygin D, Rice WG, Grummt I. 2010. The RNA polymerase I transcription machinery: an emerging target for the treatment of cancer. Annu Rev Pharmacol Toxicol 50:131–156.

Eckard SC, Rice GI, Fabre A, Badens C, Gray EE, Hartley JL, Crow YJ, Stetson DB. 2014. The SKIV2L RNA exosome limits activation of the RIG-I-like receptors. Nat Immunol 15(9):839–845.

Errett JS, Suthar MS, McMillan A, Diamond MS, Gale M, Jr. 2013. The essential, nonredundant roles of RIG-I and MDA5 in detecting and controlling West Nile virus infection. J Virol 87(21):11416–11425.

Feng Q, Hato SV, Langereis MA, Zoll J, Virgen-Slane R, Peisley A, Hur S, Semler BL, van Rij RP, van Kuppeveld FJ. 2012. MDA5 detects the double-stranded RNA replicative form in picornavirus-infected cells. Cell Rep 2(5):1187–1196.

Fensterl V, Sen GC. 2015. Interferon-induced Ifit proteins: their role in viral pathogenesis. J Virol 89(5):2462–2468.

Flanegan JB, Petterson RF, Ambros V, Hewlett NJ, Baltimore D. 1977. Covalent linkage of a protein to a defined nucleotide sequence at the 5′-terminus of virion and replicative intermediate RNAs of poliovirus. Proc Natl Acad Sci U S A 74(3):961–965.

Flick R, Neumann G, Hoffmann E, Neumeier E, Hobom G. 1996. Promoter elements in the influenza vRNA terminal structure. RNA 2(10):1046–1057.

Fodor E, Pritlove DC, Brownlee GG. 1994. The influenza virus panhandle is involved in the initiation of transcription. J Virol 68(6):4092–4096.

Fodor E, Pritlove DC, Brownlee GG. 1995. Characterization of the RNA-fork model of virion RNA in the initiation of transcription in influenza A virus. J Virol 69(7):4012–4019.

Fredericksen BL, Keller BC, Fornek J, Katze MG, Gale M, Jr. 2008. Establishment and maintenance of the innate antiviral response to West Nile Virus involves both RIG-I and MDA5 signaling through IPS-1. J Virol 82(2):609–616.

Furuichi Y, Shatkin AJ. 2000. Viral and cellular mRNA capping: past and prospects. Adv Virus Res 55:135–184.

Gack MU, Shin YC, Joo CH, Urano T, Liang C, Sun L, Takeuchi O, Akira S, Chen Z, Inoue S, Jung JU. 2007. TRIM25 RING-finger E3 ubiquitin ligase is essential for RIG-I-mediated antiviral activity. Nature 446(7138):916–920.

Gehrig S, Eberle ME, Botschen F, Rimbach K, Eberle F, Eigenbrod T, Kaiser S, Holmes WM, Erdmann VA, Sprinzl M, Bec G, Keith G, Dalpke AH, Helm M. 2012. Identification of modifications in microbial, native tRNA that suppress immunostimulatory activity. J Exp Med 209(2):225–233.

George CX, John L, Samuel CE. 2014. An RNA editor, adenosine deaminase acting on double-stranded RNA (ADAR1). J Interferon Cytokine Res 34(6):437–446.

George CX, Ramaswami G, Li JB, Samuel CE. 2016. Editing of cellular self-RNAs by adenosine deaminase ADAR1 suppresses innate immune stress responses. J Biol Chem 291(12):6158–6168.

Gerlach P, Malet H, Cusack S, Reguera J. 2015. Structural insights into bunyavirus replication and its regulation by the vRNA promoter. Cell 161(6):1267–1279.

Gilfoy FD, Mason PW. 2007. West Nile virus-induced interferon production is mediated by the double-stranded RNA-dependent protein kinase PKR. J Virol 81(20):11148–11158.

Gitlin L, Barchet W, Gilfillan S, Cella M, Beutler B, Flavell RA, Diamond MS, Colonna M. 2006. Essential role of mda-5 in type I IFN responses to polyriboinosinic:polyribocytidylic acid and encephalomyocarditis picornavirus. Proc Natl Acad Sci U S A 103(22):8459–8464.

Goubau D, Deddouche S, Reis e Sousa C. 2013. Cytosolic sensing of viruses. Immunity 38(5):855–869.

Goubau D, Schlee M, Deddouche S, Pruijssers AJ, Zillinger T, Goldeck M, Schuberth C, Van der Veen AG, Fujimura T, Rehwinkel J, Iskarpatyoti JA, Barchet W, Ludwig J, Dermody TS, Hartmann G, Reis e Sousa C. 2014. Antiviral immunity via RIG-I-mediated recognition of RNA bearing 5′-diphosphates. Nature 514(7522):372–375.

Goubau D, van der Veen AG, Chakravarty P, Lin R, Rogers N, Rehwinkel J, Deddouche S, Rosewell I, Hiscott J, Reis ESC. 2015. Mouse superkiller-2-like helicase DDX60 is dispensable for type I IFN induction and immunity to multiple viruses. Eur J Immunol 45(12):3386–3403.

Grunvogel O, Esser-Nobis K, Reustle A, Schult P, Muller B, Metz P, Trippler M, Windisch MP, Frese M, Binder M, Fackler O, Bartenschlager R, Ruggieri A, Lohmann V. 2015. DDX60L is an interferon-stimulated gene product restricting hepatitis C virus replication in cell culture. J Virol 89(20):10548–10568.

Gu L, Fullam A, Brennan R, Schroder M. 2013. Human DEAD box helicase 3 couples IkappaB kinase epsilon to interferon regulatory factor 3 activation. Mol Cell Biol 33(10):2004–2015.

Habjan M, Andersson I, Klingstrom J, Schumann M, Martin A, Zimmermann P, Wagner V, Pichlmair A, Schneider U, Muhlberger E, Mirazimi A, Weber F. 2008. Processing of genome 5′ termini as a strategy of negative-strand RNA viruses to avoid RIG-I-dependent interferon induction. PLoS One 3(4):e2032.

Habjan M, Hubel P, Lacerda L, Benda C, Holze C, Eberl CH, Mann A, Kindler E, Gil-Cruz C, Ziebuhr J, Thiel V, Pichlmair A. 2013. Sequestration by IFIT1 impairs translation of 2′O-unmethylated capped RNA. PLoS Pathog 9(10):e1003663.

Habjan M, Pichlmair A. 2015. Cytoplasmic sensing of viral nucleic acids. Curr Opin Virol 11:31–37.

Hartner JC, Walkley CR, Lu J, Orkin SH. 2009. ADAR1 is essential for the maintenance of hematopoiesis and suppression of interferon signaling. Nat Immunol 10(1):109–115.

Hopper AK. 2013. Transfer RNA post-transcriptional processing, turnover, and subcellular dynamics in the yeast *Saccharomyces cerevisiae*. Genetics 194(1):43–67.

Hornung V, Ellegast J, Kim S, Brzozka K, Jung A, Kato H, Poeck H, Akira S, Conzelmann KK, Schlee M, Endres S, Hartmann G. 2006. 5′-Triphosphate RNA is the ligand for RIG-I. Science 314(5801):994–997.

Hornung V, Hartmann R, Ablasser A, Hopfner KP. 2014. OAS proteins and cGAS: unifying concepts in sensing and re-

sponding to cytosolic nucleic acids. Nat Rev Immunol 14(8):521–528.

Hsu MT, Parvin JD, Gupta S, Krystal M, Palese P. 1987. Genomic RNAs of influenza viruses are held in a circular conformation in virions and in infected cells by a terminal panhandle. Proc Natl Acad Sci U S A 84(22):8140–8144.

Hyde JL, Gardner CL, Kimura T, White JP, Liu G, Trobaugh DW, Huang C, Tonelli M, Paessler S, Takeda K, Klimstra WB, Amarasinghe GK, Diamond MS. 2014. A viral RNA structural element alters host recognition of nonself RNA. Science 343(6172):783–787.

Imaizumi T, Yoshida H, Hayakari R, Xing F, Wang L, Matsumiya T, Tanji K, Kawaguchi S, Murakami M, Tanaka H. 2016. Interferon-stimulated gene (ISG) 60, as well as ISG56 and ISG54, positively regulates TLR3/IFN-beta/STAT1 axis in U373MG human astrocytoma cells. Neurosci Res 105: 35–41.

Isaacs A, Lindenmann J. 1957. Virus interference. I. The interferon. Proc R Soc Lond B Biol Sci 147(927):258–267.

Jockel S, Nees G, Sommer R, Zhao Y, Cherkasov D, Hori H, Ehm G, Schnare M, Nain M, Kaufmann A, Bauer S. 2012. The 2′-O-methylation status of a single guanosine controls transfer RNA-mediated Toll-like receptor 7 activation or inhibition. J Exp Med 209(2):235–241.

Kaiser S, Rimbach K, Eigenbrod T, Dalpke AH, Helm M. 2014. A modified dinucleotide motif specifies tRNA recognition by TLR7. RNA 20(9):1351–1355.

Kang R, Tang D. 2012. PKR-dependent inflammatory signals. Sci Signal 5(247):pe47.

Kato H, Takeuchi O, Mikamo-Satoh E, Hirai R, Kawai T, Matsushita K, Hiiragi A, Dermody TS, Fujita T, Akira S. 2008. Length-dependent recognition of double-stranded ribonucleic acids by retinoic acid-inducible gene-I and melanoma differentiation-associated gene 5. J Exp Med 205(7): 1601–1610.

Kato H, Takeuchi O, Sato S, Yoneyama M, Yamamoto M, Matsui K, Uematsu S, Jung A, Kawai T, Ishii KJ, Yamaguchi O, Otsu K, Tsujimura T, Koh CS, Reis e Sousa C, Matsuura Y, Fujita T, Akira S. 2006. Differential roles of MDA5 and RIG-I helicases in the recognition of RNA viruses. Nature 441(7089):101–105.

Killip MJ, Smith M, Jackson D, Randall RE. 2014. Activation of the interferon induction cascade by influenza a viruses requires viral RNA synthesis and nuclear export. J Virol 88(8):3942–3952.

Killip MJ, Young DF, Precious BL, Goodbourn S, Randall RE. 2012. Activation of the beta interferon promoter by paramyxoviruses in the absence of virus protein synthesis. J Gen Virol 93(Pt 2):299–307.

Kim HJ, Fodor E, Brownlee GG, Seong BL. 1997. Mutational analysis of the RNA-fork model of the influenza A virus vRNA promoter in vivo. J Gen Virol 78(Pt 2):353–357.

Kirchner S, Ignatova Z. 2015. Emerging roles of tRNA in adaptive translation, signalling dynamics and disease. Nat Rev Genet 16(2):98–112.

Ko C, Lee S, Windisch MP, Ryu WS. 2014. DDX3 DEAD-box RNA helicase is a host factor that restricts hepatitis B virus replication at the transcriptional level. J Virol 88(23):13689–13698.

Kohler A, Hurt E. 2007. Exporting RNA from the nucleus to the cytoplasm. Nat Rev Mol Cell Biol 8(10):761–773.

Kohlway A, Luo D, Rawling DC, Ding SC, Pyle AM. 2013. Defining the functional determinants for RNA surveillance by RIG-I. EMBO Rep 14(9):772–779.

Koppstein D, Ashour J, Bartel DP. 2015. Sequencing the cap-snatching repertoire of H1N1 influenza provides insight into the mechanism of viral transcription initiation. Nucleic Acids Res 43(10):5052–5064.

Kumar P, Sweeney TR, Skabkin MA, Skabkina OV, Hellen CU, Pestova TV. 2014. Inhibition of translation by IFIT family members is determined by their ability to interact selectively with the 5′-terminal regions of cap0-, cap1- and 5′ppp-mRNAs. Nucleic Acids Res 42(5):3228–3245.

Lassig C, Matheisl S, Sparrer KM, de Oliveira Mann CC, Moldt M, Patel JR, Goldeck M, Hartmann G, Garcia-Sastre A, Hornung V, Conzelmann KK, Beckmann R, Hopfner KP. 2015. ATP hydrolysis by the viral RNA sensor RIG-I prevents unintentional recognition of self-RNA. Elife 4:e10859.

Lee YF, Nomoto A, Detjen BM, Wimmer E. 1977. A protein covalently linked to poliovirus genome RNA. Proc Natl Acad Sci U S A 74(1):59–63.

Leung DW, Amarasinghe GK. 2016. When your cap matters: structural insights into self vs non-self recognition of 5′ RNA by immunomodulatory host proteins. Curr Opin Struct Biol 36:133–141.

Levanon EY, Eisenberg E, Yelin R, Nemzer S, Hallegger M, Shemesh R, Fligelman ZY, Shoshan A, Pollock SR, Sztybel D, Olshansky M, Rechavi G, Jantsch MF. 2004. Systematic identification of abundant A-to-I editing sites in the human transcriptome. Nat Biotechnol 22(8):1001–1005.

Liddicoat BJ, Piskol R, Chalk AM, Ramaswami G, Higuchi M, Hartner JC, Li JB, Seeburg PH, Walkley CR. 2015. RNA editing by ADAR1 prevents MDA5 sensing of endogenous dsRNA as nonself. Science 349(6252):1115–1120.

Liedmann S, Hrincius ER, Guy C, Anhlan D, Dierkes R, Carter R, Wu G, Staeheli P, Green DR, Wolff T, McCullers JA, Ludwig S, Ehrhardt C. 2014. Viral suppressors of the RIG-I-mediated interferon response are pre-packaged in influenza virions. Nat Commun 5:5645.

Lingel A, Simon B, Izaurralde E, Sattler M. 2005. The structure of the flock house virus B2 protein, a viral suppressor of RNA interference, shows a novel mode of double-stranded RNA recognition. EMBO Rep 6(12):1149–1155.

Loo YM, Fornek J, Crochet N, Bajwa G, Perwitasari O, Martinez-Sobrido L, Akira S, Gill MA, Garcia-Sastre A, Katze MG, Gale M, Jr. 2008. Distinct RIG-I and MDA5 signaling by RNA viruses in innate immunity. J Virol 82(1):335–345.

Mackenzie J. 2005. Wrapping things up about virus RNA replication. Traffic 6(11):967–977.

Maharaj NP, Wies E, Stoll A, Gack MU. 2012. Conventional protein kinase C-alpha (PKC-alpha) and PKC-beta negatively regulate RIG-I antiviral signal transduction. J Virol 86(3):1358–1371.

Malathi K, Dong B, Gale M, Jr., Silverman RH. 2007. Small self-RNA generated by RNase L amplifies antiviral innate immunity. Nature 448(7155):816–819.

Malathi K, Saito T, Crochet N, Barton DJ, Gale M, Jr, Silverman RH. 2010. RNase L releases a small RNA from HCV RNA that refolds into a potent PAMP. RNA 16(11):2108–2119.

Marq JB, Hausmann S, Veillard N, Kolakofsky D, Garcin D. 2011. Short double-stranded RNAs with an overhanging 5′ ppp-nucleotide, as found in arenavirus genomes, act as RIG-I decoys. J Biol Chem 286(8):6108–6116.

McCartney SA, Thackray LB, Gitlin L, Gilfillan S, Virgin HW, Colonna M. 2008. MDA-5 recognition of a murine norovirus. PLoS Pathog 4(7):e1000108.

McCracken S, Fong N, Rosonina E, Yankulov K, Brothers G, Siderovski D, Hessel A, Foster S, Shuman S, Bentley DL. 1997. 5′-Capping enzymes are targeted to pre-mRNA by binding to the phosphorylated carboxy-terminal domain of RNA polymerase II. Genes Dev 11(24):3306–3318.

Miyashita M, Oshiumi H, Matsumoto M, Seya T. 2011. DDX60, a DEXD/H box helicase, is a novel antiviral factor promoting RIG-I-like receptor-mediated signaling. Mol Cell Biol 31(18):3802–3819.

Molleston JM, Sabin LR, Moy RH, Menghani SV, Rausch K, Gordesky-Gold B, Hopkins KC, Zhou R, Jensen TH, Wilusz JE, Cherry S. 2016. A conserved virus-induced cytoplasmic TRAMP-like complex recruits the exosome to target viral RNA for degradation. Genes Dev 30(14):1658–1670.

Monroe KM, McWhirter SM, Vance RE. 2009. Identification of host cytosolic sensors and bacterial factors regulating the type I interferon response to *Legionella pneumophila*. PLoS Pathog 5(11):e1000665.

Moy RH, Cole BS, Yasunaga A, Gold B, Shankarling G, Varble A, Molleston JM, tenOever BR, Lynch KW, Cherry S. 2014. Stem-loop recognition by DDX17 facilitates miRNA processing and antiviral defense. Cell 158(4):764–777.

Muller-McNicoll M, Neugebauer KM. 2013. How cells get the message: dynamic assembly and function of mRNA-protein complexes. Nat Rev Genet 14(4):275–287.

Neumann G, Hobom G. 1995. Mutational analysis of influenza virus promoter elements in vivo. J Gen Virol 76(Pt 7):1709–1717.

Nikonov A, Molder T, Sikut R, Kiiver K, Mannik A, Toots U, Lulla A, Lulla V, Utt A, Merits A, Ustav M. 2013. RIG-I and MDA-5 detection of viral RNA-dependent RNA polymerase activity restricts positive-strand RNA virus replication. PLoS Pathog 9(9):e1003610.

O'Neill LA, Golenbock D, Bowie AG. 2013. The history of Toll-like receptors – redefining innate immunity. Nat Rev Immunol 13(6):453–460.

Onoguchi K, Yoneyama M, Fujita T. 2011. Retinoic acid-inducible gene-I-like receptors. J Interferon Cytokine Res 31(1):27–31.

Oshiumi H, Miyashita M, Matsumoto M, Seya T. 2013. A distinct role of Riplet-mediated K63-Linked polyubiquitination of the RIG-I repressor domain in human antiviral innate immune responses. PLoS Pathog 9(8):e1003533.

Oshiumi H, Miyashita M, Okamoto M, Morioka Y, Okabe M, Matsumoto M, Seya T. 2015. DDX60 is involved in RIG-I-dependent and independent antiviral responses, and its function is attenuated by virus-induced EGFR activation. Cell Rep 11(8):1193–1207.

Oshiumi H, Sakai K, Matsumoto M, Seya T. 2010. DEAD/H BOX 3 (DDX3) helicase binds the RIG-I adaptor IPS-1 to up-regulate IFN-beta-inducing potential. Eur J Immunol 40(4):940–948.

Painter MM, Morrison JH, Zoecklein LJ, Rinkoski TA, Watzlawik JO, Papke LM, Warrington AE, Bieber AJ, Matchett WE, Turkowski KL, Poeschla EM, Rodriguez M. 2015. Antiviral protection via RdRP-mediated stable activation of innate immunity. PLoS Pathog 11(12):e1005311.

Paul D, Bartenschlager R. 2015. Flaviviridae replication organelles: oh, what a tangled web we weave. Annu Rev Virol 2(1):289–310.

Peisley A, Lin C, Wu B, Orme-Johnson M, Liu M, Walz T, Hur S. 2011. Cooperative assembly and dynamic disassembly of MDA5 filaments for viral dsRNA recognition. Proc Natl Acad Sci U S A 108(52):21010–21015.

Peisley A, Wu B, Yao H, Walz T, Hur S. 2013. RIG-I forms signaling-competent filaments in an ATP-dependent, ubiquitin-independent manner. Mol Cell 51(5):573–583.

Pelka K, Shibata T, Miyake K, Latz E. 2016. Nucleic acid-sensing TLRs and autoimmunity: novel insights from structural and cell biology. Immunol Rev 269(1):60–75.

Pestal K, Funk CC, Snyder JM, Price ND, Treuting PM, Stetson DB. 2015. Isoforms of RNA-editing enzyme ADAR1 independently control nucleic acid sensor MDA5-driven autoimmunity and multi-organ development. Immunity 43(5):933–944.

Pflug A, Guilligay D, Reich S, Cusack S. 2014. Structure of influenza A polymerase bound to the viral RNA promoter. Nature 516(7531):355–360.

Pham AM, Santa Maria FG, Lahiri T, Friedman E, Marie IJ, Levy DE. 2016. PKR transduces MDA5-dependent signals for type I IFN induction. PLoS Pathog 12(3):e1005489.

Pichlmair A, Lassnig C, Eberle CA, Gorna MW, Baumann CL, Burkard TR, Burckstummer T, Stefanovic A, Krieger S, Bennett KL, Rulicke T, Weber F, Colinge J, Muller M, Superti-Furga G. 2011. IFIT1 is an antiviral protein that recognizes 5′-triphosphate RNA. Nat Immunol 12(7):624–630.

Pichlmair A, Schulz O, Tan CP, Naslund TI, Liljestrom P, Weber F, Reis e Sousa C. 2006. RIG-I-mediated antiviral responses to single-stranded RNA bearing 5′-phosphates. Science 314(5801):997–1001.

Pichlmair A, Schulz O, Tan CP, Rehwinkel J, Kato H, Takeuchi O, Akira S, Way M, Schiavo G, Reis e Sousa C. 2009. Activation of MDA5 requires higher-order RNA structures generated during virus infection. J Virol 83(20):10761–10769.

Pinto AK, Williams GD, Szretter KJ, White JP, Proenca-Modena JL, Liu G, Olejnik J, Brien JD, Ebihara H, Muhlberger E, Amarasinghe G, Diamond MS, Boon AC. 2015. Human and murine IFIT1 proteins do not restrict infection of negative-sense RNA viruses of the orthomyxoviridae, bunyaviridae, and filoviridae families. J Virol 89(18):9465–9476.

Portal MM, Pavet V, Erb C, Gronemeyer H. 2015. Human cells contain natural double-stranded RNAs with potential regulatory functions. Nat Struct Mol Biol 22(1):89–97.

Rassa JC, Ross SR. 2003. Viruses and toll-like receptors. Microbes Infect 5(11):961–968.

Rehwinkel J, Tan CP, Goubau D, Schulz O, Pichlmair A, Bier K, Robb N, Vreede F, Barclay W, Fodor E, Reis e Sousa C. 2010. RIG-I detects viral genomic RNA during negative-strand RNA virus infection. Cell 140(3):397–408.

Reich S, Guilligay D, Pflug A, Malet H, Berger I, Crepin T, Hart D, Lunardi T, Nanao M, Ruigrok RW, Cusack S. 2014. Structural insight into cap-snatching and RNA synthesis by influenza polymerase. Nature 516(7531):361–366.

Resa-Infante P, Jorba N, Coloma R, Ortin J. 2011. The influenza virus RNA synthesis machine: advances in its structure and function. RNA Biol 8(2):207–215.

Rice GI, Kasher PR, Forte GM, Mannion NM, Greenwood SM, Szynkiewicz M, Dickerson JE, Bhaskar SS, Zampini M, Briggs TA, Jenkinson EM, Bacino CA, Battini R, Bertini E, Brogan PA, Brueton LA, Carpanelli M, De Laet C, de Lonlay P, del Toro M, Desguerre I, Fazzi E, Garcia-Cazorla A, Heiberg A, Kawaguchi M, Kumar R, Lin JP, Lourenco CM, Male AM, Marques W, Jr., Mignot C, Olivieri I, Orcesi S, Prabhakar P, Rasmussen M, Robinson RA, Rozenberg F, Schmidt JL, Steindl K, Tan TY, van der Merwe WG, Vanderver A, Vassallo G, Wakeling EL, Wassmer E, Whittaker

E, Livingston JH, Lebon P, Suzuki T, McLaughlin PJ, Keegan LP, O'Connell MA, Lovell SC, Crow YJ. 2012. Mutations in ADAR1 cause Aicardi-Goutieres syndrome associated with a type I interferon signature. Nat Genet 44(11):1243–1248.

Roers A, Hiller B, Hornung V. 2016. Recognition of endogenous nucleic acids by the innate immune system. Immunity 44(4):739–754.

Rosenthal JJ. 2015. The emerging role of RNA editing in plasticity. J Exp Biol 218(Pt 12):1812–1821.

Runge S, Sparrer KM, Lassig C, Hembach K, Baum A, Garcia-Sastre A, Soding J, Conzelmann KK, Hopfner KP. 2014. In vivo ligands of MDA5 and RIG-I in measles virus-infected cells. PLoS Pathog 10(4):e1004081.

Saito T, Hirai R, Loo YM, Owen D, Johnson CL, Sinha SC, Akira S, Fujita T, Gale M, Jr. 2007. Regulation of innate antiviral defenses through a shared repressor domain in RIG-I and LGP2. Proc Natl Acad Sci U S A 104(2):582–587.

Sanchez David RY, Combredet C, Sismeiro O, Dillies MA, Jagla B, Coppee JY, Mura M, Guerbois Galla M, Despres P, Tangy F, Komarova AV. 2016. Comparative analysis of viral RNA signatures on different RIG-I-like receptors. Elife 5:e11275.

Sancho D, Reis e Sousa C. 2013. Sensing of cell death by myeloid C-type lectin receptors. Curr Opin Immunol 25(1): 46–52.

Sarin LP, Leidel SA. 2014. Modify or die?—RNA modification defects in metazoans. RNA Biol 11(12):1555–1567.

Satoh T, Kato H, Kumagai Y, Yoneyama M, Sato S, Matsushita K, Tsujimura T, Fujita T, Akira S, Takeuchi O. 2010. LGP2 is a positive regulator of RIG-I- and MDA5-mediated antiviral responses. Proc Natl Acad Sci U S A 107(4):1512–1517.

Schlee M. 2013. Master sensors of pathogenic RNA – RIG-I like receptors. Immunobiology 218(11):1322–1335.

Schlee M, Roth A, Hornung V, Hagmann CA, Wimmenauer V, Barchet W, Coch C, Janke M, Mihailovic A, Wardle G, Juranek S, Kato H, Kawai T, Poeck H, Fitzgerald KA, Takeuchi O, Akira S, Tuschl T, Latz E, Ludwig J, Hartmann G. 2009. Recognition of 5′ triphosphate by RIG-I helicase requires short blunt double-stranded RNA as contained in panhandle of negative-strand virus. Immunity 31(1):25–34.

Schmidt A, Schwerd T, Hamm W, Hellmuth JC, Cui S, Wenzel M, Hoffmann FS, Michallet MC, Besch R, Hopfner KP, Endres S, Rothenfusser S. 2009. 5′-Triphosphate RNA requires base-paired structures to activate antiviral signaling via RIG-I. Proc Natl Acad Sci U S A 106(29):12067–12072.

Schneider U, Martin A, Schwemmle M, Staeheli P. 2007. Genome trimming by Borna disease viruses: viral replication control or escape from cellular surveillance? Cell Mol Life Sci 64(9):1038–1042.

Schuberth-Wagner C, Ludwig J, Bruder AK, Herzner AM, Zillinger T, Goldeck M, Schmidt T, Schmid-Burgk JL, Kerber R, Wolter S, Stumpel JP, Roth A, Bartok E, Drosten C, Coch C, Hornung V, Barchet W, Kummerer BM, Hartmann G, Schlee M. 2015. A conserved histidine in the RNA sensor RIG-I controls immune tolerance to N1-2′O-methylated self RNA. Immunity 43(1):41–51.

Schulz O, Pichlmair A, Rehwinkel J, Rogers NC, Scheuner D, Kato H, Takeuchi O, Akira S, Kaufman RJ, Reis e Sousa C. 2010. Protein kinase R contributes to immunity against specific viruses by regulating interferon mRNA integrity. Cell Host Microbe 7(5):354–361.

Shi Y, Yuan B, Qi N, Zhu W, Su J, Li X, Qi P, Zhang D, Hou F. 2015. An autoinhibitory mechanism modulates MAVS activity in antiviral innate immune response. Nat Commun 6:7811.

Singh R, Reddy R. 1989. Gamma-monomethyl phosphate: a cap structure in spliceosomal U6 small nuclear RNA. Proc Natl Acad Sci U S A 86(21):8280–8283.

Strahle L, Garcin D, Kolakofsky D. 2006. Sendai virus defective-interfering genomes and the activation of interferon-beta. Virology 351(1):101–111.

Sun Z, Ren H, Liu Y, Teeling JL, Gu J. 2011. Phosphorylation of RIG-I by casein kinase II inhibits its antiviral response. J Virol 85(2):1036–1047.

Takahasi K, Yoneyama M, Nishihori T, Hirai R, Kumeta H, Narita R, Gale M, Jr, Inagaki F, Fujita T. 2008. Nonself RNA-sensing mechanism of RIG-I helicase nd activation of antiviral immune responses. Mol Cell 29(4):428–440.

Thulasi Raman SN, Liu G, Pyo HM, Cui YC, Xu F, Ayalew LE, Tikoo SK, Zhou Y. 2016. DDX3 interacts with influenza A virus NS1 and NP proteins and exerts antiviral function through regulation of stress granule formation. J Virol 90(7): 3661–3675.

Tiley LS, Hagen M, Matthews JT, Krystal M. 1994. Sequence-specific binding of the influenza virus RNA polymerase to sequences located at the 5′ ends of the viral RNAs. J Virol 68(8):5108–5116.

Topisirovic I, Svitkin YV, Sonenberg N, Shatkin AJ. 2011. Cap and cap-binding proteins in the control of gene expression. Wiley Interdiscip Rev RNA 2(2):277–298.

Triantafilou K, Vakakis E, Kar S, Richer E, Evans GL, Triantafilou M. 2012. Visualisation of direct interaction of MDA5 and the dsRNA replicative intermediate form of positive strand RNA viruses. J Cell Sci 125(Pt 20):4761–4769.

Uchikawa E, Lethier M, Malet H, Brunel J, Gerlier D, Cusack S. 2016. Structural analysis of dsRNA binding to anti-viral pattern recognition receptors LGP2 and MDA5. Mol Cell 62(4):586–602.

Venkataraman T, Valdes M, Elsby R, Kakuta S, Caceres G, Saijo S, Iwakura Y, Barber GN. 2007. Loss of DExD/H box RNA helicase LGP2 manifests disparate antiviral responses. J Immunol 178(10):6444–6455.

Versteeg GA, Garcia-Sastre A. 2010. Viral tricks to grid-lock the type I interferon system. Curr Opin Microbiol 13(4):508–516.

Weber F, Wagner V, Rasmussen SB, Hartmann R, Paludan SR. 2006. Double-stranded RNA is produced by positive-strand RNA viruses and DNA viruses but not in detectable amounts by negative-strand RNA viruses. J Virol 80(10):5059–5064.

Weber M, Gawanbacht A, Habjan M, Rang A, Borner C, Schmidt AM, Veitinger S, Jacob R, Devignot S, Kochs G, Garcia-Sastre A, Weber F. 2013. Incoming RNA virus nucleocapsids containing a 5′-triphosphorylated genome activate RIG-I and antiviral signaling. Cell Host Microbe 13(3):336–346.

Wolferstatter M, Schweneker M, Spath M, Lukassen S, Klingenberg M, Brinkmann K, Wielert U, Lauterbach H, Hochrein H, Chaplin P, Suter M, Hausmann J. 2014. Recombinant modified vaccinia virus Ankara generating excess early double-stranded RNA transiently activates protein kinase R and triggers enhanced innate immune responses. J Virol 88(24):14396–14411.

Wu B, Peisley A, Richards C, Yao H, Zeng X, Lin C, Chu F, Walz T, Hur S. 2013. Structural basis for dsRNA recognition, filament formation, and antiviral signal activation by MDA5. Cell 152(1–2):276–289.

Wu B, Peisley A, Tetrault D, Li Z, Egelman EH, Magor KE, Walz T, Penczek PA, Hur S. 2014. Molecular imprinting as a signal-activation mechanism of the viral RNA sensor RIG-I. Mol Cell 55(4):511–523.

Xu J, Mercado-Lopez X, Grier JT, Kim WK, Chun LF, Irvine EB, Del Toro Duany Y, Kell A, Hur S, Gale M, Jr, Raj A, Lopez CB. 2015. Identification of a natural viral RNA motif that optimizes sensing of viral RNA by RIG-I. MBio 6(5): e01265-15.

Yao H, Dittmann M, Peisley A, Hoffmann HH, Gilmore RH, Schmidt T, Schmid-Burgk JL, Hornung V, Rice CM, Hur S. 2015. ATP-dependent effector-like functions of RIG-I-like receptors. Mol Cell 58(3):541–548.

Yoneyama M, Kikuchi M, Matsumoto K, Imaizumi T, Miyagishi M, Taira K, Foy E, Loo YM, Gale M, Jr., Akira S, Yonehara S, Kato A, Fujita T. 2005. Shared and unique functions of the DExD/H-box helicases RIG-I, MDA5, and LGP2 in antiviral innate immunity. J Immunol 175(5):2851–2858.

Yoneyama M, Kikuchi M, Natsukawa T, Shinobu N, Imaizumi T, Miyagishi M, Taira K, Akira S, Fujita T. 2004. The RNA helicase RIG-I has an essential function in double-stranded RNA-induced innate antiviral responses. Nat Immunol 5(7): 730–737.

Zamanian-Daryoush M, Mogensen TH, DiDonato JA, Williams BR. 2000. NF-kappaB activation by double-stranded-RNA-activated protein kinase (PKR) is mediated through NF-kappaB-inducing kinase and IkappaB kinase. Mol Cell Biol 20(4):1278–1290.

Zhang B, Liu X, Chen W, Chen L. 2013. IFIT5 potentiates anti-viral response through enhancing innate immune signaling pathways. Acta Biochim Biophys Sin (Shanghai) 45(10): 867–874.

Zhang Z, Kim T, Bao M, Facchinetti V, Jung SY, Ghaffari AA, Qin J, Cheng G, Liu YJ. 2011a. DDX1, DDX21, and DHX36 helicases form a complex with the adaptor molecule TRIF to sense dsRNA in dendritic cells. Immunity 34(6):866–878.

Zhang Z, Yuan B, Lu N, Facchinetti V, Liu YJ. 2011b. DHX9 pairs with IPS-1 to sense double-stranded RNA in myeloid dendritic cells. J Immunol 187(9):4501–4508.

Address correspondence to:
Dr. Andreas Pichlmair
Innate Immunity Laboratory
Max-Planck Institute of Biochemistry
Am Klopferspitz 18
82152 Martinsried/Munich
Germany

E-mail: apichl@biochem.mpg.de

Received 19 September 2016/Accepted 5 January 2017

2.4 Restriction Factors

Sensing of nucleic acids by the aforementioned PRRs results in the activation of signaling cascades, the expression of cytokines and immune responses. A subgroup of host restriction factors is as well capable of detecting foreign nucleic acids. However, this affinity results in the direct restriction of the nucleic acid function without the activation of an immune response. Restriction factors are constitutively expressed in nearly all cell types thereby granting to act very early in the defense against incoming viruses. In infected cells, their expression is often increased by cytokine signaling. Restriction factors mostly target conserved viral structures allowing them to target a broad spectrum of viral families. In order to evade restriction factors, viruses evolved an arsenal of counter mechanisms, thereby putting evolutionary pressure on those proteins causing them to evolve rapidly.

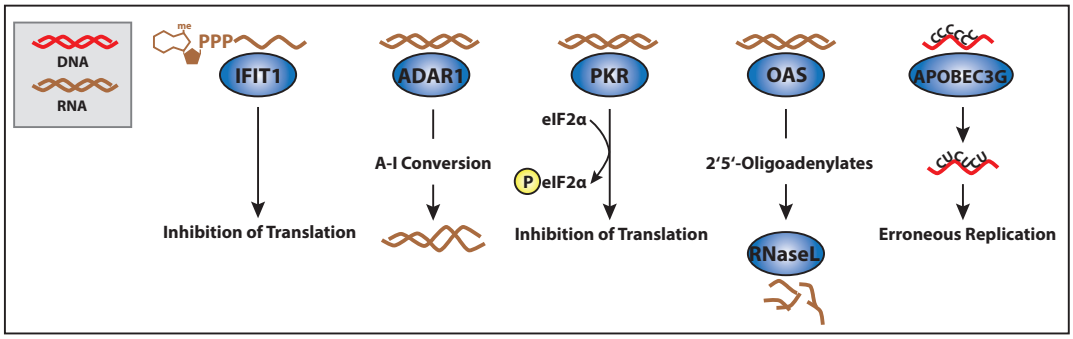

Figure 10: Overview of restriction factors important for antiviral or anti-inflammatory immunity including IFIT1 and PKR leading to an inhibition of translation, ADAR1 that destabilizes RNA, OAS inducing cleavage of nucleic acids and APOBEC proteins.

In the following section the function of RNA-binding viral restriction factors is described. These factors do either activate other proteins with effector functions (PKR and OAS), function as restriction factor on their own (IFIT1 and Schlafen family member 11) or modify the RNA (APOBEC proteins and ADAR).

One of the first restriction factors to be identified was PKR[85]. This interferon-induced protein is activated by the binding of double-stranded RNA. Upon binding, PKR dimerizes and phosphorylates the eukaryotic translation initiation factor eIF2α. This inhibits cellular ribosomal translation of mRNAs, thereby restricting the synthesis of viral proteins (Figure 10). Viruses evolved mechanisms to counteract PKR activity, highlighting its importance in antiviral defense. Mechanistically, PKR deactivation can be achieved through degradation of PKR (NSs protein of RVFV), blocking of PKR dimerization (NS5A of Hepatitis C Virus), sequestration of double-stranded RNA (NS1

of Influenza A Virus, E3L of Vaccinia Virus) and dephosphorylation of eIF2α (γ34.5 of Herpes Simplex Virus 1)[86].

The OAS system is another highly active, versatile antiviral machinery[87;88]. Binding of long double-stranded RNA leads to the activation of OAS resulting in the generation of 2'-5'-linked oligoadenylates (2'5'-OA) that serve as second messengers and activate RNase L. Binding of 2'5'-OA to RNase L induces dimerization and activation of its endonuclease activity to cleave all RNA species in the cell causing a restriction of virus growth (Figure 10)[89].

Proteins that directly act as restriction factor include the IFIT proteins were known to be induced by type I interferon and linked to regulation of translation. However, only recently it could be shown that IFIT1 and IFIT5 are able to detect 5'-triphosphorylated RNA, thereby inhibiting the replication of single-stranded RNA viruses[90;91]. At the current stage it is not clear how virus inhibition is mechanistically executed but the high number of IFIT molecules in interferon treated cells suggest a stoichiometric function. Besides binding PPP-RNA, IFIT1 is able to associate with viral capped RNAs lacking a methylation mark at the 2'-O-position of the first ribose. Such RNAs are commonly present in lower eukaryotes and certain viruses that lack 2'-O methyltransferases. IFIT1 binding leads to sequestration of 2'-O unmethylated RNA and prevents binding of the RNA to eukaryotic translation initiation factors. This leads to a highly selective block of translation while other cellular mRNAs can be properly translated (Figure 10)[92]. As for other restriction factors, viruses evolved counter mechanisms to escape IFIT1 activities. These mechanisms include generation of RNA that is methylated on the 2'-O position by acquiring 2'-O methyltransferases[93]. Moreover, alphaviruses which lack 2'-O methylation are still able to circumvent restriction by mouse Ifit1 by encoding for structural elements adjacent to the cap structure[94].

Schlafen family member 11 (SLFN11) acts more specifically in restricting retrovirus growth. It directly binds tRNAs thereby limiting specifically the availability of tRNAs for the production of proteins for HIV by exploiting a viral codon bias towards adenosines at the third position.[95].

Furthermore, the modification of nucleic acids can restrict virus growth. APOBEC3G and other APOBEC family members exert cytidine deaminase activity to mediate deoxycytidine to deoxyuridine mutations in the genome of a variety of viruses, including Human Immunodeficiency Virus (HIV). These hypermutations in the viral genome result in erroneous replication and consequently in non-infectious virions (Figure 10)[96]. The HIV protein viral infectivity factor (Vif) however counteracts this functions by ubiquitinating APOBEC3G leading to proteasomal degradation[97].

2. Nucleic Acid Immunity

Adenosine deaminase acting on RNA 1 (ADAR1) associated with double-stranded RNAs and functions as a deaminase converting adenosines to inosines in certain RNAs. Thereby the complementary base pairing between A:U is impaired making the RNA unstable (Figure 10). This mechanism prevents the formation of stimulatory double-stranded RNA molecules that could potentially activate MDA5 leading to an erroneous immune response. Therefore ADAR1 acts rather as a restriction factor of potentially stimulatory endogenous nucleic acids than as a restriction factor against viral nucleic acids[98].

2.5 Nucleases and Nucleic Acid Metabolism

Some cellular nucleases act as important factors restricting the stimulatory potential of nucleic acids, including nucleic acids of endogenous origin. Amongst those proteins is the endolysosomal DNase II, which plays an important role in the degradation of nucleic acids that accumulate during apoptotic cell death. Its importance was highlighted by the finding that mice lacking DNase II develop a chronic activation of type I interferon signaling via the cGAS-STING pathway[99] (Figure 11). Recent systematic screening approaches identified deficiency in DNAse II as causative reason for an interferonopathy in humans[100].

A surplus of endogenous nucleic acids, resulting from dead cells and chromatin debris in the extracellular space, can trigger immune responses by TLRs upon endocytosis. The extracellular DNase I represents an important nuclease prohibiting pathogenic accumulation of DNA in the extracellular space that would result in unwanted immune responses (Figure 11)[101].

The 3'-repair exonuclease (TREX1) is critical for the removal of endogenous DNA in the cytoplasm of cells. TREX1 is suggested to remove single-stranded DNA from endogenous retroelements and reverse-transcribed DNA[102]. Loss of function mutations in the human *TREX1* gene lead to increased levels of DNA species in the cytosol that can be recognized by the cGAS-STING axis and ultimately cause a severe interferonopathy named Aicardi-Goutières syndrome (AGS) (Figure 11)[103].

The RNases H are endonuclease complexes, which are involved in DNA repair cleaving the RNA moiety of RNA:DNA hybrids. Characterization of the two RNase H complexes RNase H1 and RNase H2 revealed that mutations in the three subunits of specificall RNase H2 (RNase H2A, RNase H2B and RNase H2C) can cause AGS[104]. RNA:DNA hybrids have been shown to function in vitro as endogenous stimulatory substrates for the cGAS-STING pathway[105] and TLR9[106] (Figure 11). In 2009, SAMHD1 could be added to the list of genes affected in patients suffering from AGS, the molecular

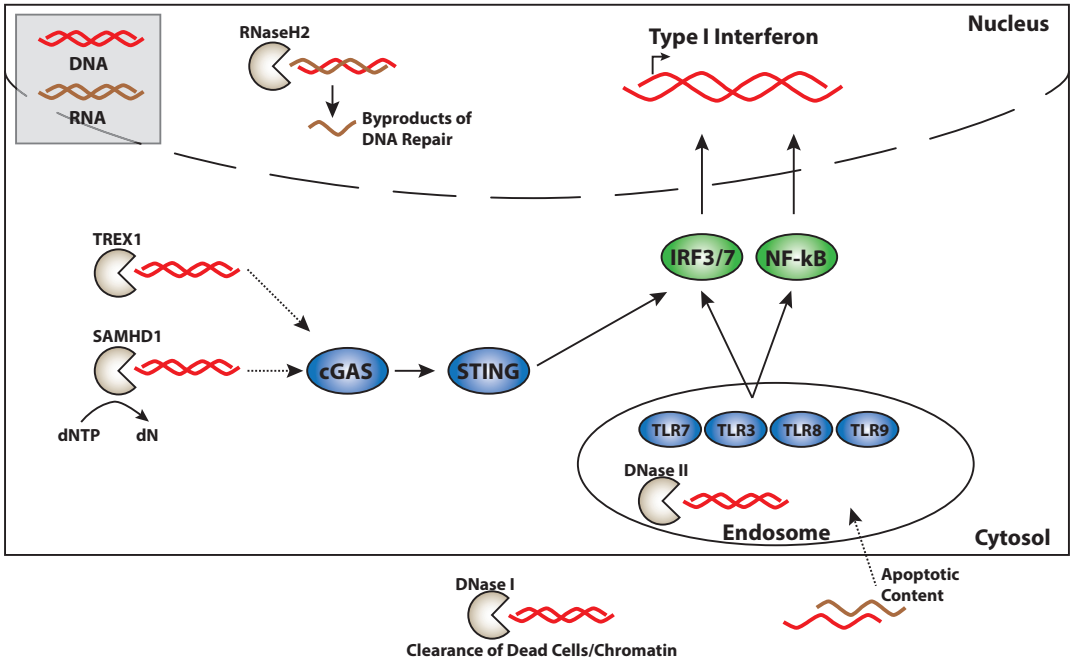

Figure 11: Cellular nucleases important for nucleic acid immunity. The cellular nucleases TREX1, RNase H2, SAMHD1, DNase I and DNase II play important roles in removing potential endogenous stimulatory nucleic acids.

mechanism however remained enigmatic (Figure 11).

Originally described as type I interferon induced protein with triphosphohydrolase activity, SAMHD1 was shown to act as a restriction factor for HIV-1 infections[107]. Besides its triphosphohydrolase activity it was proposed to function as a ribonuclease[108]. More recently, it was shown that interferon production in SAMHD1 deficient cells requires as well the cGAS-STING pathway[109] the exact substrate, however, is still unknown.

2.6 Immunopathology triggered by deregulation of Nucleic Acid Immunity

Type I interferonopathies can be characterized as a genetically heterogeneous group of autoinflammatory disorders due to an erroneous and chronic activation of the antiviral type I interferon response. The current knowledge of the pathology underlying autoinflammation was influenced by progress in our understanding of the innate immune system, foremost the identification of pattern-recognition receptors and the activation of signaling pathways culminating in the expression of type I interferons. Moreover, the

discovery of mutations in genes coding for the nucleases Trex1, Dnase I, DNase II or RNase H2 in patients with AGS further pointed to a close connection between innate immune activation and autoimmunity. The recognition of self nucleic acids by pattern recognition receptors is therefore key in the pathogenesis of type I interferonopathies since an inappropriate activation of the type I interferon axis leads to severe effects for the host by the development of autoinflammation.

The term autoinflammation was shaped when the molecular mechanisms of tumor necrosis factor receptor-associated periodic fever syndrome were elucidated. A self-directed inflammation was thereby noticed rather than an involvement of the adaptive immune system including B- or T-cells.

A uniting phenotype of type I interferonopathies is the anomalous upregulation of type I interferons. With our current knowledge, four sources of an abnormal interferon response can be classified. (1) Nucleic acids bearing atypical modifications or the accumulation of endogenous nucleic acids, (2) increased sensitivity or activation of pattern recognition receptors independent of a ligand, (3) defects in the regulation of nucleic acid-dependent interferon signaling pathways, (4) defects in the nucleic acid independent modulation of interferon responses.

Currently, more than twelve genetic disorders are known that can be categorized as a type I interferonopathy. Amongst those is the prototypic Aicardi-Goutières syndrome (AGS). It is a rare, early onset childhood disorder and characterized as a leukoencephalopathy with elevated interferon levels in the cerebrospinal fluid, cerebral calcifications, cerebral atrophy, seizures and intermittent fever[110]. An important biomarker of AGS is the interferon signature. Whereas interferon levels in the cerebrospinal fluid seem to decline over time, the upregulation of interferon-stimulated genes (ISGs) in the blood is a consistent marker[111]. AGS is a heterogeneous disease and results from mutations in any of at least seven genes including *TREX1, ADAR, RNase H2A, RNase H2B, RNase H2C, SAMHD1* and *MDA5* (Figure 12). Some AGS patients show indications which are noticed as well in patients with Systemic Lupus Erythematosus (SLE).

SLE is a chronic, autoimmune disease where patients show signs of dermatitis, arthritis, fever, rash and swollen lymph nodes[112]. Unlike AGS or other interferonopathies, SLE is a multifactorial disease where genetic and environmental factors play a role. The molecular pathology of SLE involves an immune response by the generation of autoantibodies (mostly anti-nuclear antibodies targeting DNA) that induce inflammation. Like AGS patients, SLE patients as well show signs of an interferon signature in peripheral blood[113]. Mutations in the genes of *TREX1, RNase H2A, RNase H2B* and *RNase H2C* provide a higher risk for SLE[114]. Moreover, mutations in the already previously introduced

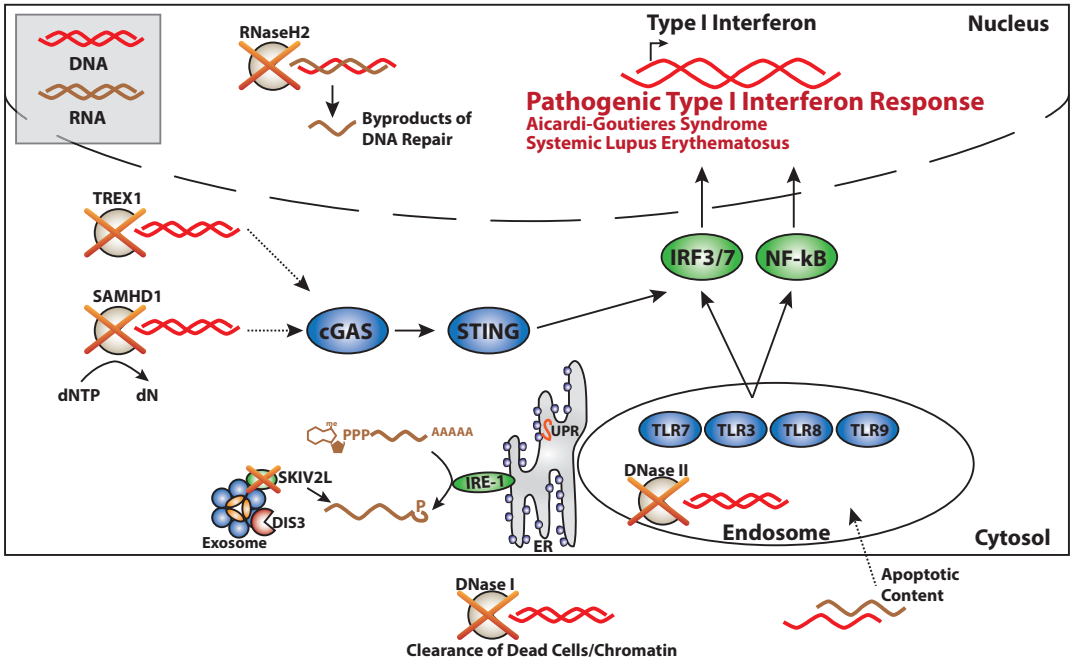

Figure 12: Type I interferonopathies triggered by genetic defects in nucleic acid immunity. Mutations in genes of cellular nucleases like TREX1, SAMHD1, RNase H2, DNase I or DNase II are causative for the development of a pathogenic type I interferon response and the development of autoinflammatory diseases.

extracellular nuclease *DNase I* have been identified in SLE patients (Figure 12)[115].

Although endogenous extracellular nucleic acids can lead to an aberrant interferon response, cytoplasmic self-nucleic acids are as harmful since most nucleic acid sensing receptors reside within the cytoplasmic cellular compartment. Defective degradation of endogenous DNA species like single-stranded DNA metabolites, which continuously emanate during DNA damage repair, single-stranded DNA polynucleotides from processing of abnormal replication intermediates, or from endogenous retroelements can activate the cGAS-STING axis. This can be prevented by the excellent waste handling of the cellular nucleases like TREX1 or RNaseH2.

However not only endogenous DNA could potentially activate cytoplasmic DNA sensors, RNA sensors like RIG-I or MDA5 could as well sense endogenous RNA species. Interestingly, only recently superkiller viralicidic activity 2-like (SKIV2L), a component of the exosome complex, was discovered to play an important role in the degradation of aberrant RNAs[116]. These abnormal RNAs containing 2'3'-cyclic phosphates originate from the regulated IRE-1-dependent RNA decay (RIDD) involved in the unfolded protein response as previously described (Figure 12)[51]. Moreover, genetic studies identified that

polymorphisms in the gene of SKIV2L lead to a potential risk of developing SLE[117]. Together, the mechanisms described above underline the outstanding importance of proper cellular nucleic acid waste handling, however it still remains unclear how for instance endogenous stimulatory triphosphorylated RNAs like 5S rRNA, or ncRNAs are rendered harmless.

CHAPTER

3

VIRAL RNA DEGRADATION

3. Viral RNA Degradation

Virus infection triggers the activation of PRRs that recognize incoming viral nucleic acids, virus replication intermediates or replication by-products. This sensing leads to the massive induction of cytokines, chemokines and the expression of antiviral genes ultimately leading to inflammation. In case of a successful defense from virus infections, an important cellular task is to remove the immune stimulatory viral nucleic acids in order to return to a homeostatic situation and to contain the effects originating from inflammation. As mentioned above, several diseases are linked to the incapability of cells to degrade stimulatory endogenous nucleic acids leading to the development of autoinflammatory diseases like the interferonopathies AGS and SLE. The genes included in these processes include nucleases like DNase I, DNase II or TREX1 that are able to degrade endogenous DNA or RNase H2 involved in the removal of RNA:DNA hybrids.

However, surprisingly little is known about the ability of cells to degrade viral or immunostimulatory nucleic acids. Yet, an interesting computational approach highlighted the importance of viral RNA degradation in Influenza A Virus (IAV) infected cells. Generating a mathematical model and calibrating it with experimental data covering all steps of the viral life cycle revealed that RNA degradation is an important parameter in the successful replication of IAV. By calculating the model parameters for viral RNA decay and diffusion time, it could be shown that the diffusion distance from the site of membrane fusion with the endosomal membrane and translocation to the nucleus impacts RNA degradation rates: the shorter the distance of diffusion to the nucleus, the lower the probability of viral RNA degradation. This computational findings could also be substantiated by experimental data showing viral RNA degradation when nuclear import was blocked by importazole[118].

As previously described, viral nucleic acids differ from cellular RNAs in several ways. This includes structural differences, double-strandedness, the lack of poly(A) tails, or the presence of 5'-PPP structures. One could hypothesize that the cell uses chemical or structural modifications that mark viral RNAs to specifically degrade such nucleic acids. However, surprisingly little is known about degradation pathways that are targeting viral nucleic acids. What is the relative contribution of the cellular known degradation mechanisms to decay viral RNA? How does perturbation of these RNA degradation mechanisms modulate virus growth *in vitro* and *in vivo*? Which proteins are mediating specificity for viral RNA degradation?

One of the major cellular RNA turnover pathways is the 5'-3' degradation pathway involving deadenylation, decapping and subsequent RNA degradation by the exonuclease XRN1. Only recently, viral nucleic acids were shown to be sensitive to this decay route. The Lemon group showed that synthetic Hepatitis C Virus (HCV) RNA harboring a

5'-triphosphate end is rapidly degraded with a half-life of around 1.5h. In contrast, the median half-life of cellular mRNAs is 9 hours and therefore much more stable[119]. This suggests a targeted degradation of viral nucleic acids compared to host RNA. Knocking down the exonuclease XRN1 led to a stabilization of the PPP-RNA by increasing the half-life to more than 3h (Figure 13)[120]. Notably, although XRN1 may be able to degrade the RNA body, degradation can only be initiated after the removal of the 5'-PPP group. This suggests involvement of a cellular enzyme that removes two of the three phosphates to leave a monophosphate on the RNA, which subsequently can be degraded by XRN1[121]. The activity of such a pyrophosphatase may be analogous to the activity of decapping enzymes that remove the 5'-cap structure in order to allow XRN1-dependnet cleavage of RNA.

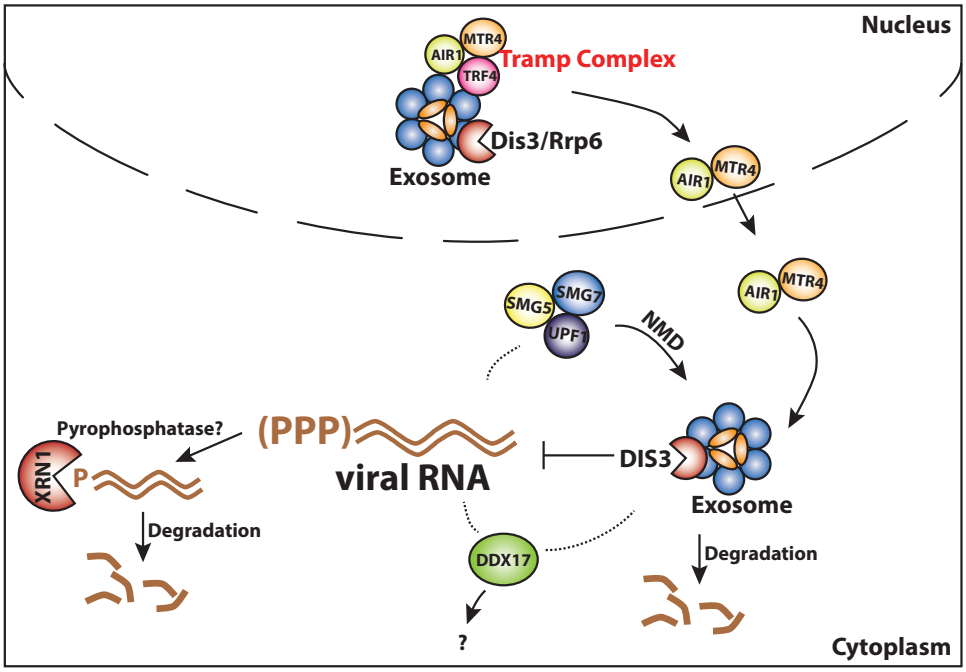

Figure 13: Viral RNA Degradation Pathways involve factors of all known cellular RNA degradation mechanisms including XRN1 from the 5'-3' decay pathway, factors of the NMD pathway and the exosome complex.

NMD is another cellular process responsible for rapid degradation of aberrant cellular mRNA[46;122;123;124]. NMD is operative on translating non-functional RNAs. Cellular mRNAs with long 3'UTRs or premature stop codons can be detected by proteins of the NMD pathway[125;126] and are subsequently eliminated by the exosome complex. Since viral nucleic acids possess features of aberrant RNAs there is increasing evidence that they are recognized as targets of the cellular RNA degradation machinery. A genome-

wide siRNA screen that tested for host factors restricting Semliki Forest Virus (SFV) growth, identified the NMD components SMG5, SMG7 and UPF1 as targets and their depletion led to an increase in virus replication during the early phase of infection[127]. This indicates that viruses with single-stranded, positive-sense RNA genomes can be detected and degraded by NMD (Figure 13). Due to the fact that NMD is translation-dependent, the genomes of DNA viruses, retroviruses and negative-sense RNA viruses can most likely not be targeted by NMD.

Besides being targeted for degradation by NMD or the 5'-3' decay pathway, the 3'-5' decay pathway including the exosome complex was implicated in degradation of viral RNA. Multiple RNA binding proteins linked to antiviral immunity were shown to interact with the exosome complex implying that RNA degradation is accomplished through those complexes. Amongst factors that associate with viral RNA and the exosome is DDX17, which restricts Rift Valley Fever Virus (RVFV) growth and is directly binding the exosome (Figure 13). Though, the mechanism of influencing RVFV growth is not clear yet[128;129].

Recent work by the Sara Cherry group, revealed that the TRAMP complex components MTR4 and AIR1 (Zcchc7) are antiviral against several RNA viruses including RVFV, Vesicular Stomatitis Virus (VSV) and Sindbis Virus (SINV). Interestingly, these components are generally part of the strictly nuclear TRAMP complex. Notably, in infected cells MTR4 and AIR1 translocate to the cytoplasm where they form a complex with the cytoplasmic exosome and viral RNAs (Figure 13). The RNA of RVFV was found to be stabilized in the absence of AIR1, suggesting targeted degradation of viral transcripts by this newly identified cytoplasmic TRAMP complex. Attaching GFP to the 3' UTR of RVFV and subsequently infecting the cells was sufficient to target the GFP-tagged transcript for degradation, implying that infectious conditions trigger a selective degradation by the exosome complex[130].

A further study showed that the cytidine deaminase (AID), a member of the APOBEC family, interacts with a viral RNP complex of Hepatitis B Virus (HBV) consisting of the viral P protein and the epsilon RNA sequence essential for HBV replication. Besides binding to the viral RNP complex, AID was as well shown to recruit the RNA exosome (Figure 14). Moreover HBV-levels are reduced in an AID-dependent manner indicating that interaction of AID with the viral RNP complex and the RNA exosome leads to RNA degradation by the exosome[131]. HBV is able to evade the induction of the interferon system. However, the virus can still be cleared in most patients to a high extent, suggesting cellular restriction pathways that efficiently restrict HBV replication in an interferon-independent manner. In a functional screen for helicases

that could potentially modulate HBV replication, the SKIV2L helicase, member of the cytoplasmic Ski complex, was identified. Furthermore, interaction of SKIV2L with the HBV X-RNA was shown to be indispensable for degradation of the X-mRNA. This degradation seems to involve the protein HBS1, which is a factor also involved in the cellular RNA surveillance pathways (Figure 14)[132].

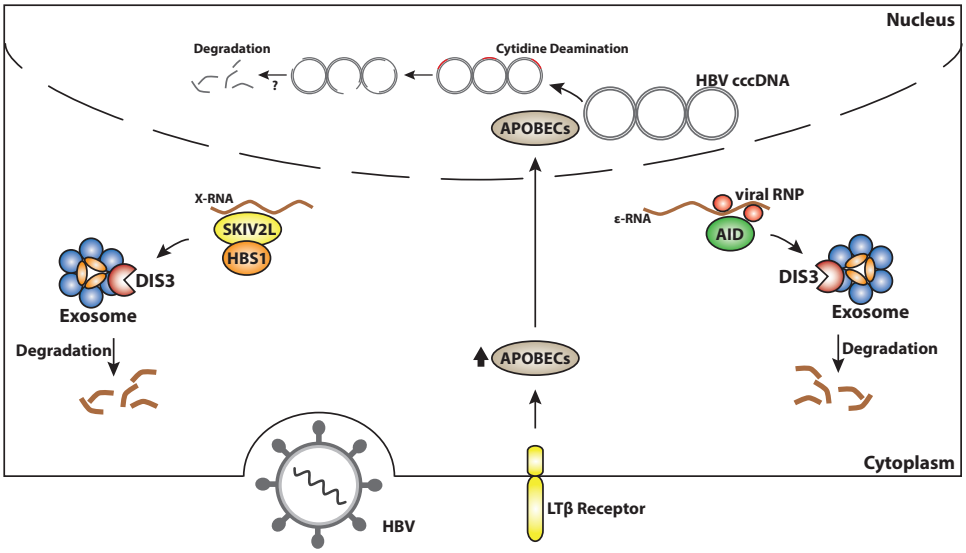

Figure 14: Degradation of HBV nucleic acids. Different HBV nucleic acids (X-RNA, and -RNA are recognized by RNA binding proteins leading to degradation by the exosome complex. In the nucleus APOBEC proteins deaminate the covalently closed circular DNA (cccDNA) which leads to degradation by nuclear nucleases.

Additionally, the Protzer laboratory showed that stimulation of the lymphotoxin beta receptor (LTβR) upon HBV infection leads to the expression of proteins of the APOBEC family. APOBEC3A and APOBEC3B translocate to the nucleus in HBV infected cells and lead to cytidine deamination of the nuclear covalently closed circular DNA (cccDNA), a highly stable state of the genomic HBV DNA. Deamination of the cccDNA led to degradation in cell culture (Figure 14)[133]. However it is yet unclear how the modified RNA gets degraded in the nucleus. In patients with chronic HBV infection no impact on cccDNA turnover could be observed despite activation of LTβR gets[134].

The interferon system is the main executor of antiviral responses and a number of interferon stimulated genes bear nuclease activity. Amongst those is the interferon-induced RNase L, which cleaves a broad range of RNAs without apparent discrimination between viral and cellular nucleic acids (Figure 15). However some reports point towards a partial selectivity of viral nucleic acids. First, cellular RNAs especially tRNAs and rRNAs are modified heavily on internal nucleotides thereby representing only suboptimal

3. Viral RNA Degradation

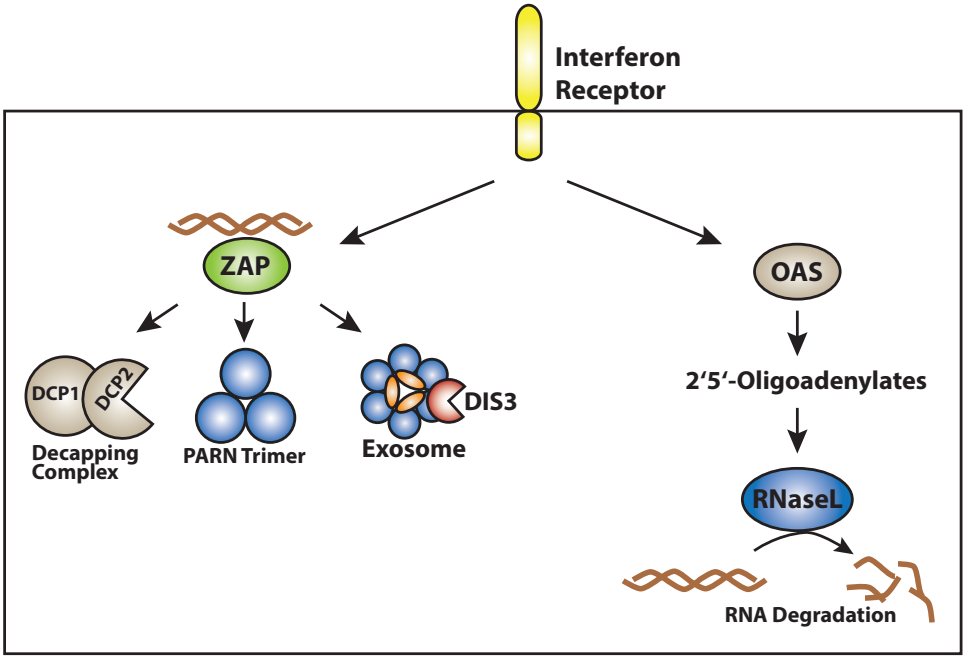

Figure 15: Interferon-induced nucleic acid degradation pathways. The interferon-induced zinc-finger antiviral protein (ZAP) is able to recruit the RNA decay machinery upon viral RNA binding. RNaseL stimulated by the interferon-induced generation of 2'5'-oligoandenylates is activated to cleave various nucleic acids

substrates for RNase L[135]. Second, RNase L strongly favors UU or UA sequences as cleavage sites, which are not found frequently in mammalian codons[136]. Another example for an interferon induced nuclease is zinc-finger antiviral protein (ZAP) that has the ability to specifically target RNAs bearing ZAP response elements though its zinc finger domain. ZAP response elements commonly found in many viruses[137;138]. Upon RNA binding, ZAP recruits the whole RNA decay machinery including the exosome complex, the deadenylase PARN and the decapping enzymes DCP1 and DCP2 (Figure 15)[139]. The mechanism, however, is still not entirely explored and it is not clear if ZAP-dependent restriction of virus growth is due to degradation of the viral RNAs or any other potential mechanism.

In sum, several lines of evidence suggest involvement of the exosome complex as well as XRN1 – dependent degradation in the turnover of viral nucleic acids. However, currently it is enigmatic how specificity is conferred to viral RNA in order to allow specificity. To date, no mechanism was identified that would specifically target viral nucleic acids for degradation.

CHAPTER

4

THE MAMMALIAN PHOSPHATOME

4. The Mammalian Phosphatome

The phosphatome refers to the entire set of proteins with phosphatase activity encoded in the genome. Phosphatases are enzymes capable of removing a phosphate moiety from various biomolecules and thereby fulfil important biological functions in metabolism, signaling and nucleic acid processing. The biochemistry of phosphate removal represents a typical hydrolysis reaction with a water molecule as attacking group and results in the generation of a phosphate ion and a molecule with a free hydroxyl (OH) group. The attack of the water molecule can be catalyzed by divalent metal ions or histidine-, cysteine-, or serine-residues. The classification of phosphatases is nearly as diverse as their molecular functions and includes categorization into either alkaline phosphatases or acid phosphatases, classification according to their active-site catalytic group (metalphosphatases, serinephosphatases, histidinphosphatases or cysteinphosphatases[140]) or according to their protein structural fold[141]. Typically, phosphatases do not recognize their substrate within the active site but rather bind multiple residues with weak binding affinity. However the cumulative effect of multiple weak interactions provides an increase in binding specificity to the substrate[142].

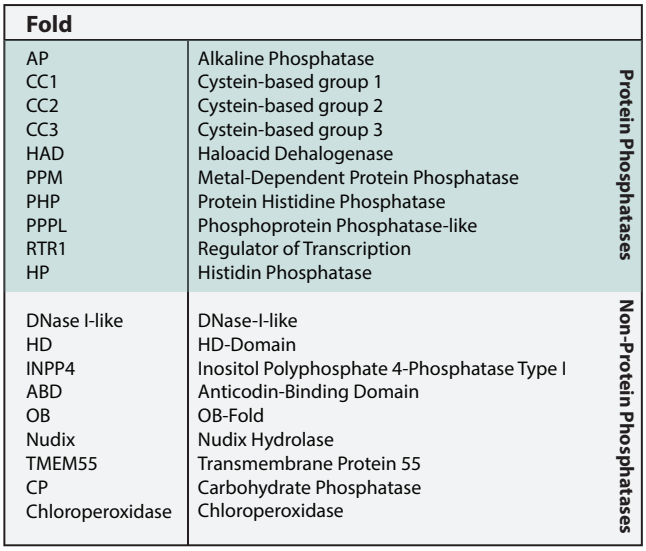

Figure 16: The human phosphoproteome subdivided in 19 protein structural folds. Depicted in blue are protein-phosphatases and in grey non-protein phosphatases

Only recently, Chen et al. classified human phosphatases[141]. By including input from databases, protein sequence similarity searches and literature it was possible to create a phosphatome of 264 phosphatases. Based on structural databases, the human phosphatome can be subdivided into proteins with 19 different protein folds (Figure 16).The largest group is comprised of the human protein phosphatases, which dephosphorylate post-translationally modified proteins on tyrosine or serine/threonine residues. The group of protein phosphatases includes alkaline phosphatases (AP), the cysteine-based

phosphatases (CC1, CC2, CC3), haloacid dehydrogenases (HAD), metal-dependent protein phosphatases (PPM), protein histidine phosphatases (PHP), Phosphoprotein phosphatase-like phosphatases (PPPL), histidine phosphatases (HP), and a phosphatase of the regulator of transcription fold (RTR1). The group of non-protein phosphatases is more diverse and less well studied. However, they play important roles in metabolism where the addition or removal of phosphate groups changes the energy of metabolic intermediates, in the processing of nucleic acids, or in the regulatory role of phosphoinositide lipids.

Nudix Hydrolases

Non-protein phosphatases with a Nudix fold comprise a protein superfamily of metal-dependent phosphatases. These Nudix hydrolases are conserved in 250 species including bacteria, archea and eukaryotes[143]. Proteins of the Nudix superfamily catalyze the hydrolysis of nucleoside diphosphates linked to other moieties (X) and contain the conserved sequence motif GX_5EX_5[UA]$XREX_2EEXGU$ where U is a bulky amino acid and X can be any amino acid[144].

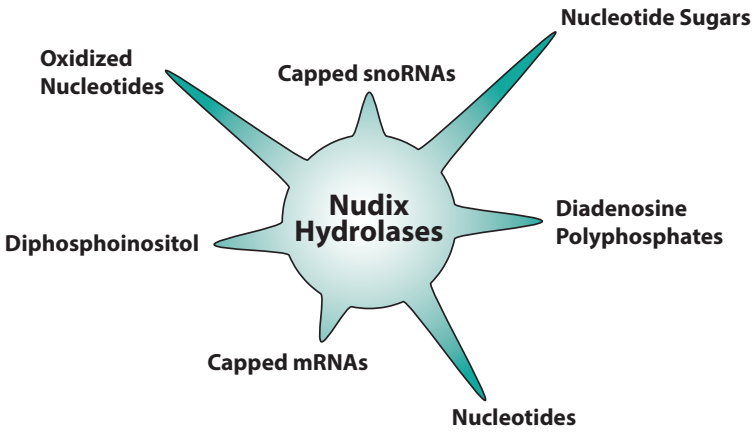

Figure 17: Substrates of Nudix Hydrolases. Substrates of human Nudix hydrolases are very diverse and range from single nucleotides to nucleotide sugars, capped RNA and nucleotide polyphosphates.

This so called Nudix box forms a structural motif of a loop - α-helix - loop structure, which harbors the catalytic residues. This motif is part of an $\alpha/\beta/\alpha$ sandwich making up the Nudix fold[145]. The substrates that are dephosphorylated by Nudix hydrolases are very diverse ranging from nucleoside triphosphates, polyphosphates, and nucleotide-sugars to capped mRNAs (Figure 17). Consequently, they are known to play very diverse

roles in cellular metabolism and cell homeostasis, as well as mRNA processing[146;147]. The mechanism of Nudix hydrolases resembles that of other metal-dependent phosphatases with a nucleophilic attack of a water molecule on the γ-phosphate of the substrate and formation of a trigonal bypyramidal intermediate[148]. The double bond is then reformed thereby displacing a monophosphorylated moiety as leaving group (Figure 18). The attacking water ligand is properly aligned by the electrostatic interactions with divalent cations, mostly Mn^{2+} or Mg^{2+} that as well enhance the nucleophilicity of water. In addition, two conserved glutamate residues in the Nudix box are critical for the hydrogen bonding of the water molecule and the coordination of the metal ions. In some cases, a third Mg^{2+} ion stabilizes the negatively charged phosphate of the leaving group (Figure 18). The substrate specificity is not provided by residues within the active site but rather by motifs elsewhere in the structure.

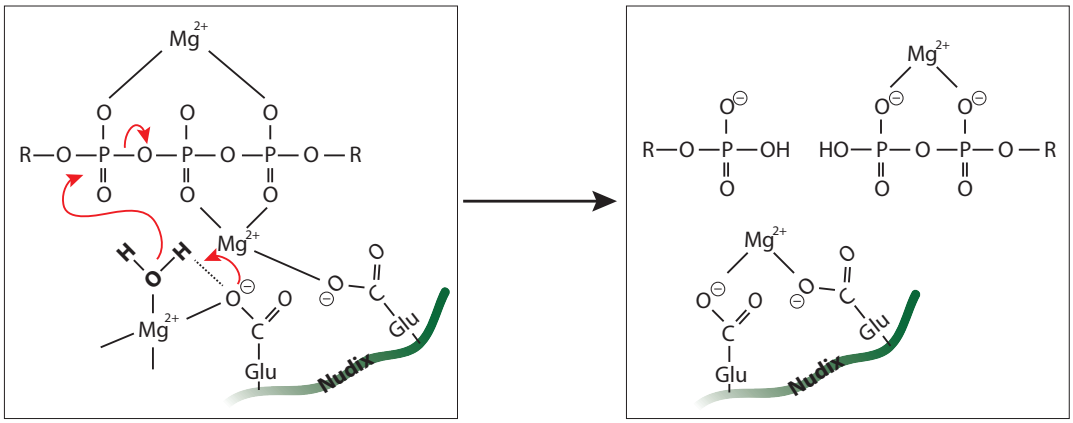

Figure 18: Mechanism of phosphate removal by Nudix hydrolases. Metal-dependent hydrolysis reaction by nucleophilic attack of a water molecule and displacement of a monophosphorylated moiety.

The human genome encodes for 24 Nudix genes. Although the first NUDIX member was already defined in 1954, the biological role of most of the Nudix hydrolases still remains unknown[146]. Only recently, a comprehensive study profiled the family of Nudix hydrolases in more detail in terms of structural similarities, mRNA expression levels and by screening 52 different substrates for their sensitivity to Nudix activity[149]. Although this study expanded our knowledge on Nudix hydorlases, the molecular functions and their cellular targets remain enigmatic.

CHAPTER

5

AIM OF THE THESIS

Aim of the Thesis

Viruses are the most abundant pathogens on earth and represent a major threat to human health. In order to grow and spread, viruses are strongly dependent on their genetic material. In comparison to the highly processed host nucleic acids, viral nucleic acids miss several of those features. Therefore sensing of virus infections mostly involves the recognition of viral nucleic acids. In the past years, remarkable progress has been made in the understanding of how foreign nucleic acids are sensed by the cell. However, only little is known about the pathways of cells to degrade specifically viral nucleic acids.

The genome of RNA viruses is protected from degradation by a 5'-triphosphate group. Similar to mRNA degradation in eukaryotes where mRNA decay needs to be initiated by the removal of the protecting 5'-cap structure by DCP2, the viral RNA would need to be prepared for degradation by 5'-exonucleases. Therefore, the aim of this thesis was to identify a mechanism that could specifically target viral nucleic acids for degradation. The curiosity was sparked by a publication of Deana et al., who identified a bacterial pyrophosphatase of the Nudix hydrolase superfamily (RppH) to be able to dephosphorylate triphosphorylated bacterial mRNA. Interestingly, the eukaryotic decapping enzyme DCP2 belongs as well to the Nudix hydrolase superfamily. Therefore, I first set out to screen all mammalian Nudix hydrolases for having an impact on virus growth. After selecting four, I found only one Nudix hydrolase, namely NUDT2, to dephosphorylate triphosphorylated RNA. I could show that NUDT2 releases two phosphate groups of a triphosphorylated RNA in a sequential manner, leaving behind a monophosphorlyated RNA that could serve as a substrate for the cellular 5'-exonuclease XRN1. Thereby NUDT2 initiates a RNA degradation pathway specific to viral triphosphorylated RNAs.

Additionally, discriminating self- from non-self nucleic acids is of upmost importance for host cells to launch a proper immune response. The crystal structure of the viral restriction factor interferon-induced protein with tetratricopeptide repeats 1 (IFIT1) revealed novel insights in the binding of capped viral RNA. In collaboration with Bhushan Nagar I aimed at functionally validating that cap-RNA binding of specific residues in the cap-binding pocket are important for IFIT1-mediated inhibition of virus growth.

Part II

Results

CHAPTER

6

PUBLICATION 1

NUDT2 initiates viral RNA degradation by removal of 5'-phosphates

Beatrice T. Laudenbach, Alexander Reim, Markus Moser, Arno Meiler, Janos Ludwig and Andreas Pichlmair. NUDT2 initiates viral RNA degradation by removal of 5'-phosphates. Submitted to *Science* (2018)

Viruses are dependent on their genetic material in order to spread. However, if this viral genetic material is subjected to degradation by cellular nucleases is not explored yet. The genome of many RNA viruses is protected by a 5'-triphosphate group which does not allow digestion by 5'-3' nucleases. Very similar, host messenger RNAs are protected as well by a chemical structure, namely the 5'- cap. Prior to mRNA degradation, the cap structure needs to be removed by decapping protein 2 (DCP2). The generated monophosphorylated RNA is thereby rendered susceptible to degradation by cellular exonuclease 1 (XRN1). In my PhD work, I discovered that NUDT2, very similar to DCP2, removes phosphates from RNA substrates generating a monophosphorylated RNA that serves as substrate for XRN1. This represents a novel mechanism to degrade specifically viral nucleic acids. Its importance is highlighted by the increased virus-load in cells lacking the *Nudt2* gene.

NUDT2 initiates viral RNA degradation by removal of 5'-phosphates

Beatrice T. Laudenbach[1], Alexander Reim[2], Markus Moser[3], Arno Meiler[1], Janos Ludwig[4] and Andreas Pichlmair[1,5,6]

[1]Innate Immunity Laboratory, [2]Department of Proteomics and Signaltransduction, [3]Department of Molecular Medicine, Max-Planck Institute of Biochemistry, Martinsried/Munich, 82152, Germany, [4]Institute of Clinical Chemistry and Clinical Pharmacology, University Hospital Bonn, 53127 Bonn, Germany, [5]Technical University of Munich, School of Medicine, Institute of Virology, 81675 Munich, Germany, [6]German Center for Infection Research (DZIF), Munich, Germany

Corresponding author:

Andreas Pichlmair, PhD, DVM
Innate Immunity Laboratory
Max-Planck Institute of Biochemistry
Am Klopferspitz 18
82152 Martinsried/Munich, Germany
Email: apichl@biochem.mpg.de
Telephone: +49 89 8578 2220

6. Publication 1

Laudenbach *et al.*

Abstract

In course of an infection, viruses rapidly amplify their genetic material. Relatively little is known regarding cellular mechanisms to degrade viral RNA, although this may represent an essential step to successfully clear viral infections. Here we identified a mechanism that allows processing of viral triphosphorylated (PPP)-RNA into P-RNA, which serves as substrate for 5'-3' RNA degradation. Nudix hydrolase 2 (NUDT2) removes 5'-phosphates from PPP-RNA in a RNA sequence- and structure-independent manner and prepares this RNA for XRN1 mediated degradation. Ablation of NUDT2 resulted in increased growth of a PPP-RNA virus, highlighting this PPP-RNA processing as an important control mechanism to prevent virus infection.

Main text

5'-3' RNA degradation is an evolutionary highly conserved process. Eukaryotic messenger (m) RNA is protected from 5'-3' degradation by a 5'-m7G cap structure, which needs to be removed by decapping protein 2 (DCP2) in order to generate a monophosphorylated (P-) RNA substrate for the 5' to 3' exonuclease 1 (XRN1) (Fig. 1a) (*1, 2*). Some viral genomic RNAs and viral RNA transcripts do not bear a 5'-cap but present a 5'triphosphate (PPP-) group, which also serves as a chemical modification preventing 5'-3' degradation. In this regards, viral RNA is very similar to prokaryotic mRNA, which also bears a 5'-PPP or 5'-PP group. In case of bacteria, these phosphates are removed by the RNA pyrophosphatase H (RppH) to prepare RNA for degradation by the bacterial nuclease RNase E (*3, 4*) (Fig. 1a). Interestingly, both, DCP2 and RppH belong to the superfamily of Nudix hydrolases (*5*), a protein family that is highly diverse in terms of sequence, domain organization and substrate specificity (*6*) (Fig. 1b). Nudix hydrolases are most commonly pyrophosphohydrolases active towards substrates with the structure NDP-X (nucleoside diphosphate linked to another moiety, *X*) usually resulting in NMP (nucleoside monophosphate) and P-X as products (*7-9*). Nudix proteins are characterized by a Nudix hydrolase domain, which contains characteristic catalytic and metal-binding amino acids (*9*). We

hypothesized that processing of viral PPP-RNA in eukaryotic cells may involve a Nudix hydrolase and that such a protein should contribute to virus growth restriction.

We therefore individually depleted all mammalian Nudix genes that are known to have a role in nucleotide metabolism (*7*) or the pattern recognition receptor RIG-I as positive control, and tested for growth of Vesicular stomatitis virus expressing GFP (VSV-GFP) and the interferon stimulating variant VSV-AV3-GFP (*10*). Notably, depletion of four Nudix hydrolases (NUDT2, NUDT12, NUDT14 and NUDT17) led to an increase in VSV-GFP or VSV-AV3-GFP growth (Fig. 1b), without affecting cell viability (Supplementary Fig. 1a). NUDT5, NUDT21 and NUDT22 showed a negative impact on VSV growth. We selected NUDT2, -12, -14 and -17 for further experiments. Depleting the four Nudix hydrolases in A549 and HeLa cells and using renilla-luciferase expressing Influenza A virus (FluAV-ren) as alternative PPP-RNA generating virus showed that depletion of only NUDT2 significantly increased growth of FluAV in both cell types (Fig. 1c, Supplementary Fig. 1c, d). NUDT12 and NUDT17 exhibited inconsistent results between the two cell types.

To characterize the four selected Nudix hydrolases for their ability to dephosphorylate PPP-RNA, we generated recombinant NUDT2, -12, -14 and -17. As controls we mutated the metal-coordinating glutamic acid residue (E) in their conserved Nudix hydrolase domain motif generating NUDT2 E58A, NUDT12 E369A, NUDT14 E121A and NUDT17 E124A (Fig. 2a). We tested the recombinant proteins for their ability to release phosphates from a double-stranded PPP-RNA substrate (IVT4) (*11*). Notably, of all proteins tested, only NUDT2, but no other tested Nudix hydrolase, released phosphates when co-incubated with PPP-RNA (Fig. 2b). The phosphate release mediated by NUDT2 was comparable to the amounts of phosphates released by calf intestinal phosphatase (CIP). Importantly, the NUDT2 E58A mutant showed no activity, indicating specificity in this assay (Fig. 2b). Despite phosphate release, the RNA substrate itself remained intact after NUDT and CIP treatment, indicating that the phosphates are not released from the RNA backbone and that the here tested Nudix hydrolases do not have RNAse activity (Fig. 2c). In sum, this analysis indicated NUDT2 as PPP-RNA processing enzyme that negatively

regulates virus growth. NUDT2 is highly conserved from nematodes to mammals (Supplementary Fig. 2a), further indicating an important role. The major substrate of NUDT2 is the stress-induced diadenosine tetraphosphate (Ap4A) (*12, 13*). In mammalian cells, Ap_4A is generated by most aminoacyl-tRNA synthetases, acyl-CoA synthetases and DNA ligases (*14, 15*). Intracellular Ap_4A can act as a second messenger (*16*), as transcriptional regulator (*17*), is involved in the regulation of DNA replication (*18*) and is known to bind a number of proteins including protein kinases (*19*), the chaperone GroEL, cAMP receptor protein (*20*), and the HINT1 tumor suppressor (*21*). Extracellularly, Ap_4A can as well act as messenger molecule by binding to P2-type purinergic receptors (*22*). Besides proteins of the nucleotide pyrophosphatases/phosphodiesterases family of proteins (*23*), NUDT2 plays the principle role in cleaving Ap_4A to reduce intracellular levels (*24*). 5'-PPP RNA as a substrate for NUDT2 was not indicated so far.

To assess the substrate specificity, we next tested the ability of NUDT2 to release phosphates from different substrates. Phosphates were released when a single-stranded 44mer RNA was used (Fig. 2d). We designed substrates with diverse length of single-stranded overhangs and variable nucleotides (A, G, U and C) at the second position (Supplementary Fig. 2b, c). NUDT2 and the positive control CIP released similar amounts of phosphates from substrates with ssRNA overhangs and a guanosine as first and variable nucleotides at the second position, while NUDT2 E58A showed reduced activity (Supplementary Fig. 2b). NUDT2 was also able to dephosphorylate RNA templates with adenines at the 5' end, irrespective of the 5' single-stranded RNA overhang (Supplementary Fig. 2c). We could not observe degradation of the used RNA templates by NUDT2 (Supplementary Fig. 2d). Notably, no phosphates were released when single nucleotides (ATP, GTP, UTP and CTP) were used (Fig. 2e), indicating that NUDT2 requires polynucleotides as substrates. We concluded from these experiments, that NUDT2 can dephosphorylate PPP-RNA substrates with no obvious sequence or structural preference.

Since NUDT2 does not have exonuclease activity itself (Fig. 2c, Supplementary Fig. 2d), we next tested whether PPP-RNA could in principle be converted into P-RNA, to serve as a XRN1 substrate. We generated PPP-RNA with radioactive [^{32}P] labelled γ-phosphate. Thin layer chromatography (TLC)

experiments clearly showed that incubation with NUDT2 specifically released a radiolabelled phosphate and reduced radioactive labelling of the substrate RNA (Fig. 3a). In contrast, NUDT12, NUDT14 and NUDT17 did not show γ-phosphate release or reduced labelling of the substrate RNA (Fig. 3a). This reaction was time dependent and required a functional Nudix domain (Supplementary Fig. 3a). The substrate single- or double-strandedness did not affect γ-phosphate release by NUDT2 in TLC assays (Supplementary Fig. 3b).

In order to assess the mode of removal of phosphates by NUDT2, we synthesized triphosphorylated RNA dinucleotides (PPP-GpA and PPP-ApG) and tested these substrates for removal of mono- or diphosphates. As expected (*3*), bacterial RppH released pyrophosphates (PP_i) from PPP-GpA (Fig. 3b). Surprisingly, NUDT2 released single phosphates in a consecutive manner resulting in a di-phosphorylated intermediate that is further converted into a mono-phosphorylated product (Fig. 3b, Supplementary Fig. 3c) irrespective of the first nucleotide (Fig. 3c, Supplementary Fig. 3c). This was a time-dependent event that required a fully functional Nudix hydrolase domain (Fig. 3c, d). No removal of phosphates could be observed for the control protein NUDT14 (Supplementary Fig. 3d).

We next tested whether NUDT2 has the ability to prepare viral PPP-RNA for degradation by the canonical 5'-3' RNA degradation machinery using a Hepatitis C virus (HCV) encoding RNA as template. While incubation with NUDT2 or XRN1 did not affect stability of the triphosphorylated HCV RNA, combination of NUDT2 with XRN1 led to RNA degradation (Fig. 3e, f). To assess whether NUDT2 and XRN1 have a similar synergistic effect during infection of cells with a virus, we infected Huh7.5 control cells and cells that were deleted for NUDT2 and XRN1 expression by CRISPR/Cas9 targeting with VSV wt. To focus on incoming viral RNA, virus replication was blocked using cycloheximide (Fig. 3g, scheme). Notably, control Huh7.5 cells showed significantly reduced levels of VSV-N transcripts as compared to NUDT2 or XRN1 knockout cells (Fig. 3g), indicating that NUDT2 negatively affects virus replication at an early stage.

6. Publication 1

Laudenbach *et al.*

We generated Nudt2 deficient mice from targeted embryonic stem cells (Fig. 4a, Supplementary Fig. 4a). Correct targeting of the *Nudt2* locus and loss of Nudt2 protein expression was confirmed by PCR and mass spectrometric analysis of mouse bone marrow cells (Supplementary Fig. 4b, Fig. 4a). Homozygous knockout mice were viable, bred with expected mendelian ratios and did not show an obvious phenotype under non-infected conditions (Supplementary Fig. 4c). Notably, accumulation of infectious virus particles was increased in supernatants of bone marrow cells or MEFs lacking *Nudt2* as compared to *Nudt2*$^{+/+}$ littermate controls by more than 10-fold or 100-fold, respectively (Fig. 4b, c). At the same time, accumulation of HSV-1, which does not generate PPP-RNA, was comparable in both cell types (Fig. 4c). Similarly, cytopathic effects and accumulation of viral RNA was significantly higher in VSV infected *Nudt2*$^{-/-}$ MEFs as compared to controls (Fig. 4d, Supplementary Fig. 4d). The observed increase in viral RNA levels was specific to PPP-RNA generating VSV, since wt and *Nudt2* deficient cells showed similar accumulation of mRNA for HSV-1 and SFV (Fig. 4d), which do not generate PPP-RNA. We concluded from these studies that mouse Nudt2 impairs growth of PPP-RNA generating viruses, but it does not affect accumulation of other viruses.

Overall, NUDT2 is part of a degradation pathway specifically targeting viral nucleic acids. With its broad activity of removing phosphates from a wide variety of single- and double-stranded triphosphorylated RNA substrates, the degradation of the RNA body by exonucleases like XRN1 can be initiated.

Discussion

RNA turnover is a highly conserved process and tightly controlled to regulate RNA abundance and to target erroneous RNAs for degradation. Viral triphosphorylated RNA cannot be degraded by known cellular decay pathways, yet, the disposal of viral nucleic acids appears to be a fundamental component of the cellular antiviral response (*25, 26*). Interestingly, when synthetic Hepatitis C virus (HCV) RNA is electroporated into cells, it is degraded rapidly with a half-life of ~1.5-2.0 hours (*27*). In contrast the half-life of cellular mRNAs is with a median of 9 hours much more stable (*28*). In addition, decay of HCV-RNA, for instance, is XRN1-dependent (*29*) and regulates virus persistence and spread. It was however unclear how HCV-RNA is processed to serve as substrate for XRN1, which exclusively acts on 5'-P RNA. Stanley Lemon and others hypothesized that an as yet unidentified cellular pyrophosphatase has to prepare the HCV-RNA for degradation (*30-32*). Using a siRNA screen and phosphate release assays, we identified the protein NUDT2 to have an impact on virus growth and the capability to release phosphates from 5'-PPP RNA substrates. NUDT2 is active on a broad range of triphosphorylated RNA substrates, potentially hinting towards involvement of NUDT2 activity in degradation of RNAs derived from diverse viruses. By releasing two phosphates in a sequential manner, a monophosphorylated RNA is generated that can serve as a substrate for the cellular exonuclease XRN1.

Since the Nudix hydrolase RppH was already shown to play a role in the dephosphorylation of 5'-PPP RNA in bacteria (*3*) and NUDT2 itself is highly conserved throughout evolution, this form of antiviral immunity may represent an ancient antiviral defense mechanism. Although the sequence and structure of different Nudix hydrolases differs a lot and homology searches would not suggest a high similarity of NUDT2 and RppH, the mechanism of dephosphorylating 5'-PPP RNA is shared by both Nudix hydrolases.

6. Publication 1

The importance of RNA degradation is highlighted by the fact that many viruses evolved mechanisms to evade such RNA decay pathways and potentially hide from NUDT2 activity. Potential evasion strategies include capping of RNA by either employing the virus-derived capping machinery or seizing it from cellular mRNAs in a process called cap snatching (*33, 34*) thereby shielding the 5'-PPP group from NUDT2 activity. Other RNA viruses like viruses of the family Caliciviridae protect their RNA by attaching a viral genome-linked protein (VPg). RNA of some viruses like Picornaviruses carry a structural element named internal ribosome entry site (IRES) that could as well present a barrier for exonucleases like XRN1 (*35*). HCV employs an unconventional mechanism to protect its RNA from degradation. It recruits the liver-specific microRNA miR-122 to its 5'-end. By complementary binding to the HCV RNA, the RNA was shown to be protected from degradation by XRN1 (*36*) by sterically hindering binding to the 5'-end. Activity of NUDT2 would likely be inhibited in the same way. Flaviruses employ a different evasion strategy. Formation of membranous replication factories covers viral RNA from cellular proteins (*37*). It is not clear yet, if NUDT2 is able to access such intracellular sub-compartments or if the activity of NUDT2 is limited to free 5'-PPP RNAs in the cytoplasm. Screening the impact of NUDT2 on more viruses would greatly enhance our understanding of the impact of NUDT2 dependent viral restriction and RNA decay. Moreover, we cannot exclude that other cellular pyrophosphatases have redundant functions. Testing their activity on the growth of other virus classes will be the focus of further studies.

With PPP-RNA as novel substrate identified for NUDT2, one could hypothesize that not only viral 5'-PPP RNAs, but also endogenous 5'-PPP-RNAs are processed by NUDT2. It is commonly believed that such RNAs rarely exist in cells, evidenced by minute activation of RIG-I by endogenous RNA. Endogenous PPP-RNA would have detrimental effects due to chronic and inappropriate activation of the antiviral immune response, which could lead to autoinflammation. Few RNA Polymerase III transcripts including noncoding RNAs and the 5S ribosomal RNA could potentially remain with unprocessed 5'-PPP ends. In addition, RNA Polymerase III transcripts were shown to serve as well as mRNAs generating functional proteins without bearing a 5'-cap structure or poly(A) tail (*38*), although they may be

stimulatory. Thereby, this could indicate that NUDT2 plays an additional role in clearing the cell from such potential self-stimulatory nucleic acids. Sequencing genomes of patients with interferonopathies could give more detailed insights into the relevance of NUDT2 in the development of autoinflammatory diseases. However, *Nudt2*$^{-/-}$ mice do not show any phenotype. Some autoinflammatory diseases only become evident by triggering the system. Therefore, events leading to an increase in RNA production could be necessary to induce autoinflammatory phenotypes in mice or patients.

Given that clearance of viral nucleic acids from infected cells is of fundamental importance for antiviral immunity, we envisage a central role of the highly conserved protein NUDT2 in launching a novel RNA degradation pathway specific to viral nucleic acids. RNA degradation mechanisms would target the virus at its most vulnerable point: its genetic integrity and the ability to transfer its information between cells. Here we show that NUDT2 serves as cellular factor that pertains viral RNA integrity and reduces the ability of viruses to spread.

6. Publication 1

Laudenbach *et al.*

Author Contributions

B.T.L., A.R., and B.H. conducted experiments. B.T.L and A.R. analyzed data. A.M. performed homology searches. J.L. contributed critical reagents. B.T.L. and A.P. designed the experiments and wrote the paper.

Acknowledgements

We want to acknowledge the innate immunity laboratory for critical discussions and suggestions. We further thank Korbinian Mayr, Igor Paron and Gaby Sowa for maintaining mass spectrometers and the MPI-B core facility for support. We further thank Georg Kochs for the A549 cells, Soren Riis Paludan for HSV-1, Gerd Zimmer for VSV-Luc, Andres Merits for SFV and Marco Binder for the pFK-JFH plasmid. Work in the author's laboratories was supported by the Max-Planck Free Floater program, an ERC starting grant (ERC-StG iVIP, 311339), the German Research Foundation (PI 1084/2, PI 1084/3 and TRR179, MS 632/15), Infect-Era and the German Federal Ministry of Education and Research (ERASE) to A.P.

Competing financial interests

The authors declare no competing financial interests.

Materials and Methods

Cells, reagents and viruses

HeLa and HEK293T cells were described previously (*39*). Huh7.5 cells were a kind gift of Marco Binder (DKFZ, Germany) and A549 cells of Georg Kochs (University of Freiburg, Germany). Mouse embryonic fibroblasts (MEFs) were isolated from 13.5 day old embryos from heterozygous breeding pairs. Murine bone marrow-derived macrophages were generated by culturing bone marrow from mouse femur and tibia in DMEM supplemented with 10% fetal calf serum, 10 mM HEPES pH 7.4, 1 mM sodium pyruvate and 2 mM L-glutamine. Cell lines were maintained in DMEM (PAA Laboratories) containing 10% fetal calf serum (GE Healthcare) and antibiotics (100 U/ml penicillin, 100 µg/ml streptomycin).

All viruses used are classified as BSL2 pathogens in Germany and all experiments were carried out according to official regulations. A/SC35M-NS1-2A-Renilla-2A-NEP (FluAV-ren) (*40*), VSV, VSV-M2 (*41*), VSV-GFP, VSV-AV3-GFP have been previously described. HSV-1 (F-strain) was from Soren Riis Paludan (Uni Aarhus, Denmark), VSV-Luc was a gift from Gert Zimmer (University Bern, Switzerland) and SFV was a gift from Andres Merits (University of Tartu, Estonia).

Recombinant XRN1, CIP and RppH and restriction enzymes for in vitro transcriptions were obtained from NEB, single nucleotides for in vitro transcriptions and phosphate release assays were from Jena Bioscience, RNasin was from Promega, TURBO DNase was obtained from Thermo Fisher Scientific and T7 RNA polymerase was produced by the Core Facility of the MPI of Biochemistry. The CellTiter-Glo assay kit and the luciferase substrate d-Luciferin (E1602) were purchased from Promega. siRNAs were purchased from Qiagen or were synthesized by the Core Facility of the MPI of Biochemistry (see Supplementary Table 1)

Primary antibodies used in this study were as follows: NUDT2 (Santa Cruz: sc-271410), β-Actin (Santa Cruz: sc-47778 HRP) and secondary antibodies detecting mouse IgG (Jackson ImmunoResearch, Dako) were horseradish peroxidase (HRP)-coupled.

Preparation of triphosphorylated RNA

As RNA substrate, IVT4, a defined double-stranded triphosphorylated RIG-I ligand was used as described (*11*). The DNA template was generated from pairs of complementary oligodeoxynucleotides (Supplementary Table 2).

To test the sequence specificity of NUDT2, RNA substrates with varying starting nucleotides including single-stranded and double-stranded 5-ends were used as described (*42*). For in vitro transcription, DNA templates were generated from annealed pairs of complementary oligodeoxynucleotides (Supplementary Table 2). RNA Sequences beginning with 5'-AG contained a T7 φ2.5 promoter; all other templates contained a T7 φ6.5 promoter. Single-stranded oligo templates were mixed 1:1 at a final concentration of 10 µM each in 25mM Tris pH 7.4 and 25mM NaCl, heated to 95 °C for 5 min, and slow-cooled on the bench. For preparation of HCV RNA, the pFK-JFH plasmid DNA (*43*) was linearized by MluI cleavage.

Transcription was carried out for 6-8 hours at 37 °C in 5x transcription buffer (200mM Tris pH 8, 30mM $MgCl_2$, 10mM Spermidine and 5mM DTT), 2.5 mM ATP, 2.5 mM UTP, 2.5 mM CTP, 2.5 mM GTP, RNasin (Promega), and 1000 U T7 RNA polymerase (Core Facility of the MPI of Biochemistry), in 100µl final volume. 2µl TURBO DNase (Thermo Fisher Scientific) was added for 30 minutes at 37°C. Reactions were purified with mini Quick Spin RNA Columns (Roche) according to the manufacturer's protocol.

For the 44mer single stranded RNA the pGEX-6P-T7-44mer-RNA (*44*) plasmid linearized by EcoRI cleavage served as template. RNA was synthesized by in vitro transcription according to the MEGAscript T7 Kit (Thermo Fisher Scientific). After incubation for 16h at 37°C and TURBO DNase (Thermo Fisher Scientific) treatment for 30 minutes at 37°C, the RNA was purified according to the Direct-zol RNA extraction kit (Zymo Research). For generation of double stranded RNA a 20nt antisense RNA (Metabion) (5'- acucucucucucucucccc-3') was annealed to the in vitro transcribed RNA.

siRNA-mediated knockdown experiments

Duplex siRNAs were transfected using either siPrime transfection reagent (GE Healthcare) for the Nudix Hydrolase siRNA screen or Metafectine Pro transfection reagent with the SI^+ Buffer (Biontex) for targeted gene knockdowns.

Transfection was performed according to the manufacturer's instructions for HeLa or A549 cells. Briefly, we transfected 15 pmol of pooled siRNAs per 1×10^5 cells in a 24 well format. Cells were infected 48 hours after siRNA knockdown. Duplex siRNAs were either purchased from Qiagen or synthesized by the Core Facility at the MPI of Biochemistry (Supplementary Table 1). Cell viability after siRNA-mediated knockdown was assessed with the CellTiter-Glo (Promega) luminescent cell viability assay according to the manufacturer's protocol.

Virus infections and determination of virus titres and growth

To determine the impact of *Nudt2* knockout on virus growth, MEFs and bone marrows were seeded the day before infection. Cells were infected with VSV wt at a multiplicity of infection (MOI) of 0.001, SFV at a MOI of 0.001, HSV-1 at a MOI of 2, VSV-luc at an MOI of 0.001, FluAV-renilla at an MOI of 0.1, and HSV-luc at an MOI of 2. Only for bone marrows, cells were infected with VSV wt, VSV M2 and VSV AV3-GFP at a MOI of 1. 24 h post infection or as indicated specifically in the Fig. legend, cells were harvested for quantitative RT-PCR, Western Blot or and supernatant was harvested to test for virus accumulation by 50% tissue culture-infective dose (TCID50) assays on Vero E6 cells.

To quantify the effects of siRNA-mediated knockdown of Nudix hydrolases, cells were infected 48h after the knockdown was performed with VSV-Luciferase at an MOI of 0.001 for 24h, IAV-Renilla at an MOI of 1 for 48h, VSV-GFP at an MOI of 0.001 for 24h, and VSV-M2-GFP at an MOI of 0.0001 for 24h. GFP-levels were determined fluorometrically. Z-scores were calculated from three independent experiments individually for every gene and virus.

For RT PCR analysis, RNA was isolated using the NucleoSpin RNA Plus kit (Macherey Nagel) according to the manufacturer`s protocol. For proteomic analysis, cell pellets were snap frozen in liquid

nitrogen before further processing. For western blot analysis, cells were lysed in Laemmli buffer, boiled for 10 min at 95 °C and subjected to SDS-polyacrylamide gel electrophoresis and western blot analysis. For GFP-tagged viruses, virus growth was measured by determining GFP levels in a microplate reader (Tecan Infinite 200 Pro) with an excitation wavelength of 485nm and an emission wavelength of 535 nm. For luciferase-tagged viruses, cells were lysed in Passive Lysis Buffer (Promega) and virus load was determined by measuring Firefly or Renilla-luciferase.

Protein expression and purification

DNA sequences of NUDT2, NUDT2 E58A, NUDT12, NUDT12 E369A, NUDT14, NUDT14 E121A, NUDT17, NUDT17 E124A were obtained as gBlocks from IDT containing overhangs suitable for SLIC cloning. All constructs were cloned into pCoofy4 providing a *N*-terminal His6-MBP tag. Protein expression and purification was performed by the Core Facility of the MPI of Biochemistry. Briefly, plasmids were transformed in BL21 -AI pRARE bacteria and protein expression was carried out in autoinduction medium containing 0.2% arabinose. Cells were lysed using an AVESTIN high pressure homogenizers and cleared lysate was used for protein purification using a HisTrap HP column (GE Healthcare: 17-5247-01) and further purified by gel filtration using a Superose 6 PC 3.2/30 (GE Healthcare: 17-0673-01) (mobile phase: 20 mM Tris-HCl pH 7.5, 250 mM NaCl, 10mM $MgCl_2$). Proteins were dialyzed with D-Tube Dialyser Midi (cutoff 6-8kDa) in a buffer containing 20 mM Tris-HCl pH 7.5, 250 mM NaCl, 10mM $MgCl_2$ and 1mM DTT. Identity of recombinant proteins was confirmed by mass spectrometry.

Phosphate release assay

The ability of NUDIX hydrolases to release phosphates from RNA was tested with a double-stranded RNA. The assay was performed with 900ng substrate and two enzyme concentrations of recombinant NUDIX hydrolases (NUDT2, NUDT2 E58A, NUDT12, NUDT12 E369A, NUDT14, NUDT14 E121A,

NUDT17, NUDT17 E124A), low (300nM) and high (600nM). Activity was assessed in triplicates in NEB2 buffer after incubating for 3 h at 37°C.

In order to test NUDT2 activity on a panel of possible substrates, NUDT2 (600nM) and NUDT2 E58A (600nM) were incubated for 3 h with substrates (2.5µM) including ATP, GTP, UTP, CTP, double-stranded RNA, and single-stranded RNA at 37°C in NEB2 reaction buffer.

To assess sequence specificity of NUDT2, RNAs with different starting nucleotides including double-stranded and single-stranded 5'-ends (1200ng) were tested with NUDT2 and NUDT2 E58A at low (300nM) and high (600nM) concentrations. Incubation of substrate and enzyme was performed in NEB2 reaction buffer for 3 h at 37°C. CIP (10U) (NEB) and RppH (5U) (NEB) served as controls for released inorganic phosphate in all experiments. The generated inorganic phosphate was detected after 2 hours of incubation by addition of 50µl malachite green reagent (1 volume 4.2 % [w/v] ammonium molybdate in 4 N HCl, 3 volumes 0.045 % [w/v] Malachite green solution and 0.01% v/v Tween20) to 25µl reaction samples in 384-well plates. The absorbance was read at 600nm in a microplate reader (Tecan Infinite 200 Pro). The amount of phosphate released is calculated from a phosphate standard curve.

Phosphate release from γ-32P-labelled RNA

γ-32P labelled RNA was synthesized by in vitro transcription according to the MEGAscript T7 Kit (Thermo Fisher Scientific) supplemented with 0.17µM [γ-32P] GTP (Perkin Elmer). For the 44mer single stranded RNA, the pGEX-6P-T7-44mer-RNA (10.1038/nature11783) plasmid linearized by EcoRI cleavage served as template. For the dsRNA IVT4, two annealed primer pairs (Supplementary Table 2) (*11*) were used as template. After incubation for 16h at 37°C and DNase digestion with TURBO DNase (Thermo Fisher Scientific) for 30 minutes at 37°C, the RNA was purified according to the Direct-zol RNA extraction kit (Zymo Research). For generation of a double stranded RNA of the 44mer ssRNA a 20nt antisense RNA (Metabion) (5'- acucucucucucucucccc-3') was annealed to the in vitro transcribed RNA.

The labelled RNAs were incubated with purified NUDT2 (600nM), NUDT12 (600nM), NUDT14 (600nM), NUDT17 (600nM), and RppH (10units) purchased from NEB in a solution (20µl) containing NEB2 Buffer (1x) at 37°C. Reaction samples (10µl) were taken at 0 and 90 minutes and quenched with 2.5 µl of EDTA (100 mM, pH 8.0), analyzed by TLC on PEI-cellulose (Merck Millipore) and developed with potassium phosphate buffer (0.3 M, pH 7.5). Spot intensities imaged by using a GE Typhoon FLA 9000 Imager.

For time course experiments the labelled RNA was incubated with purified NUDT2 or NUDT2 E58A (600nM) in a solution (50µl) containing NEB2 Buffer (1x) for 0–90 min at 37 °C. Reaction samples (10 µl) were quenched at time intervals with 2.5 µl of EDTA (100 mM, pH 8.0) and analyzed by TLC on PEI-cellulose (Merck Millipore) developed with potassium phosphate buffer (0.3 M, pH 7.5). Spot intensities imaged by using a GE Typhoon FLA 9000 Imager.

Synthesis of pppApG and pppGpA

Dinucleotides were synthesized using DMT-2′-O-TBDMS-rA(bz), DMT-2′-O-TBMDS-rG(ib) amidites and rA(Bz) and rG(ibu) CPG (Chemgenes) on 10-micromol scale by using standard solid phase oligoribonucleotide coupling techniques. The CPG-bound dimers were triphosphorylated using the cyclotriphosphate protocol of triphosphate synthesis (*45*), with the exception that after deprotection of the dinucleotides the reaction mixture was converted into the triethylamoniumsalt using Dowex Et3NH+ before reverse phase chromatography on a Source RP column. DecNHpppApG and DecNHpppGpA RP-HPLC product peaks were converted into pppApG and pppGpA as described, the pure pppGpA and pppApG was isolated as triethylammoniumsalts by ion exchange chromatography on a Hi Screen DEAE FF column using a gradient of 0-0.6 MTriethylammonium bicarbonate . The structure of the pppApG and pppGpA dimers was verified by LC-MS analysis.

HPLC Analysis

A short RNA (pppGpA, 0.1 OD260) was incubated for 2 h at 37°C in a solution (15µl) containing NEB2 Buffer (1x) with recombinant NUDT2 (600nM), NUDT2 E58A (600nM), RppH (5 units) or left untreated. Reactions mixtures were quenched with 3.75 µl of EDTA (100 mM, pH 8.0) and diluted 1:20 with water. For timecourse measurements, the two short RNAs (pppGpA or pppApG, 0.1 OD260 each) were incubated with purified recombinant NUDT2 (600nM), NUDT14 (600nM), and NUDT2 E58A (600nM), respectively, in a solution (75µl) containing NEB2 Buffer (1x) at 37°C. Reaction samples (15µl) were taken after 0, 1, 3, 6 and 19 hours, quenched with 3.75 µl of EDTA (100 mM, pH 8.0) and diluted 1:20 with water. Aliquots (80 µl) were analyzed by reversed phase (RP)-HPLC on an AGILENT 1100 System using an XBridge C18 column (3.5 µm, 150x2.1mm, WATERS). Chromatography was performed using a two eluent buffer system. Buffer A consists of an aqueous solution of 100 mM Et3NHOAc, pH 7.8, and buffer B consists of an aqueous solution of 100 mM Et3NHOAc, pH 7.8 and 40% (v/v) MeCN. Chromatograms were recorded at a wavelength of 260 nm. HPLC was performed using the following gradient condition: 0% B over 4 min, to 15% B over 20 min, to 18% B over 16 min to 100% B over 10 min, held at 100% B for 15 min, to 0% B over 2 min, held at 0% B for 13 min with a flow rate of 0.3 ml/min. Quantification of eluted compounds was performed by integration of the corresponding peak areas.

Assessment of RNA integrity

To assess RNA integrity after treatment with recombinant Nudix Hydrolases, small reaction samples were analyzed by the Bioanalyzer (Agilent) using the Agilent Small RNA kit according to the manufacturer's protocol.

Quantitative RT PCR analysis

Total RNA was isolated using the NucleoSpin RNA Plus kit (Machery-Nagel). Next, 200–500 ng of RNA was reverse-transcribed with PrimeScript RT Master Mix (TAKARA) and thereafter quantified by real-time PCR using the QuantiFast SYBR Green RT-PCR Kit (Qiagen) and a CFX96 Touch Real-Time PCR

Detection System (Bio-Rad). Each cycle included 10 s at 95 °C and 30 s at 60 °C, followed by a melting curve analysis. Primer sequences are depicted in Supplementary Table 3.

Generation of CRISPR/Cas9 knockout cells

Double-stranded 30 nucleotide guide sequences (Supplementary Table 4) targeting the human *Nudt2* and *Xrn1* gene, were designed and cloned into pLentiCRISPRv2 (Addgene #52961) as previously described (*46, 47*). HEK 293T cells were co-transfected with the obtained plentiCRISPR v2 vector (6 µg), pxPAX2 (3 µg) and pMD2G (1.5 µg) in a 10cm dish using PEI. 24 h post-transfection, the medium was replaced with 10 ml of fresh DMEM. 72 h post-transfection the medium was collected, filtered through a 0.45 µm pore size membrane (Millipore) and Huh7.5 cells were infected with the lentivirus. 24 h post-infection, medium was replaced with DMEM containing puromycin (1 µg/ml) for four passages. Knockout efficiency was analyzed by western blotting.

RNA degradation assays

Degradation of 1000ng of an in vitro transcribed HCV RNA carrying a firefly luciferase was assessed by incubating it either with 10 u RNase, 600 nM recombinant NUDT2, 1 unit recombinant XRN1 or both 600 nM NUDT2 and 1 unit XRN1 for 4h at 37°C. To determine RNA levels after incubation, firefly luciferase RNA was quantified using qPCR.

Degradation of viral RNA, was evaluated in cell culture. Huh7.5 cells carrying a knockout of NUDT2, XRN1 or a double-knockout of NUDT2 and XRN1 were infected on ice with VSV wt at MOI 1for 1 h. Cycloheximid was added when cells were shifted to 37°C. Total RNA was harvested 4 h post infection. Viral RNA levels were quantified using qPCR.

Generation of Nudt2 knockout mice

The *Nudt2* allele was deleted by introducing a poly(A) signal after exon 1 in a construct purchased from the European Conditional Mouse Mutagenesis consortium (EUCOMM). This genetically modified ES

cell clone (Clone ID: EPD0146_2_H06, Cell type: JM8.N4) was injected into C57BL/6 blastocyst donors. Male chimeras were bred with C57BL/6 females to produce heterozygous Nudt2 tm1a mice containing a cassette encoding for the lacZ gene, a neomycin resistance, a splice acceptor and a polyA site flanked by FRT sites.

For genotyping Nudt2 knockout mice, ear punches were collected from 21-23-day old mice and genotyped by PCR using the following primers: Nudt2_fwd: 5'-ccagctttcttgtacaaagtgg-3', Nudt2 wt_fwd: 5'-gaatttctgctgctgcaggc-3', Nudt2_rev: 5'-cctagtgaagggacaaagcagc-3'and using the following parameters: 94°C for 1 min, followed by 35 cycles of 94°C for 30 s, 65°C for 20 s, and 72°C for 1 min. The wildtype allele was detected as a band at 492 bp, whereas the inserted tm1a cassette was detected as bands of 417 bp and 912bp.

lacZ expression in mouse organs

For determining expression levels of Nudt2 in different mouse organs, tissue of wild-type and heterozygous mice were isolated and lysed using a FastPrep-24 homogenizer with SS matrix beads (MP Biomedicals). Lysates were cleared by centrifugation and the β-galactosidase expression driven from the lacZ gene of the tm1a cassette was assessed by the FluoReporter lacZ/Galactosidase Quantification kit (Thermo Fisher Scientific) according to the manufacturer's protocol except that the assay was performed in a 384-well format and half of the indicated volumes were used.

Proteomic analysis of Nudt2 knock-out in mouse bone marrow cells

For proteomic analysis, wildtype and Nudt2 knockout bone marrow cells ($5x10^6$/cell line/replicate; 4 replicates) were lysed in 300µl of lysis buffer (4% SDS, 10 mM DTT in 50 mM Tris pH 7.6) supplemented with complete protease inhibitor (Roche) and boiled for 10 minutes at 95°C. Protein concentration of cleared cell lysates was assessed using Pierce 660nm Protein Assay (Thermo Fisher Scientific) according to the manufacturer's protocol. Protein concentrations for all cell lines and replicates were equalized to 35µg protein content and alkylated with 55 mM IAA for 20 min in the dark. Proteins

were precipitated with acetone and resuspended in 150µl of denaturation buffer (6 M Urea / 2 M Thiourea in 10 mM HEPES pH 8.0). Protein digestion was performed by adding 1:100 (protein:enzyme) trypsin and LysC overnight at room temperature and peptides were purified on stage tips and analysed by LC-MS/MS using the Easy nano LC 1200 system coupled to a Q Exactive HF mass spectrometer (Thermo Fisher Scientific). Peptide mixtures were separated on a 50cm C18-reversed phase column (Reprosil-Pur 120 C18-AQ, 1.9 µM, 200×0.075 mm; Dr. Maisch) using a 180 minute linear gradient of 5 to 30% buffer B (0.1% formic acid and 80% ACN) with a flow rate of 250 nL/min. The mass spectrometer was set up to run a Top10 method acquiring full scans (300-1,600 m/z, R = 60,000 at 200 m/z) at a target of 3e6 ions, followed by isolation of the ten most abundant ions, HCD fragmentation (target 1e5 ions, maximum injection time 120 ms, isolation window 1.4 m/z, NCE 27%, and underfill ratio of 20%) and detection the Orbitrap cell.

Phylogenetic Analysis

To establish the phylogenetic relationship between *different human Nudix hydrolases and bacterial RppH*, protein sequences from all H. sapiens Nudix hydrolases and E.coli RppH were analyzed using the ClustalW tool

Homology Searches

Orthologous sequences were collected using the web-server morFeus (*48*) (http://chimborazo.biochem.mpg.de/morfeus). The multiple sequence alignment was generated using mafft (*49*) and submitted to the Gblocks web-server (*50*) to select conserved blocks for further phylogenetic analysis. The phylogenetic tree was calculated with Phyml (*51*) using standard parameters and bootstrapping with 100 iterations. The resulting tree was displayed using Dendroscope (*52*) and visually adapted using Adobe Illustrator.

Figure Legends

Figure 1: Nudix hydrolases prepare RNA for degradation

(a) Schematic representation of processes involved in 5'-3' RNA degradation. Eukaryotic and bacterial messenger (m)RNA are processed by proteins DCP2 and RppH, respectively, to generate monophosphorylated substrates for the 5'-3' exonuclease XRN1 or RNase E. We hypothesize that a mammalian Nudix Hydrolase could prepare viral RNA for degradation by removing pyrophosphate groups. **(b)** GFP expression in HeLa cells that were transfected with siRNA pools targeting the indicated NUDT gene for 48 hours and infected with VSV-GFP (x-axis) or VSV-AV3-GFP (y-axis). 24 h after infection GFP expression was analysed by fluorometric anaylsis for GFP. Dot colour indicates maximum z-score of the two viruses. **(c)** A549 cells (left panel) or HeLa cells (right panel) were treated with siRNA pools for 48 hours targeting NUDT2, NUDT12, NUDT14, NUDT17 or non-targeting siRNA control (siScrambled) and infected with Influenza A reporter virus expressing the renilla luciferase at MOI 1 . 48 h post infection renilla luciferase activity was determined by luminescence measurements. Histograms show means of three technical replicates and SE of three independent measurements. RLU, relative light units; *** $P<0.001$, ** $P<0.01$, * $P<0.05$ as analyzed by two-way analysis of variance (ANOVA) statistics with Bonferroni`s post-test.

Figure 2: Nudt2 releases phosphates from a triphosphorylated RNA substrate

(a) Coomassie gel of His6-MBP-tagged recombinant Nudix hydrolases including mutants having point mutations in the catalytic Nudix box. **(b)** Phosphate release activity of recombinant wildtype and mutant Nudix hydrolases at low (300nM) and high (600nM) concentration and CIP as control. Phosphate release activity was assessed after 3 h incubation in a malachite green assay using 900ng *in vitro* transcribed double-stranded triphosphorylated RNA (IVT4) as substrate. One out of three independent experiments with similar results is shown. **(c)** RNA was incubated for 3h with the indicated Nudix hydrolase and its integrity was determined using a Bioanalyzer. **(d)** As (b), but 900ng single-stranded triphosphorylated RNA was used as substrate for the indicated recombinant protein. **(e)** As (b) but 2.5µM single nucleotides

were included as additional substrates for NUDT2. 2.5µM 44mer double-stranded RNA was used as control. One out of three independent experiment is shown.

Figure 3: NUDT2 is preparing RNA to serve as a substrate for XRN1

(a) γ-32P-radiolabelled in vitro transcribed 44mer ssRNA substrate was left untreated or was subjected to a 4 h incubation of 600nM NUDT2, NUDT12, NUDT14, NUDT17 or RppH at 37°C. Reaction mixtures were analyzed by TLC and autoradiography. P_i, organic phosphate; remaining input RNA after treatment in comparison to untreated RNA is depicted on the bottom. **(b)** RNA species generated by mock-treatment, or incubation with NUDT2, NUDT2 E58A, or RppH of a very short triphosphorylated RNA substrate (pppGpA) for 2h at 37°C were separated by HPLC. Histograms show the absorbance at 260nm. **(c)** Separation of RNA species by HPLC of a short RNA substrate (pppGpA) treated with 600nM NUDT2 for 0 h, 1h, or 19h. **(d)** Time-resolved quantification of the amount of generated RNA species after treatment of pppGpa with 600 nM NUDT2 or NUDT2 E58A. **(e)** HCV-firefly luciferase RNA levels after mock-treatment or incubation with 10 u RNase, 600nM NUDT2, 1 u XRN1 or 600 nM NUDT2 together with 1u XRN1. RNA was amplified and quantified by qRT-PCR using primers specific to the firefly luciferase tag. Histogram shows the fold change compared to input RNA and SD of two independent experiments **(f)** Degradation of incoming viral RNA was determined by infecting Huh 7.5 cells lacking the exonuclease XRN1, NUDT2, XRN1 and NUDT2, or NUDT17 as control with VSV at MOI 1. Virus replication blocked using cycloheximid. Total RNA was isolated 4h post infection and cycloheximid addition and levels of the N-transcript of Vesicular stomatitis virus were determined by qRT-PCR. AU, arbitrary units; VSV, Vesicular stomatitis virus.

Figure 4: Impact of Nudt2 on virus growth

(a) Depletion of the NUDT2 protein in mice was assessed by proteomic analysis of bone marrow cells isolated from *Nudt2* wildtype or *Nudt2* knockout mice. LFQ intensity of NUDT2 and GAPDH peptides is depicted. **(b)** Accumulation of infectious viral particles in supernatants of *Nudt2* wildtype or *Nudt2*

knockout bone marrow cells infected with either wildtype VSV, M2-mutated VSV, or VSV AV3-GFP at a MOI of 1 for 16 h was quantified by the TCID50 method. **(c)** Accumulation of infectious viral particles in supernatants collected to the indicated timepoints of *Nudt2* wildtype or *Nudt2* knockout MEFs infected with either wildtype VSV at a MOI of 0.001 or HSV-1 at a MOI of 2 for 16 h was quantified by the TCID50 method. **(d)** Viral RNA load in *Nudt2* wildtype and knockout MEFs infected with either VSV, HSV-1 or SFV. RNA levels were quantified by qRT-PCR analysis using specific primers for the N-transcript of VSV, DNA polymerase I of HSV or nsp3-transcript of SFV. Data were normalized to murine *ActB* RNA and the mean of two technical replicates are represented. Arbitrary units of three biological repetitions are shown. *** $P<0.001$, ** $P<0.01$, * $P<0.05$ as analyzed by two-way analysis of variance (ANOVA) statistics with Bonferroni`s post-test. LFQ, label-free-quantification; VSV, Vesicular stomatitis virus; HSV-1, Herpes simplex virus 1; SFV, Semliki forest virus.

Supplementary Figure 1: Nudix hydrolases have an impact on virus growth

(a) Cell viability was determined 72 h after siRNA knockdown using a luminescence-based assay. Relative cell viability was assessed by assuming the average cell viability of the whole siRNA screen set as 100% viable. **(b)** Phylogenetic analysis of all human Nudix hydrolases and the bacterial RppH was performed using ClustalW. **(c)** Knockdown efficiency of NUDT2, NUDT12, NUDT14 and NUDT17 was determined by quantifying the respective RNA levels in siRNA knockdown cells by qRT-PCR using primers specific for the amplification of human NUDT2, NUDT12, NUDT14 and NUDT17. The knockdown efficiency was determined in comparison to a non-targeting siRNA control (siScrambled). **(d)** NUDT2 knockdown was as well determined by Western Blot against NUDT2 and β-actin as loading control.

Suppmentary Figure 2: NUDT2 is broadly active on triphosphorylated RNA substrates

(a) Phylogenetic tree of the Nudt2 family of proteins. Nudt2 is conserved from nematodes to mammals and is also found in insects and fish. **(b-c)** Phosphate release activity of recombinant wildtype and mutant

NUDT2 in a low (300nM) and high (600nM) concentration and CIP as control was assessed after 3 h incubation on RNA substrates with varying starting nucleotides and varying lengths of single stranded 5'-ends as indicated using a malachite green assay as readout. One out of three independent experiments is shown. **(d)** Integrity of 900 ng of the indicated RNA was determined on an Agilent Small RNA chip after incubation for 3 h with 600nM recombinant wildtype NUDT2.

Supplementary Figure 3: NUDT2 cleaves the γ-phosphate of various triphosphorylated RNA substrates

(a) γ-32P-radiolabelled in vitro transcribed 44mer RNA substrate was subjected to a 4 h incubation with 600 nM NUDT2, 600nM NUDT2 E58A or 5 units RppH for the indicated time intervals and analysed by TLC and autoradiography demonstrating γ-phosphate release. P_i, organic phosphate; RNA, remaining input RNA after treatment in comparison to untreated RNA. **(b)** γ-32P-radiolabelled in vitro transcribed single-stranded 44mer RNA was subjected to a 4 h incubation of 600nM NUDT2 and 5 units RppH as control. In addition, γ-32P-radiolabelled double-stranded RNA substrates having a double-stranded 5'-end to the previously used 44mer RNA (dsRNA) or a known double-stranded RIG-I ligand (IVT4) were subjected to NUDT2 treatment. γ-phosphate (P_i) release was analysed by TLC and autoradiography. **(c)** Separation of a short RNA substrate (pppApG) treated with 600 nM NUDT2 for 0 h, 1h, or 19h by HPLC. **(d)** Time-resolved quantification of the amount of generated RNA species after treatment of pppGpA with 600 nM NUDT14. Quantification was performed by the integration of the corresponding peak area generated by HPLC separation.

Supplementary Figure 4: Characterization of *Nudt2* knockout mice

(a) Schematic overview of the inserted promoter-driven tm1a cassette. Depicted is the *Nudt2* gene locus with the cassette inserted after the first exon encoding for the lacZ gene, with a splice acceptor and a polyA site as well as a neomycin resistance. **(b)** Genotyping PCR of Nudt2 tm1a mice. PCR amplification results in a wildtype allele detectable at 492 bp, whereas the inserted tm1a casette is detectable as bands

of 417 bp and 912bp. **(c)** Mendelian ratios observed from 192 weaned animals originating from *Nudt2*$^{+/-}$ breeding pairs compared to the expected mendelian distribution. **(d)** Cytopathic effects after infection of wildtype and *Nudt2* knockout mouse embryonic fibroblasts with VSV wildtype and VSV M2.

References

1. M. Arribas-Layton, D. Wu, J. Lykke-Andersen, H. Song, Structural and functional control of the eukaryotic mRNA decapping machinery. *Biochim Biophys Acta* **1829**, 580-589 (2013).

2. O. Pellegrini, N. Mathy, C. Condon, L. Benard, In vitro assays of 5' to 3'-exoribonuclease activity. *Methods Enzymol* **448**, 167-183 (2008).

3. A. Deana, H. Celesnik, J. G. Belasco, The bacterial enzyme RppH triggers messenger RNA degradation by 5' pyrophosphate removal. *Nature* **451**, 355-358 (2008).

4. D. R. Schoenberg, The end defines the means in bacterial mRNA decay. *Nat Chem Biol* **3**, 535-536 (2007).

5. J. G. Belasco, All things must pass: contrasts and commonalities in eukaryotic and bacterial mRNA decay. *Nat Rev Mol Cell Biol* **11**, 467-478 (2010).

6. J. Carreras-Puigvert *et al.*, A comprehensive structural, biochemical and biological profiling of the human NUDIX hydrolase family. *Nat Commun* **8**, 1541 (2017).

7. A. G. McLennan, The Nudix hydrolase superfamily. *Cell Mol Life Sci* **63**, 123-143 (2006).

8. A. S. Mildvan *et al.*, Structures and mechanisms of Nudix hydrolases. *Arch Biochem Biophys* **433**, 129-143 (2005).

9. M. J. Bessman, D. N. Frick, S. F. O'Handley, The MutT proteins or "Nudix" hydrolases, a family of versatile, widely distributed, "housecleaning" enzymes. *J Biol Chem* **271**, 25059-25062 (1996).

10. D. F. Stojdl *et al.*, VSV strains with defects in their ability to shutdown innate immunity are potent systemic anti-cancer agents. *Cancer Cell* **4**, 263-275 (2003).

11. M. Goldeck, M. Schlee, G. Hartmann, V. Hornung, Enzymatic synthesis and purification of a defined RIG-I ligand. *Methods Mol Biol* **1169**, 15-25 (2014).

12. P. C. Lee, B. R. Bochner, B. N. Ames, AppppA, heat-shock stress, and cell oxidation. *Proc Natl Acad Sci U S A* **80**, 7496-7500 (1983).

13. A. G. McLennan, Dinucleoside polyphosphates-friend or foe? *Pharmacol Ther* **87**, 73-89 (2000).

14. O. Goerlich, R. Foeckler, E. Holler, Mechanism of synthesis of adenosine(5')tetraphospho(5')adenosine (AppppA) by aminoacyl-tRNA synthetases. *Eur J Biochem* **126**, 135-142 (1982).

15. O. Madrid, D. Martin, E. A. Atencia, A. Sillero, M. A. Gunther Sillero, T4 DNA ligase synthesizes dinucleoside polyphosphates. *FEBS Lett* **433**, 283-286 (1998).

16. F. Martin *et al.*, Intracellular diadenosine polyphosphates: a novel second messenger in stimulus-secretion coupling. *FASEB J* **12**, 1499-1506 (1998).

17. I. Carmi-Levy, N. Yannay-Cohen, G. Kay, E. Razin, H. Nechushtan, Diadenosine tetraphosphate hydrolase is part of the transcriptional regulation network in immunologically activated mast cells. *Mol Cell Biol* **28**, 5777-5784 (2008).

18. A. S. Marriott *et al.*, Diadenosine 5', 5'''-P(1),P(4)-tetraphosphate (Ap4A) is synthesized in response to DNA damage and inhibits the initiation of DNA replication. *DNA Repair (Amst)* **33**, 90-100 (2015).

19. S. Pype, H. Slegers, Inhibition of casein kinase II by dinucleoside polyphosphates. *Enzyme Protein* **47**, 14-21 (1993).

20. J. A. Tanner, M. Wright, E. M. Christie, M. K. Preuss, A. D. Miller, Investigation into the interactions between diadenosine 5',5'''-P1,P4-tetraphosphate and two proteins: molecular chaperone GroEL and cAMP receptor protein. *Biochemistry* **45**, 3095-3106 (2006).

21. Y. N. Lee, H. Nechushtan, N. Figov, E. Razin, The function of lysyl-tRNA synthetase and Ap4A as signaling regulators of MITF activity in FcepsilonRI-activated mast cells. *Immunity* **20**, 145-151 (2004).

22. V. N. Mutafova-Yambolieva, L. Durnin, The purinergic neurotransmitter revisited: a single substance or multiple players? *Pharmacol Ther* **144**, 162-191 (2014).

23. P. Vollmayer *et al.*, Hydrolysis of diadenosine polyphosphates by nucleotide pyrophosphatases/phosphodiesterases. *Eur J Biochem* **270**, 2971-2978 (2003).

24. A. Guranowski, Specific and nonspecific enzymes involved in the catabolism of mononucleoside and dinucleoside polyphosphates. *Pharmacol Ther* **87**, 117-139 (2000).

25. M. Schelker *et al.*, Viral RNA Degradation and Diffusion Act as a Bottleneck for the Influenza A Virus Infection Efficiency. *PLoS Comput Biol* **12**, e1005075 (2016).

26. H. Oshiumi, E. J. Mifsud, T. Daito, Links between recognition and degradation of cytoplasmic viral RNA in innate immune response. *Rev Med Virol* **26**, 90-101 (2016).

27. Y. Li, T. Masaki, D. Yamane, D. R. McGivern, S. M. Lemon, Competing and noncompeting activities of miR-122 and the 5' exonuclease Xrn1 in regulation of hepatitis C virus replication. *Proc Natl Acad Sci U S A* **110**, 1881-1886 (2013).

28. B. Schwanhausser *et al.*, Global quantification of mammalian gene expression control. *Nature* **473**, 337-342 (2011).

29. Y. Li, D. Yamane, S. M. Lemon, Dissecting the roles of the 5' exoribonucleases Xrn1 and Xrn2 in restricting hepatitis C virus replication. *J Virol* **89**, 4857-4865 (2015).

30. Y. Li, D. Yamane, T. Masaki, S. M. Lemon, The yin and yang of hepatitis C: synthesis and decay of hepatitis C virus RNA. *Nat Rev Microbiol* **13**, 544-558 (2015).

31. J. A. Wilson, A. Huys, miR-122 promotion of the hepatitis C virus life cycle: sound in the silence. *Wiley Interdiscip Rev RNA* **4**, 665-676 (2013).

32. P. A. Charley, J. Wilusz, Standing your ground to exoribonucleases: Function of Flavivirus long non-coding RNAs. *Virus Res* **212**, 70-77 (2016).

33. F. Ferron, E. Decroly, B. Selisko, B. Canard, The viral RNA capping machinery as a target for antiviral drugs. *Antiviral Res* **96**, 21-31 (2012).

34. E. Decroly, F. Ferron, J. Lescar, B. Canard, Conventional and unconventional mechanisms for capping viral mRNA. *Nat Rev Microbiol* **10**, 51-65 (2011).

35. L. Balvay, R. Soto Rifo, E. P. Ricci, D. Decimo, T. Ohlmann, Structural and functional diversity of viral IRESes. *Biochim Biophys Acta* **1789**, 542-557 (2009).

36. E. S. Machlin, P. Sarnow, S. M. Sagan, Masking the 5' terminal nucleotides of the hepatitis C virus genome by an unconventional microRNA-target RNA complex. *Proc Natl Acad Sci U S A* **108**, 3193-3198 (2011).

37. I. Romero-Brey, R. Bartenschlager, Membranous replication factories induced by plus-strand RNA viruses. *Viruses* **6**, 2826-2857 (2014).

38. S. Gunnery, M. B. Mathews, Functional mRNA can be generated by RNA polymerase III. *Mol Cell Biol* **15**, 3597-3607 (1995).

39. C. Holze *et al.*, Oxeiptosis, a ROS-induced caspase-independent apoptosis-like cell-death pathway. *Nat Immunol* **19**, 130-140 (2018).

40. P. Reuther *et al.*, Generation of a variety of stable Influenza A reporter viruses by genetic engineering of the NS gene segment. *Sci Rep* **5**, 11346 (2015).

41. M. Habjan *et al.*, Sequestration by IFIT1 impairs translation of 2'O-unmethylated capped RNA. *PLoS Pathog* **9**, e1003663 (2013).

42. P. K. Hsieh, J. Richards, Q. Liu, J. G. Belasco, Specificity of RppH-dependent RNA degradation in Bacillus subtilis. *Proc Natl Acad Sci U S A* **110**, 8864-8869 (2013).

43. T. Schaller *et al.*, Analysis of hepatitis C virus superinfection exclusion by using novel fluorochrome gene-tagged viral genomes. *J Virol* **81**, 4591-4603 (2007).

44. Y. M. Abbas, A. Pichlmair, M. W. Gorna, G. Superti-Furga, B. Nagar, Structural basis for viral 5'-PPP-RNA recognition by human IFIT proteins. *Nature* **494**, 60-64 (2013).

45. M. Goldeck, T. Tuschl, G. Hartmann, J. Ludwig, Efficient solid-phase synthesis of pppRNA by using product-specific labeling. *Angew Chem Int Ed Engl* **53**, 4694-4698 (2014).

46. N. E. Sanjana, O. Shalem, F. Zhang, Improved vectors and genome-wide libraries for CRISPR screening. *Nat Methods* **11**, 783-784 (2014).

47. O. Shalem *et al.*, Genome-scale CRISPR-Cas9 knockout screening in human cells. *Science* **343**, 84-87 (2014).

48. I. Wagner *et al.*, morFeus: a web-based program to detect remotely conserved orthologs using symmetrical best hits and orthology network scoring. *BMC Bioinformatics* **15**, 263 (2014).

49. K. Katoh, D. M. Standley, MAFFT: iterative refinement and additional methods. *Methods Mol Biol* **1079**, 131-146 (2014).

50. J. Castresana, Selection of conserved blocks from multiple alignments for their use in phylogenetic analysis. *Mol Biol Evol* **17**, 540-552 (2000).

51. S. Guindon, F. Delsuc, J. F. Dufayard, O. Gascuel, Estimating maximum likelihood phylogenies with PhyML. *Methods Mol Biol* **537**, 113-137 (2009).

52. D. H. Huson *et al.*, Dendroscope: An interactive viewer for large phylogenetic trees. *BMC Bioinformatics* **8**, 460 (2007).

Figure 1

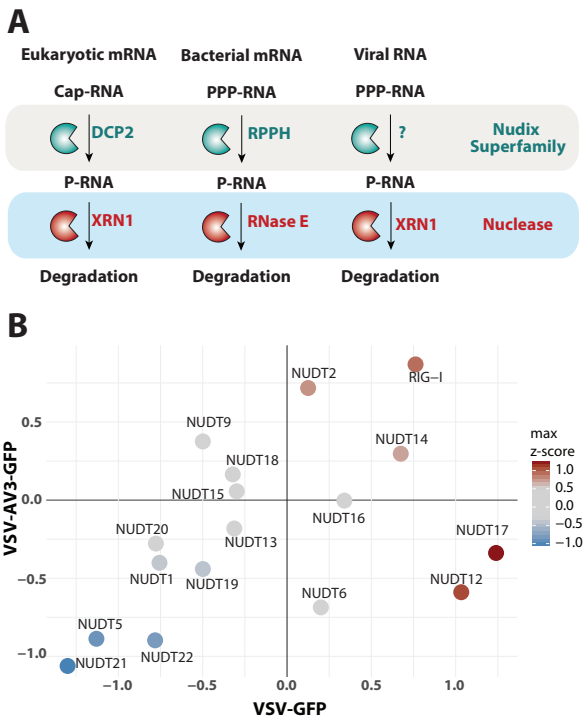
A
Eukaryotic mRNA
Bacterial mRNA
Viral RNA
Cap-RNA
PPP-RNA
PPP-RNA
DCP2
RPPH
?
Nudix Superfamily
P-RNA
P-RNA
P-RNA
XRN1
RNase E
XRN1
Nuclease
Degradation
Degradation
Degradation
B
NUDT2
RIG–I
NUDT9
NUDT14
NUDT18
NUDT15
NUDT16
NUDT17
NUDT20
NUDT13
NUDT1
NUDT19
NUDT6
NUDT12
NUDT5
NUDT22
NUDT21
VSV-AV3-GFP
VSV-GFP
max z-score
1.0
0.5
0.0
−0.5
−1.0
C
FluAV-ren
FluAV-ren
RLU X10^4
siScrambled
siNUDT2
siNUDT12
siNUDT14
siNUDT17

Figure 2

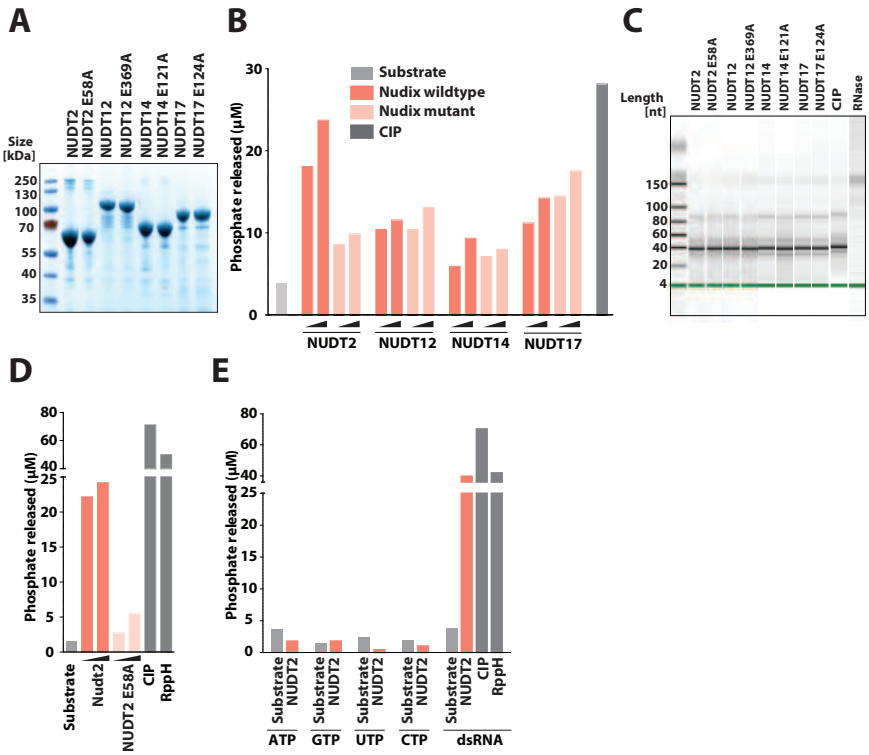
A
Size [kDa]
NUDT2
NUDT2 E58A
NUDT12
NUDT12 E369A
NUDT14
NUDT14 E121A
NUDT17
NUDT17 E124A
250
130
100
70
55
40
35
B
Substrate
Nudix wildtype
Nudix mutant
CIP
Phosphate released (µM)
30
20
10
0
NUDT2
NUDT12
NUDT14
NUDT17
C
Length [nt]
NUDT2
NUDT2 E58A
NUDT12
NUDT12 E369A
NUDT14
NUDT14 E121A
NUDT17
NUDT17 E124A
CIP
RNase
150
100
80
60
40
20
4
D
Phosphate released (µM)
80
60
40
25
20
15
10
5
0
Substrate
Nudt2
NUDT2 E58A
CIP
RppH
E
Phosphate released (µM)
80
60
40
25
20
15
10
5
0
Substrate
NUDT2
CIP
RppH
ATP
GTP
UTP
CTP
dsRNA

Figure 3

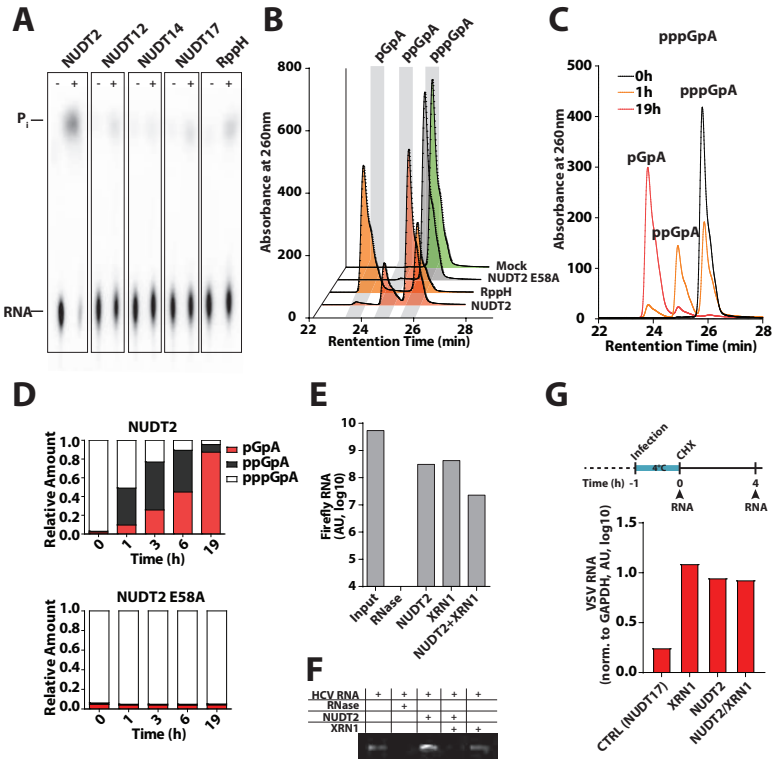
A
NUDT2
NUDT12
NUDT14
NUDT17
RppH
P i
RNA
B
pGpA
ppGpA
pppGpA
Absorbance at 260nm
Mock
NUDT2 E58A
RppH
NUDT2
Rentention Time (min)
C
pppGpA
0h
1h
19h
pGpA
ppGpA
Absorbance at 260nm
Rentention Time (min)
D
NUDT2
pGpA
ppGpA
pppGpA
Relative Amount
Time (h)
NUDT2 E58A
E
Firefly RNA (AU, log10)
Input
RNase
NUDT2
XRN1
NUDT2+XRN1
F
HCV RNA
RNase
NUDT2
XRN1
G
Infection
CHX
Time (h) -1
RNA
RNA
VSV RNA (norm. to GAPDH, AU, log10)
CTRL (NUDT17)
XRN1
NUDT2
NUDT2/XRN1

Figure 4

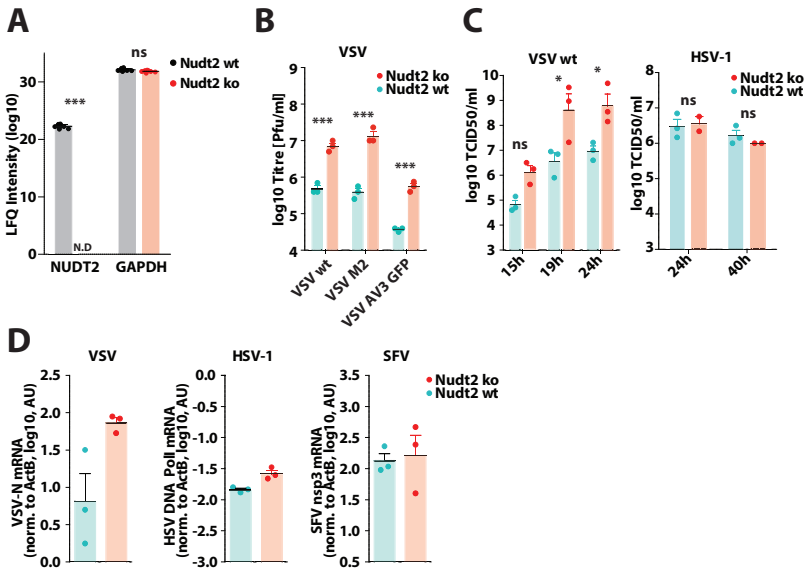
A
B
C
D
LFQ Intensity (log10)
Nudt2 wt
Nudt2 ko
ns
***
N.D
NUDT2
GAPDH
VSV
log10 Titre [Pfu/ml]
VSV wt
VSV M2
VSV AV3 GFP
VSV wt
log10 TCID50/ml
15h
19h
24h
HSV-1
24h
40h
VSV-N mRNA (norm. to ActB, log10, AU)
HSV DNA Pol mRNA (norm. to ActB, log10, AU)
SFV
SFV nsp3 mRNA (norm. to ActB, log10, AU)

Supplementary Figure 1

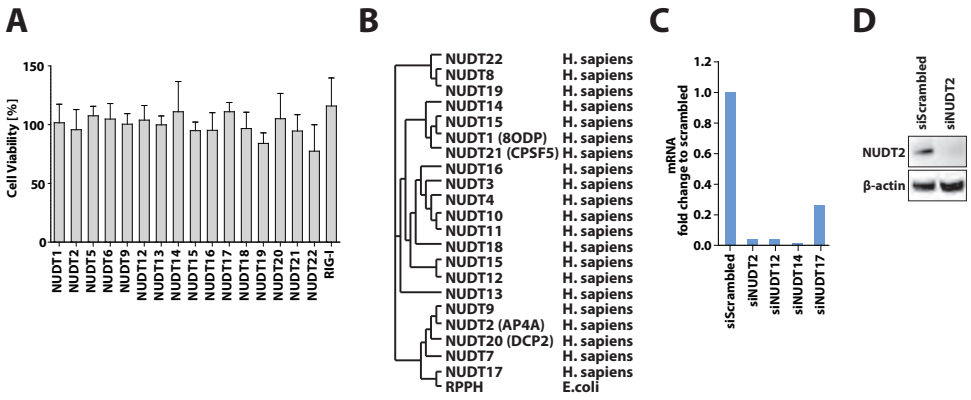

Supplementary Figure 2

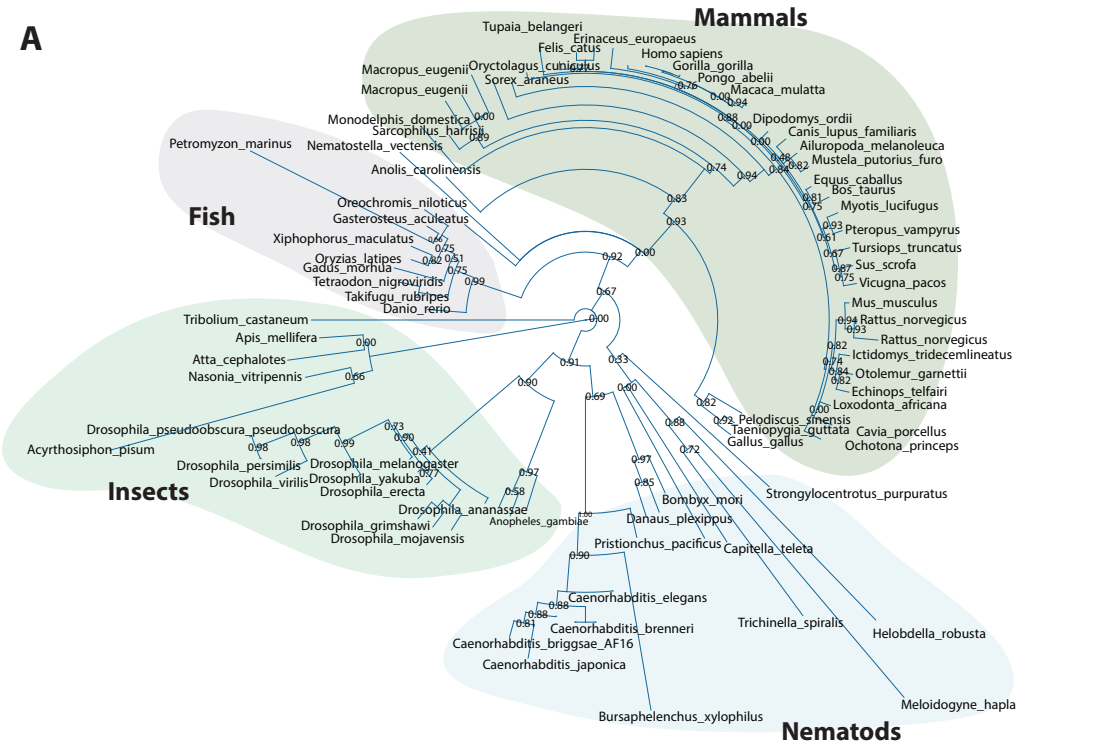

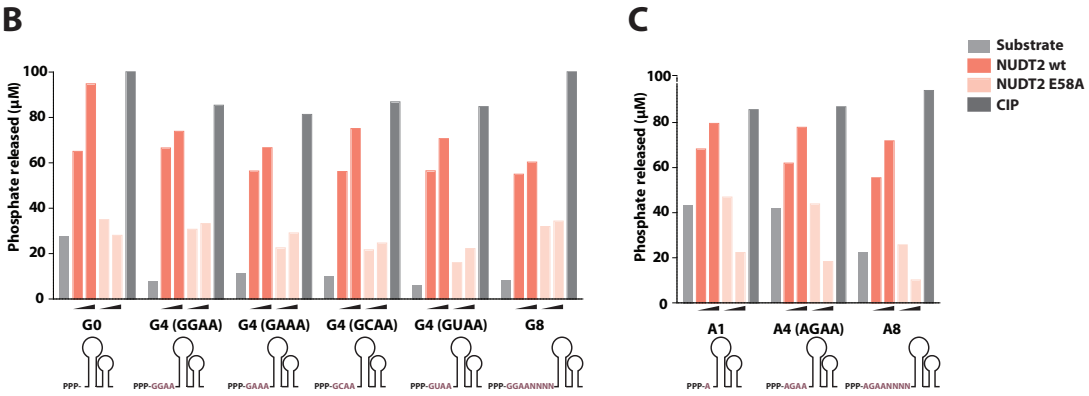

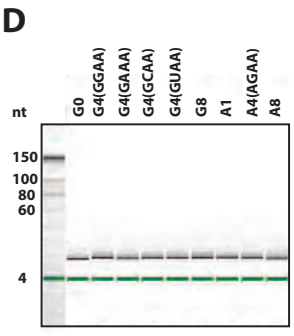

Supplementary Figure 3

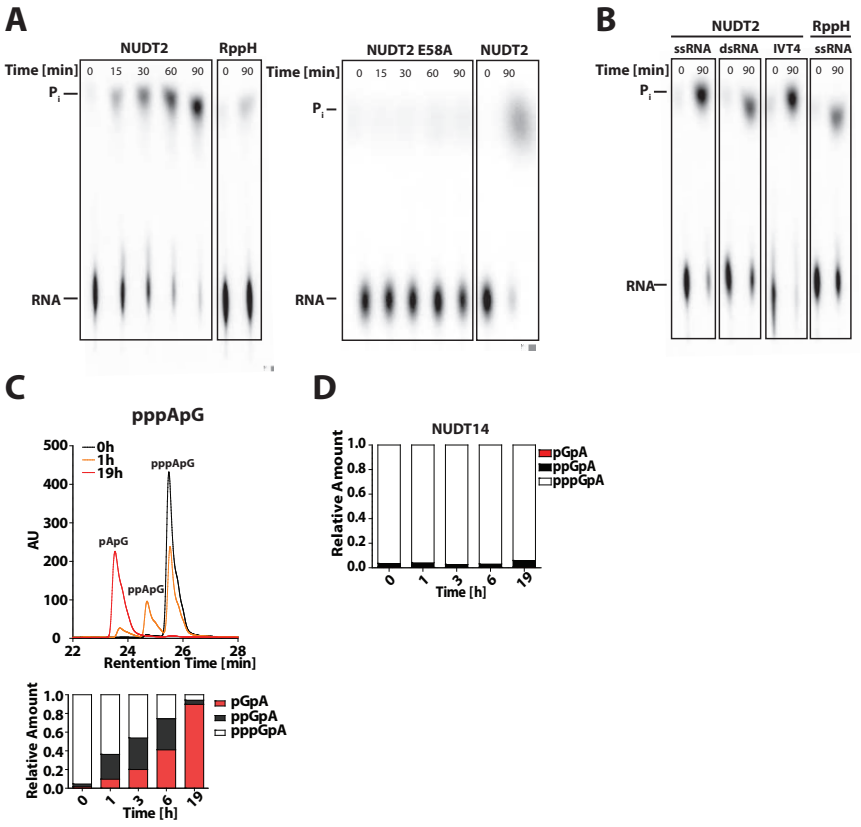

Supplementary Figure 4

A

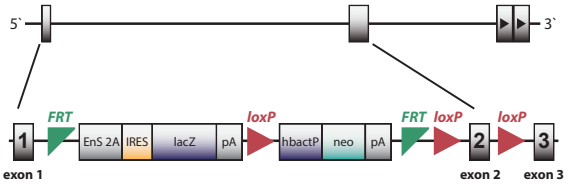

B

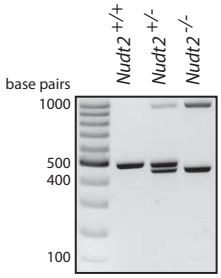

C

	Weaned Animals	
Genotype	**Oberserved**	**Expected**
Nudt2 $^{+/+}$	**53 (27.6%)**	**48 (25%)**
Nudt2 $^{+/-}$	**87 (45.3%)**	**96 (50%)**
Nudt2 $^{-/-}$	**52 (27.1%)**	**48 (25%)**

Preweaning mortality: 22%

D

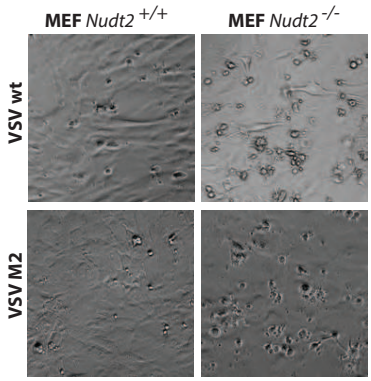

Supplementary Table 1

siRNA target sequences used in the siRNA screen

Sequence Name	siRNA target sequence 5'->3'
Hs_NUDT1_3	CTCCTGCTTCAGAAGAAGAAA
Hs_NUDT1_4	CCGGGTTTCATCTGGAATTAA
Hs_NUDT1_5	CCGCGAGGTGGACACGGTCTA
Hs_NUDT2_10	CAGGCATCAGATGGCATTCAT
Hs_NUDT2_7	TGCCAGGGTCCTGCAGTTATA
Hs_NUDT2_8	AGGATCCTTGTGGGCCTTCTA
Hs_NUDT5_2	CAGGCTTGTCAAACTGTACTA
Hs_NUDT5_3	TACATGGATCCTACTGGTAAA
Hs_NUDT5_6	TTCCTACGCTCTAGCACTGAA
Hs_NUDT6_5	CACGCAGAATCGGATTCATCA
Hs_NUDT6_6	CTGGTTGTACAAGATCGAAAT
Hs_NUDT6_7	GAGCTGTATTTGATGAAAGTA
Hs_NUDT9_5	ATGGATAATCTTATGCTAGAA
Hs_NUDT9_6	CACGCTGCAGATCCCATTATA
Hs_NUDT9_3	AAGATTAGTGCCACACTGAAA
Hs_NUDT12_6	AGCCGAGCTATTGCACATCAA
Hs_NUDT12_7	ATGATTGGTTGCTTAGCTCTA
Hs_NUDT12_5	AAGGTCGGATATTAAATAAGT
Hs_NUDT13_6	CAGGGAACGGAAGCCGTTGAA
Hs_NUDT13_5	CCACAACGTGTTGATTAACAA
Hs_NUDT13_7	TAGCCCGGATCAAGTCACTTA
Hs_NUDT14_1	CAGCGTGACCGTTCTCTTATT
Hs_NUDT14_2	AAAGGCTTGCATAGCTCCAAA
Hs_NUDT14_4	CTCCAGACAGACCATGTTCTA
Hs_NUDT15_4	CAGCAGTACTCTTCTCACTAA
Hs_NUDT15_6	CTCAAGAGCCTTTCAAGGGTA
Hs_NUDT15_7	ATCTGGTGTGATATTGTAATA
Hs_NUDT16_1	CTCCCTGTTTATATGCGTACA
Hs_NUDT16_2	CAGGTCAACACTAATACCACT
Hs_NUDT16_3	ATGTATGAAGGTGGTTCTCAA
Hs_NUDT17_7	CCCAACCATGGCAGAGGACAA
Hs_NUDT17_6	CCCGGATCCAACCAAACCCAA
Hs_NUDT17_5	TACCATCACATTGTTCTGTAT
Hs_NUDT18_1	CTGGGCCGAGATCACAGTGAT
Hs_NUDT18_2	AAGCGAGGAGTCCAAAGCTCA
Hs_NUDT18_3	ATCCTGCACCTGGTTGAACTA
Hs_NUDT19_4	TACGAAGTGAGAAGACTTGCA
Hs_NUDT19_3	CACGTTTATCCTAAGAACTCT
Hs_NUDT19_2	CACCGGATAGTGACATACCAT
Hs_DCP2_5	CCGGTGATTCATGTTTGTGAA
Hs_DCP2_6	CTGCTTATAAATGTTATTGTA
Hs_DCP2_1	CTGGGTTATCAGAGTAATGAA
Hs_NUDT21_5	CTGCACATATTACAAAGCCTA
Hs_NUDT21_1	ATCGTGATGAGAAACCTAATA
Hs_NUDT21_3	CCAAGTGTAGCTGAGCAATTA
Hs_NUDT22_4	AGGCGCCATCATCCTCTACAA
Hs_NUDT22_1	CTGGGCCTTACTTCCTACCGA
Hs_NUDT22_3	CCGAGACTTCCTGGGCACCAA
Hs_DDX58_6 (RIG-I)	AACGTTTACAACCAGAATTTA
Hs_DDX58_10 (RIG-I)	TTCTACAGATTTGCTCTACTA
Hs_DDX58_11 (RIG-I)	CTCCTCCTACCCGGCTTTAAA
Scrambled (control)	AAGGTAATTGCGCGTGCAACT

Supplementary Table 2

Nucleotide sequences used as templates in in vitro transcriptions

Sequence Name	Sequence 5' -> 3'
dsRNA IVT4	TTGTAATACGACTCACTATAGGGACGCTGACCCAGAAGATCTACTAGAAATAGTAGATCTTCTGGGTCAGCGTCCC
dsRNA IVT4_as	GGGACGCTGACCCAGAAGATCTACTATTTCTAGTAGATCTTCTGGGTCAGCGTCCCTATAGTGAGTCGTATTACAA
G0	AATTCCTGCAGTAATACGACTCACTATAGGCGCCGCGGTAACGCGGCGCCACGCGGAAACGCGCC
G0_as	GGCGCGTTTCCGCGTGGCGCCGCGTTACCGCGGCGCCTATAGTGAGTCGTATTACTGCAGGAATT
G8	AATTCCTGCAGTAATACGACTCACTATAGGAACAACGGCGCCGCGGTAACGCGGCGCCACGCGGAAACGCGCC
G8_as	GGCGCGTTTCCGCGTGGCGCCGCGTTACCGCGGCGCCGTTGTTCCTATAGTGAGTCGTATTACTGCAGGAATT
G4[GGAA]	AATTCCTGCAGTAATACGACTCACTATAGGAAGGCGCCGCGGTAACGCGGCGCCACGCGGAAACGCGCC
G4[GGAA]_as	GGCGCGTTTCCGCGTGGCGCCGCGTTACCGCGGCGCCTTCCTATAGTGAGTCGTATTACTGCAGGAATT
G4[GAAA]	AATTCCTGCAGTAATACGACTCACTATAGAAAGGCGCCGCGGTAACGCGGCGCCACGCGGAAACGCGCC
G4[GAAA]_as	GGCGCGTTTCCGCGTGGCGCCGCGTTACCGCGGCGCCTTTCTATAGTGAGTCGTATTACTGCAGGAATT
G4[GCAA]	AATTCCTGCAGTAATACGACTCACTATAGCAAGGCGCCGCGGTAACGCGGCGCCACGCGGAAACGCGCC
G4[GCAA]_as	GGCGCGTTTCCGCGTGGCGCCGCGTTACCGCGGCGCCTTGCTATAGTGAGTCGTATTACTGCAGGAATT
G4[GUAA]	AATTCCTGCAGTAATACGACTCACTATAGTAAGGCGCCGCGGTAACGCGGCGCCACGCGGAAACGCGCC
G4[GUAA]_as	GGCGCGTTTCCGCGTGGCGCCGCGTTACCGCGGCGCCTTACTATAGTGAGTCGTATTACTGCAGGAATT
A8	AATTCCTGCAGTAATACGACTCACTATTAGAACAACGGCGCCGCGGTAACGCGGCGCCACGCGGAAACGCGCC
A8_as	GGCGCGTTTCCGCGTGGCGCCGCGTTACCGCGGCGCCGTTGTTCTAATAGTGAGTCGTATTACTGCAGGAATT
A4[AGAA]	AATTCCTGCAGTAATACGACTCACTATTAGAAGGCGCCGCGGTAACGCGGCGCCACGCGGAAACGCGCC
A4[AGAA]_as	GGCGCGTTTCCGCGTGGCGCCGCGTTACCGCGGCGCCTTCTAATAGTGAGTCGTATTACTGCAGGAATT
A1	AATTCCTGCAGTAATACGACTCACTATTAGGCGCCGCGGTAACGCGGCGCCACGCGGAAACGCGCC
A1_as	GGCGCGTTTCCGCGTGGCGCCGCGTTACCGCGGCGCCTAATAGTGAGTCGTATTACTGCAGGAATT

Supplementary Table 3

qRT-PCR primers used in this study

Sequence Name	Sequence 5' -> 3'
hu_NUDT2_fw	CACTGGACTCCTCCCAAAGG
hu_NUDT2_rv	TCCTCTTGGGTCTCCCTCAG
hu_NUDT12_fw	TTGGGCAAAACTTGTATCGAC
hu_NUDT12_rv	CTTCATCCTCCTATGCCAGC
hu_NUDT14_fw	AAGAGAACGGTCACGCTGTC
hu_NUDT14_rv	CCGCCTCACCCTACCTG
hu_NUDT17_fw	GACTGTCTTGCTAACCCGAAG
hu_NUDT17_rv	GGCAGGTGTAGTCCACTCTC
VSV-N_fw	ATCGGAATATTTGACCTTGTA
VSV-N_rv	ACTGTTCATTGATCATTTTGC
ms_ActB_fw	CTCTGGCTCCTAGCACCATGAAGA
ms_ActB_rv	GTAAAACGCAGCTCAGTAACAGTCCG
SFV-nsp3_fw	GCAAGAGGCAAACGAACAGA
SFV-nsp3_rev	GGGAAAAGATGAGCAAACCA
HSV-DNA Polymerase I_fw	AGCCTGTACCCCAGCATCAT
HSV-DNA Polymerase I_rv	TGGGCCTTCACGAAGAACA
Firefly Luc_fw	CTCACTGAGACTACATCAGC
Firefly Luc_rv	TCCAGATCCACAACCTTCGC
hu_GAPDH_fw	GATTCCACCCATGGCAAATTC
hu_GAPDH_fw	AGCATCGCCCCACTTGATT

Supplementary Table 4

Nucleotide guide sequences cloned in pLentiCRISPRv2

Sequence Name	Sequence 5' -> 3'
NUDT2_gRNA1	ATGAGCACCAAGCCTACCGC
NUDT2_gRNA2	AATTGCATTGTTGTCCACTT
NUDT2_gRNA3	TAACTAGGCCATGTGGAACC
NUDT2_gRNA4	CATCAGATGGCATTCATCAC
NUDT2_gRNA5	TCTCCTTGAACTGAGCCAAC
NUDT2_gRNA6	CCATTATTGAGGGGTTCAAA
XRN1_gRNA1	TTAAGAGAAGAAGTTCGATT
XRN1_gRNA2	TAAAACGCCTCCCACGCTGC
XRN1_gRNA3	GCTTGGATTAACAAGTCATG
XRN1_gRNA4	TAATGCGAAACAACACCTCC
XRN1_gRNA5	GTATCCCTGTCTCAGCGAAG
XRN1_gRNA6	TTTCACCACTTCGCTGAGAC

CHAPTER

7

PUBLICATION 2

Structure of human IFIT1 with capped RNA reveals adaptable mRNA binding and mechanisms for sensing N1 and N2 ribose 2-O methylations

Yazan M. Abbas, **Beatrice Theres Laudenbach**, Saúl Martínez-Montero, Regina Cencic, Matthias Habjan, Andreas Pichlmair, Masad J. Damha, Jerry Pelletier, and Bhushan Nagar. Structure of human IFIT1 with capped RNA reveals adaptable mRNA binding and mechanisms for sensing N1 and N2 ribose 2'-O methylations. *Proc Natl Acad Sci U S A* 114, E2106-E2115 (2017).

The collaborative manuscript 'Structure of human IFIT1 with capped RNA reveals adaptable mRNA binding and mechanisms for sensing N1 and N2 ribose 2-O methylations' published in the Proceedings of the National Academy of Sciences (PNAS) presents novel insights into the binding of capped RNA by IFIT1. The crystal structure of IFIT1 with capped RNA revealed that a central positively charged tunnel that sterically excludes RNAs that are methylated at the 2'-OH positions of the ribose of the first and second nucleotides. This structural feature thereby provides specificity for viral capped RNAs that do not show these specific methylation marks in contrast to cellular RNAs. The sequestration of capped RNAs lacking 2'-OH methylation by IFIT1 prohibits binding of eIF4E and thereby inhibits translation of these RNAs. I contributed with functional validation of IFIT1 mutant cells infected with a human coronavirus mutant lacking the 2'-OH methyltransferase. My findings highlighted the importance of RNA binding to IFIT1 and consequential IFIT1-mediated inhibition on virus growth.

Structure of human IFIT1 with capped RNA reveals adaptable mRNA binding and mechanisms for sensing N1 and N2 ribose 2′-O methylations

Yazan M. Abbas[a], Beatrice Theres Laudenbach[b,1], Saúl Martínez-Montero[c,1], Regina Cencic[d,1], Matthias Habjan[b], Andreas Pichlmair[b], Masad J. Damha[c], Jerry Pelletier[d,e,f], and Bhushan Nagar[a,2]

[a]Department of Biochemistry and Groupe de Recherche Axe sur la Structure des Proteines, McGill University, Montreal, QC, Canada H3G 0B1; [b]Innate Immunity Laboratory, Max-Planck Institute of Biochemistry, 82152 Martinsried/Munich, Germany; [c]Department of Chemistry, McGill University, Montreal, QC, Canada H3A 0B8; [d]Department of Biochemistry, McGill University, Montreal, QC, Canada H3G 1Y6; [e]The Rosalind and Morris Goodman Cancer Research Center, Montreal, QC, Canada H3A 1A3; and [f]Department of Oncology, McGill University, Montreal, QC, Canada H3G 1Y6

Edited by Joseph D. Puglisi, Stanford University School of Medicine, Stanford, CA, and approved February 3, 2017 (received for review July 27, 2016)

IFIT1 (IFN-induced protein with tetratricopeptide repeats-1) is an effector of the host innate immune antiviral response that prevents propagation of virus infection by selectively inhibiting translation of viral mRNA. It relies on its ability to compete with the translation initiation factor eIF4F to specifically recognize foreign capped mRNAs, while remaining inactive against host mRNAs marked by ribose 2′-O methylation at the first cap-proximal nucleotide (N1). We report here several crystal structures of RNA-bound human IFIT1, including a 1.6-Å complex with capped RNA. IFIT1 forms a water-filled, positively charged RNA-binding tunnel with a separate hydrophobic extension that unexpectedly engages the cap in multiple conformations (*syn* and *anti*) giving rise to a relatively plastic and nonspecific mode of binding, in stark contrast to eIF4E. Cap-proximal nucleotides encircled by the tunnel provide affinity to compete with eIF4F while allowing IFIT1 to select against N1 methylated mRNA. Gel-shift binding assays confirm that N1 methylation interferes with IFIT1 binding, but in an RNA-dependent manner, whereas translation assays reveal that N1 methylation alone is not sufficient to prevent mRNA recognition at high IFIT1 concentrations. Structural and functional analysis show that 2′-O methylation at N2, another abundant mRNA modification, is also detrimental for RNA binding, thus revealing a potentially synergistic role for it in self- versus nonself-mRNA discernment. Finally, structure-guided mutational analysis confirms the importance of RNA binding for IFIT1 restriction of a human coronavirus mutant lacking viral N1 methylation. Our structural and biochemical analysis sheds new light on the molecular basis for IFIT1 translational inhibition of capped viral RNA.

IFIT1 crystal structure | innate immunity | mRNA cap recognition | self vs. nonself | 2′-O methylation

Infection by a virus relies on its ability to exploit the host's translational machinery to convert its genome into protein products that can ultimately be used to assemble new viral particles. In eukaryotes, endogenous mRNA is protected by a highly conserved 5′ cap structure consisting of an *N7*-methylguanosine triphosphate (m7Gppp/Cap0) moiety. This is recognized by the eukaryotic translation initiation factor 4E to promote cap-dependent translation (eIF4E together with eIF4G and eIF4A comprise eIF4F) (1). In higher eukaryotes, the mRNA cap is further modified by ribose 2′-O methylation on the first and sometimes second cap-proximal nucleotides (N1 and N2, where N is any nucleotide) (Fig. S1*A*), resulting in Cap1- (m7GpppNmN) or Cap2- (m7GpppNmNm) mRNA (2, 3). N1 methylation was recently shown to serve as a molecular signature of "self," which can subvert mammalian antiviral responses (4, 5). As such, many viruses also produce Cap1-mRNA, either through the action of host- or virally encoded 2′-O methyltransferases (MTases) or through viral "cap-snatching" enzymes (6, 7). Hence, Cap0-mRNAs (along with other virus-derived RNAs) are marked as "nonself" and can trigger responses, such as the type I IFN antiviral program (5, 8, 9), which culminates in the induction of hundreds of IFN-stimulated genes (ISGs) (10).

Among the most potently induced of the ISGs are the IFITs (IFN-induced proteins with tetratricopeptide repeats), a family of antiviral effectors whose expression can also be triggered downstream of IFN-independent signaling (11). IFITs are conserved throughout vertebrate evolution, with humans and most mammals encoding five paralogues—IFIT1, IFIT1B, IFIT2, IFIT3, and IFIT5—although many also possess species-specific duplications and deletions. For example, mice lack IFIT5 and were only recently discovered to have also lost IFIT1 (12). Therefore, what is currently known as mouse Ifit1 (54% sequence identity with human IFIT1) is actually an ortholog of human IFIT1B. In humans, IFIT1B (67% sequence identity with human IFIT1) is not known to be IFN-inducible (11), and recent data suggest that it may be nonfunctional (12). IFITs are structurally related and are composed of tandem copies of the tetratricopeptide repeat (TPR), a helix–turn–helix motif. Structures of several IFITs have shown that their TPRs coalesce into distinct superhelical subdomains that form clamp-shaped structures (13–16).

Significance

IFIT1 is an antiviral effector of host innate-immunity that selectively recognizes the 5′-end of viral mRNAs, which are often capped to mimic host mRNA, and blocks their translation. Our X-ray structural analysis reveals that the cap and four additional nucleotides are encircled by IFIT1 through a central tunnel in an adaptable manner, which gives it the flexibility required to defend against many different viruses, and to deter their ability to rapidly evolve. Host mRNA, normally ribose methylated at the first and second nucleotides following the cap, avoids IFIT1 recognition through tight complementary interfaces at these positions. This study uncovers the molecular basis for how IFIT1 selectively recognizes viral mRNAs and will help guide development of viral vaccines and mRNA therapeutics.

Author contributions: Y.M.A. and B.N. designed research; Y.M.A. performed structural work and binding assays; B.T.L. performed viral infection assays; R.C. performed in vitro translation assays; M.H. performed viral infection assays; S.M.-M. and M.J.D. contributed new reagents/analytic tools; Y.M.A., B.T.L., R.C., M.H., A.P., J.P., and B.N. analyzed data; and Y.M.A. and B.N. wrote the paper.

The authors declare no conflict of interest.

This article is a PNAS Direct Submission.

Data deposition: The atomic coordinates and structure factors have been deposited in the Protein Data Bank, www.rcsb.org/pdb/home/home.do (PDB ID codes 5UDI, 5UDJ, 5UDK, and 5UDL).

[1]B.T.L., S.M-M., and R.C. contributed equally to this work.

[2]To whom correspondence should be addressed. Email: bhushan.nagar@mcgill.ca.

This article contains supporting information online at www.pnas.org/lookup/suppl/doi:10.1073/pnas.1612444114/-/DCSupplemental.

Recently, it was discovered that IFITs play a prominent role in impeding viral replication by directly binding the 5′ end of viral RNA (17). Thus, IFIT1 and IFIT1B can compete with eIF4F to selectively bind and sequester viral Cap0-mRNA, resulting in its translational inhibition (18–20). In this manner, mouse Ifit1 has been shown to restrict a broad spectrum of wild-type and mutant viruses lacking 2′-O MTase activity, including alphaviruses, coronaviruses, flaviviruses, and vaccinia virus (4, 18, 21–25), whereas mutating viral N1 methylation enhanced coronavirus and flavivirus sensitivity to human IFIT1 (18, 23, 24, 26). In contrast, host cellular mRNA is not targeted as it bears N1 2′-O methylation, which interferes with IFIT1 and IFIT1B binding (18–20). That many cytoplasmic virus families have adapted by acquiring 2′-O MTases to generate their own Cap1-mRNA, thereby potentially escaping IFIT1/IFIT1B restriction, underscores the importance of these proteins in this process (7). Furthermore, alphaviruses, which display only Cap0-mRNA, can still subvert mouse Ifit1 activity by encoding cap-proximal structural elements (21, 22), which has also been shown to interfere with RNA binding and enhance pathogenicity.

IFIT1, along with IFIT5, can also recognize uncapped viral triphosphate (PPP)-RNA (another nonself marker of infection) to potentially inhibit the replication of some negative-sense single-stranded (ss) RNA viruses (13, 17). The crystal structure of human IFIT5 bound to uncapped PPP-RNA revealed that the RNA sits in a narrow, positively charged tunnel at the core of the protein, with a network of electrostatic interactions specifically recognizing the PPP moiety (13). Up to four nucleotides are also stably bound within the tunnel in a sequence-nonspecific manner. The sequence identity between IFIT5 and IFIT1 (55%) and a structure of the N-terminal region of IFIT1 suggested that IFIT1 accommodates capped RNA in a similar fashion. However, IFIT5 cannot bind capped mRNA (13, 18, 19), and indeed protein residues at the base of the tunnel would block any further progression beyond the PPP moiety. Thus, how IFIT1-like proteins can accommodate Cap0-mRNA remains unclear.

We report here several crystal structures of RNA-bound human IFIT1. The structures reveal that the positively charged RNA-binding tunnel of IFIT1 is distinct from that found in IFIT5 and further extended to allow binding of both capped and uncapped RNAs. Strikingly, mRNA binding and cap recognition by IFIT1 appears to be adaptable and its mechanism is evolutionarily divergent from eIF4E and other cap-binding proteins. The shape of the tunnel in the vicinity of the 2′-hydroxyls of N1 and N2 sterically occludes RNA methylated at these positions. A comprehensive analysis of the interaction between human IFIT1 and differentially methylated capped RNAs corroborates the structural findings, revealing that either N1 or N2 methylation alone interferes with IFIT1 binding, but in an RNA-dependent manner. Combining N1 and N2 methylation resulted in an additive and potentially synergistic effect in inhibiting IFIT1 activity, particularly toward susceptible RNA sequences and at high IFIT1 concentrations. Our structural and biochemical analysis therefore sheds light on IFIT1 antiviral activity and reveals a previously uncharacterized role for N2 ribose methylation and Cap2 structures as signatures of self mRNA.

Results

RNA Binding and Inhibition of in Vitro Translation by Human IFIT1. The interaction between IFIT1 and capped-RNA is well established, but the precise structural determinants of the viral RNA important for binding are as yet unclear. Thus, we began by carrying out EMSAs between human IFIT1 and two 5′ capped sequences derived from genomes of coronaviruses known to be restricted by human IFIT1 or mouse Ifit1: human coronavirus strain 229E (HCoV) and murine hepatitis virus strain A59 (MHV) (18). Human IFIT1 bound the capped-RNAs with apparent affinities of ∼250 nM and <100 nM, respectively (Fig. 1*A*). Binding strength decreased as the stability and proximity of RNA secondary structure to the 5′-end increased (Fig. 1*A* and Fig. S1*B*), confirming the preference for ssRNA as previously demonstrated for human IFIT1 and mouse Ifit1 (13, 21). As with IFIT5, RNA binding is generally sequence-nonspecific and replacing the first 3 nt of HCoV (sequence ACU) with GGG resulted in only a modest enhancement of binding (Fig. 1*A*, *Right*). IFIT1 also binds uncapped PPP-RNA, but this is inherently weaker and more sensitive to the presence of predicted secondary structure at the 5′-end (Fig. S1*C*). This finding is in contrast to IFIT5, which binds PPP-RNA but cannot accommodate capped RNA, as shown by its crystal structure and a variety of biochemical assays from several groups (13, 18, 19).

To understand the contribution of IFIT1 binding to capped RNA in a more physiological context, we used an in vitro translation system to assess the effect on translation initiation. The system consists of Krebs extracts programmed with a bicistronic Cap0-mRNA reporter (27). The 5′-cistron expresses a Firefly luciferase (FF) reporter that is translated in a cap-dependent manner, whereas the 3′-cistron expresses a *Renilla* luciferase (Ren) reporter under the control of an internal ribosome entry site (IRES) from hepatitis C virus (HCV) (Fig. 1*B*). Ren expression serves as an internal control for nonspecific translational inhibition by IFIT1. Titrating human IFIT1 into these extracts at concentrations ranging from ∼30 nM to 5 μM showed that IFIT1 could inhibit Cap0-dependent translation with IC_{50} values of ∼50–200 nM (Fig. 1*C*, and other figures herein). Interestingly, addition of IFIT1 after the reporter was preincubated with translation extracts for 10 min resulted in its inhibitory activity being reduced by more than an order-of-magnitude (IC_{50} > 5 μM), presumably because of the formation of a closed-loop mRNP that facilitates ribosome reinitiation (28). This result suggests that optimal IFIT1 activity in vivo is probably only realized in cells that are already expressing the protein before infection, as might be the case for cells activated by IFN signaling in a paracrine manner.

In all cases, cap-independent translation of Ren was reduced by at most 15–20%, which is likely because of nonspecific binding of IFIT1 to either the IRES, ribosomal RNA (19), transfer RNA (19), or translation factors (e.g., eIF3e) (29). This finding is in contrast to one report showing nearly complete inhibition of HCV–IRES-mediated translation by 600 nM IFIT1 in rabbit reticulocyte lysates (30). This discrepancy may be attributed to differences in translation efficiency between Krebs extracts and rabbit reticulocyte lysates. Finally, titration of IFIT5 in these assays did not produce the same level of translational inhibition (Fig. S1*D*) (IC_{50} ≥ 5 μM), consistent with the notion that IFIT5 cannot specifically bind capped-RNA. Taken together, our data are consistent with an IFIT1 antiviral mechanism that is dependent on the recognition of mRNA cap structures to compete with eIF4F (18, 19).

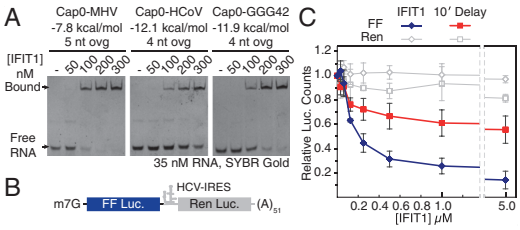

Fig. 1. RNA binding and inhibition of in vitro translation by human IFIT1. (*A*) EMSAs between human IFIT1 and capped-RNA visualized by SYBR Gold staining. Cap0-MHV, first 41 nt of MHV strain A59; Cap0-HCoV, first 42 nt of HCoV strain 229E; Cap0-GGG42, ACU to GGG modification of HCoV. The RNA secondary structure minimum free energy (kcal/mol) and 5′-overhang length (ovg) are indicated (see also Fig. S1*B*). (*B*) Schematic of bicistronic mRNA reporter. (*C*) Translation assay with IFIT1 titrated into Krebs extracts programmed with Cap0/m7Gppp reporter, and titration following a 10-min preincubation of the reporter with extracts. FF and Ren luciferase (luc.) activities at each concentration were normalized against buffer control, which was set to 1. Data represent the mean of two independent measurements performed in duplicate ± SD.

Overall Structure of Full-Length Human IFIT1. To gain insight into the mechanisms of viral RNA binding by IFIT1, we initially crystallized RNA-bound, full-length, wild-type human IFIT1 (residues 1–478) in complex with short PPP- and m7Gppp-containing oligoadenosines. The IFIT1–RNA complex purified and crystallized as a dimer with two molecules in the asymmetric unit, but diffracted X-rays to only ~2.7 Å. To improve the resolution, we mutated the dimerization interface at the C-terminal end of the protein to produce a monomeric version that crystallized in a different space group and diffracted X-rays to 1.58-Å resolution (Table S1). The overall folds of the wild-type and monomeric mutant are essentially the same (rmsd 0.35 Å). Henceforth, we describe only the high-resolution structures with respect to RNA binding, whereas all functional assays were performed with wild-type protein.

Human IFIT1 is made up of 23 α-helices, 18 of which form 9 TPR motifs that together form three distinct subdomains interrupted by non-TPR structural elements (Fig. 2 *A* and *B* and Fig. S2 *A–C*). The overall structure is similar to the previously determined RNA-bound structure of human IFIT5 (rmsd 1.9 Å) (Fig. S2*D*) and the N-terminal region of human IFIT1 (rmsd 0.8 Å) (Fig. S2*E*) (13). The subdomains are arranged to form a clamp-shaped structure with a central RNA-binding tunnel that is ~30–40 Å in length and 12–19 Å in width, accommodating only ssRNA with a total of five nucleotides (cap + four RNA nucleotides) (Fig. 2 *B–D*). As with IFIT5, a pair of long non-TPR pivot helices connect the second and third subdomains and likely function in an analogous fashion to regulate closure of the protein around the RNA (13) (Fig. S2*C*). About 30–40% of the tunnel volume is occupied by bound water molecules (Fig. 2*E*), which appears to be an important facet for recognition of different RNA sequences and structures (discussed below). We demarcate four distinct regions of the tunnel according to their role in RNA binding: (*i*) the cap-binding pocket, which houses the *N7*-methylguanosine moiety; (*ii*) the triphosphate channel, which links the cap-binding pocket to the 5′-end of the RNA; (*iii*) the first dinucleotide (N1 and N2), where the presence of 2′-O methylation is sensed; and (*iv*) the second dinucleotide (N3 and N4), where the requirement for single stranded 5′-ends is reinforced.

The IFIT1 RNA-Binding Tunnel Houses a Functionally Distinct Cap-Binding Pocket. IFIT1 and IFIT5 were previously characterized as PPP-RNA binding proteins (17), although more recent evidence revealed that the primary role of IFIT1 is in binding capped-RNA. Conversely, the role of IFIT5 remains restricted to recognition of 5′-phosphorylated RNAs (13, 14, 16). The structure of IFIT1 bound to PPP-RNA revealed that, like IFIT5, the PPP moiety is ligated by numerous specific electrostatic interactions from protein side chains (Fig. S3 *A–C*). However, there are some key differences. IFIT5 recognition of PPP-RNA uses a positively charged metal ion bound between the α- and γ-phosphates, which stabilizes a bent conformation of the PPP facilitated by T37 at the base of the tunnel in IFIT5 (Fig. 3*A*). The corresponding position in IFIT1 is occupied by an arginine (R38), and an ion is no longer part of its PPP binding. This results in a more extended conformation of the PPP that allows it to reach toward the entrance of a neighboring unoccupied pocket.

The crystal structure of IFIT1 bound to m7Gppp-RNA revealed that this adjacent pocket harbors the cap moiety. Whereas most of the RNA-binding tunnel is positively charged, the cap-binding pocket is generally more hydrophobic and interactions with the cap occur predominantly through nonspecific van der Waals contacts (Figs. 2*C* and 3*B*). Surprisingly, we found that the m7G base adopts both *syn*- and *anti*-conformations with approximately equal occupancies (Fig. 3*C* and Fig. S3*D*) (discussed in detail below). In either conformation, m7G sits atop a tryptophan residue (W147) making π–π stacking interactions, reminiscent of other cap-binding proteins, such as eIF4E (31) (Fig. 3 *D* and *E*). Additionally, the base is abutted by I183 from the same side as W147, and on the other side by L46 and T48 emanating from a flexible loop that forms the outer wall of the pocket, which we term the "cap-binding loop" (Fig. 3 *D* and *E* and Fig. S2*F*). The ribose of m7G is similar in the *syn*- and *anti*-modes of binding, adopting an S-type conformation that is stabilized by an intramolecular hydrogen bond between the ribose 3′-OH and the bridging β-phosphate (Fig. S3*D*). It sits in a pocket formed by Q42, L46, R187, Y218, I183, and L150 (Fig. 3*E*), and two ordered water molecules: the first coordinated by Q42 and the second bridging the ribose 3′-OH to the backbone carbonyl of W147 (Fig. S3*F*).

As in PPP-RNA–bound IFIT1, the bridging triphosphate in the cap-bound structure is in an extended conformation stabilized by numerous electrostatic interactions, although pulled slightly toward the cap-binding pocket (Fig. 3*F* and Fig. S3*E*). The γ-phosphate interacts with K151, R255, Y218, and R187, and the β-phosphate is coordinated by K151, R187, and R38. Additionally, six highly ordered water molecules mediate hydrogen bonds with the α- and γ-phosphates (Fig. S3*F*). Finally, m7Gppp binding is facilitated by a high degree of interresidue coordination: for example, R38 is held in place by D34, and W147 is coordinated by E176 (Fig. S3*G*).

In IFIT5, although most of these cap-binding residues are conserved, substitutions at a few key positions render it unable to bind cap productively. As described above, replacement of R38 in IFIT1 with T37 in IFIT5 causes it to recognize a more compact conformation of the PPP in a metal-dependent manner. This positions the γ-phosphate away from the putative cap-binding pocket, which draws in several residues, such as Q41 (from helix α2) and K48 (from the putative cap-binding loop), causing them to block access to its putative cap-binding pocket (Fig. 3*G* and Fig. S3 *H* and *I*). Therefore, the formation of a positively charged RNA-binding tunnel with an accessible and spatially separated cap-binding pocket in IFIT1 explains, at least in part, why it can bind capped-RNA, whereas IFIT5 cannot. The preference for an arginine or threonine on helix α2 is highly conserved among IFIT1/1B-like and IFIT5-like sequences, respectively (Fig. S3*J*), and the identity of this PPP bridging residue (Arg or Thr) appears to play a major role in determining the 5′ specificities of IFIT1/1B- or IFIT5-like proteins. Interestingly, a small group of mammalian IFIT5-like proteins retain an arginine at this position; these sequences probably have a hybrid IFIT1/IFIT5 character, and possibly resemble an ancestral IFIT1/IFIT5 precursor protein, because they all belong to nonplacental mammals (e.g., opossum and platypus) (Fig. S3*K*).

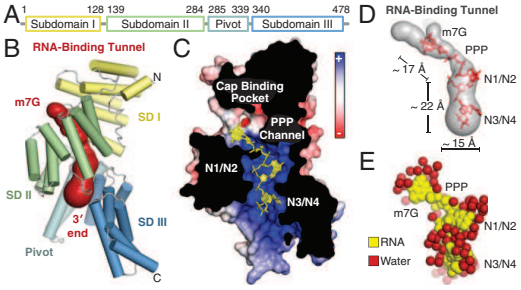

Fig. 2. Overall structure of monomeric, RNA-bound human IFIT1. (*A*) Schematic of IFIT1 subdomains. (*B*) Cartoon representation of human IFIT1 colored by subdomain (SD) and surface representation of the tunnel (dark red) determined by CAVER (50). (*C*) Cross-section of IFIT1 colored by surface electrostatic potential from negative (−10 kTe^{-1}; red) to positive (+10 kTe^{-1}; blue) with capped-RNA (yellow sticks). (*D*) Dimensions of the IFIT1 tunnel (gray surface) and capped RNA (red sticks). (*E*) Waters surrounding the RNA inside the tunnel.

IFIT1 Can Nonspecifically Accommodate Multiple Forms and Conformations of the Cap. The high-resolution structure of the monomeric IFIT1 mutant (1.58 Å) allowed us to unambiguously build two conformations for the m7G base that are consistent with the

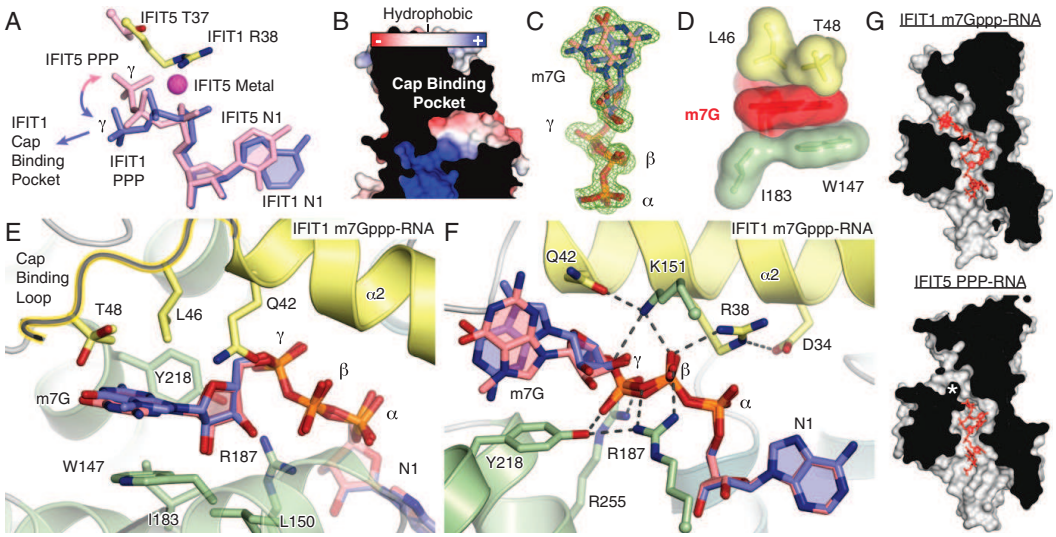

Fig. 3. IFIT1 mRNA cap-binding mechanism. (*A*) The IFIT1 PPP (blue) adopts an extended conformation compared with the "bent" IFIT5 PPP (pink). The γ-phosphate from PPP–RNA-bound IFIT1 points toward the nearby unoccupied cap-binding pocket. (*B*) Protein cross-section and close-up the cap-binding pocket. This view is rotated by ∼180° compared with Fig. 2*C*. (*C*) Simulated annealing $2F_o$–F_c omit map of the m7Gppp-moiety contoured at 1σ. *Syn*- and *anti*-configuration carbons are colored light blue and salmon, respectively. (*D*) Surface/stick representation of residues (colored by subdomain) abutting the m7G base moiety from above and below. The interplanar distance between m7G and Trp-147 is 3.4–3.7 Å. (*E* and *F*) Cartoon/stick representation of residues interacting with the m7Gppp-moiety. See also Movie S1. Shown are both conformations of the m7GpppA dinucleotide, which was modeled as a single residue during model building and refinement. (*G*) Cross-sections of the IFIT1 and IFIT5 RNA-binding tunnels (gray/black) with m7Gppp- or PPP-RNA (red sticks). The asterisk (*) shows where K48 and Q41 block the IFIT5 putative cap-binding pocket (see Fig. S3 *H*–*K*).

electron density, which has a relatively symmetric shape because of an ∼180° rotation about the *N*-glycosidic bond connecting the base to the ribose. Multiple base conformations were also evident in the lower-resolution wild-type m7Gppp-RNA cocrystals. This results in the interactions at the base periphery being quite distinct in the two conformations (Fig. 4*A*). Notably, there are no direct hydrogen bonds from the protein toward the base in either conformation, but there are a small number of water-mediated interactions. In the *anti*-orientation, *N3* of the base is weakly hydrogen bonded to a water molecule that is coordinated by Q42. The *N7*-methyl (*C7*) and *O6* groups make van der Waals contacts with N216, and the remainder of the base is partially oriented toward water molecules near the proximal opening of the tunnel leading to bulk solvent. In the *syn*-orientation, the *N7*-methyl and *O6* are instead pointing toward the bulk solvent, whereas *N2* is nestled between Y218 and N216.

Because of the presence of the *N7*-methyl group on m7G, it acquires a delocalized positive charge on its imidazole ring that could in principle enhance the stacking with W147 through additional cation–π interactions (31, 32). However, the geometry of cation–π stacking changes with the base orientation (Fig. 4*A*). Whereas the *anti*-conformation places the positive charge at an angle away from W147, the *syn*-conformation places it directly over the indole ring of W147. To test whether *N7*-methylation and associated positive charge controls cap orientation, we determined the structure of Gppp-RNA (lacking the *N7*-methyl group) bound to IFIT1 (1.7 Å) (Fig. 4*B* and Fig. S4*A*). Here, the base exists only in the *anti*-conformation, indicating that the ability of the base to adopt two conformations depends, at least in part, on *N7*-methylation. The presence of two base conformations is also determined by the chemical environment surrounding the base, because the structure of an N216 mutant of monomeric IFIT1 (N216A) bound to m7Gppp-RNA also resulted in the base adopting only the *anti*-conformation (Fig. S4*B*).

Despite these observations, IFIT1 appears not to be selective for *N7*-methylation. In fact, gel-shift assays suggest that Gppp-RNA binding is, in some cases, more efficient than m7Gppp-RNA binding (Fig. S4*C*) (18, 19), in stark contrast to the case with eIF4E, whose cap binding is strongly dependent on proper methylation (31). In the absence of the methyl group, the guanine ring moves closer to N216, making a hydrogen bond with it through *O6* (Fig. 4*B*, *Left*), although removing this hydrogen bond through mutation (N216A or N216D) does not weaken Gppp-RNA binding (Fig. S4*D*). Interestingly, the water structure surrounding Gppp-RNA changes compared with m7Gppp-RNA, such that almost all hydrogen bond donor and acceptor sites on the unmethylated base are now satisfied (Fig. 4*B*, *Right*), and this may be a contributing factor for maintaining strong Gppp-RNA binding (relative to m7Gppp-RNA).

The physiological relevance of Gppp-RNA binding by IFIT1 is unclear, but one possibility is that it may facilitate targeting of transient intermediates formed during viral mRNA capping. We therefore tested IFIT1 activity in extracts programmed with a Gppp-capped reporter (Fig. S4*E*). In this system, although overall translation is less efficient than in Cap0-programmed extracts, translation initiation still proceeds through binding of the cap-proximal nucleotides via eIF4G (33). IFIT1 titration resulted in translational inhibition similar to m7Gppp-capped mRNA (IC_{50} ∼ 200 nM), highlighting the importance of binding not only the cap, but also the proximal nucleotides to provide additional affinity to allow competition with eIF4F (19).

Because cap binding does not rely on any guanine-specific hydrogen bonds, we wondered whether IFIT1 could also recognize Appp-capped RNAs. Indeed, IFIT1 can bind Appp-RNA (Fig. S4*F*) and inhibit translation initiation from an Appp-capped reporter (IC_{50} ∼ 500 nM) (Fig. S4*E*). Thus, it appears that IFIT1 has evolved to recognize not only canonically capped mRNA, but rather diverse 5′-5′ linked base modifications of the mRNA

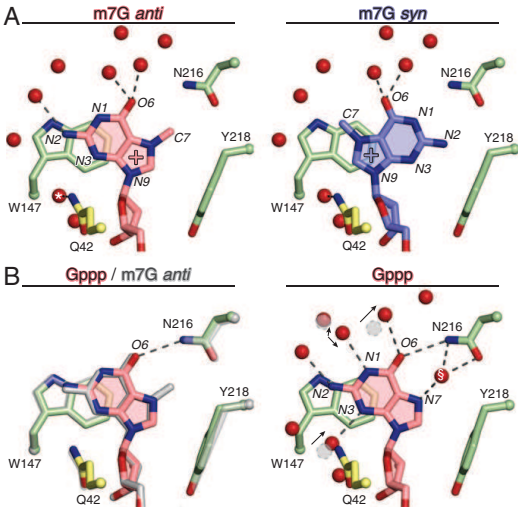

Fig. 4. IFIT1 can accommodate multiple forms and conformations of the cap. (*A*) m7G base interactions at its periphery in the *anti*- or *syn*-modes of binding. The water H-bonded to Q42 (*) is 3.3 Å away from *N3* in the *anti*-mode. (*B, Left*) The Gppp-moiety adopts only *anti*, and approaches N216 to form a weak H-bond through *O6;* m7Gppp-RNA bound IFIT1 is superposed in gray. (*Right*) The water structure surrounding the G moiety changes compared with m7G, and satisfies almost all H-bond donor and acceptor groups. The arrows depict the movement of waters from the m7Gppp-bound form (gray circles) to the Gppp-bound form (red spheres). The water molecule H-bonded to Q42 and *N3* becomes more ordered in the Gppp-RNA structure (same resolution and crystal form but B-factor decreases from 28 $Å^2$ to 15.3 $Å^2$). The water at *N7* (§) appears only in the Gppp-bound form. The water at N1 appears to be in two conformations and was modeled as two water molecules.

through relatively nonspecific interactions in the pocket. The notion of lack of specificity is underscored by the structure of IFIT1 with PPP-RNA, where the cap-binding pocket is occupied by PEG (polyethylene glycol) molecules from the crystallization solution, which form interactions that mimic cap binding (Fig. S4*G*).

Mutational Analysis of Cap Recognition. To test whether our structural findings are functionally valid, we mutated several residues involved in cap binding and assayed them in fluorescent gel-shift binding assays (with m7Gppp-43 RNA) (Table S2) and the translational inhibition assays described above (Fig. 5 and Fig. S4*I*). Both R38A and K151M are critical for binding, and K151M reduces IFIT1 inhibitory activity by one to two orders-of-magnitude (IC_{50} > 5 μM). Y218A and Q42A weakened binding to capped RNA and reduced IFIT1 inhibitory activity. N216A retains full binding to m7Gppp-RNA, indicating that the N216–cap interactions (e.g., with the *N7*-methyl) are dispensable. W147 is perhaps the most important residue inside the cap-binding pocket as W147M essentially abolished m7Gppp-RNA binding, whereas mutation to another aromatic residue (W147F) largely retained binding. Accordingly, W147M reduced IFIT1 translation inhibition ~40-fold, and W147F mostly retained inhibitory activity (compared with W147M). Mutation of E176, which coordinates W147, had similar effects as W147F. From the cap-binding loop, T48 was deemed dispensable, but L46 was required for optimal binding and translational inhibition. All cap-binding pocket mutants tested here retained binding toward PPP-RNA, except for R38A and K151M (which target the PPP moiety), indicating that the protein fold was not disrupted by the mutations (Fig. S4*J*). Taken together, the data in the mutational analysis confirm the importance of cap binding and the role of the RNA-binding tunnel in mediating translational inhibition by IFIT1.

Our results are in agreement with previous mutational binding assays based on in silico modeling (19). In this model, Phe-45 and Tyr-50 from the cap-binding loop were also predicted to interact with the base; however, our structures reveal that these two residues are distal from the m7G moiety and are probably important for maintaining subdomain contacts, or helping pre-organize the cap-binding loop (Fig. S4*K*).

The Cap-Binding Mechanism Is Conserved in IFIT1 and IFIT1B Proteins Across Mammalian Evolution. The mode of cap binding identified here likely applies to all mammalian IFIT1- and IFIT1B-like proteins, as the residues involved in *N7*-methylguanosine triphosphate recognition are highly conserved (Figs. S4*M* and S5). Two notably prevalent differences in cap-binding residues compared with human IFIT1 include Q42 and N216, which are replaced with a glutamate and aspartate, respectively, in many of the orthologs and paralogs (including human IFIT1B). Both substitutions are conservative, because neither would disrupt hydrogen-bonding patterns nor interfere with the van der Waals interactions with the cap. We tested this by carrying out an EMSA between m7Gppp-RNA and IFIT1 N216D or IFIT1 Q42E (Fig. S4*L*). Whereas N216D had no impact on RNA binding, Q42E weakened the interaction and in translation assays, Q42E reduced IFIT1 activity similarly to Q42A (Fig. 5*B*, *Right*). In other IFIT1-like proteins, such as rabbit IFIT1 and rabbit IFIT1B [both of which bind m7Gppp-RNA with ~20 and 10 nM affinity, respectively (19)], the natural Q42E variation is likely overcome by compensatory interactions.

Unlike IFIT1B from other species, human IFIT1B lacks an apparent function in RNA binding (12). Sequence comparison shows that, along with Q42E, human IFIT1B has acquired additional substitutions that could impact RNA recognition: L150 is replaced with an Ala, which would affect cap ribose interactions, and R255 with Gln, which would disrupt a salt-bridge with the γ-phosphate (Fig. 3 *E* and *F*). Supporting this theory, mutation of R255 in human IFIT1 (R255M) was shown to disrupt capped- and PPP-RNA binding (13, 18). On the other hand, mice lack a bona fide IFIT1 ortholog and instead encode three copies of IFIT1B-like proteins (12), currently annotated as mouse Ifit1, mouse Ifit1b, and mouse Ifit1c (Fig. S5). Mouse

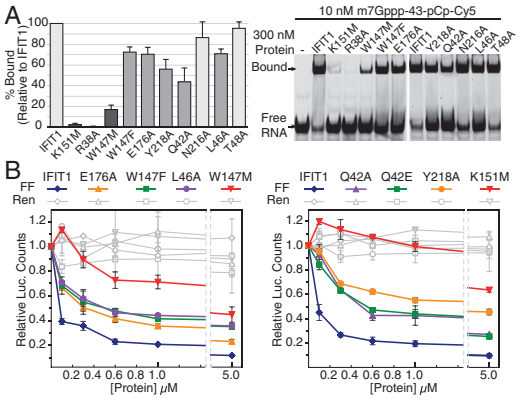

Fig. 5. Functional validation of cap recognition. (*A*) Mutational analysis of cap-binding residues investigated by fluorescent EMSA with 3′-end–labeled (pCp-Cy5) RNA. (*Left*) Quantification of percent bound (*Upper* band, *Right*) for each mutant normalized against IFIT1. Data represent the mean of three independent measurements ± SD. (*B*) In vitro translation assays with RNA binding mutants and Cap0 reporter. Data represent the mean of two measurements ± SD.

Ifit1b and Ifit1c harbor several substitutions that would disrupt RNA binding, such as R255G and Q42T in both, and R187H in Ifit1b (Fig. S5). Consistent with this finding, pull-downs showed that mouse Ifit1c cannot bind capped RNA directly (18).

IFIT1 Cap Binding Is Distinct from Canonical Cap-Binding Proteins. The IFIT1 cap-binding mechanism described here is quite distinct from canonical cap-binding proteins such as eIF4E (34), cap-binding complex (CBC) (35), and VP39 (vaccinia virus N1 2′-O MTase) (36). Through convergent evolution these proteins evolved a highly specific cap-binding slot between two aromatic side-chains that engage the methylated guanine in a cation–π sandwich (31). Charge–charge interactions with the delocalized positive charge and van der Waals contacts with the *N7*-methyl also play a role (31). In these proteins, the absence of *N7*-methylation and associated positive charge on the base results in >100-fold loss in binding affinity (37). These proteins also rely on hydrogen bonds targeting groups at the m7G base periphery. The cumulative effect of these restrictions results in highly specific recognition of the cap in a single *anti*-conformation of m7G (Fig. 6).

In contrast, IFIT1 engagement of the cap is relatively less specific, permitting both *syn*- and *anti*-base orientations, as described above. Although IFIT1 does use one aromatic residue for cap stacking, the remainder of its sandwich is formed by aliphatic side chains (Leu-46, Thr-48, and Ile-183) rather than another aromatic residue. Therefore, the lack of an electron-rich, aromatic cap-binding slot reduces the dependence on an electron-deficient, *N7*-methylated base. Additionally, protein contacts with the *N7*-methyl are dispensable (e.g., the N216A mutant), and they are altogether absent when the cap is in the *syn*-configuration. Importantly, IFIT1 lacks any sequence specific hydrogen bonding from protein residues, and instead uses a more plastic, water-mediated hydrogen-bonding network for base recognition.

Finally, at physiological pH m7G exists in an equilibrium between two forms: a positively charged "keto tautomer" and a zwitterionic "enolate tautomer" (in which *N1* is deprotonated) (Fig. S4*H*) (34). The canonical cap-binding proteins are highly selective for guanine as the base and in particular, its keto form. These aspects are enforced by two elements: (*i*) the cation–π sandwich, which is only compatible with an electron-deficient, positively charged keto tautomer (38); and (*ii*) Asp or Glu residues at one end of the cap-binding slot, which hydrogen bond with a protonated *N1* and the *N2*-amino group. Conversely, IFIT1 does not form any keto- or enolate-specific interactions with the base, suggesting that IFIT1 is not selective for the tautomerization state, reinforcing the lack of guanine specificity.

Binding of Cap-Proximal Nucleotides. Recognition of the four RNA nucleotides following the cap is conformation-specific and can be divided into two distinct dinucleotide groups diverging between N2 and N3 (Fig. 2 *C*–*E*). The RNA backbone lies along the superhelical axis of the protein, and is recognized by specific hydrogen bonds and salt bridges from protein residues targeting the 5′-phosphates and 2′-hydroxyls of N2 and N3 (Fig. S6 *A* and *B*). In contrast, recognition of the bases is predominantly through sequence-nonspecific van der Waals and stacking interactions. The first dinucleotide (N1 and N2) adopts geometry similar to CpG dinucleotides found within Z-form RNA and UUCG tetraloops (39), and is tightly sandwiched between multiple protein residues (Fig. S6 *A* and *C*). The second dinucleotide (N3 and N4) adopts A-form helical geometry with the bases also stacked upon each other and abutted by protein residues from above and below (Fig. S6 *B* and *D*). The large water network inside the tunnel interacts with all groups of the RNA, and mediates both intermolecular protein–RNA and intramolecular RNA–RNA interactions (Fig. S6*E*). Interestingly, a large part of this extensive water network is involved in protein–base contacts, allowing IFIT1 to recognize a wide variety of RNA sequences that may exist at the 5′-end of viral RNA. A small degree of sequence-dependent binding affinity variation may exist because there are two adenine-specific hydrogen

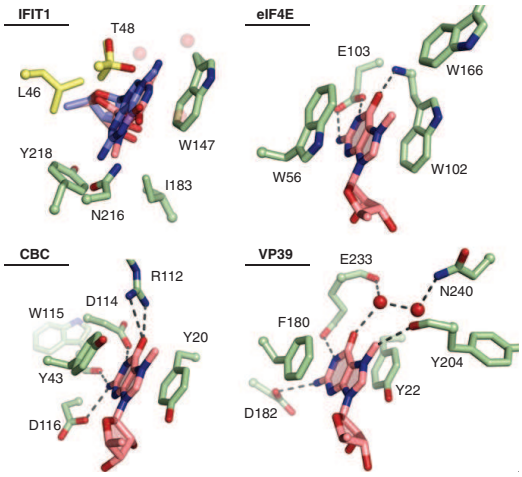

Fig. 6. Comparison with the canonical cap-binding proteins eIF4E (PDB ID code 1EJ1), CBC (PDB ID code 1H2T), and VP39 (PDB ID code 1V39). In IFIT1, some of the nearby water molecules are shown as transparent red spheres, and T48 adopts two conformations.

bonds at N2 and N4 (Fig. S6 *A* and *B*), although RNA binding assays show that adenosines are not strictly required at these positions.

The 3′-end of the RNA (N4) emerges from the C-terminal opening of the tunnel and points toward a positively charged, solvent-exposed groove formed by the pivot helices and the third subdomain (Fig. 7). This surface is contiguous with the RNA-binding tunnel and also appears to contribute to RNA interactions because the analogous region in IFIT5 can apparently bind tRNA (14). In IFIT1, the groove does play some role in RNA binding, as primer-extension toe-printing assays suggested that IFIT1 has a 6- to 8-nt footprint at the 5′-end of mRNA, and mutational analysis of this region had an impact on mRNA binding (19). However, cocrystal structures of IFIT1 with longer oligonucleotides (6–8 nt in length) revealed extra electron density for only the 5′-phosphate of a fifth nucleotide, as was shown for IFIT5 (13), suggesting that only the first four nucleotides are stably bound by IFIT1, whereas residues in the positively charged groove probably contribute to nonspecific RNA binding.

IFIT1 Senses Ribose 2′-O Methylation at N1 and N2. The mRNA of higher eukaryotes is normally modified by ribose 2′-O methylation at N1 and N2 (40). Whereas all cellular mRNAs are methylated at N1 in the nucleus by the endogenous Cap1-methyltransferase (CMTr1) (2), ribose methylation at N2 arises from secondary methylation in the cytoplasm through the action of CMTr2 (3, 41), and accompanies N1 methylation on up to 50% of cellular mRNAs (42, 43). N1 ribose methylation is a molecular determinant of self that can protect mRNA from IFIT1/IFIT1B recognition (18, 19), but the role of N2 methylation in this process is unknown. To gain additional insight into self- vs. nonself-mRNA discernment by IFIT1, and to explore the uncharacterized role of ribose N2 methylation in this process, we examined the interaction between human IFIT1 and differentially methylated RNA. Note that, to distinguish the naturally occurring Cap1 and Cap2 structures (m7GpppNmN- and m7GpppNmNm-) from capped RNAs that contain ribose N2 methylation only (m7GpppNNm-), we refer to the latter as Cap0^{N2Me}-RNA.

When bound to IFIT1, N1 and N2 adopt a rare Z-RNA–like conformation that is dependent on their respective ribose conformations (Fig. S6*F*) (39). Whereas N2 is in the favorable C3′-*endo* conformation, N1 adopts a C2′-*endo* conformation and

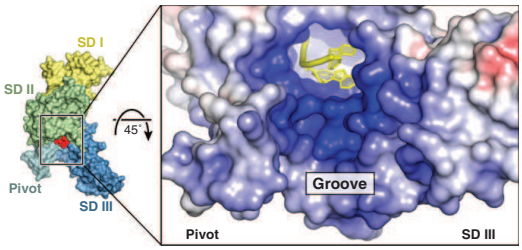

Fig. 7. IFIT1 forms a positively charged, solvent-exposed RNA binding groove. See Fig. S5 for residues in this region.

places its 2′-OH in close proximity to the side chains of two highly conserved residues, R187 and Y157 (Fig. 8*A* and Fig. S6*A*). Modeling of ribose 2′-O methylation on N1 to mimic Cap1-mRNA shows that the methyl group would clash with these protein residues (Fig. 8*A*). Rotating the methyl group away introduces a steric clash with the RNA itself and interferes with the water network. Interestingly, N2 ribose methylation is also predicted to disrupt RNA binding to IFIT1, because of hydrogen bonds with H289 and steric hindrance by Q290 (Fig. 8*A* and Fig. S6*A*). Thus, the IFIT1 tunnel is restricted to interact with RNAs not methylated at these 2′-hydroxyls.

Consistent with this finding, either N1 or N2 methylation of HCoV and GGG42 RNAs is sufficient to disrupt binding with up to 2.5 μM IFIT1 (Fig. 8*B* and Fig. S7 *A* and *B*). Surprisingly, at the same concentrations, individual N1 or N2 methylation only partially reduced the interaction between IFIT1 and MHV RNA, and combining both was required to fully abolish binding for this sequence (Fig. 8*B* and Fig. S7 *A*–*C*). This RNA-dependent effect is likely because of the longer overhang and decreased secondary structure stability of the MHV sequence compared with HCoV/GGG42 (Fig. 1*A* and Fig. S1*B*), allowing it to maintain relatively strong binding to IFIT1, even when modified with a single ribose methylation, and requiring the additive effect of multiple methylations (N1+N2) to avoid IFIT1 recognition. However, we cannot rule out the existence of RNA-sequence or other structural elements within MHV that intrinsically enhance its affinity for IFIT1. At higher protein concentrations (5 μM IFIT1) where nonspecific interactions may play a role, the additive effects of N1+N2 ribose methylations also became apparent for the GGG42 RNA (Fig. S7 *D* and *E*).

Consistent with the above findings, single N1 or N2 methylation of the reporter mRNA reduced IFIT1 inhibitory activity in translation assays by ∼10-fold (IC_{50} ∼ 1 μM) (Fig. 8*C*), whereas translation of Cap1- and $Cap0^{N2Me}$-mRNA was still strongly inhibited by 5 μM IFIT1. This finding intriguingly suggests that N1- or N2-methyl steric hindrance can be overcome at very high IFIT1 concentrations, possibly from nonspecific RNA interactions contributed by the solvent exposed groove of IFIT1. As before, combining N1 and N2 methylations (Cap2 reporter) resulted in a striking rescue of translational inhibition, restoring FF levels to 90% even in the presence of 5 μM IFIT1 (Fig. 8*C*). Taken together, our combined structural and functional analysis confirms the role of N1 methylation in interfering with IFIT1 inhibitory activity, and reveals an analogous function for N2 methylation. Importantly, our data suggest that the combination of N1 and N2 methylation, as found in nearly half of endogenous mRNAs, produces an additive and potentially synergistic protective effect against IFIT1 recognition, which is particularly evident under circumstances where IFIT1 can overcome individual 2′-O methylation in an RNA-dependent or protein concentration-dependent manner.

To further confirm the importance of 2′-O methyl sensing for IFIT1 activity, we mutated the residues predicted to clash with N1 or N2 ribose methylations, and tested their impact on RNA binding and translational inhibition (Fig. 8 *D* and *E*). At N1, Y157F had only a minor effect on capped RNA binding, but both R187H and R187A abolished the interaction. At N2, mutating either H289 (H289A) or Q290 (Q290E) partially reduced binding, and combining either mutant with Y157F (DM-YH, Y157F/H289A; or DM-YQ, Y157F/Q290E) completely disrupted binding. Translation assays also showed reductions in IFIT1 inhibitory activity for all mutants, with R187H and the two double mutants having the greatest effect. It should be noted, however, that these residues are highly conserved (Fig. S4*M*), and as such, play an integral role in general RNA binding that extends beyond 2′-O methyl sensing (Fig. S6 *A* and *B*). Thus, capped-RNA recognition and 2′-O methyl sensing by IFIT1 are two tightly linked processes that have likely coevolved.

Functional Validation of IFIT1 Activity Against 2′-O Methyltransferase Deficient Human Coronavirus. Human IFIT1 has been shown to inhibit replication of viruses lacking N1 ribose 2′-O methylation, such as HCoV 229E bearing a D129A (DA) mutation in its viral 2′-O MTase gene (18). Therefore, to functionally validate our results in a biological context, we tested the antiviral activity of IFIT1 RNA-binding mutants against wild-type HCoV 229E and HCoV 229E DA. First, we verified that the IFIT1 mutants used in cell-based assays (R187H, W147M, Y157F, and Q290E) disrupted the interaction with Cap0-HCoV RNA (Fig. S7*F*). Next, we reconstituted Flp-In T-REx 293 IFIT1 knockout cells with human IFIT1 or IFIT1 mutants, and assayed HCoV growth in these cells (Fig. 8 *F* and *G*). Although expression of a control protein (GFP) led to comparable accumulation of both wild-type and DA virus in the supernatant of infected cells, expression of IFIT1 significantly reduced growth of the DA mutant virus, but not wild-type virus (Fig. 8*F*). In contrast, IFIT1 R187H, which disrupts interactions with the cap ribose and bridging triphosphate (Fig. 3 *E* and *F*), was unable to impair HCoV 229E DA virus growth (Fig. 8*F*). Similarly, W147M, which disrupts cap recognition, or Y157F and Q290E, which impair binding to Cap0-HCoV RNA (Fig. S7*F*), lost their antiviral activity against HCoV 229E DA (Fig. 8*G*). Thus, IFIT1 binding to 2′-O unmethylated viral RNA is required for its antiviral properties.

Discussion

The ability of many viruses to cap their mRNA and mimic the host's allows them to hijack a cell's translational machinery and replicate new virus particles. To counteract this, host cells have evolved as part of their antiviral program, the IFIT proteins. By competing with eIF4E/eIF4F for binding to capped RNA, IFIT1 can prevent viral propagation by latching onto the ends of mRNA and preventing assembly of ribosomal initiation complexes (18, 19). Whereas recognition of the cap by eIF4E and other cap-binding proteins occurs in a highly specific manner (31, 37), we surprisingly found that recognition of the cap moiety by IFIT1 is instead nonspecific with regards to both sequence and structure. Through its highly water-filled cap-binding pocket, IFIT1 can accommodate not only bona fide cap in different orientations, but also an unmethylated cap, adenine cap, and presumably other structures too. This built-in plasticity may in part be to allow IFIT1 to maintain a broad spectrum of antiviral activity, and to thwart the ability of viral structures to rapidly evolve. Another possibility is that IFIT1 genes simply have not had enough time to evolve exquisite cap specificity, because they emerged relatively recently in evolution [jawed vertebrates (12)] compared with eIF4E and CBC, which are essential genes in all eukaryotes (34, 35). Regardless, the penalty for this plasticity is likely a reduction in affinity for the cap moiety and in this respect, the recognition of nucleotides beyond the cap provides IFIT1 the additional affinity required to compete with an otherwise very tight eIF4F–5′-cap complex.

The recognition of cap-proximal nucleotides by IFIT1 also plays a critical role in discerning self from nonself. Our structural analysis revealed that IFIT1 forms a tight interacting surface around the ribose 2′-hydroxyls of N1 and N2, thus preventing recognition of endogenous mRNAs methylated at these positions

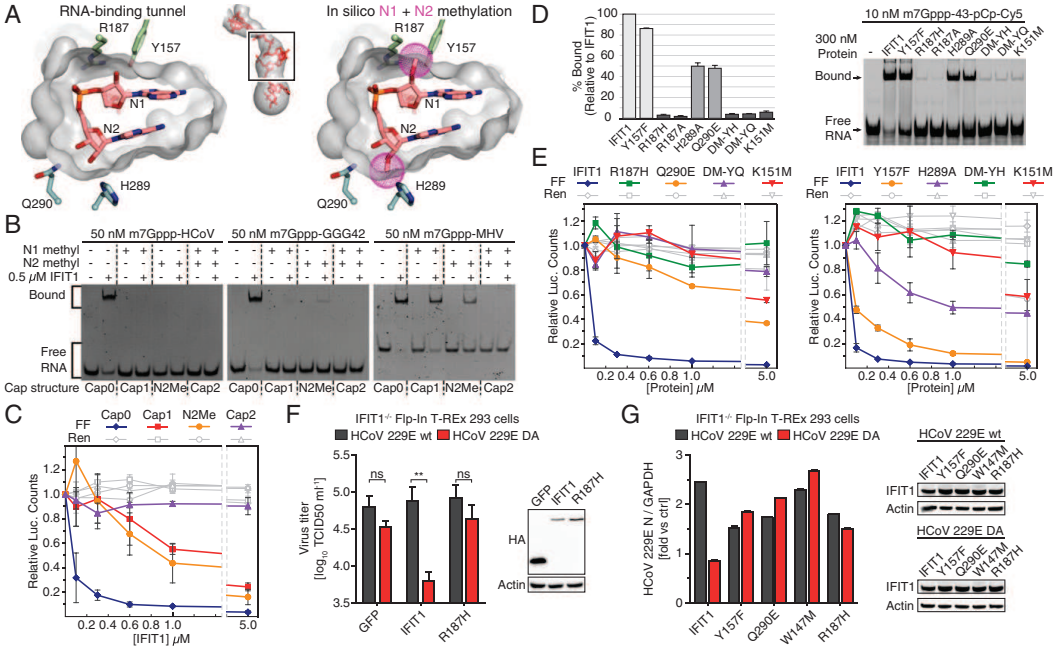

Fig. 8. Sensing of N1 and N2 ribose 2′-O methylation by IFIT1. (*A*, *Left*) Cross-section of the IFIT1 tunnel van der Waals surface (gray) and residues predicted to clash with N1 and N2 methylations. (*Right*) In silico rigid body modeling of N1 and N2 methylations (purple dots). (*B*) SYBR Gold-stained EMSAs between 0.5 μM IFIT1 and differentially methylated m7Gppp-RNA. The dashed lines demarcate lanes with different cap structures, as indicated by the labels below the gel. See Fig. S7 *A–E* for additional gel shifts. (*C*) Translation assay with differentially methylated reporter mRNA. Data represent the mean of three independent measurements performed in duplicate ± SD. (*D*) Mutational analysis of 2′-O methyl sensing residues investigated by fluorescent EMSA similar to Fig. 5*A*. (*E*) In vitro translation assays with 2′-O methyl sensing mutants and Cap0 reporter. Data represent the mean of two measurements ± SD. (*F*) Flp-In T-REx 293 IFIT1 knockout cells were cotransfected with expression plasmids for CD13 and either GFP control, wild-type IFIT1, or IFIT1 R187H and infected with HCoV 229E wild-type or HCoV 239E DA. Virus titers in supernatants were determined by $TCID_{50}$ 18 h postinfection. Data represent the mean of three independent experiments ± SD. $^{**}P < 0.01$ as analyzed by two-way ANOVA with Bonferroni posttest. The Western blots show expression of proteins at the time of infection. (*G*) Similar to *F*, except IFIT1 knockout cells were reconstituted with the indicated IFIT1 constructs or GFP, and virus growth determined by quantitative PCR. Data represent the mean fold-change ± SD of triplicate measurements of the viral *N*-gene signal, relative to GFP control (ctrl). One representative experiment of three is shown. Western blots show protein expression at the end of the experiment.

and restricting IFIT1 activity to unmethylated viral mRNAs. This finding is supported by a comprehensive gel-shift analysis that showed a preference for recognizing Cap0 structures over N1 or N2 methylated RNA, in vitro translation assays that showed a reduction in IFIT1's ability to inhibit translation of N1 or N2 methylated mRNA reporters, and human coronavirus infectivity assays that showed enhanced IFIT1 antiviral activity when viral N1 methylation was mutated. In this way, IFIT1 effector function complements RIG-I receptor activity (summarized in Fig. S7 *H–J*), as RIG-I detects blunt-ended, base-paired PPP- and Cap0-RNAs to up-regulate IFIT1 and other ISGs (8, 9).

Cellular N1 methylation was generally thought to be the primary determinant of self, protecting endogenous mRNA from IFIT1 recognition, but we discovered that the ability to discern between Cap0 and Cap1 structures is diminished for one of our RNAs (MHV) (Fig. 8*B*), an effect that is possibly linked to its 5′-sequence or secondary structure. This finding is in accordance with a recent study by Daugherty et al., who demonstrated that human IFIT1 can target both Cap0 and Cap1 mRNAs when overexpressed in a yeast system (12). Furthermore, while this manuscript was under revision, Young et al. similarly showed that N1 methylation of a reporter gene only partially reduced its sensitivity to human IFIT1 in an in vitro translation system (44). Interestingly, using viral mRNA in the same system, Young et al. also noted potential RNA-dependent effects for N1 methylation. Taken together, these observations lead to the conclusion that N1 methylation alone may not be enough to protect all endogenous mRNAs from IFIT1, and that there are other determinants of self that govern IFIT1 activity.

Our structural and functional analysis reveals that N2 methylation by CMTr2 could fulfill this role, providing an additional safeguard against aberrant recognition of mRNAs that are otherwise susceptible to IFIT1 (Fig. 8*B*). However, as Cap2 structures are not as ubiquitous as Cap1 (40), other elements may prevent self-recognition. For example, actively translating mRNAs are generally found in preformed mRNP complexes and, as indicated by our order-of-addition experiment (Fig. 1*C*), would be protected from IFIT1 competition. Similarly, newly synthesized mRNAs undergo a pioneer round of translation directed by the CBC (45), which may also offer protection from IFIT1. Adenosine *N6*-methylation of the first transcribed nucleotide is another modification that accompanies ribose N1 methylation on ∼20–30% of cellular mRNAs, in the form of *N6*,O2′-dimethyladenosine (m6Am) (46, 47). Our structure suggests that m6Am could protect self-mRNAs by disrupting water-mediated interactions and impinging on nearby residues (Fig. S6 *A* and *E*), and thus merits further investigation. Finally, cap-proximal secondary structure

elements could combine with mRNA modifications to further prevent self-recognition.

To what extent do viruses exploit these mechanisms to alter IFIT1 activity? Our observations support the model whereby viral N1 methylation evades or dampens IFIT1 activity (Fig. 8 *F* and *G*), and is consistent with previous studies showing enhanced sensitivity of coronaviruses and flaviviruses to IFIT1 when viral N1 methylation was mutated (18, 23, 24, 26). Similarly, Young et al. recently showed that parainfluenza virus type 5 (PIV5) was more sensitive to human IFIT1-mediated restriction than PIV3, partly because PIV5 mRNAs were not completely N1-methylated during infection (44). On the other hand, vesicular stomatitis virus (VSV) has been shown to uniformly N1-methylate its mRNAs in vivo (48, 49), yet it remains sensitive to IFIT1 restriction (12). One explanation is that the short and potentially unstructured 5′ UTRs of VSV mRNAs could allow IFIT1 to overcome N1 methylation (as described here for MHV RNA). Alternatively, VSV mRNAs may display another pattern specifically recognized by IFIT1 (as proposed by Daugherty et al.), such as RNA-sequence or -structural elements (12). Further work is needed to validate either notion, and to determine if this ability to overcome viral N1 methylation is an adaptation that allows IFIT1 to target other Cap1-containing viruses, or if it is restricted to VSV and related viruses.

IFIT1B (which includes mouse Ifit1) is the only other IFIT family member known to specifically recognize capped RNAs to inhibit viral replication (18, 19). Our analysis supports the notion that both proteins use a similar mode of cap-recognition, and thus should display overlapping antiviral activities. However, recent evidence suggested otherwise (12). Based on our structural and functional data, we propose that both IFIT1 and IFIT1B can target Cap0-containing viruses, but they may differ in their sensitivity to cap-proximal modifications, such as methylation, RNA-sequence, or RNA-structure. These differences and underlying molecular mechanisms are not entirely clear yet, but one possibility is that the ability to overcome N1 methylation in an RNA-dependent manner could distinguish IFIT1 from IFIT1B proteins, and may explain why IFIT1 overexpression inhibited wild-type VSV replication (a Cap1-containing ssRNA virus), whereas IFIT1B overexpression did not (12). Regardless, in humans IFIT1B appears to be nonfunctional, and has been deleted or pseudogenized in several other mammals, consistent with the notion that widespread viral evasion strategies (e.g., N1 methylation) have generally defeated IFIT1B (12), whereas IFIT1 was retained possibly because of its adaptable nature.

Taken together, through a relatively nonspecific cap-binding pocket and a potentially plastic RNA binding mechanism, IFIT1 appears to have grafted adaptability onto an otherwise germ-line–encoded member of the innate immune system, to broadly defend against rapidly evolving viral pathogens. At the same time, the host evolved multiple mechanisms that combine to limit detrimental IFIT1 activity against endogenous mRNAs. Clearly, further work is needed to validate the physiological relevance of these notions, particularly with respect to understanding how IFIT1 can overcome N1 methylation in an RNA-dependent manner, the differential specificities of IFIT1 and IFIT1B proteins, and if viruses exploit CMTr2 and other enzymes to modify their mRNA and evade IFIT1. Finally, it has been established that human IFIT1 can form complexes with other IFIT family members (IFIT2 and IFIT3) and several host factors (17), which could play a role in modulating self- vs. nonself-mRNA recognition and translational inhibition. Our structural and functional analysis of IFIT1-capped RNA interactions will provide a framework for future structure-guided studies of IFIT function. Moreover, these efforts will provide important contributions to the development of mRNA therapeutics and to vaccine design, as emerging research suggests that rendering viruses more susceptible to IFIT1-like antiviral responses, by inhibiting their mRNA 2′-O methylation or modifying their 5′-secondary structure, is a strategy for the rapid development of live, attenuated vaccines (e.g., refs 21–24).

Materials and Methods

Detailed discussions of the materials and methods used in this study are provided in *SI Materials and Methods*.

Protein Expression and Purification. IFIT proteins, RNMT (Human N7-MTase), and TbMTr2 (*Trypanosoma brucei* Cap2 MTase) were expressed in *Escherichia coli*, and purified by Ni-affinity, ion-exchange, and size-exclusion chromatography. CMTr2 (Human Cap2 MTase) was expressed in *Sf9* insect cells and purified by Ni-affinity and size-exclusion chromatography.

IFIT1 Crystallography. IFIT1 monomeric mutants (L457E/L464E or N216A/L457E/L464E) were purified to homogeneity and mixed with molar excess chemically synthesized oligos (see *SI Materials and Methods* for synthesis, purification, and MS of oligos) and crystallized in 27–32% (vol/vol) PEG 200, 0.1 M Tris pH 8.1, and 200 mM $CaCl_2$. Crystals were flash-frozen in liquid nitrogen without additional cryoprotection, and diffraction data were collected at Canadian Light Source beamline 08ID-1 (Table S1). Initial structures were determined by molecular replacement, subsequent structures by rigid body refinement.

RNA EMSA. RNAs for EMSAs were prepared using T7 RNA polymerase and purified by denaturing PAGE. Appp-GGG42 was capped cotranscriptionally; other modifications were performed with CIP (New England Biolabs), vaccinia capping enzyme (New England Biolabs), Cap1 2′-O MTase (New England Biolabs), or home-made CMTr2 or TbMTr2. All 5′ caps and RNA sequences were confirmed by LC/MS. RNA sequences and mass spec summary are in Tables S2 and S3, respectively. The 3′-end labeling of m7Gppp-43 with pCp-Cy5 was performed with T4 RNA ligase (New England Biolabs). For EMSAs, purified proteins and RNA were mixed at the indicated concentrations in each figure, and resolved by native PAGE [1× TBE, 10% (vol/vol) gels]. Bands were visualized with SYBR Gold and UV imaging (unlabeled RNA), or with a Typhoon R3 imager (for pCp-Cy5 labeled RNA). Band densitometry was performed with ImageJ.

Reporter mRNA Preparation and in Vitro Translation Assay. The bicistronic reporter (5′-UTR sequence is in Table S2) was in vitro transcribed with SP6 RNA polymerase in the presence of either m7GpppG, GpppG, or ApppG RNA Cap Analog (New England Biolabs). N1/N2 methylations were performed post transcriptionally using mRNA Cap1 2′-O MTase (New England Biolabs) and/or TbMTr2. In vitro translations were set up at a final volume of 10 μL with 4 ng/μL reporter mRNA (~4 nM final) and 1 μL protein in untreated Krebs-2 extracts, and performed as described in *SI Materials and Methods*.

Virus Infectivity Assay. Flp-In T-REx 293 IFIT1$^{-/-}$ cells were cotransfected with plasmids for IFIT1 and CD13 (HCoV receptor). Cells were treated with 20 units of IFN-β or left untreated and 24 h later infected with HCoV 229E wild-type and HCoV 229E DA with a multiplicity of infection of 1 and 1.25, respectively. Eighteen hours postinfection, virus accumulation was tested by quantitative RT-PCR or $TCID_{50}$ analysis.

ACKNOWLEDGMENTS. We thank the Canadian Macromolecular Crystallography Facility staff for X-ray data collection (Canadian Light Source); Dr. A. Wahba for LC-MS (McGill University); A. Gorelik, Dr. N. Siddiqui, and Dr. M. W. Górna for feedback and reading of the manuscript; A. Gorelik and K. Illes for *Sf9* expression; and P. Sénéchal for assistance with translation assays. Support was provided by the Canadian Institutes of Health Research Strategic Training Initiative in Chemical Biology and the Natural Sciences and Engineering Research Council CREATE Training Program in Bionanomachines (Y.M.A.); a Canada Research Chair (B.N.); Canadian Institutes of Health Research Grants MOP-133535 (to B.N.) and MOP-115126 (to J.P.); a Discovery grant from the Natural Sciences and Engineering Research Council of Canada (to M.J.D.); the McGill Canadian Institutes of Health Research Drug Development Training Program (S.M.-M.); and the Max-Planck Free Floater program, the European Research Council (StG iVIP, 311339), InfectERA (ERASE), and the German Federal Ministry of Education and Research (A.P.).

1. Pelletier J, Graff J, Ruggero D, Sonenberg N (2015) Targeting the eIF4F translation initiation complex: A critical nexus for cancer development. *Cancer Res* 75(2):250–263.
2. Bélanger F, Stepinski J, Darzynkiewicz E, Pelletier J (2010) Characterization of hMTr1, a human Cap1 2′-O-ribose methyltransferase. *J Biol Chem* 285(43):33037–33044.
3. Werner M, et al. (2011) 2′-O-ribose methylation of cap2 in human: Function and evolution in a horizontally mobile family. *Nucleic Acids Res* 39(11):4756–4768.
4. Daffis S, et al. (2010) 2′-O methylation of the viral mRNA cap evades host restriction by IFIT family members. *Nature* 468(7322):452–456.

5. Züst R, et al. (2011) Ribose 2′-O-methylation provides a molecular signature for the distinction of self and non-self mRNA dependent on the RNA sensor Mda5. *Nat Immunol* 12(2):137–143.
6. Decroly E, Ferron F, Lescar J, Canard B (2011) Conventional and unconventional mechanisms for capping viral mRNA. *Nat Rev Microbiol* 10(1):51–65.
7. Hyde JL, Diamond MS (2015) Innate immune restriction and antagonism of viral RNA lacking2′′-O methylation. *Virology* 479-480:66–74.
8. Schuberth-Wagner C, et al. (2015) A conserved histidine in the RNA sensor RIG-I controls immune tolerance to N1-2′O-methylated self RNA. *Immunity* 43(1):41–51.
9. Devarkar SC, et al. (2016) Structural basis for m7G recognition and 2′-O-methyl discrimination in capped RNAs by the innate immune receptor RIG-I. *Proc Natl Acad Sci USA* 113(3):596–601.
10. Fensterl V, Chattopadhyay S, Sen GC (2015) No love lost between viruses and interferons. *Annu Rev Virol* 2(1):549–572.
11. Fensterl V, Sen GC (2015) Interferon-induced Ifit proteins: Their role in viral pathogenesis. *J Virol* 89(5):2462–2468.
12. Daugherty MD, Schaller AM, Geballe AP, Malik HS (2016) Evolution-guided functional analyses reveal diverse antiviral specificities encoded by IFIT1 genes in mammals. *elife* 5:60.
13. Abbas YM, Pichlmair A, Górna MW, Superti-Furga G, Nagar B (2013) Structural basis for viral 5′-PPP-RNA recognition by human IFIT proteins. *Nature* 494(7435):60–64.
14. Katibah GE, et al. (2013) tRNA binding, structure, and localization of the human interferon-induced protein IFIT5. *Mol Cell* 49(4):743–750.
15. Yang Z, et al. (2012) Crystal structure of ISG54 reveals a novel RNA binding structure and potential functional mechanisms. *Cell Res* 22(9):1328–1338.
16. Feng F, et al. (2013) Crystal structure and nucleotide selectivity of human IFIT5/ISG58. *Cell Res* 23(8):1055–1058.
17. Pichlmair A, et al. (2011) IFIT1 is an antiviral protein that recognizes 5′-triphosphate RNA. *Nat Immunol* 12(7):624–630.
18. Habjan M, et al. (2013) Sequestration by IFIT1 impairs translation of 2′O-unmethylated capped RNA. *PLoS Pathog* 9(10):e1003663.
19. Kumar P, et al. (2014) Inhibition of translation by IFIT family members is determined by their ability to interact selectively with the 5′-terminal regions of cap0-, cap1- and 5′ppp- mRNAs. *Nucleic Acids Res* 42(5):3228–3245.
20. Kimura T, et al. (2013) Ifit1 inhibits Japanese encephalitis virus replication through binding to 5′ capped 2′-O unmethylated RNA. *J Virol* 87(18):9997–10003.
21. Hyde JL, et al. (2014) A viral RNA structural element alters host recognition of nonself RNA. *Science* 343(6172):783–787.
22. Reynaud JM, et al. (2015) IFIT1 differentially interferes with translation and replication of alphavirus genomes and promotes induction of type I interferon. *PLoS Pathog* 11(4):e1004863.
23. Menachery VD, et al. (2014) Attenuation and restoration of severe acute respiratory syndrome coronavirus mutant lacking 2′-o-methyltransferase activity. *J Virol* 88(8):4251–4264.
24. Züst R, et al. (2013) Rational design of a live attenuated dengue vaccine: 2′-o-methyltransferase mutants are highly attenuated and immunogenic in mice and macaques. *PLoS Pathog* 9(8):e1003521.
25. Szretter KJ, et al. (2012) 2′-O methylation of the viral mRNA cap by West Nile virus evades ifit1-dependent and -independent mechanisms of host restriction in vivo. *PLoS Pathog* 8(5):e1002698.
26. Pinto AK, et al. (2015) Human and murine IFIT1 proteins do not restrict infection of negative-sense RNA viruses of the orthomyxoviridae, bunyaviridae, and filoviridae families. *J Virol* 89(18):9465–9476.
27. Novac O, Guenier AS, Pelletier J (2004) Inhibitors of protein synthesis identified by a high throughput multiplexed translation screen. *Nucleic Acids Res* 32(3):902–915.
28. Amrani N, Ghosh S, Mangus DA, Jacobson A (2008) Translation factors promote the formation of two states of the closed-loop mRNP. *Nature* 453(7199):1276–1280.
29. Guo J, Hui DJ, Merrick WC, Sen GC (2000) A new pathway of translational regulation mediated by eukaryotic initiation factor 3. *EMBO J* 19(24):6891–6899.
30. Wang C, et al. (2003) Alpha interferon induces distinct translational control programs to suppress hepatitis C virus RNA replication. *J Virol* 77(7):3898–3912.
31. Quiocho FA, Hu G, Gershon PD (2000) Structural basis of mRNA cap recognition by proteins. *Curr Opin Struct Biol* 10(1):78–86.
32. Dougherty DA (2013) The cation-π interaction. *Acc Chem Res* 46(4):885–893.
33. De Gregorio E, Preiss T, Hentze MW (1998) Translational activation of uncapped mRNAs by the central part of human eIF4G is 5′ end-dependent. *RNA* 4(7):828–836.
34. Marcotrigiano J, Gingras AC, Sonenberg N, Burley SK (1997) Cocrystal structure of the messenger RNA 5′ cap-binding protein (eIF4E) bound to 7-methyl-GDP. *Cell* 89(6):951–961.
35. Mazza C, Segref A, Mattaj IW, Cusack S (2002) Large-scale induced fit recognition of an m(7)GpppG cap analogue by the human nuclear cap-binding complex. *EMBO J* 21(20):5548–5557.
36. Hodel AE, Gershon PD, Shi X, Wang SM, Quiocho FA (1997) Specific protein recognition of an mRNA cap through its alkylated base. *Nat Struct Biol* 4(5):350–354.
37. Fechter P, Brownlee GG (2005) Recognition of mRNA cap structures by viral and cellular proteins. *J Gen Virol* 86(Pt 5):1239–1249.
38. Hu G, Tsai AL, Quiocho FA (2003) Insertion of an N7-methylguanine mRNA cap between two coplanar aromatic residues of a cap-binding protein is fast and selective for a positively charged cap. *J Biol Chem* 278(51):51515–51520.
39. D'Ascenzo L, Leonarski F, Vicens Q, Auffinger P (2016) 'Z-DNA like' fragments in RNA: A recurring structural motif with implications for folding, RNA/protein recognition and immune response. *Nucleic Acids Res* 44(12):5944–5956.
40. Banerjee AK (1980) 5′-Terminal cap structure in eucaryotic messenger ribonucleic acids. *Microbiol Rev* 44(2):175–205.
41. Perry RP, Kelley DE (1976) Kinetics of formation of 5′ terminal caps in mRNA. *Cell* 8(3):433-442.
42. Wei CM, Moss B (1975) Methylated nucleotides block 5′-terminus of vaccinia virus messenger RNA. *Proc Natl Acad Sci USA* 72(1):318–322.
43. Cleaves GR, Dubin DT (1979) Methylation status of intracellular dengue type 2 40 S RNA. *Virology* 96(1):159–165.
44. Young DF, et al. (2016) Human IFIT1 inhibits mRNA translation of rubulaviruses but not other members of the paramyxoviridae family. *J Virol* 90(20):9446–9456.
45. Maquat LE, Tarn W-Y, Isken O (2010) The pioneer round of translation: Features and functions. *Cell* 142(3):368–374.
46. Wei C, Gershowitz A, Moss B (1975) N6, O2′-dimethyladenosine a novel methylated ribonucleoside next to the 5′ terminal of animal cell and virus mRNAs. *Nature* 257(5523):251–253.
47. Wei CM, Gershowitz A, Moss B (1976) 5′-Terminal and internal methylated nucleotide sequences in HeLa cell mRNA. *Biochemistry* 15(2):397–401.
48. Rose JK (1975) Heterogeneous 5′-terminal structures occur on vesicular stomatitis virus mRNAs. *J Biol Chem* 250(20):8098–8104.
49. Liang B, et al. (2015) Structure of the L protein of vesicular stomatitis virus from electron cryomicroscopy. *Cell* 162(2):314–327.
50. Pavelka A, et al. (2016) CAVER: Algorithms for analyzing dynamics of tunnels in macromolecules. *IEEE/ACM Trans Comput Biol Bioinformatics* 13(3):505–517.
51. Mossessova E, Lima CD (2000) Ulp1-SUMO crystal structure and genetic analysis reveal conserved interactions and a regulatory element essential for cell growth in yeast. *Mol Cell* 5(5):865–876.
52. Thillier Y, et al. (2012) Synthesis of 5′ cap-0 and cap-1 RNAs using solid-phase chemistry coupled with enzymatic methylation by human (guanine-N^7)-methyl transferase. *RNA* 18(4):856–868.
53. Berger I, Fitzgerald DJ, Richmond TJ (2004) Baculovirus expression system for heterologous multiprotein complexes. *Nat Biotechnol* 22(12):1583–1587.
54. Grochulski P, Fodje MN, Gorin J, Labiuk SL, Berg R (2011) Beamline 08ID-1, the prime beamline of the Canadian Macromolecular Crystallography Facility. *J Synchrotron Radiat* 18(Pt 4):681–684.
55. Otwinowski Z, Minor W (1997) Processing of X-ray diffraction data collected in oscillation mode. *Methods Enzymol* 276:307–326.
56. Winn MD, et al. (2011) Overview of the CCP4 suite and current developments. *Acta Crystallogr D Biol Crystallogr* 67(Pt 4):235–242.
57. McCoy AJ, et al. (2007) Phaser crystallographic software. *J Appl Cryst* 40(Pt 4):658–674.
58. Moriarty NW, Grosse-Kunstleve RW, Adams PD (2009) Electronic Ligand Builder and Optimization Workbench (eLBOW): A tool for ligand coordinate and restraint generation. *Acta Crystallogr D Biol Crystallogr* 65(Pt 10):1074–1080.
59. Adams PD, et al. (2010) PHENIX: A comprehensive Python-based system for macromolecular structure solution. *Acta Crystallogr D Biol Crystallogr* 66(Pt 2):213–221.
60. Emsley P, Lohkamp B, Scott WG, Cowtan K (2010) Features and development of Coot. *Acta Crystallogr D Biol Crystallogr* 66(Pt 4):486–501.
61. Chen VB, et al. (2010) MolProbity: All-atom structure validation for macromolecular crystallography. *Acta Crystallogr D Biol Crystallogr* 66(Pt 1):12–21.
62. Baker NA, Sept D, Joseph S, Holst MJ, McCammon JA (2001) Electrostatics of nanosystems: Application to microtubules and the ribosome. *Proc Natl Acad Sci USA* 98(18):10037–10041.
63. Robert X, Gouet P (2014) Deciphering key features in protein structures with the new ENDscript server. *Nucleic Acids Res* 42(Web Server issue):W320–W324.
64. Zuker M (2003) Mfold web server for nucleic acid folding and hybridization prediction. *Nucleic Acids Res* 31(13):3406–3415.
65. Schneider TD, Stephens RM (1990) Sequence logos: A new way to display consensus sequences. *Nucleic Acids Res* 18(20):6097–6100.
66. Hall MP, Ho CK (2006) Functional characterization of a 48 kDa *Trypanosoma brucei* cap 2 RNA methyltransferase. *Nucleic Acids Res* 34(19):5594–5602.
67. Robert F, et al. (2006) Initiation of protein synthesis by hepatitis C virus is refractory to reduced eIF2.GTP.Met-tRNA(i)(Met) ternary complex availability. *Mol Biol Cell* 17(11): 4632–4644.
68. Svitkin YV, Sonenberg N (2004) An efficient system for cap- and poly(A)-dependent translation in vitro. *mRNA Processing and Metabolism,* Methods in Molecular Biology, ed Schoenberg DR (Humana, Totowa, NJ), Vol 257, pp 155–170.
69. Zlatev I, et al. (2010) Efficient solid-phase chemical synthesis of 5′-triphosphates of DNA, RNA, and their analogues. *Org Lett* 12(10):2190–2193.
70. Zlatev I, Manoharan M, Vasseur J-J, Morvan F (2012) Solid-phase chemical synthesis of 5′-triphosphate DNA, RNA, and chemically modified oligonucleotides. *Curr Protoc Nucleic Acid Chem* Chapter 1:Unit1.28.

Part III

Discussion

The arms race between viruses and their hosts greatly advanced both, the viral strategies to exploit the host cell as well as the host defense system. Over the course of evolution, the host cell developed simple but effective mechanisms to detect and clear viral pathogens and thereby adapted to the sophisticated strategies viruses themselves evolved to evade the cellular defense system. The repertoire of host cells include pattern recognition receptors which are able to specifically sense viral genetic material, that lacks features host nucleic acids evolved to have. Moreover, host restriction factors represent a simple yet effective method to contain virus growth and nucleic acid turnover serves as an effective instrument to clear the cell from nucleic acids and thereby prohibits further virus spread. In this dissertation, I identified novel aspects of the host defense system. In particular, I present a novel strategy of the host to specifically degrade viral and furthermore insights into how a restriction factor inhibits translation of capped viral transcripts.

Novel aspects in antiviral immunity

The full potential of antiviral immunity is not yet known. However, in recent years it became clear that sensing by pattern recognition receptors and the subsequent induction of cytokines and type I interferons is not the only layer of nucleic acid immunity. Another layer of complexity was added, when first insights revealed specific degradation of viral nucleic acids. In general, RNA degradation is a process that is tightly regulated in order to regulate the abundance of mRNA and to spot aberrant cellular RNAs that need to be degraded. Targeted degradation of mRNA lowers the expression levels of specific proteins and thereby recycles the nucleotides needed for the synthesis of other transcripts the cell requires. The RNAs degraded by 5'- and 3'-exonucleases also include viral nucleic acids. However, the proteins involved to specifically degrade pathogenic nucleic acids are not known yet. Comparing the RNA degradation mechanisms of eukaryotes and prokaryotes revealed some striking similarities. mRNAs of both kingdoms are protected from degradation by either a 5'-cap structure in case of eukaryotes or a 5'-PPP group in case of bacteria. In order to be degraded, both chemical structures need to be removed. Notably, removal of the 5'-cap structure by DCP2 and dephosphorylation of the 5'-PPP group by RppH involves two proteins of the Nudix hydrolase family of proteins. Given that the genetic material of RNA viruses is chemically very similar to the mRNA of bacteria I took this assumption as a starting point to explore potential phosphatases of the human Nudix hydrolase family to use PPP-RNA as a substrate. In the work presented here, I could identify a novel mechanism involving NUDT2 that is specifically preparing 5'-PPP RNA substrates for degradation by the exonuclease XRN1. Furthermore, this mechanism seems to be universal and demands no specific sequence or structural feature

of the RNA substrate. Since the activity of Nudix hydrolases and especially of NUDT2 is conserved throughout evolution, this form or immunity may represent an ancient defense mechanism. Using Vesicular Stomatitis Virus (VSV) as model virus elucidated the antiviral capacity of NUDT2 in mouse embryonic fibroblasts and its importance is highlighted by the impact on the mortality of VSV infected mice that lack the *Nudt2* gene. The RNA of VSV serves as an ideal substrate for NUDT2 since its 5'-end is triphosphorylated and VSV is replicating in the cytoplasm of infected cells. Besides being localized to the cytoplasm, NUDT2 is also found in the nucleus. Since other classes of RNA viruses (e.g. IAV) use the nucleus of the host cell for their replication purposes, NUDT2 could serve as a broad acting surveillance system for viruses bearing 5'-PPP groups. Further studies, including different classes of RNA viruses as well as DNA viruses will give more detailed insights into the specificity of NUDT2. Already previously it was shown that the RNA of HCV is degraded in an XRN1 dependent manner[150]. However, it was unclear how the 5'-PPP RNA is prepared for degradation by the exonuclease XRN1 that strictly uses only 5'-monophosphorylated RNA as a substrate. It was hypothesized by Stanley Lemon and others[121;151;152] that an as yet unidentified cellular pyrophosphatase would need to remove phosphates from the 5'-end of viral RNAs to make it amenable for XRN1 cleavage. The mechanism of NUDT2 to remove phosphates from 5'-PPP RNA substrates to launch RNA degradation represents the first mechanism of a RNA degradation pathway that specifically targets viral RNAs. Several publications already emphasized the importance of viral RNA degradation or implied cellular proteins and pathways relevant for viral RNA degradation. This included both canonical cellular RNA turnover routes, the 5'-3' decay mediated by XRN1 or 3'-5' degradation by the exosome complex. However, none of the published data showed a targeted viral RNA degradation. NUDT2 could serve this role, since 5'-PPP RNAs are not present in cells under steady-state conditions and enter the cells only through virus infection. At the current stage, the observed phenotype is correlative since we could not show an active degradation of a specific viral RNA. To address this point, it would be insightful to develop targeted experiments, for instance pulse-chase experiments, which allow to unequivocally determine the stability of viral and cellular RNAs.

The relevance of NUDT2 is as well emphasized by the fact that many viruses evolved a variety of mechanisms to shield their triphosphorylated RNA ends to evade such a degradation mechanism. Many viruses hide from NUDT2 by protecting their nucleic acids with a 5'-cap structure just as their host does. The capping of host mRNAs takes place in the nucleus, therefore many viruses that replicate in the cytoplasm either achieve

a cap structure by encoding for their own capping machinery or by abducting it from cellular mRNAs in a process called cap snatching[153]. Other viruses like Picornaviruses bear a structural element at their 5'-end called internal ribosome entry site (IRES) that could offer a barrier for exonucleases[154]. Some RNA viruses also protect their RNA by the attachment of a viral genome-linked protein (VPg). HCV employs an unconventional mechanism to stabilize its RNA by recruiting miR-122 to its 5'-end. This liver-specific miRNA was shown to protect the viral nucleic acids from degradation by XRN1[155]. In addition, counter-measures of other plus-strand RNA viruses (e.g. flaviviruses) could be the formation of membranous replication factories that shield the viral nucleic acids from cellular proteins[156]. It is not clear yet, how NUDT2 would gain access to such cellular compartments or if the impact of NUDT2 on growth of those viruses is indeed limited by these viral counter-mechanisms. Screening more viruses would enhance our understanding of the comprehensiveness by which NUDT2 initiates RNA degradation.

An important point to consider is the impact of NUDT2 on the functionality of the innate immune system. NUDT2 is constitutively expressed and not induced upon stimulation by type I interferons (Philipp Hubel, unpublished data). However, NUDT2 is removing triphosphates from viral RNAs and may thereby modulate the stimulatory potential of viral PAMPs. It could well be, that the activity of NUDT2 needs to be tightly regulated in order to allow a proper immune response besides the clearance of viral genomic material. This could either involve a kinetic regulation where pattern recognition receptors like RIG-I find enough time to sense their putative ligand and initiate an antiviral response or a spatial separation of NUDT2 and pattern recognition receptors in different cellular compartments or cytoplasmic sub-compartments induced by specific viruses. Moreover, NUDT2 could potentially be held in an inactive state by other proteins bound to it. Stimulation with cytokines like type I interferons may abrogate these inhibitory factors and release fully active NUDT2. Identifying potential interaction partners of NUDT2 by affinity purification coupled to mass spectrometry would give valuable insights into such a potential regulation mechanism of NUDT2 on the protein level. Such findings could theoretically be used to develop therapeutic antiviral strategies. Boosting NUDT2 activity by modulating its activity would elevate the degradation of viral nucleic acids and decrease virus load.

In this PhD work, I chose growth of Vesicular stomatitis virus as functional readout to discover mammalian pyrophosphatases able to initiate a viral RNA degradation pathway. Thereby I found exclusively NUDT2 to have an impact on virus growth and the ability to release phosphates from a triphosphorylated RNA substrate. However, it could well be that other mammalian Nudix hydrolases have redundant functions. Testing their

potential on growth of other viruses including viruses with for instance capped nucleic acids could reveal the importance of other Nudix proteins. Moreover, I cannot exclude that NUDT2 had redundant function to other proteins. It could be that alternative cellular phosphatases similarly prepare viral RNA for degradation by nucleases. Most cellular phosphatases use post-translationally modified proteins as substrate and were not shown to be active on RNA. Another prerequisite for 5'-3' degradation of the RNA body would be a remaining monophosphate group since OH-RNA cannot serve as substrate for XRN1.

Further roles of dephosphorylation by NUDT2 in cellular homeostasis

The novel role of NUDT2 introduced here raises the question of cellular triphosphorylated RNA substrates for NUDT2. The principal substrate of NUDT2 is the thermal or genotoxic stress-induced diadenosine tetraphosphate (Ap4A)[157]. It is synthesized by a number of proteins including DNA ligases, firefly luciferase and most aminoacyl-tRNA synthetases[158]. Besides some other proteins, NUDT2 plays the major role in cleaving Ap4A to reduce intracellular levels[159]. Intracellular Ap4A was implicated to act as a second messenger, as transcriptional regulator and to be involved in the regulation of DNA replication[160;161]. 5'-PPP RNA as a substrate for NUDT2 was not indicated so far. However, with the new role identified here one could speculate that besides clearing the cell from viral triphosphorylated nucleic acids, endogenous triphosphorylated RNAs can serve as substrate as well. Only little is known about the presence of such endogenous 5'-PPP RNAs. Most nucleic acid species generated by the RNA polymerases in the nucleus are processed and modified in such a manner, that no stimulatory motif is present when being exported to the cytoplasm. However, some Pol-III transcripts including 5S rRNA and many ncRNAs were not shown to be modified at the 5'-end and probably bear triphosphorylated 5'-ends. Although, being mostly sequestered in protein complexes (e.g. 5S rRNA in ribosomes, vault ncRNA in the major vault complex) such endogenous 5'-PPP RNAs would be highly stimulatory by activating the intracellular pattern recognition receptor RIG-I. It may be that another essential function of NUDT2 involves rendering such potential stimulatory self-nucleic acids harmless. This would put NUDT2 on par with nucleases like TREX1 or DNase II that clear the cell from self-stimulatory DNA molecules and prohibit the development of autoinflammation through a chronic induction of type I interferons. However, several important questions remain to be solved. In light of improvements of increasingly sophisticated, sensitive and fast genomics methods, mutations in the genome of patients with type I interferonopathies

could elucidate the importance of NUDT2 in the onset of autoinflammatory diseases. Moreover, exploring the identity of potential stimulatory endogenous RNA molecules or the identification of triggers that lead to the release or detachment of such RNAs in the cytosol would greatly enhance our understanding of type I interferonopathies.

Antiviral restriction factor specificity

A further aspect of my work stresses the counter mechanisms cells evolved to contain viral replication. The restriction factor IFIT1 sequesters capped viral RNAs lacking methylation marks host mRNAs normally have. By binding to these RNAs the translation of specifically viral transcripts is inhibited. Interestingly, the crystal structure of IFIT1 with capped RNA revealed that the cap-binding pocket is relatively unspecific. Besides accommodating the canonical m7G-cap structure, unmethylated cap structures and adenine caps could as well fit. A stricter specificity is introduced by a tight tunnel that excludes methylation on the ribose of the first (N1) and second nucleotide (N2). Previously, N1 methylation alone was thought to be a sufficient feature of self. However, observations from the crystal structure and experimental data of others[162;163] suggest that probably N2 methylation could provide an additional layer of safety to protect cellular mRNAs from IFIT1 restriction. This novel insights could potentially aid the development of live attenuated vaccines that only recently with the development of a 2'-O-methyltransferase mutant dengue virus showed promising first results[164].

Together with IFIT5, IFIT1 was originally described as a PPP-RNA binding protein. However, differences is some key residues are responsible that IFIT1 is able to bind capped-RNA, whereas access to the cap-binding pocket is blocked in IFIT5. Replacement of an arginine residue in IFIT1 to a threonine residue in IFIT5 causes several residues to be pulled into the putative cap-binding pocket, which is then blocked. Interestingly, nonplacental mammals seem to have an IFIT5-like protein that still carries the arginine residue as IFIT1 does. These proteins therefore probably show a hybrid IFIT5/IFIT1 function and present a genealogical IFIT5/IFIT1 precursor protein. Together, the work presented in this dissertation provides novel insights into important areas of nucleic acid immunity. Restricting virus replication and spread is the most important objective innate immunity is able to accomplish and represents an efficient and powerful mechanism to prevent detrimental outcomes for the organism.

REFERENCES

[1] Katherine E. Sloan, Ahmed S. Warda, Sunny Sharma, Karl-Dieter Entian, Denis L. J. Lafontaine, and Markus T. Bohnsack. Tuning the ribosome: The influence of rRNA modification on eukaryotic ribosome biogenesis and function. *RNA Biology*, 14(9):1138–1152, dec 2016.

[2] Anthony K. Henras, Célia Plisson-Chastang, Marie-Françoise ODonohue, Anirban Chakraborty, and Pierre-Emmanuel Gleizes. An overview of pre-ribosomal RNA processing in eukaryotes. *Wiley Interdisciplinary Reviews: RNA*, 6(2):225–242, oct 2014.

[3] Robert J. White. Transcription by RNA polymerase III: more complex than we thought. *Nature Reviews Genetics*, 12(7):459–463, may 2011.

[4] D. Raha, Z. Wang, Z. Moqtaderi, L. Wu, G. Zhong, M. Gerstein, K. Struhl, and M. Snyder. Close association of RNA polymerase II and many transcription factors with pol III genes. *Proceedings of the National Academy of Sciences*, 107(8):3639–3644, feb 2010.

[5] Giorgio Dieci, Gloria Fiorino, Manuele Castelnuovo, Martin Teichmann, and Aldo Pagano. The expanding RNA polymerase III transcriptome. *Trends in Genetics*, 23(12):614–622, dec 2007.

[6] Yong Xiong and Thomas A Steitz. A story with a good ending: trna 3'-end maturation by cca-adding enzymes. *Current opinion in structural biology*, 16:12–17, February 2006.

[7] Jane E. Jackman and Juan D. Alfonzo. Transfer RNA modifications: natures combinatorial chemistry playground. *Wiley Interdisciplinary Reviews: RNA*, 4(1):35–48, nov 2012.

[8] A J Shatkin. Capping of eucaryotic mrnas. *Cell*, 9:645–653, December 1976.

[9] Magdalena Byszewska, Mirosław Śmietański, Elżbieta Purta, and Janusz M Bujnicki. Rna methyltransferases involved in 5' cap biosynthesis. *RNA biology*, 11:1597–1607, 2014.

[10] J Zhao, L Hyman, and C Moore. Formation of mrna 3' ends in eukaryotes: mechanism, regulation, and interrelationships with other steps in mrna synthesis. *Microbiology and molecular biology reviews : MMBR*, 63:405–445, June 1999.

[11] Y Huang and G G Carmichael. Role of polyadenylation in nucleocytoplasmic transport of mrna. *Molecular and cellular biology*, 16:1534–1542, April 1996.

[12] A. Gregory Matera, Rebecca M. Terns, and Michael P. Terns. Non-coding RNAs: lessons from the small nuclear and small nucleolar RNAs. *Nature Reviews Molecular Cell Biology*, 8(3):209–220, mar 2007.

[13] John Karijolich and Yi-Tao Yu. Spliceosomal snrna modifications and their function. *RNA biology*, 7:192–204, 2010.

[14] Thomas M. Carlile, Maria F. Rojas-Duran, Boris Zinshteyn, Hakyung Shin, Kristen M. Bartoli, and Wendy V. Gilbert. Pseudouridine profiling reveals regulated mRNA pseudouridylation in yeast and human cells. *Nature*, 515(7525):143–146, nov 2014.

[15] Schraga Schwartz, Douglas A. Bernstein, Maxwell R. Mumbach, Marko Jovanovic, Rebecca H. Herbst, Brian X. León-Ricardo, Jesse M. Engreitz, Mitchell Guttman, Rahul Satija, Eric S. Lander, Gerald Fink, and Aviv Regev. Transcriptome-wide mapping reveals widespread dynamic-regulated pseudouridylation of ncRNA and mRNA. *Cell*, 159(1):148–162, sep 2014.

[16] Xiaoyu Li, Ping Zhu, Shiqing Ma, Jinghui Song, Jinyi Bai, Fangfang Sun, and Chengqi Yi. Chemical pulldown reveals dynamic pseudouridylation of the mammalian transcriptome. *Nature Chemical Biology*, 11(8):592–597, jun 2015.

[17] Françoise Wyers, Mathieu Rougemaille, Gwenaël Badis, Jean-Claude Rousselle, Marie-Elisabeth Dufour, Jocelyne Boulay, Béatrice Régnault, Frédéric Devaux, Abdelkader Namane, Bertrand Séraphin, Domenico Libri, and Alain Jacquier. Cryptic pol ii transcripts are degraded by a nuclear quality control pathway involving a new poly(a) polymerase. *Cell*, 121:725–737, June 2005.

[18] Roy Parker and Haiwei Song. The enzymes and control of eukaryotic mrna turnover. *Nature structural & molecular biology*, 11:121–127, February 2004.

References

[19] J Chen, J Rappsilber, Y C Chiang, P Russell, M Mann, and C L Denis. Purification and characterization of the 1.0 mda ccr4-not complex identifies two novel components of the complex. *Journal of molecular biology*, 314:683–694, December 2001.

[20] Nga-Chi Lau, Annemieke Kolkman, Frederik M. A. van Schaik, Klaas W. Mulder, W. W. M. Pim Pijnappel, Albert J. R. Heck, and H. Th. Marc Timmers. Human ccr4–not complexes contain variable deadenylase subunits. *Biochemical Journal*, 422(3):443–453, sep 2009.

[21] Morgan Tucker, Robin R. Staples, Marco A. Valencia-Sanchez, Denise Muhlrad, and Roy Parker. Ccr4p is the catalytic subunit of a ccr4p/pop2p/notp mRNA deadenylase complex inSaccharomyces cerevisiae. *The EMBO Journal*, 21(6):1427–1436, mar 2002.

[22] Akio Yamashita, Tsung-Cheng Chang, Yukiko Yamashita, Wenmiao Zhu, Zhenping Zhong, Chyi-Ying A Chen, and Ann-Bin Shyu. Concerted action of poly(a) nucleases and decapping enzyme in mammalian mRNA turnover. *Nature Structural & Molecular Biology*, 12(12):1054–1063, nov 2005.

[23] Eva Dehlin, Michael Wormington, Christof G. Körner, and Elmar Wahle. Cap-dependent deadenylation of mRNA. *The EMBO Journal*, 19(5):1079–1086, mar 2000.

[24] M Gao, D T Fritz, L P Ford, and J Wilusz. Interaction between a poly(a)-specific ribonuclease and the 5' cap influences mrna deadenylation rates in vitro. *Molecular cell*, 5:479–488, March 2000.

[25] Ryohei Ishii, Osamu Nureki, and Shigeyuki Yokoyama. Crystal structure of the tRNA processing enzyme RNase PH fromAquifex aeolicus. *Journal of Biological Chemistry*, 278(34):32397–32404, may 2003.

[26] M F Symmons, G H Jones, and B F Luisi. A duplicated fold is the structural basis for polynucleotide phosphorylase catalytic activity, processivity, and regulation. *Structure (London, England : 1993)*, 8:1215–1226, November 2000.

[27] Andrzej Dziembowski, Esben Lorentzen, Elena Conti, and Bertrand Séraphin. A single subunit, dis3, is essentially responsible for yeast exosome core activity. *Nature Structural & Molecular Biology*, 14(1):15–22, dec 2006.

[28] Fabien Bonneau, Jérôme Basquin, Judith Ebert, Esben Lorentzen, and Elena Conti. The yeast exosome functions as a macromolecular cage to channel rna substrates for degradation. *Cell*, 139:547–559, October 2009.

[29] Elmar Wahle. Wrong PH for RNA degradation. *Nature Structural & Molecular Biology*, 14(1):5–7, jan 2007.

[30] Hudan Liu, Nancy D Rodgers, Xinfu Jiao, and Megerditch Kiledjian. The scavenger mrna decapping enzyme dcps is a member of the hit family of pyrophosphatases. *The EMBO journal*, 21:4699–4708, September 2002.

[31] Quansheng Liu, Jaclyn C Greimann, and Christopher D Lima. Reconstitution, activities, and structure of the eukaryotic rna exosome. *Cell*, 127:1223–1237, December 2006.

[32] C Allmang, J Kufel, G Chanfreau, P Mitchell, E Petfalski, and D Tollervey. Functions of the exosome in rrna, snorna and snrna synthesis. *The EMBO journal*, 18:5399–5410, October 1999.

[33] John LaCava, Jonathan Houseley, Cosmin Saveanu, Elisabeth Petfalski, Elizabeth Thompson, Alain Jacquier, and David Tollervey. Rna degradation by the exosome is promoted by a nuclear polyadenylation complex. *Cell*, 121:713–724, June 2005.

[34] J T Brown, X Bai, and A W Johnson. The yeast antiviral proteins ski2p, ski3p, and ski8p exist as a complex in vivo. *RNA (New York, N.Y.)*, 6:449–457, March 2000.

[35] Felix Halbach, Peter Reichelt, Michaela Rode, and Elena Conti. The yeast ski complex: Crystal structure and RNA channeling to the exosome complex. *Cell*, 154(4):814–826, aug 2013.

[36] Marcos Arribas-Layton, Donghui Wu, Jens Lykke-Andersen, and Haiwei Song. Structural and functional control of the eukaryotic mrna decapping machinery. *Biochimica et biophysica acta*, 1829:580–589, 2013.

[37] Meenakshi Kshirsagar and Roy Parker. Identification of edc3p as an enhancer of mrna decapping in saccharomyces cerevisiae. *Genetics*, 166:729–739, February 2004.

[38] Tracy Nissan, Purusharth Rajyaguru, Meipei She, Haiwei Song, and Roy Parker. Decapping activators in saccharomyces cerevisiae act by multiple mechanisms. *Molecular cell*, 39:773–783, September 2010.

References

[39] L. S. Cohen, C. Mikhli, X. Jiao, M. Kiledjian, G. Kunkel, and R. E. Davis. Dcp2 decaps m2,2,7gpppn-capped RNAs, and its activity is sequence and context dependent. *Molecular and Cellular Biology*, 25(20):8779–8791, sep 2005.

[40] Man-Gen Song, You Li, and Megerditch Kiledjian. Multiple mrna decapping enzymes in mammalian cells. *Molecular cell*, 40:423–432, November 2010.

[41] You Li, Mangen Song, and Megerditch Kiledjian. Differential utilization of decapping enzymes in mammalian mrna decay pathways. *RNA (New York, N.Y.)*, 17:419–428, March 2011.

[42] Ewa Grudzien-Nogalska, Xinfu Jiao, Man-Gen Song, Ronald P Hart, and Megerditch Kiledjian. Nudt3 is an mrna decapping enzyme that modulates cell migration. *RNA (New York, N.Y.)*, 22:773–781, May 2016.

[43] Christopher Iain Jones, Maria Vasilyevna Zabolotskaya, and Sarah Faith Newbury. The 5' 3' exoribonuclease xrn1/pacman and its functions in cellular processes and development. *Wiley interdisciplinary reviews. RNA*, 3:455–468, 2012.

[44] Olivier Pellegrini, Nathalie Mathy, Ciarán Condon, and Lionel Bénard. In vitro assays of 5' to 3'-exoribonuclease activity. *Methods in enzymology*, 448:167–183, 2008.

[45] Mai Sun, Björn Schwalb, Nicole Pirkl, Kerstin C. Maier, Arne Schenk, Henrik Failmezger, Achim Tresch, and Patrick Cramer. Global analysis of eukaryotic mRNA degradation reveals xrn1-dependent buffering of transcript levels. *Molecular Cell*, 52(1):52–62, oct 2013.

[46] Olaf Isken and Lynne E Maquat. Quality control of eukaryotic mrna: safeguarding cells from abnormal mrna function. *Genes & development*, 21:1833–1856, August 2007.

[47] Meenakshi K Doma and Roy Parker. Endonucleolytic cleavage of eukaryotic mrnas with stalls in translation elongation. *Nature*, 440:561–564, March 2006.

[48] Thomas Becker, Jean-Paul Armache, Alexander Jarasch, Andreas M Anger, Elizabeth Villa, Heidemarie Sieber, Basma Abdel Motaal, Thorsten Mielke, Otto Berninghausen, and Roland Beckmann. Structure of the no-go mRNA decay complex dom34–hbs1 bound to a stalled 80s ribosome. *Nature Structural & Molecular Biology*, 18(6):715–720, may 2011.

[49] Dario O Passos, Meenakshi K Doma, Christopher J Shoemaker, Denise Muhlrad, Rachel Green, Jonathan Weissman, Julie Hollien, and Roy Parker. Analysis of dom34 and its function in no-go decay. *Molecular biology of the cell*, 20:3025–3032, July 2009.

[50] Pamela A Frischmeyer, Ambro van Hoof, Kathryn O'Donnell, Anthony L Guerrerio, Roy Parker, and Harry C Dietz. An mrna surveillance mechanism that eliminates transcripts lacking termination codons. *Science (New York, N.Y.)*, 295:2258–2261, March 2002.

[51] Julie Hollien and Jonathan S. Weissman. Decay of endoplasmic reticulum-localized mRNAs during the unfolded protein response. *Science*, 313(5783):104–107, jul 2006.

[52] Philipp Kimmig, Marcy Diaz, Jiashun Zheng, Christopher C Williams, Alexander Lang, Tomas Aragón, Hao Li, and Peter Walter. The unfolded protein response in fission yeast modulates stability of select mRNAs to maintain protein homeostasis. *eLife*, 1, oct 2012.

[53] E A Mudd, H M Krisch, and C F Higgins. Rnase e, an endoribonuclease, has a general role in the chemical decay of escherichia coli mrna: evidence that rne and ams are the same genetic locus. *Molecular microbiology*, 4:2127–2135, December 1990.

[54] G J Cao and N Sarkar. Identification of the gene for an escherichia coli poly(a) polymerase. *Proceedings of the National Academy of Sciences of the United States of America*, 89:10380–10384, November 1992.

[55] E Hajnsdorf, F Braun, J Haugel-Nielsen, J Le Derout, and P Régnier. Multiple degradation pathways of the rpso mrna of escherichia coli. rnase e interacts with the 5' and 3' extremities of the primary transcript. *Biochimie*, 78:416–424, 1996.

[56] Helena Celesnik, Atilio Deana, and Joel G Belasco. Initiation of rna decay in escherichia coli by 5' pyrophosphate removal. *Molecular cell*, 27:79–90, July 2007.

[57] Atilio Deana, Helena Celesnik, and Joel G Belasco. The bacterial enzyme rpph triggers messenger rna degradation by 5' pyrophosphate removal. *Nature*, 451:355–358, January 2008.

References

[58] Nathalie Mathy, Lionel Bénard, Olivier Pellegrini, Roula Daou, Tingyi Wen, and Ciarán Condon. 5'-to-3' exoribonuclease activity in bacteria: role of rnase j1 in rrna maturation and 5' stability of mrna. *Cell*, 129:681–692, May 2007.

[59] Alessandro Fatica and David Tollervey. Making ribosomes. *Current opinion in cell biology*, 14:313–318, June 2002.

[60] Christophe Dez, Jonathan Houseley, and David Tollervey. Surveillance of nuclear-restricted pre-ribosomes within a subnucleolar region of saccharomyces cerevisiae. *The EMBO journal*, 25:1534–1546, April 2006.

[61] Frederick J LaRiviere, Sarah E Cole, Daniel J Ferullo, and Melissa J Moore. A late-acting quality control process for mature eukaryotic rrnas. *Molecular cell*, 24:619–626, November 2006.

[62] Sarah E. Cole, Frederick J. LaRiviere, Christopher N. Merrikh, and Melissa J. Moore. A convergence of rRNA and mRNA quality control pathways revealed by mechanistic analysis of nonfunctional rRNA decay. *Molecular Cell*, 34(4):440–450, may 2009.

[63] Claudine Kraft, Anna Deplazes, Marc Sohrmann, and Matthias Peter. Mature ribosomes are selectively degraded upon starvation by an autophagy pathway requiring the ubp3p/bre5p ubiquitin protease. *Nature cell biology*, 10:602–610, May 2008.

[64] Sujatha Kadaba, Anna Krueger, Tamyra Trice, Annette M Krecic, Alan G Hinnebusch, and James Anderson. Nuclear surveillance and degradation of hypomodified initiator trnamet in s. cerevisiae. *Genes & development*, 18:1227–1240, June 2004.

[65] Andrei Alexandrov, Irina Chernyakov, Weifeng Gu, Shawna L Hiley, Timothy R Hughes, Elizabeth J Grayhack, and Eric M Phizicky. Rapid trna decay can result from lack of nonessential modifications. *Molecular cell*, 21:87–96, January 2006.

[66] I. Chernyakov, J. M. Whipple, L. Kotelawala, E. J. Grayhack, and E. M. Phizicky. Degradation of several hypomodified mature tRNA species in saccharomyces cerevisiae is mediated by met22 and the 5-3 exonucleases rat1 and xrn1. *Genes & Development*, 22(10):1369–1380, may 2008.

[67] G Hartmann. Nucleic acid immunity. *Advances in immunology*, 133:121–169, 2017.

[68] C.A. Janeway. Approaching the asymptote? evolution and revolution in immunology. *Cold Spring Harbor Symposia on Quantitative Biology*, 54(0):1–13, jan 1989.

[69] J LINDENMANN, D C BURKE, and A ISAACS. Studies on the production, mode of action and properties of interferon. *British journal of experimental pathology*, 38:551–562, October 1957.

[70] A ISAACS, R A COX, and Z ROTEM. Foreign nucleic acids as the stimulus to make interferon. *Lancet (London, England)*, 2:113–116, July 1963.

[71] B Lemaitre, E Nicolas, L Michaut, J M Reichhart, and J A Hoffmann. The dorsoventral regulatory gene cassette spätzle/toll/cactus controls the potent antifungal response in drosophila adults. *Cell*, 86:973–983, September 1996.

[72] Ruslan Medzhitov, Paula Preston-Hurlburt, and Charles A. Janeway. A human homologue of the drosophila toll protein signals activation of adaptive immunity. *Nature*, 388(6640):394–397, jul 1997.

[73] Ruey-Bing Yang, Melanie R. Mark, Alane Gray, Arthur Huang, Ming Hong Xie, Min Zhang, Audrey Goddard, William I. Wood, Austin L. Gurney, and Paul J. Godowski. Toll-like receptor-2 mediates lipopolysaccharide-induced cellular signalling. *Nature*, 395(6699):284–288, sep 1998.

[74] H Hemmi, O Takeuchi, T Kawai, T Kaisho, S Sato, H Sanjo, M Matsumoto, K Hoshino, H Wagner, K Takeda, and S Akira. A toll-like receptor recognizes bacterial dna. *Nature*, 408:740–745, December 2000.

[75] L Alexopoulou, A C Holt, R Medzhitov, and R A Flavell. Recognition of double-stranded rna and activation of nf-kappab by toll-like receptor 3. *Nature*, 413:732–738, October 2001.

[76] Florian Heil, Hiroaki Hemmi, Hubertus Hochrein, Franziska Ampenberger, Carsten Kirschning, Shizuo Akira, Grayson Lipford, Hermann Wagner, and Stefan Bauer. Species-specific recognition of single-stranded rna via toll-like receptor 7 and 8. *Science (New York, N.Y.)*, 303:1526–1529, March 2004.

[77] Mitsutoshi Yoneyama, Mika Kikuchi, Takashi Natsukawa, Noriaki Shinobu, Tadaatsu Imaizumi, Makoto Miyagishi, Kazunari Taira, Shizuo Akira, and Takashi Fujita. The RNA helicase RIG-i has an essential function in double-stranded

RNA-induced innate antiviral responses. *Nature Immunology*, 5(7):730–737, jun 2004.

[78] Andreas Pichlmair, Oliver Schulz, Choon Ping Tan, Tanja I Näslund, Peter Liljeström, Friedemann Weber, and Caetano Reis e Sousa. Rig-i-mediated antiviral responses to single-stranded rna bearing 5'-phosphates. *Science (New York, N.Y.)*, 314:997–1001, November 2006.

[79] Veit Hornung, Jana Ellegast, Sarah Kim, Krzysztof Brzózka, Andreas Jung, Hiroki Kato, Hendrik Poeck, Shizuo Akira, Karl-Klaus Conzelmann, Martin Schlee, Stefan Endres, and Gunther Hartmann. 5'-triphosphate rna is the ligand for rig-i. *Science (New York, N.Y.)*, 314:994–997, November 2006.

[80] Andrea Ablasser, Franz Bauernfeind, Gunther Hartmann, Eicke Latz, Katherine A Fitzgerald, and Veit Hornung. Rig-i-dependent sensing of poly(da:dt) through the induction of an rna polymerase iii-transcribed rna intermediate. *Nature immunology*, 10:1065–1072, October 2009.

[81] Fabio Martinon, Kimberly Burns, and Jürg Tschopp. The inflammasome: a molecular platform triggering activation of inflammatory caspases and processing of proil-beta. *Molecular cell*, 10:417–426, August 2002.

[82] Veit Hornung and Eicke Latz. Intracellular dna recognition. *Nature reviews. Immunology*, 10:123–130, February 2010.

[83] J. Wu, L. Sun, X. Chen, F. Du, H. Shi, C. Chen, and Z. J. Chen. Cyclic GMP-AMP is an endogenous second messenger in innate immune signaling by cytosolic DNA. *Science*, 339(6121):826–830, dec 2012.

[84] Hiroki Ishikawa, Zhe Ma, and Glen N Barber. Sting regulates intracellular dna-mediated, type i interferon-dependent innate immunity. *Nature*, 461:788–792, October 2009.

[85] G C Sen, H Taira, and P Lengyel. Interferon, double-stranded rna, and protein phosphorylation. characteristics of a double-stranded rna-activated protein kinase system partially purified from interferon treated ehrlich ascites tumor cells. *The Journal of biological chemistry*, 253:5915–5921, September 1978.

[86] M A García, E F Meurs, and M Esteban. The dsrna protein kinase pkr: virus and cell control. *Biochimie*, 89:799–811, 2007.

[87] K Yang, H Samanta, J Dougherty, B Jayaram, R Broeze, and P Lengyel. Interferons, double-stranded rna, and rna degradation. isolation and characterization of homogeneous human (2'-5')(a)n synthetase. *The Journal of biological chemistry*, 256:9324–9328, September 1981.

[88] C Baglioni, M A Minks, and P A Maroney. Interferon action may be mediated by activation of a nuclease by pppa2'p5'a2'p5'a. *Nature*, 273:684–687, June 1978.

[89] Sarah E Brennan-Laun, Heather J Ezelle, Xiao-Ling Li, and Bret A Hassel. Rnase-l control of cellular mrnas: roles in biologic functions and mechanisms of substrate targeting. *Journal of interferon & cytokine research : the official journal of the International Society for Interferon and Cytokine Research*, 34:275–288, April 2014.

[90] Andreas Pichlmair, Caroline Lassnig, Carol-Ann Eberle, Maria W Górna, Christoph L Baumann, Thomas R Burkard, Tilmann Bürckstümmer, Adrijana Stefanovic, Sigurd Krieger, Keiryn L Bennett, Thomas Rülicke, Friedemann Weber, Jacques Colinge, Mathias Müller, and Giulio Superti-Furga. Ifit1 is an antiviral protein that recognizes 5'-triphosphate rna. *Nature immunology*, 12:624–630, June 2011.

[91] Yazan M Abbas, Andreas Pichlmair, Maria W Górna, Giulio Superti-Furga, and Bhushan Nagar. Structural basis for viral 5'-ppp-rna recognition by human ifit proteins. *Nature*, 494:60–64, February 2013.

[92] Matthias Habjan, Philipp Hubel, Livia Lacerda, Christian Benda, Cathleen Holze, Christian H Eberl, Angelika Mann, Eveline Kindler, Cristina Gil-Cruz, John Ziebuhr, Volker Thiel, and Andreas Pichlmair. Sequestration by ifit1 impairs translation of 2'o-unmethylated capped rna. *PLoS pathogens*, 9:e1003663, 2013.

[93] T. Kimura, H. Katoh, H. Kayama, H. Saiga, M. Okuyama, T. Okamoto, E. Umemoto, Y. Matsuura, M. Yamamoto, and K. Takeda. Ifit1 inhibits japanese encephalitis virus replication through binding to 5 capped 2-o unmethylated RNA. *Journal of Virology*, 87(18):9997–10003, jul 2013.

[94] J. L. Hyde, C. L. Gardner, T. Kimura, J. P. White, G. Liu, D. W. Trobaugh, C. Huang, M. Tonelli, S. Paessler, K. Takeda, W. B. Klimstra, G. K. Amarasinghe, and M. S. Diamond. A viral RNA structural element alters host recognition of nonself RNA. *Science*, 343(6172):783–787, jan 2014.

References

[95] Manqing Li, Elaine Kao, Xia Gao, Hilary Sandig, Kirsten Limmer, Mariana Pavon-Eternod, Thomas E. Jones, Sebastien Landry, Tao Pan, Matthew D. Weitzman, and Michael David. Codon-usage-based inhibition of HIV protein synthesis by human schlafen 11. *Nature*, 491(7422):125–128, sep 2012.

[96] Ann M Sheehy, Nathan C Gaddis, Jonathan D Choi, and Michael H Malim. Isolation of a human gene that inhibits hiv-1 infection and is suppressed by the viral vif protein. *Nature*, 418:646–650, August 2002.

[97] Silvestro G Conticello, Reuben S Harris, and Michael S Neuberger. The vif protein of HIV triggers degradation of the human antiretroviral DNA deaminase APOBEC3g. *Current Biology*, 13(22):2009–2013, nov 2003.

[98] Kazuko Nishikura. A-to-i editing of coding and non-coding rnas by adars. *Nature reviews. Molecular cell biology*, 17:83–96, February 2016.

[99] K. Kawane, K. Motani, and S. Nagata. DNA degradation and its defects. *Cold Spring Harbor Perspectives in Biology*, 6(6):a016394–a016394, jun 2014.

[100] Mathieu P. Rodero, Alessandra Tesser, Eva Bartok, Gillian I. Rice, Erika Della Mina, Marine Depp, Benoit Beitz, Vincent Bondet, Nicolas Cagnard, Darragh Duffy, Michael Dussiot, Marie-Louise Frémond, Marco Gattorno, Flavia Guillem, Naoki Kitabayashi, Fabrice Porcheray, Frederic Rieux-Laucat, Luis Seabra, Carolina Uggenti, Stefano Volpi, Leo A H. Zeef, Marie-Alexandra Alyanakian, Jacques Beltrand, Anna Monica Bianco, Nathalie Boddaert, Chantal Brouzes, Sophie Candon, Roberta Caorsi, Marina Charbit, Monique Fabre, Flavio Faletra, Muriel Girard, Annie Harroche, Evelyn Hartmann, Dominique Lasne, Annalisa Marcuzzi, Bénédicte Neven, Patrick Nitschke, Tiffany Pascreau, Serena Pastore, Capucine Picard, Paolo Picco, Elisa Piscianz, Michel Polak, Pierre Quartier, Marion Rabant, Gabriele Stocco, Andrea Taddio, Florence Uettwiller, Erica Valencic, Diego Vozzi, Gunther Hartmann, Winfried Barchet, Olivier Hermine, Brigitte Bader-Meunier, Alberto Tommasini, and Yanick J. Crow. Type i interferon-mediated autoinflammation due to DNase II deficiency. *Nature Communications*, 8(1), dec 2017.

[101] M. K. Atianand and K. A. Fitzgerald. Molecular basis of DNA recognition in the immune system. *The Journal of Immunology*, 190(5):1911–1918, feb 2013.

[102] Daniel B Stetson, Joan S Ko, Thierry Heidmann, and Ruslan Medzhitov. Trex1 prevents cell-intrinsic initiation of autoimmunity. *Cell*, 134:587–598, August 2008.

[103] Yanick J Crow, Bruce E Hayward, Rekha Parmar, Peter Robins, Andrea Leitch, Manir Ali, Deborah N Black, Hans van Bokhoven, Han G Brunner, Ben C Hamel, Peter C Corry, Frances M Cowan, Suzanne G Frints, Joerg Klepper, John H Livingston, Sally Ann Lynch, Roger F Massey, Jean François Meritet, Jacques L Michaud, Gerard Ponsot, Thomas Voit, Pierre Lebon, David T Bonthron, Andrew P Jackson, Deborah E Barnes, and Tomas Lindahl. Mutations in the gene encoding the 3'-5' dna exonuclease trex1 cause aicardi-goutières syndrome at the ags1 locus. *Nature genetics*, 38:917–920, August 2006.

[104] Yanick J Crow, Andrea Leitch, Bruce E Hayward, Anna Garner, Rekha Parmar, Elen Griffith, Manir Ali, Colin Semple, Jean Aicardi, Riyana Babul-Hirji, Clarisse Baumann, Peter Baxter, Enrico Bertini, Kate E Chandler, David Chitayat, Daniel Cau, Catherine Déry, Elisa Fazzi, Cyril Goizet, Mary D King, Joerg Klepper, Didier Lacombe, Giovanni Lanzi, Hermione Lyall, María Luisa Martínez-Frías, Michèle Mathieu, Carole McKeown, Anne Monier, Yvette Oade, Oliver W Quarrell, Christopher D Rittey, R Curtis Rogers, Amparo Sanchis, John B P Stephenson, Uta Tacke, Marianne Till, John L Tolmie, Pam Tomlin, Thomas Voit, Bernhard Weschke, C Geoffrey Woods, Pierre Lebon, David T Bonthron, Chris P Ponting, and Andrew P Jackson. Mutations in genes encoding ribonuclease h2 subunits cause aicardi-goutières syndrome and mimic congenital viral brain infection. *Nature genetics*, 38:910–916, August 2006.

[105] Arun K Mankan, Tobias Schmidt, Dhruv Chauhan, Marion Goldeck, Klara Höning, Moritz Gaidt, Andrew V Kubarenko, Liudmila Andreeva, Karl-Peter Hopfner, and Veit Hornung. Cytosolic rna:dna hybrids activate the cgas-sting axis. *The EMBO journal*, 33:2937–2946, December 2014.

[106] Rachel E Rigby, Lauren M Webb, Karen J Mackenzie, Yue Li, Andrea Leitch, Martin A M Reijns, Rachel J Lundie, Ailsa Revuelta, Donald J Davidson, Sandra Diebold, Yorgo Modis, Andrew S MacDonald, and Andrew P Jackson. Rna:dna hybrids are a novel molecular pattern sensed by tlr9. *The EMBO journal*, 33:542–558, March 2014.

[107] Diana Ayinde, Nicoletta Casartelli, and Olivier Schwartz. Restricting HIV the SAMHD1 way: through nucleotide starvation. *Nature Reviews Microbiology*, 10(10):675–680, aug 2012.

[108] Jeongmin Ryoo, Jongsu Choi, Changhoon Oh, Sungchul Kim, Minji Seo, Seok-Young Kim, Daekwan Seo, Jongkyu Kim, Tommy E White, Alberto Brandariz-

Nuñez, Felipe Diaz-Griffero, Cheol-Heui Yun, Joseph A Hollenbaugh, Baek Kim, Daehyun Baek, and Kwangseog Ahn. The ribonuclease activity of SAMHD1 is required for HIV-1 restriction. *Nature Medicine*, 20(8):936–941, jul 2014.

[109] Jonathan Maelfait, Anne Bridgeman, Adel Benlahrech, Chiara Cursi, and Jan Rehwinkel. Restriction by SAMHD1 limits cGAS/STING-dependent innate and adaptive immune responses to HIV-1. *Cell Reports*, 16(6):1492–1501, aug 2016.

[110] J. Aicardi and F. Goutières. A progressive familial encephalopathy in infancy with calcifications of the basal ganglia and chronic cerebrospinal fluid lymphocytosis. *Annals of Neurology*, 15(1):49–54, jan 1984.

[111] Gillian I Rice, Gabriella M A Forte, Marcin Szynkiewicz, Diana S Chase, Alec Aeby, Mohamed S Abdel-Hamid, Sam Ackroyd, Rebecca Allcock, Kathryn M Bailey, Umberto Balottin, Christine Barnerias, Genevieve Bernard, Christine Bodemer, Maria P Botella, Cristina Cereda, Kate E Chandler, Lyvia Dabydeen, Russell C Dale, Corinne De Laet, Christian G E L De Goede, Mireia Del Toro, Laila Effat, Noemi Nunez Enamorado, Elisa Fazzi, Blanca Gener, Madli Haldre, Jean-Pierre S-M Lin, John H Livingston, Charles Marques Lourenco, Wilson Marques, Patrick Oades, Pärt Peterson, Magnhild Rasmussen, Agathe Roubertie, Johanna Loewenstein Schmidt, Stavit A Shalev, Rogelio Simon, Ronen Spiegel, Kathryn J Swoboda, Samia A Temtamy, Grace Vassallo, Catheline N Vilain, Julie Vogt, Vanessa Wermenbol, William P Whitehouse, Doriette Soler, Ivana Olivieri, Simona Orcesi, Mona S Aglan, Maha S Zaki, Ghada M H Abdel-Salam, Adeline Vanderver, Kai Kisand, Flore Rozenberg, Pierre Lebon, and Yanick J Crow. Assessment of interferon-related biomarkers in aicardi-goutières syndrome associated with mutations in trex1, rnaseh2a, rnaseh2b, rnaseh2c, samhd1, and adar: a case-control study. *The Lancet. Neurology*, 12:1159–1169, December 2013.

[112] Anisur Rahman and David A Isenberg. Systemic lupus erythematosus. *The New England journal of medicine*, 358:929–939, February 2008.

[113] Emily C Baechler, Franak M Batliwalla, George Karypis, Patrick M Gaffney, Ward A Ortmann, Karl J Espe, Katherine B Shark, William J Grande, Karis M Hughes, Vivek Kapur, Peter K Gregersen, and Timothy W Behrens. Interferon-inducible gene expression signature in peripheral blood cells of patients with severe lupus. *Proceedings of the National Academy of Sciences of the United States of America*, 100:2610–2615, March 2003.

[114] Min Ae Lee-Kirsch, Maolian Gong, Dipanjan Chowdhury, Lydia Senenko, Kerstin Engel, Young-Ae Lee, Udesh de Silva, Suzanna L Bailey, Torsten Witte, Timothy J Vyse, Juha Kere, Christiane Pfeiffer, Scott Harvey, Andrew Wong, Sari Koskenmies, Oliver Hummel, Klaus Rohde, Reinhold E Schmidt, Anna F Dominiczak, Manfred Gahr, Thomas Hollis, Fred W Perrino, Judy Lieberman, and Norbert Hübner. Mutations in the gene encoding the 3'-5' dna exonuclease trex1 are associated with systemic lupus erythematosus. *Nature genetics*, 39:1065–1067, September 2007.

[115] K Yasutomo, T Horiuchi, S Kagami, H Tsukamoto, C Hashimura, M Urushihara, and Y Kuroda. Mutation of dnase1 in people with systemic lupus erythematosus. *Nature genetics*, 28:313–314, August 2001.

[116] Sterling C Eckard, Gillian I Rice, Alexandre Fabre, Catherine Badens, Elizabeth E Gray, Jane L Hartley, Yanick J Crow, and Daniel B Stetson. The skiv2l rna exosome limits activation of the rig-i-like receptors. *Nature immunology*, 15:839–845, September 2014.

[117] Michelle M A Fernando, Christine R Stevens, Pardis C Sabeti, Emily C Walsh, Alasdair J M McWhinnie, Anila Shah, Todd Green, John D Rioux, and Timothy J Vyse. Identification of two independent risk factors for lupus within the mhc in united kingdom families. *PLoS genetics*, 3:e192, November 2007.

[118] Max Schelker, Caroline Maria Mair, Fabian Jolmes, Robert-William Welke, Edda Klipp, Andreas Herrmann, Max Flöttmann, and Christian Sieben. Viral RNA degradation and diffusion act as a bottleneck for the influenza a virus infection efficiency. *PLOS Computational Biology*, 12(10):e1005075, oct 2016.

[119] Björn Schwanhäusser, Dorothea Busse, Na Li, Gunnar Dittmar, Johannes Schuchhardt, Jana Wolf, Wei Chen, and Matthias Selbach. Global quantification of mammalian gene expression control. *Nature*, 473(7347):337–342, may 2011.

[120] You Li, Takahiro Masaki, Daisuke Yamane, David R McGivern, and Stanley M Lemon. Competing and noncompeting activities of mir-122 and the 5' exonuclease xrn1 in regulation of hepatitis c virus replication. *Proceedings of the National Academy of Sciences of the United States of America*, 110:1881–1886, January 2013.

[121] You Li, Daisuke Yamane, Takahiro Masaki, and Stanley M Lemon. The yin and

yang of hepatitis c: synthesis and decay of hepatitis c virus rna. *Nature reviews. Microbiology*, 13:544–558, September 2015.

[122] Stephanie Kervestin and Allan Jacobson. Nmd: a multifaceted response to premature translational termination. *Nature reviews. Molecular cell biology*, 13:700–712, November 2012.

[123] Christoph Schweingruber, Simone C Rufener, David Zünd, Akio Yamashita, and Oliver Mühlemann. Nonsense-mediated mrna decay - mechanisms of substrate mrna recognition and degradation in mammalian cells. *Biochimica et biophysica acta*, 1829:612–623, 2013.

[124] Jens Lykke-Andersen and Eric J Bennett. Protecting the proteome: Eukaryotic cotranslational quality control pathways. *The Journal of cell biology*, 204:467–476, February 2014.

[125] Kristian E Baker and Roy Parker. Nonsense-mediated mrna decay: terminating erroneous gene expression. *Current opinion in cell biology*, 16:293–299, June 2004.

[126] J Robert Hogg and Stephen P Goff. Upf1 senses 3'utr length to potentiate mrna decay. *Cell*, 143:379–389, October 2010.

[127] Giuseppe Balistreri, Peter Horvath, Christoph Schweingruber, David Zünd, Gerald McInerney, Andres Merits, Oliver Mühlemann, Claus Azzalin, and Ari Helenius. The host nonsense-mediated mrna decay pathway restricts mammalian rna virus replication. *Cell host & microbe*, 16:403–411, September 2014.

[128] Ryan H Moy, Brian S Cole, Ari Yasunaga, Beth Gold, Ganesh Shankarling, Andrew Varble, Jerome M Molleston, Benjamin R tenOever, Kristen W Lynch, and Sara Cherry. Stem-loop recognition by ddx17 facilitates mirna processing and antiviral defense. *Cell*, 158:764–777, August 2014.

[129] Michal Lubas, Marianne S Christensen, Maiken S Kristiansen, Michal Domanski, Lasse G Falkenby, Søren Lykke-Andersen, Jens S Andersen, Andrzej Dziembowski, and Torben Heick Jensen. Interaction profiling identifies the human nuclear exosome targeting complex. *Molecular cell*, 43:624–637, August 2011.

[130] Jerome M Molleston, Leah R Sabin, Ryan H Moy, Sanjay V Menghani, Keiko Rausch, Beth Gordesky-Gold, Kaycie C Hopkins, Rui Zhou, Torben Heick Jensen,

Jeremy E Wilusz, and Sara Cherry. A conserved virus-induced cytoplasmic tramp-like complex recruits the exosome to target viral rna for degradation. *Genes & development*, 30:1658–1670, July 2016.

[131] Guoxin Liang, Guangyan Liu, Kouichi Kitamura, Zhe Wang, Sajeda Chowdhury, Ahasan Md Monjurul, Kousho Wakae, Miki Koura, Miyuki Shimadu, Kazuo Kinoshita, and Masamichi Muramatsu. Tgf- suppression of hbv rna through aid-dependent recruitment of an rna exosome complex. *PLoS pathogens*, 11:e1004780, April 2015.

[132] Hussein H. Aly, Junya Suzuki, Koichi Watashi, Kazuaki Chayama, Shin ichi Hoshino, Makoto Hijikata, Takanobu Kato, and Takaji Wakita. RNA exosome complex regulates stability of the hepatitis b virus x-mRNA transcript in a non-stop-mediated (NSD) RNA quality control mechanism. *Journal of Biological Chemistry*, 291(31):15958–15974, jun 2016.

[133] J. Lucifora, Y. Xia, F. Reisinger, K. Zhang, D. Stadler, X. Cheng, M. F. Sprinzl, H. Koppensteiner, Z. Makowska, T. Volz, C. Remouchamps, W.-M. Chou, W. E. Thasler, N. Huser, D. Durantel, T. J. Liang, C. Munk, M. H. Heim, J. L. Browning, E. Dejardin, M. Dandri, M. Schindler, M. Heikenwalder, and U. Protzer. Specific and nonhepatotoxic degradation of nuclear hepatitis b virus cccDNA. *Science*, 343(6176):1221–1228, feb 2014.

[134] M.-A. Meier, A. Suslov, S. Ketterer, M. H. Heim, and S. F. Wieland. Hepatitis b virus covalently closed circular DNA homeostasis is independent of the lymphotoxin pathway during chronic HBV infection. *Journal of Viral Hepatitis*, 24(8):662–671, mar 2017.

[135] B. R. Anderson, H. Muramatsu, B. K. Jha, R. H. Silverman, D. Weissman, and K. Kariko. Nucleoside modifications in RNA limit activation of 2-5-oligoadenylate synthetase and increase resistance to cleavage by RNase l. *Nucleic Acids Research*, 39(21):9329–9338, aug 2011.

[136] Maher Al-Saif and Khalid SA Khabar. UU/UA dinucleotide frequency reduction in coding regions results in increased mRNA stability and protein expression. *Molecular Therapy*, 20(5):954–959, may 2012.

[137] Age Utt, Tania Quirin, Sirle Saul, Kirsi Hellström, Tero Ahola, and Andres Merits. Versatile trans-replication systems for chikungunya virus allow functional analysis and tagging of every replicase protein. *PLOS ONE*, 11(3):e0151616, mar 2016.

References

[138] S. Muller, P. Moller, M. J. Bick, S. Wurr, S. Becker, S. Gunther, and B. M. Kummerer. Inhibition of filovirus replication by the zinc finger antiviral protein. *Journal of Virology*, 81(5):2391–2400, dec 2006.

[139] Xuemin Guo, Jing Ma, Jing Sun, and Guangxia Gao. The zinc-finger antiviral protein recruits the rna processing exosome to degrade the target mrna. *Proceedings of the National Academy of Sciences of the United States of America*, 104:151–156, January 2007.

[140] R L Van Etten. Human prostatic acid phosphatase: a histidine phosphatase. *Annals of the New York Academy of Sciences*, 390:27–51, 1982.

[141] Mark J. Chen, Jack E. Dixon, and Gerard Manning. Genomics and evolution of protein phosphatases. *Science Signaling*, 10(474):eaag1796, apr 2017.

[142] J. Roy and M. S. Cyert. Cracking the phosphatase code: Docking interactions determine substrate specificity. *Science Signaling*, 2(100):re9–re9, dec 2009.

[143] A G McLennan. The mutt motif family of nucleotide phosphohydrolases in man and human pathogens (review). *International journal of molecular medicine*, 4:79–89, July 1999.

[144] M J Bessman, D N Frick, and S F O'Handley. The mutt proteins or "nudix" hydrolases, a family of versatile, widely distributed, "housecleaning" enzymes. *The Journal of biological chemistry*, 271:25059–25062, October 1996.

[145] C Abeygunawardana, D J Weber, A G Gittis, D N Frick, J Lin, A F Miller, M J Bessman, and A S Mildvan. Solution structure of the mutt enzyme, a nucleoside triphosphate pyrophosphohydrolase. *Biochemistry*, 34:14997–15005, November 1995.

[146] A G McLennan. The nudix hydrolase superfamily. *Cellular and molecular life sciences : CMLS*, 63:123–143, January 2006.

[147] Man-Gen Song, Sophie Bail, and Megerditch Kiledjian. Multiple nudix family proteins possess mrna decapping activity. *RNA (New York, N.Y.)*, 19:390–399, March 2013.

[148] A S Mildvan, Z Xia, H F Azurmendi, V Saraswat, P M Legler, M A Massiah, S B Gabelli, M A Bianchet, L-W Kang, and L M Amzel. Structures and mechanisms of nudix hydrolases. *Archives of biochemistry and biophysics*, 433:129–143, January 2005.

[149] Jordi Carreras-Puigvert, Marinka Zitnik, Ann-Sofie Jemth, Megan Carter, Judith E. Unterlass, Björn Hallström, Olga Loseva, Zhir Karem, José Manuel Calderón-Montaño, Cecilia Lindskog, Per-Henrik Edqvist, Damian J. Matuszewski, Hammou Ait Blal, Ronnie P. A. Berntsson, Maria Häggblad, Ulf Martens, Matthew Studham, Bo Lundgren, Carolina Wählby, Erik L. L. Sonnhammer, Emma Lundberg, Pål Stenmark, Blaz Zupan, and Thomas Helleday. A comprehensive structural, biochemical and biological profiling of the human NUDIX hydrolase family. *Nature Communications*, 8(1), nov 2017.

[150] You Li, Daisuke Yamane, and Stanley M. Lemon. Dissecting the roles of the 5′ exoribonucleases xrn1 and xrn2 in restricting hepatitis c virus replication. *Journal of Virology*, 89(9):4857–4865, feb 2015.

[151] Joyce A. Wilson and Adam Huys. miR-122 promotion of the hepatitis c virus life cycle: sound in the silence. *Wiley Interdisciplinary Reviews: RNA*, 4(6):665–676, jul 2013.

[152] Phillida A. Charley and Jeffrey Wilusz. Standing your ground to exoribonucleases: Function of flavivirus long non-coding RNAs. *Virus Research*, 212:70–77, jan 2016.

[153] Etienne Decroly, François Ferron, Julien Lescar, and Bruno Canard. Conventional and unconventional mechanisms for capping viral mrna. *Nature reviews. Microbiology*, 10:51–65, December 2011.

[154] Laurent Balvay, Ricardo Soto Rifo, Emiliano P Ricci, Didier Decimo, and Théophile Ohlmann. Structural and functional diversity of viral ireses. *Biochimica et biophysica acta*, 1789:542–557, 2009.

[155] Erica S Machlin, Peter Sarnow, and Selena M Sagan. Masking the 5' terminal nucleotides of the hepatitis c virus genome by an unconventional microrna-target rna complex. *Proceedings of the National Academy of Sciences of the United States of America*, 108:3193–3198, February 2011.

[156] Inés Romero-Brey and Ralf Bartenschlager. Membranous replication factories induced by plus-strand RNA viruses. *Viruses*, 6(7):2826–2857, jul 2014.

[157] P C Lee, B R Bochner, and B N Ames. Appppa, heat-shock stress, and cell oxidation. *Proceedings of the National Academy of Sciences of the United States of America*, 80:7496–7500, December 1983.

References

[158] A Sillero and M A Sillero. Synthesis of dinucleoside polyphosphates catalyzed by firefly luciferase and several ligases. *Pharmacology & therapeutics*, 87:91–102, 2000.

[159] A Guranowski. Specific and nonspecific enzymes involved in the catabolism of mononucleoside and dinucleoside polyphosphates. *Pharmacology & therapeutics*, 87:117–139, 2000.

[160] I. Carmi-Levy, N. Yannay-Cohen, G. Kay, E. Razin, and H. Nechushtan. Diadenosine tetraphosphate hydrolase is part of the transcriptional regulation network in immunologically activated mast cells. *Molecular and Cellular Biology*, 28(18):5777–5784, jul 2008.

[161] Andrew S Marriott, Nikki A Copeland, Ryan Cunningham, Mark C Wilkinson, Alexander G McLennan, and Nigel J Jones. Diadenosine 5', 5"'-p(1),p(4)-tetraphosphate (ap4a) is synthesized in response to dna damage and inhibits the initiation of dna replication. *DNA repair*, 33:90–100, September 2015.

[162] D. F. Young, J. Andrejeva, X. Li, F. Inesta-Vaquera, C. Dong, V. H. Cowling, S. Goodbourn, and R. E. Randall. Human IFIT1 inhibits mRNA translation of rubulaviruses but not other members of the paramyxoviridae family. *Journal of Virology*, 90(20):9446–9456, aug 2016.

[163] Matthew D Daugherty, Aaron M Schaller, Adam P Geballe, and Harmit S Malik. Evolution-guided functional analyses reveal diverse antiviral specificities encoded by IFIT1 genes in mammals. *eLife*, 5, may 2016.

[164] Roland Züst, Hongping Dong, Xiao-Feng Li, David C. Chang, Bo Zhang, Thavamalar Balakrishnan, Ying-Xiu Toh, Tao Jiang, Shi-Hua Li, Yong-Qiang Deng, Brett R. Ellis, Esther M. Ellis, Michael Poidinger, Francesca Zolezzi, Cheng-Feng Qin, Pei-Yong Shi, and Katja Fink. Rational design of a live attenuated dengue vaccine: 2ı-o-methyltransferase mutants are highly attenuated and immunogenic in mice and macaques. *PLoS Pathogens*, 9(8):e1003521, aug 2013.

ACKNOWLEDGMENT

First of all, I am grateful to my supervisor Andreas Pichlmair for supporting me all the way from my studies to pursuing the PhD degree, for opening doors and creating a unique and inspiring environment. It is a privilege to work in your lab! You taught me how to think about, present about, and write about science. I value your scientific education and amazing support as generous gift.

My special thanks go to Prof. Dr. Matthias Mann for taking the responsibility to be my official doctoral advisor, for all the support during TAC meetings and my PhD time and for heading a really outstanding department with a great atmosphere.

My appreciation goes to all of my lab mates of the 'Innate Lab'. Thank you for sharing your valuable knowledge tackling everyday 'surprises' and making me enjoy every single day in the lab.

Pietro, many thanks for all the discussions and your ideas. You are a really great scientist and I really appreciate your intellectual input and wet lab knowledge! I wouldn't have learned that much without you being in the lab!

Many thanks to my lab girls: Anna, Renate, Cathleen, Darya and Angelika. For all the laughs we had together, for everlasting help in the lab and for all the great evenings with good food and all the fun!

Dear Anna, I am blessed and couldn't be more greatful that you walked in to my life. You really made a difference to my life and taught me so much more than science! I am glad that we had such an amazing PhD time together and can't imagine yet how it feels going to work every day without meeting you!

Furthermore, I thank Igor and Korbi for being genius with the mass spectrometers and Gaby for unfaltering high quality and reliability of the columns.

Acknowledgement

I am greatful to have wonderful friends around me: Lisa for the valuable support throughout the entire process of our studies and all the phone calls about science and everything else. The whole Tübingen-Crew for always being around although being spread so far. Björn, thank you for your friendship, for all the coffee dates, the fun times but also all the serious talks we had together. I hope we can resume our early-bird runs soon.

Finally my love and deep gratitude goes to my family. To my grandmother for your cheers and thoughts, I wish you could see this day. And particulary to my sister and my parents for your unconditional support, dedication and overwhelming faith that encourages me to achieve my plans and dreams. I owe it all to you.